NUEVAS METODOLOGÍAS EN ANÁLISIS DE ALIMENTOS CON EL USO DE NANOPARTÍCULAS

NEW METHODOLOGIES IN FOOD ANALYSIS USING NANOPARTICLES

Tesis Doctoral
Juan Godoy Navajas
Marzo 2014

TITULO: *Nuevas metodologías en análisis de alimentos con el uso de nanopartículas. New metodologies in food analysis using nanoparticles*

AUTOR: *Juan Godoy Navajas*

Campus de Rabanales
Ctra. Nacional IV, Km. 396 A
14071 Córdoba

www.uco.es/publicaciones
publicaciones@uco.es

NUEVAS METODOLOGÍAS EN ANÁLISIS DE ALIMENTOS CON EL USO DE NANOPARTÍCULAS

NEW METHODOLOGIES IN FOOD ANALYSIS USING NANOPARTICLES

LOS DIRECTORES

Fdo: **Agustina Gómez Hens,**
Catedrática del Departamento de Química Analítica de la Universidad de Córdoba

Fdo: **Mª de la Paz Aguilar Caballos,**
Profesora Titular del Departamento de Química Analítica de la Universidad de Córdoba

Trabajo presentado para aspirar
al Grado de Doctor en Ciencias

EL DOCTORANDO,

Fdo: **Juan Godoy Navajas**
Licenciado en Química

Agustina Gómez Hens, Catedrática del Departamento de Química Analítica de la Universidad de Córdoba y **Mª de la Paz Aguilar Caballos**, Profesora Titular del citado Departamento, en calidad de directores de la Tesis Doctoral presentada por el Licenciado en Química, Juan Godoy Navajas,

CERTIFICAN:

Que la Tesis Doctoral "NUEVAS METODOLOGÍAS ANALÍTICAS CON EL USO DE NANOPARTÍCULAS" ha sido desarrollada en los Laboratorios del Departamento de Química Analítica de la Universidad de Córdoba y del Departamento de Biotecnología de la Universidad de Turku (Finlandia) y que, a nuestro juicio, reúne todos los requisitos exigidos a este tipo de trabajo.

Y para que conste y surta los efectos pertinentes, expiden el presente certificado en la ciudad de Córdoba, a 20 de Enero de 2014.

Agustina Gómez Hens **Mª de la Paz Aguilar Caballos**

TÍTULO DE LA TESIS: NUEVAS METODOLOGÍAS EN ANÁLISIS DE ALIMENTOS CON EL USO DE NANOPARTÍCULAS

DOCTORANDO: Juan Godoy Navajas

INFORME RAZONADO DE LOS DIRECTORES DE LA TESIS

El doctorando Juan Godoy Navajas cursó brillantemente los estudios del Máster en Química Fina Avanzada, obteniendo excelentes calificaciones en las asignaturas del mismo. El trabajo fin de Máster se publicó en la revista Journal of Fluorescence.

La temática de la Tesis se encuadra en una línea de investigación puntera, como es la Nanociencia y la Nanotecnología aplicadas al análisis de alimentos. En este sentido, el doctorando ha sintetizado nanopartículas de sílice dopadas con fluoróforos de larga longitud de onda para utilizarlas en inmunoensayo. También ha desarrollado nuevas metodologías aplicables a la determinación de antioxidantes en alimentos, utilizando en una de ellas nanopartículas de óxido de terbio.

La realización de la investigación recogida en la Memoria que se presenta ha permitido al doctorando adquirir, además de una sólida formación analítica, experiencia en el manejo de las técnicas espectroscópicas UV-visible y fluorimetría y en microscopía de transmisión, así como en la síntesis de materiales nanoestructurados, en el desarrollo de procesos analíticos en microplacas, en la automatización y en el análisis de muestras reales. Todo ello ha dado lugar a seis artículos científicos, de los cuales cuatro se han publicado ya, tres de ellos en revistas situadas en el primer cuartil y uno en el segundo cuartil, otro ha sido enviado a publicar y el sexto está en fase de redacción. También han sido fruto de esta Tesis Doctoral catorce comunicaciones a Congresos nacionales e internacionales, cuatro de ellas en forma oral y el resto en forma de póster.

La estancia realizada en el grupo de investigación del Prof. Soukka (Universidad de Turku, Finlandia) durante el desarrollo de la Tesis Doctoral ha completado de forma satisfactoria dicha formación, permitiendo al doctorando adquirir conocimientos sobre el uso y aplicación de otros tipos de nanomateriales como son los *Upconverting Phosphors*, lo que dio lugar a una comunicación a un Congreso internacional en formato de póster.

Por todo ello, consideramos que la investigación desarrollada, y recogida en esta Memoria, reúne todos los requisitos necesarios en cuanto a innovación y calidad, y autorizamos la presentación de la Tesis Doctoral de D. Juan Godoy Navajas.

Córdoba, Marzo de 2014

Firma de los Directores

Fdo: Agustina Gómez Hens

Fdo: María de la Paz Aguilar Caballos

Mediante la defensa de esta Memoria se pretende optar a la obtención de la Mención "Doctorado Internacional" habida cuenta de que el doctorando reúne los requisitos exigidos para tal mención:

1. Cuenta con los informes favorables de dos doctores pertenecientes a Instituciones de Enseñanza Superior de países europeos distintos a España.

2. Uno de los miembros del tribunal que ha de evaluar la Tesis pertenece a un centro de enseñanza superior de otro país europeo.

3. Parte de la defensa de la Memoria se realizará en la lengua oficial de otro país europeo.

4. El doctorando ha realizado una estancia en el Departamento of Biotecnología de la Universidad de Turku, Finlandia, de tres meses de duración, que ha contribuido a su formación y permitido desarrollar parte del trabajo experimental de esta Memoria.

Quisiera mostrar mi más sincero agradecimiento a mis directoras de Tesis Doctoral, Tina y Mari Paz.

Gracias Tina por darme la oportunidad de trabajar contigo durante estos años y por ver en mi algo que nadie había visto anteriormente.

Mari Paz, gracias por volcar todos tus conocimientos conmigo, por sacar lo mejor de mí y por enseñarme lo fascinante que puede llegar a ser el mundo de la investigación.

A ambas os estaré eternamente agradecido.

A Juan Manuel Fernández Romero que siempre ha estado ahí cuando lo he necesitado.

Gracias a mis compañeras de laboratorio. Todas habéis conseguido que mi día a día sea mucho más ameno. Siempre es mucho más fácil trabajar rodeado de sonrisas y alegría.

A mis compañeros y amigos del departamento de Química Analítica (Paco, María, Isa Montesinos, María José, Jose, Noelia Luque, Noelia Caballero, Antoñito, Carmen, Ana Ballesteros, Laura Soriano, Guille, Lola, Nani, Isa Márquez…) pero especialmente a mi grandísimo amigo JuanMa Jiménez. A veces la vida pone en mitad de tu camino pruebas muy difíciles de superar. Pero en otras ocasiones, coloca a gente maravillosa que te ayuda a superar estas pruebas. Muchas gracias por todo y nunca os olvidaré.

No puedo olvidarme de vosotros, de mis compañeros de piso y de carrera. Este camino lo comenzamos juntos hace ya más de una década y lo

estamos finalizando juntos. Muchas gracias de todo corazón a Jesús, Alejandro, Pepe, Puri, Kaquisco, Jose, Trócoli, Carlos, Cristel, porque gracias a vosotros tengo la gran suerte de recordar todos estos años con una sonrisa en los labios.

Gracias a mi familia, especialmente a mis hermanos: Puri, Carmen y Jose. Fui el pequeño de una familia numerosa pero, sobre todo, me sentí siempre el más querido. Hemos vivido muchos momentos buenos y algunos muy malos, pero siempre hemos estado todos unidos. Muchísimas gracias por todo vuestro apoyo incondicional.

He dejado para el final a las personas más importantes en mi vida. Mis padres. Vosotros habéis sido los pilares de mi vida, de mi educación y formación. Gracias a vosotros, hoy soy lo que soy. Vosotros habéis luchado durante toda vuestra vida para que pudiésemos llegar a lo más. No hay palabras para agradecer todo lo que habéis hecho por mí y por mis hermanos. Esta Tesis Doctoral es vuestra.

I would like to thank Prof. Tero Soukka for offering me the opportunity to work with him in the Department of Biotechnology of the University of Turku (Finland).

Special thanks should be given to PhD. Terhi Riuttamäki for her support and unconditional help in both academic and personal fields, and for the time devoted to me.

I also thank to other colleagues (Timo, Sami, Ari and Rikka) for their valuable help and kindness during my stay in Finland.

Agradezco a la Consejería de Economía, Innovación, Ciencia y Empleo de la Junta de Andalucía la concesión de una beca pre-doctoral adscrita al Proyecto de Excelencia P09-FQM4933 que me ha permitido dedicar estos últimos 4 años al desarrollo de esta Tesis.

INDICE

ÍNDICE **Página**

OBJETO

AIM

El objetivo genérico de las investigaciones que constituyen esta Memoria ha sido el desarrollo de métodos rápidos para el análisis de alimentos utilizando, básicamente, las especiales propiedades que presentan distintos nanomateriales. Los estudios realizados han pretendido expandir la aplicabilidad analítica de la Nanotecnología para abrir nuevas vías, alternativas a las ya establecidas, que mejoren el control de la calidad alimentaria. Para alcanzar este objetivo se han realizado las siguientes investigaciones:

- Síntesis y caracterización de nanopartículas de sílice dopadas con los fluoróforos de larga longitud de onda azul nilo y violeta de cresilo y su utilización para formar marcadores aplicables a la determinación de macromoléculas y moléculas pequeñas en alimentos mediante inmunoensayo heterogéneo.
- Desarrollo de nuevas metodologías analíticas para la determinación de parámetros globales en alimentos, tales como la capacidad antioxidante y contenido de polifenoles, utilizando fluorimetría de larga longitud de onda y nanopartículas de óxido de terbio, respectivamente.
- Estudio sistemático de la utilidad del fenómeno de transferencia de energía de resonancia luminiscente (LRET) entre nanocristales de iones lantánidos, que presentan luminiscencia anti-Stokes (upconverting phosphors), y fluoróforos orgánicos para la determinación de biotina mediante ensayos de afinidad en medio homogéneo.

The general aim of the investigations included in this Dissertation has been the development of fast methods for food analysis mainly using the especial properties of nanomaterials. The studies performed have tried to expand the application field of Nanotechnology and open new possibilities by developing analytical methods alternative to those already established in order to improve food quality control processes. The investigations performed to achieve this goal are described below:

- Synthesis and characterization of silica nanoparticles doped with the long-wavelength fluorophores cresyl violet and nile blue and their further use to obtain tracers to be applied to the determination of either macromolecules or haptens in foods by heterogeneous immunoassay.

- Development of new analytical methodologies to estimate global parameters in foods, such as the antioxidant capacity and total polyphenol content, using long wavelength fluorometry and terbium oxide nanoparticles, respectively.

- Study of the potential usefulness of luminescent resonance energy transfer (LRET) between nanocrystals of lanthanide ions that show anti-Stokes luminescence (upconverting phosphors) and organic fluorophores to develop homogeneous affinity assays for biotin.

INTRODUCCIÓN

Las investigaciones que se presentan en esta Memoria han dado lugar a diversos métodos determinativos orientados principalmente a ampliar el campo de aplicación de la Nanotecnología en análisis de alimentos. Como preámbulo a estas investigaciones se describen a continuación algunos aspectos relacionados con las metodologías desarrolladas, incidiendo en los tres tipos de nanomateriales utilizados en esta Memoria, en los fluoróforos de larga longitud de onda y en el inmunoensayo. Al inicio de cada capítulo se describirán aspectos más concretos relacionados con su contenido. Esta introducción general se ha dividido en cuatro apartados: 1) nanopartículas de sílice, 2) nanomateriales basados en lantánidos, principalmente "upconverting phosphors" y óxidos de lantánidos, 3) fluoróforos de larga longitud de onda, y 4) técnicas de inmunoensayo y su uso en análisis de alimentos.

1. Nanopartículas de sílice

Las numerosas investigaciones que se están desarrollando en el campo de la Nanotecnología, y los procesos involucrados en la síntesis, manipulación y desarrollo de nanomateriales, están dando lugar a nuevas herramientas metodológicas e instrumentales con aplicaciones en distintas áreas analíticas [1]. Entre la variedad de los nanomateriales actualmente disponibles, el uso de nanopartículas de sílice (SiO_2NPs) constituye una opción muy útil como se describe a continuación.

El interés que presenta la utilización de SiO_2NPs con fines analíticos es atribuible a sus especiales características. No solo muestran

ausencia de toxicidad, elevada solubilidad en agua y estabilidad, principalmente en medio acuoso, sino también otras características tales como su fácil funcionalización y enlace a biomóleculas, la posibilidad de controlar su porosidad, su transparencia a la radiación, su bajo coste y su capacidad para utilizarlas como portadores de una amplia variedad de reactivos [2]. Estas propiedades hacen de las SiO_2NPs un material muy adecuado para su uso en bioensayos.

Los fluoróforos convencionalmente utilizados como marcadores moleculares están siendo sustituidos por SiO_2NPs dopadas con dichos fluoróforos ya que éstas poseen propiedades ópticas superiores, una mayor estabilidad química y una menor fotodescomposición. Además, se han desarrollado NPs dopadas con especies electroquimioluminiscentes con fines bioanalíticos por su gran estabilidad y mayor señal luminiscente, siendo fácilmente aplicables en sistemas miniaturizados [3]. También se han sintetizado otros tipos de SiO_2NPs usando materiales semiconductores, metálicos, magnéticos e incluso orgánicos. Además, la elevada concentración de grupos silanoles que existe en la superficie de las SiO_2NPs facilita una gran variedad de reacciones de funcionalización y unión a biomoléculas como son anticuerpos y otras proteínas, ADN u otras moléculas para ensayos de bioafinidad, como son los sistemas biotina-avidina y biotina-estreptavidina.

1.1 Síntesis de nanopartículas de sílice

Existen dos métodos principales para la síntesis de SiO_2NPs: el método Stöber y el método de microemulsión de micelas inversas.

El método Stöber es el proceso tradicionalmente utilizado, con el que se obtienen SiO_2NPs de diámetro medio inferior a 100 nm. El proceso implica la hidrólisis de un precursor alcóxido de sílice (como puede ser el tetraetoxisilano, TEOS) en una mezcla de etanol e hídroxido amónico. Durante esta hidrólisis tiene lugar la generación de ácido silícico y, cuando la concentración de éste supera su solubilidad en etanol, se produce la nucleación, dando lugar a la formación de las NPs. El diámetro de estas partículas puede ser controlado mediante modificación de diversas variables experimentales como las concentraciones de los diferentes reactivos y la temperatura de la reacción [4]. El diámetro de las NPs obtenidas puede oscilar entre 10 nm y 1 μm, lo que da lugar a un conjunto bastante heterogéneo. La incorporación de fluoróforos orgánicos a estas NPs puede realizarse mediante enlace covalente para lo que es necesario modificar los fluoróforos con grupos funcionales como el isocianato, el cual se une a grupos aminos procedentes de algún precursor de sílice, como el 3-aminopropiltrietoxisilano, APTES, por lo que los reactivos TEOS y APTES se incluyen simultáneamente en el proceso de síntesis.

El método de microemulsión de micelas inversas, también conocido como método de microemulsión de agua-en-aceite (W/O), origina agregados termodinámicamente estables a partir de un surfactante anfifílico. Las cabezas hidrofílicas se orientan de forma que aíslan multitud de gotas de agua de tamaño nanométrico, mientras que las colas hidrofóbicas quedan orientadas hacia el disolvente orgánico. Estas nanogotas aisladas del medio orgánico actúan como nanoreactores donde se lleva a cabo la formación de las NPs. Al igual que en el método Stöber,

las NPs se forman por hidrólisis del precursor de sílice y el diámetro de éstas puede ser controlado variando la proporción entre el agua y el surfactante (W_0) ya que la reacción tiene lugar en el núcleo acuoso. En comparación con el método Stöber, este proceso de síntesis necesita un mayor tiempo de reacción, pero las NPs obtenidas son más esféricas, presentan mayor dispersión entre ellas y una distribución de tamaños más homogénea. Este método de microemulsión de micelas inversas puede ser utilizado para preparar SiO_2NPs dopadas con fluoróforos o materiales metálicos tales como núcleos magnéticos o semiconductores tipo quantum dots (QDs) [5].

1.2 Nanopartículas dopadas

En los últimos años se han desarrollado numerosos métodos analíticos en los que se utilizan marcadores formados por SiO_2NPs dopadas con fluróroforos orgánicos, QDs, partículas magnéticas o partículas activas a la radiación Raman, aprovechando las ventajas que proporciona el uso de estos materiales encapsulados en la matriz de la sílice, mencionadas anteriormente. A continuación se describen algunos ejemplos:

1.2.1 Nanopartículas dopadas con fluoróforos orgánicos

Las moléculas marcadas con fluoróforos han sido ampliamente utilizadas en bioanálisis. Los fluoróforos convencionales, tales como el isotiocianato de fluoresceína, rodaminas o cianinas, presentan ciertas desventajas como son su elevada inestabilidad, sensibilidad a procesos de fotodescomposición y estrecho desplazamiento Stokes. Además,

normalmente, sólo un número limitado de fluoróforos puede unirse a las biomoléculas debido a problemas de impedimento estérico y a enlaces inespecíficos con potenciales interferentes.

Por el contrario, las SiO_2NPs dopadas con moléculas fluorescentes presentan varias ventajas. Poseen una elevada fluorescencia, buena estabilidad, gracias a la protección que confiere la sílice, y amplia aplicabilidad en el campo del bioanálisis mediante la modificación de su superficie para enlazarse a diversos tipos de moléculas. Tanto reactivos orgánicos como inorgánicos pueden ser incorporados al interior de la sílice usando diferentes métodos de síntesis, obteniendo NPs que contienen un elevado número de estos fluoróforos y que son especialmente útiles para formar marcadores en ensayos ultrasensibles. El isotiocianato de fluoresceína ha sido ampliamente utilizado para obtener SiO_2NPs fluorescentes aplicables a la determinación de biomoléculas. También se ha descrito la utilización de SiO_2NPs dopadas con tris(2,2´-bipiridil)diclororutenio(II) hexahidratado ($Ru(bpy)_3^{2+}$) para desarrollar ensayos con detección electroquimioluminiscente (unidas a un electrodo para diseñar un sensor, en microplacas o en sistemas microfluídicos) para determinar marcadores tumorales [6 – 9], ADN [10] y otras biomoléculas [11, 12]. Recientemente, estas NPs dopadas con $Ru(bpy)_3^{2+}$ se han utilizado como marcadores quimioluminiscentes para determinar ácidos nucleicos en ensayos de flujo lateral [13] así como para la determinación de iones metálicos [14]. Otro derivado fluorescente de rutenio(II), diclorotris-(1,10-fenantrolin)rutenio(II) hidratado [$Ru(phen)_3^{2+}$], se ha utilizado para sintetizar NPs fluorescentes y diseñar un nuevo método para la

determinación de ozono basado en el fenómeno de transferencia de energía resonante electroquimioluminiscente (ECRET). En este caso, las NPs dopadas con $Ru(phen)_3^{2+}$ (RuSiNPs) transfieren la energía a otro fluoróforo que actúa como aceptor [15].

1.2.2 Nanopartículas de sílice dopadas con quelatos de iones lantánidos

Las NPs dopadas con quelatos de iones lantánidos poseen propiedades luminiscentes únicas tales como un elevado rendimiento cuántico, estrechas bandas de absorción y emisión, y una excelente fotoestabilidad. Estos quelatos de iones lantánidos unidos a la superficie de SiO_2NPs se han utilizado en un ensayo inmunofluorimétrico de tiempo resuelto para la determinación de la hormona estimulante del tiroides humano [16]. También se han encapsulado en el interior de las NPs para, por ejemplo, aplicaciones en imagen celular mediante luminiscencia de tiempo resuelto [17].

1.2.3 Nanopartículas de sílice dopadas con quantum dots (QDs)

Se han encapsulado diversos tipos de quantum dots (QDs) en el interior de SiO_2NPs para formar marcadores y utilizarlos en bioanálisis. Por ejemplo, se ha descrito un nuevo inmunosensor electroquimioluminiscente que emite en el infrarrojo cercano para la determinación de proteínas haciendo uso de estos QDs encapsulados en la matriz de sílice [18]. Este tipo de nanomaterial dopado también se ha utilizado en ensayos basados en el fenómeno de transferencia de energía resonante de fluorescencia (FRET) donde el QD actúa como dador del

sistema para la determinación de iones mercurio [19] o de melamina [20]. Otra combinación de los QDs con las SiO_2NPs ha sido la unión de estos nanocristales a la superficie de la sílice mediante enlaces covalentes para ser utilizados en la determinación de células y marcadores tumorales [21 – 23], anticuerpos y otras proteínas [24, 25], así como moléculas de menor tamaño como el trinitrotolueno [26].

1.2.4 Nanopartículas de sílice activas a la radiación Raman

Las señales generadas mediante dispersión Raman contienen una elevada información aunque suelen ser poco sensibles. Esta limitación puede evitarse en parte inmovilizando la molécula de interés sobre una superficie metálica (especialmente sobre metales nobles tales como plata u oro). Esta primera etapa da lugar a un incremento en la intensidad de señal de varios órdenes de magnitud. Para conseguir metodologías Raman más robustas, estos metales pueden ser combinados con SiO_2NPs. Por ejemplo, se ha desarrollado un método simple para preparar marcadores Raman con nanopartículas de plata (AgNPs), enlazadas a ácido 4-mercaptobenzoico y encapsuladas en el interior de SiO_2NPs [27]. Para la síntesis se ha utilizado tanto el método de microemulsión de micelas inversas [28] como el método Stöber [29]. También se ha descrito un método para sintetizar nanopartículas híbridas de plata y sílice utilizando un polímero orgánico, como el etilenglicol, el cual actúa como soporte entre las AgNPs y la superficie de sílice para, combinarlas posteriormente con óxido de grafeno. Utilizando este procedimiento se ha descrito un nuevo biosensor para la determinación de glucosa en muestras de orina y suero [30].

Las NPs de oro (AuNPs), al igual que las AgNPs, pueden incorporarse en el interior de las SiO_2NPs durante el proceso de síntesis o bien unirse a la superficie. Por ejemplo, se han utilizado AuNPs@SiO_2NPs para diseñar un biosensor basado en la dispersión Raman superficial donde las NPs actúan como marcador mediante su enlace a un aptámero para la determinación de adenosina trifosfato [31] o a anticuerpos para determinar la bacteria del cólera utilizando un inmunoensayo [32]. Otra opción es la combinación de las AuNPs y las SiO_2NPs con otros materiales para conseguir una amplificación de la señal. Por ejemplo, utilizando óxidos metálicos, como el ZrO_2, se ha desarrollado un inmunosensor para la determinación del virus de la hepatitis C [33] y, utilizando óxido de grafeno reducido y AuNPs retenidas en una matriz de SiO_2/quitosán, se ha descrito un biosensor electroquímico para la determinación de dopamina y ácido úrico [34]. También se han combinado SiO_2NPs dopadas con oro y enzimas y se han utilizado para catalizar una reacción quimioluminiscente para la determinación de residuos de estreptomicina [35]. Otra aplicación descrita para estas NPs ha sido su combinación con nanotubos de carbono (CNTs) y óxido de grafeno para el diseño de un inmunosensor electróquimico para la determinación de gonadotropina coriónica humana (hCG) [36], así como la utilización de AuNPs y acetilcolinesterasa en una matriz sol-gel y CNTs de pared múltiple (MWCNTs) para modificar un electrodo de platino y aplicarlo a la determinación de acetilcolina [37].

1.2.5 Nanopartículas magnéticas

Las nanopartículas magnéticas (MNPs) tienen un gran atractivo en el ámbito científico debido a su elevado potencial en diversos campos,

como es el suministro y liberación controlados de fármacos, diagnóstico por imagen en resonancia magnética (MRI), terapia tumoral mediante hipertermia magnética, biomarcadores y bioseparación. Estas aplicaciones normalmente requieren estabilidad química y fácil dispersión en medio líquido, por lo que las SiO_2NPs con núcleo magnético son una buena opción debido a la estabilidad que presenta la sílice en medio acuoso, su biocompatibilidad y fácil funcionalización que permite su unión a especies biológicamente activas. En Química Analítica, las MNPs han sido utilizadas con diferentes fines. Por ejemplo, las SiO_2NPs dopadas con materiales magnéticos se han usado como medio de separación en la determinación simultánea de dos marcadores tumorales (α-fetoproteína y antígeno carcinoembriónico) mediante una reacción electroquimio-luminiscente [38]. En otra aplicación, se han combinado con AuNPs para la determinación de trazas de proteína C reactiva mediante un immunosensor piezoeléctrico utilizando un anticuerpo y peroxidasa de rábano inmovilizados en las AuNPs [39].

1.3 Métodos para modificar la superficie de las nanopartículas de sílice

El uso de SiO_2NPs en aplicaciones analíticas se ha extendido gracias a la relativa facilidad para modificar su superficie. Existen precursores de sílice que permiten introducir grupos funcionales como aminas, carboxilos, y tioles, creando así puntos de unión a biomoléculas. Por ejemplo, los oligonucleótidos pueden ser inmovilizados en la superficie de las SiO_2NPs usando la reacción de acoplamiento del disulfuro, donde las SiO_2NPs se funcionalizan con 3-mercaptopropiltrimetoxisilano. Una reacción de intercambio tiol-disulfuro permite la conjugación de las

SiO_2NPs modificadas con grupos tioles con los oligonucleótidos modificados con grupos disulfuro sin ningún tipo de reacción adicional. Un protocolo comúnmente utilizado para la unión de enzimas y anticuerpos es la unión vía glutaraldehido. Para ello, se funcionalizan las NPs utilizando el 3-aminopropiltrietoxisilano o el N-[3-(trimetoxisilil)-propil]dietilentriamino y los grupos amino de la superficie funcionalizada se unen a los grupos amino de estas biomoléculas mediante entrecruzamiento con glutaraldehido o disuccinidimidil glutarato. Por otro lado, las SiO_2NPs pueden modificarse también con carbonato sódico o con grupos –OCN mediante reacción con bromuro de cianógeno en acetonitrilo [3].

Como se ha indicado anteriormente, las SiO_2NPs son un soporte adecuado debido a su superficie químicamente inerte y su fácil modificación con grupos funcionales. Cuando estas NPs son utilizadas como medios de transporte deben presentar una buena dispersión y una morfología superficial homogénea para conseguir una concentración de especies similar entre las diferentes nanoesferas, requisito necesario para conseguir buena sensibilidad, reproducibilidad y otras propiedades analíticas deseables. Diferentes moléculas fluorescentes pueden ser inmovilizadas en la superficie de las NPs. El fluoróforo $Ru(bpy)_3^{2+}$ se ha utilizado para el diseño de un sensor para la determinación de inmunoglobulina G mediante la combinación de estas NPs con CNTs proporcionando una señal quimioluminiscente [40]. En otros casos, la superficie de las NPs se ha modificado con materiales electroactivos, como

el ácido fosfónico, para la determinación de glucosa en muestras reales en presencia de glucosa oxidasa, midiéndose la corriente eléctrica [41].

Las biomoléculas más utilizadas para inmovilizarlas en la superficie de las SiO_2NPs son las enzimas y los anticuerpos, debido a su elevada selectividad, pero es imprescindible la generación de algún tipo de señal que pueda medirse y relacionarse con la concentración de analito. Por ejemplo, se han utilizado enzimas unidas a la superficie de SiO_2NPs que pueden catalizar reacciones quimioluminiscentes. Se ha descrito el uso de SiO_2NPs marcadas con anticuerpos anti-*staphylococcal enterotoxin B* y peroxidasa de rábano (HRP) para obtener una señal luminiscente en presencia de peróxido de hidrógeno y luminol [42]. También se han utilizado especies magnéticas como método de separación. Por ejemplo, en una separación basada en una inmunoreacción tipo sándwich para microcistina-LR, se ha marcado uno de los anticuerpos con NPs ferromagnéticas, mientras que el segundo anticuerpo se ha enlazado a SiO_2NPs sobre las que se ha inmovilizado previamente la HRP. En presencia del analito, ambos conjugados quedan unidos y se separan del resto de la matriz de la muestra utilizando un imán, debido a las propiedades magnéticas de uno de los conjugados. A continuación, se adiciona un precursor quimioluminiscente que actúa como sustrato de la enzima y se registra la señal quimioluminiscente [43].

La confinación física de biomoléculas en la superficie de las SiO_2NPs, por ejemplo, mediante atrapamiento en una matriz porosa de este material, puede ser una alternativa útil en ciertas técnicas biomédicas, biotecnológicas y bioanalíticas. Utilizando las características de la matriz

de sílice se ha desarrollado un sensor combinando MWCNTs y SiO_2NPs para la determinación de epinefrina [44]. Una tecnología similar se ha usado para desarrollar varios tipos de biosensores para la determinación indirecta de dibutilftalato utilizando materiales de reconocimiento molecular y SiO_2NPs, donde se lleva a cabo la polimerización [45], o para el reconomiento de tert-butilhidroquinona utilizando un sensor electroquímico de impresión molecular [46].

1.4. Uso de nanopartículas de sílice en análisis de alimentos

En lo que respecta al análisis de alimentos haciendo uso de las SiO_2NPs, se han descrito diversas aplicaciones interesantes, aunque su uso no está generalizado. Estos nanomateriales se han utilizado como nuevos soportes sólidos en métodos de extracción y separación del analito de la muestra, previos a la etapa de determinación. Una opción descrita en la que se utilizan SiO_2NPs para la separación ha consistido en su dopaje con un núcleo magnético y su posterior funcionalización con un anticuerpo. Utilizando estas NPs como medio de extracción, se ha determinado Salmonella en muestras de zumo de limón y leche pasteurizada vía PCR [47].

Como se ha descrito anteriormente, las SiO_2NPs se han utilizado para formar marcadores y desarrollar nuevas metodologías aplicables al análisis de alimentos. Por ejemplo, se han aplicado a la determinación de enterotoxina B en leche [42] y tert-butilhidroquinona en aceites [46].

Los métodos de "screening" o tests de respuesta rápida desempeñan una función destacable en análisis de alimentos,

concretamente en el control de sustancias prohibidas, gracias a la posibilidad de realizar dichos ensayos *in situ* sin necesidad de instrumentación costosa y sofisticada. Las SiO_2NPs se han utilizado en estos métodos de "screening" dopándolas con algún fluoróforo y funcionalizándolas con un anticuerpo. Estas NPs se han usado como marcadores en el desarrollo de inmunocromatografías utilizando tiras reactivas para la determinación rápida de enrofloxacina en muestras de carne de pollo [48] o residuos de β-agonistas en orina de cerdo [49].

En resumen, aunque la aplicación de las SiO_2NPs al análisis de alimentos ha sido relativamente limitada, sus especiales características ofrecen nuevas posibilidades de utilidad en este área analítica.

2. Nanomateriales basados en lantánidos

Esta sección se centrará en la descripción de las principales características y aplicaciones de los nanomateriales basados en lantánidos utilizados en las investigaciones incluidas en esta Memoria, tales como los "upconverting phosphors" y las nanopartículas de óxidos de lantánidos. Aunque existen otros materiales utilizados con fines analíticos, tales como las NPs de sílice dopadas con quelatos de iones lantánidos, su descripción se realizó en el apartado anterior de esta Introducción por lo que no se incluye en esta sección.

2.1 "Upconverting phosphors"

Debido a que en el Capítulo IV de esta Memoria se describen las investigaciones realizadas con un tipo especial de nanomateriales como son los "upconverting phosphors", se dedica una parte de esta Introducción a la descripción de sus características y de algunas aplicaciones analíticas.

El fenómeno de "upconversion" es un proceso en el cual se genera una intensa emisión de energía a partir de una radiación menos energética. Este incremento de energía se debe a la absorción de varios fotones, normalmente dos o tres, por cada fotón emitido. La transición del estado electrónico excitado superior al estado electrónico más bajo, o a otros niveles menos energéticos, da lugar a una emisión luminiscente a longitudes de onda más cortas que la longitud de onda de excitación. Este proceso óptico no lineal, también conocido como fotoluminiscencia anti-Stokes, implica estados de energía intermedios, imprescindibles para llevar a cabo el salto electrónico y la emisión de energía [50].

A diferencia de los fenómenos de fluorescencia basados en desplazamiento Stokes, donde se lleva a cabo la excitación a longitudes de onda más cortas y la emisión tiene lugar a una longitud de onda mayor, el fenómeno de "upconversion" requiere una menor energía de excitación que los fenómenos Stokes (Figura 1). Por lo tanto, este proceso permite irradiar la muestra sin el riesgo de descomposición fotoquímica de la misma. Además, se minimizan las interferencias espectrales procedentes de dicha matriz, como se comentará posteriormente.

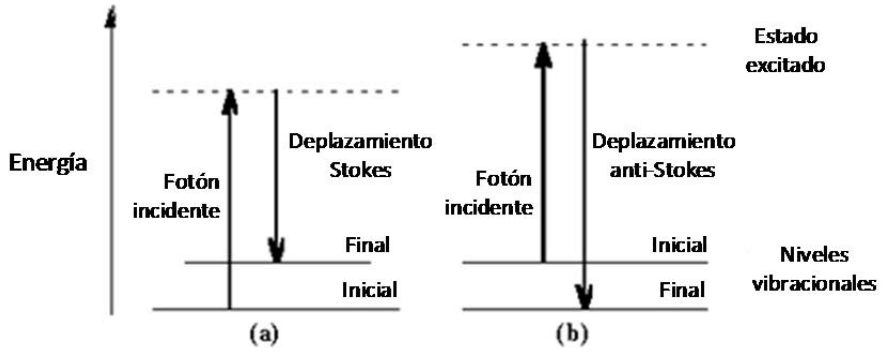

Figura 1. Representación esquemática de los fenómenos de fluorescencia con desplazamiento Stokes (a) y anti-Stokes (b).

Las aplicaciones analíticas de la luminiscencia anti-Stokes se han incrementado en las últimas décadas debido a la disponibilidad de nanomateriales inorgánicos capaces de llevar a cabo este fenómeno luminiscente, denominados "upconverting phosphors" (UCPs). Estos materiales están compuestos por una estructura inorgánica, siendo el más utilizado el $NaYF_4$, aunque también se puede usar Gd y La en lugar de Y, y se suelen dopar con iones, normalmente lantánidos, modelando así sus características espectrales. Los diferentes métodos utilizados para la síntesis de UCPs con fines analíticos son optimizados para que estos nanomateriales presenten las siguientes características: monodispersos, forma homogénea, fácil dispersión en agua y una estructura cristalográfica pura con un tamaño uniforme (preferiblemente con un diámetro inferior a 50 nm), así como elevada luminiscencia. Los UCPs de tamaño nanométrico se han sintetizado usando varios procesos, los cuales van desde el más

comúnmente utilizado proceso de co-precipitación, descomposición térmica y cristalización en disolvente orgánico por encima del punto de ebullición hasta los métodos de síntesis hidro- y solvotermal [51].

Los iones dopantes desempeñan una función crucial en lo que respecta a la absorción y emisión de fotones. Estos iones determinan, por ejemplo, la longitud de onda de la radiación emitida. Algunos lantánidos trivalentes poseen estados electrónicos intermedios metaestables muy útiles para la generación de la emisión anti-Stokes. Las propiedades fotoluminiscentes vienen definidas por sus electrones *4f*, los cuales están bien protegidos por los electrones de menor energía *5s* y *5p,* localizados en orbitales más externos [52]. Los saltos energéticos de los niveles electrónicos de los iones Er(III), Tm(III) y Ho(III), son muy apropiados para utilizarlos como iones dopantes en materiales cuya finalidad es la producción del fenómeno anti-Stokes, mientras que los iones Pr(III), Nd(III) y Dy(III), presentan niveles energéticos menos adecuados.

Con el fin de aumentar la eficiencia del proceso de emisión de fluorescencia con desplazamiento anti-Stokes, estos UCPs son normalmente co-dopados con el ion Yb(III), el cual presenta una elevada capacidad de absorción [53]. Además, los iones Yb(III) son menos susceptibles que otros lantánidos al fenómeno de inhibición por concentración, es decir, a la pérdida de fluorescencia cuando se utilizan concentraciones elevadas. Por lo tanto, se pueden usar elevadas concentraciones de Yb(III) para aumentar la probabilidad de excitación de los iones dopantes [54]. Además, los niveles electrónicos del Yb(III) y de los iones dopantes Er(III), Ho(III) y Tm(III) responsables de la transferencia

electrónica y del fenómeno de fluorescencia, son energéticamente muy similares, lo que facilita el salto de los electrones de unos iones a otros, obteniéndose así emisiones fotoluminiscentes anti-Stokes muy intensas.

Los UCPs son cristales inorgánicos hidrofóbicos que, originalmente, no disponen de grupos funcionales. Por lo tanto, la modificación de su superficie es un aspecto fundamental para transformar estas partículas en un material más hidrofílico y con grupos funcionales en su superficie para utilizarlos con fines analíticos. Con este fin, estos se recubren con sílice y, posteriormente, se funcionalizan mediante los métodos descritos anteriormente [4, 5].

Los UCPs están emergiendo en el campo de la Química Analítica como una alternativa a los biomarcadores fluorescentes tradicionales, los cuales se basan en la emisión de fluorescencia con desplazamiento Stokes. Su uso para preparar marcadores presenta una serie de ventajas. Muestran un alto rendimiento cuántico, estrechas bandas de emisión, gran desplazamiento anti-Stokes, baja toxicidad y buena estabilidad fotoquímica. Además, la excitación de los UCPs se lleva a cabo a una longitud de onda situada en el infrarrojo cercano, por lo que la relación señal-ruido es mayor que a longitudes de onda más bajas, mejorando así la sensibilidad gracias a la disminución del fenómeno de autofluorescencia. Las excelentes características de los UCPs los hacen muy útiles para su uso en bioanálisis gracias a la disminución de la señal de fondo, obteniéndose límites de detección más bajos.

La combinación de los UCPs con biomoléculas selectivas, como son las implicadas en las interacciones antígeno-anticuerpo o biotina-estreptavidina, constituyen una excelente alternativa para su uso en aplicaciones bioanalíticas. Tanto la biomolécula como el UCP, deben presentar grupos funcionales adecuados para poder unirse mediante enlaces covalentes. La adsorción física de las biomoléculas sobre la superficie de los UCPs ha sido estudiada aunque la inestabilidad que presentan las hace inapropiadas para los bioensayos [55].

Se han desarrollado varias aplicaciones bioanalíticas utilizando los UCPs como marcadores en ensayos homogéneos [56 - 59] y heterogéneos [60 - 62], en ensayos de flujo lateral [63 - 66] y como sensores [67, 68] basándose algunas de estas aplicaciones, especialmente los ensayos homogéneos, en sistemas basados en transferencia de energía resonante luminiscente (LRET). En el capítulo IV correspondiente a las investigaciones realizadas con el uso de "upconverting phosphors" se abordará con más profundidad la utilidad de estos nanocristales en el desarrollo de sistemas LRET.

2.2. Nanopartículas de óxidos lantánidos

Las nanopartículas de óxidos lantánidos, y más específicamente las nanopartículas de óxido de terbio y de europio, a pesar de haberse utilizado en numerosas aplicaciones industriales, tales como en el desarrollo de dispositivos de iluminación en estado sólido, han presentado hasta la fecha escasas aplicaciones analíticas. Se ha descrito recientemente el uso de las nanopartículas de Eu_2O_3 para la determinación del antibiótico

tetraciclina en muestras de orina animal y miel [69]. El método está basado en la interacción directa de dicho antibiótico con las Eu_2O_3NPs, para producir una intensa luminiscencia sensibilizada. Esta emisión luminiscente presenta características similares a la luminiscencia observada con quelatos de iones europio, tales como estrechas bandas de emisión, un amplio desplazamiento Stokes y una larga duración de la luminiscencia [70]. Esta última característica posibilita la realización de medidas en el modo de tiempo resuelto, que permite eliminar la interferencia de señales fluorescentes de más corta duración. Las nanopartículas de Eu_2O_3 se han utilizado también para el desarrollo de inmunoensayos en fase sólida [71, 72]. Estas NPs no tienen grupos funcionales en su superficie, por lo que ésta ha de modificarse para poder ser utilizadas como marcador, lo que puede conducir a la inhibición de su luminiscencia por la acción de los reactivos requeridos para la activación y conjugación. Para evitar esto, se recurre a su encapsulamiento en matrices de sílice o alúmina, como se ha descrito para un inmunoensayo para la determinación de atrazina, en el que las Eu_2O_3 NPs se han recubierto de sílice para formar el marcador [72]. La luminiscencia sensibilizada de las nanopartículas de óxido de terbio(III,IV), también denominado terbia (Tb_4O_7), por salicilato y lasalocid se ha estudiado de forma sistemática, desarrollándose finalmente un método para la determinación de lasalocid en muestras de agua, de pienso y de huevos [73]. La selectividad del método propuesto ha permitido la determinación de dicho antibiótico con un tratamiento sencillo de las muestras. En las investigaciones incluidas en esta Memoria no se abordará el uso de la luminiscencia sensibilizada de estas nanopartículas, sino que se

describirá una nueva propiedad como activador de la enzima laccasa para la determinación de polifenoles en vinos.

3. Fluoróforos de larga longitud de onda

El uso de fluoróforos de larga longitud de onda (LWFs) en Química Analítica es una alternativa útil para mejorar la selectividad espectral de las medidas fluorescentes frente a los fluoróforos tradicionales. La emisión de fluorescencia a larga longitud de onda tiene lugar en una zona del espectro electromagnético (>600 nm) donde prácticamente no se produce la absorción o emisión de posibles interferentes presentes en la matriz de la muestra. Además, debido a la baja energía utilizada para excitar el fluoróforo, el riesgo de degradación de la muestra es bajo mientras que las interferencias que originan señales Raman también se reducen considerablemente [74]. Por otro lado, la posibilidad de sufrir fenómenos de inhibición es muy reducida ya que los LWFs muestran un tiempo de vida corto. La utilidad de este tipo de fluoróforos se ha demostrado ampliamente, especialmente en análisis biológico, donde la señal procedente de la matriz de la muestra puede ser una fuente de interferencias muy importante.

La versatilidad de estos compuestos se ha puesto de manifiesto en el desarrollo de nuevos sustratos enzimáticos, actuando como marcadores en inmunoensayos, en secuenciación de ácidos nucleicos y como reactivos derivatizantes en electroforesis capilar (CE) y cromatografía de líquidos (LC). Además, estos fluoróforos se han utilizado para el desarrollo de

metodologías basadas en sistemas FRET y de nuevos sensores, así como en metodologías cinéticas [75].

3.1 Tipos y propiedades de los fluoróforos de larga longitud de onda

En los últimos años se han utilizado diferentes tipos de fluoróforos de larga longitud de onda como reactivos, entre los que se pueden destacar tres grupos bien diferenciados: materiales inorgánicos, fluoróforos orgánicos y compuestos organometálicos (Figura 2).

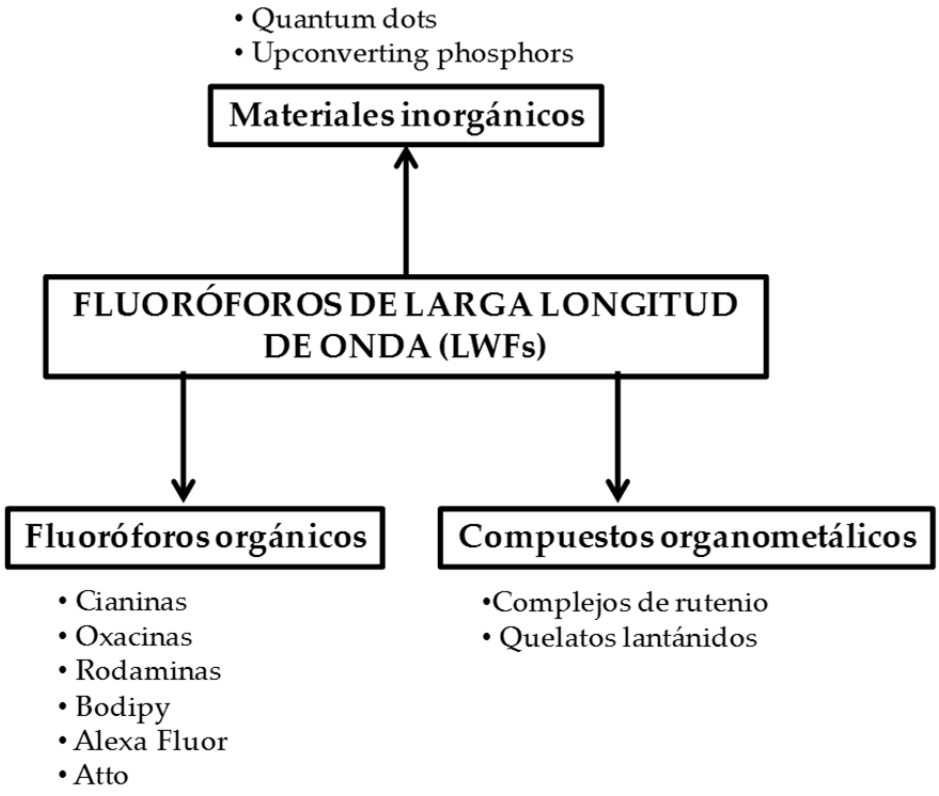

Figura 2. Clasificación de los fluoróforos de larga longitud de onda.

Dentro de los materiales inorgánicos, se pueden destacar dos tipos, los quantum dots (QDs) [76] y los upconverting phosphors (UCPs) [77], estos últimos descritos en el apartado anterior. Los QDs suelen estar formados por una estructura sintetizada a partir de materiales semiconductores como CdSe, CdTe, PbS, o materiales similares, y cuya composición y tamaño inciden en las longitudes de onda máximas de excitación y emisión que presentan estos materiales.

Aunque el número de fluoróforos orgánicos de larga longitud de onda es menor que el de los fluoróforos convencionales, se ha sintetizado una gran variedad de compuestos de este tipo en los últimos años, los cuales se han utilizado en muchos casos en el diseño de láseres de colorantes. Un LWF debe presentar una estructura rígida con enlaces conjugados o anillos aromáticos condensados. Este sistema de conjugación puede favorecer la inestabilidad del reactivo así como procesos de foto-descomposición cuando es excitado. También pueden mostrar otros inconvenientes tales como estrechos desplazamientos Stokes, baja solubilidad, y procesos de foto-oxidación. Sin embargo, las ventajas anteriormente indicadas justifican su aplicación en Química Analítica [78, 79], describiéndose a continuación algunas características de los LWFs más utilizados.

Los fluoróforos de la familia de las cianinas constituyen uno de los principales grupos de LWFs. Su estructura presenta dos anillos aromáticos y heterocíclicos unidos mediante una cadena de polimetina con dobles enlaces carbono-carbono conjugados (Figura 3). Estos fluoróforos tienen máximos de excitación en el intervalo 600-900 nm, obteniéndose amplios

desplazamientos espectrales batocrómicos con la adición de grupos vinilo a la cadena de polimetina. Las cianinas presentan algunas limitaciones: no tienen grupos reactivos para unirlos a los analitos, su vida media en el estado excitado es muy corta, bajo rendimiento cuántico y tienden a agregarse en disolución, lo que origina un rápido descenso de la intensidad de fluorescencia [80]. Sin embargo, la fotofísica de estos compuestos puede mejorarse añadiendo macromoléculas o disolventes orgánicos al medio. La adición de grupos sulfonato a la estructura del fluoróforo puede mejorar su solubilidad en agua, el rendimiento cuántico y su estabilidad fotoquímica. Además, la adición de grupos funcionales, como el isotiocianato, permite su uso como marcador ya que puede unirse a otras moléculas. Los derivados indolio de estos colorantes muestran una buena estabilidad fotoquímica, la cual puede incluso mejorarse incluyendo una estructura anular a la cadena de polimetina [81].

Dos fluoróforos cianina ampliamente utilizados con fines analíticos son Cy5 y verde de indocianina (ICG), denominado también IR125 (Figura 3). Se han descrito numerosas aplicaciones analíticas para Cy5, principalmente en CE [82] y sensores [83]. El ICG es un fluoróforo cargado negativamente, soluble en agua, que se utilizó inicialmente para técnicas de diagnóstico médico ya que no es tóxico para el organismo humano [84]. Aunque el ICG por sí solo presenta una baja intensidad de fluorescencia en disolución acuosa, ésta aumenta después de su unión a algunos compuestos, tales como proteínas [85].

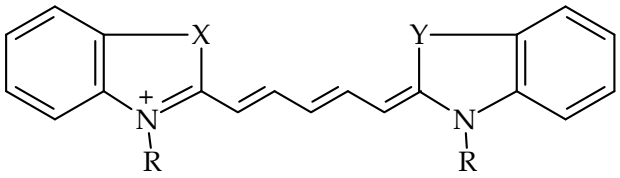

X,Y = O,S, -$C(CH_3)_2$ o -C_2H_2-; n=4, R: (CH_2)-SO_3^-

a)

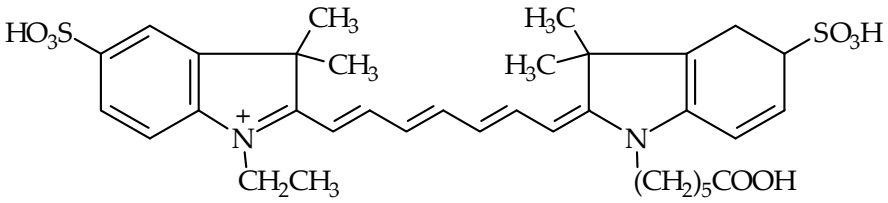

b)

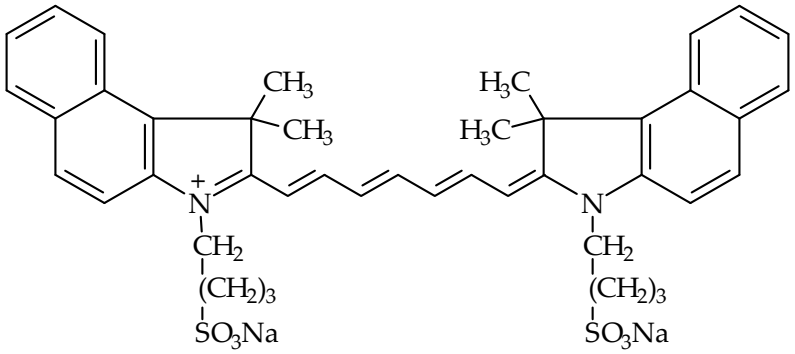

c)

Figura 3. Estructura de los fluoróforos cianina: a) Estructura básica, b) Cy5, c) verde de indocianina.

Los fluoróforos oxacina constituyen otro grupo de LWFs que presentan mejor estabilidad fotoquímica que los fluoróforos anteriores. Las estructuras de estos compuestos se muestran en la Figura 4, donde puede observarse que son más compactos que los colorantes cianina. Se han descrito algunas aplicaciones analíticas con violeta de cresilo [86, 87], azul nilo [88 - 91] y Oxacina 750 [92].

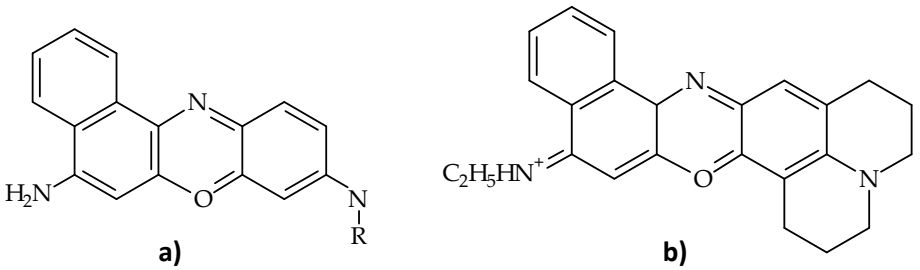

Figura 4. Estructura de los colorantes oxacina: a) violeta de cresilo (R: -H_2) y azul nilo (R: -C_2H_5), b) Oxacina 750.

El tercer grupo de LWF de tipo orgánico son los derivados de la rodamina. Existen algunos ejemplos de la utilidad analítica de dos de sus derivados, Rodamina 800 [93 - 97] y Rojo Texas [98 - 100] (Figura 5). El primero de ellos se ha utilizado recientemente para la determinación de metales pesados en muestras acuosas y como sensor de pH intracelular [95]. El Rojo Texas también se ha utilizado en diversas metodologías analíticas. Por ejemplo, este fluoróforo se ha encapsulado junto con una enzima (peroxidasa de rábano) en el interior de NPs para el diseño de un sensor para la determinación de peróxido de hidrógeno [98].

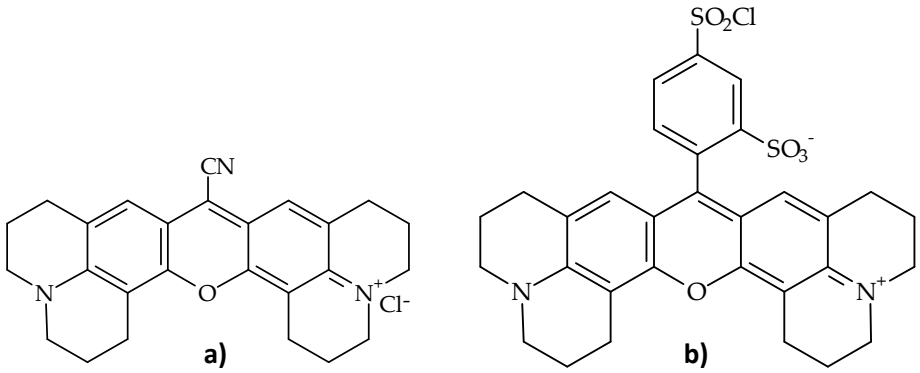

Figura 5. Estructura de: a) Rodamina 800, b) Rojo Texas.

Los colorantes BODIPY son una familia de compuestos que responden a la fórmula general 4,4-difluoro-4-bora-3a,4a-diaza-s-indaceno (Figura 6). La sustitución en distintas posiciones del sistema de anillos heterocíclicos origina diferencias en el comportamiento luminiscente de estos compuestos. Los primeros colorantes sintetizados, que incluían fundamentalmente sustituyentes alquílicos en su estructura, presentaban algunos inconvenientes, como la emisión en la zona verde del espectro electromagnético (entre 400-600 cm^{-1}) y cortos desplazamientos Stokes. No obstante, se han sintetizado recientemente algunos derivados que emiten a longitudes de onda más largas [101 - 103]. Estos colorantes incluyen grupos fenólicos o naftólicos en la posición 8 de su estructura y otros sustituyentes en las posiciones 3 y 5, que contribuyen a aumentar la conjugación con respecto a la de la estructura básica. La fluorescencia de algunos de estos colorantes aumenta en medio ácido, por lo que se ha propuesto su uso como sensores de pH [101].

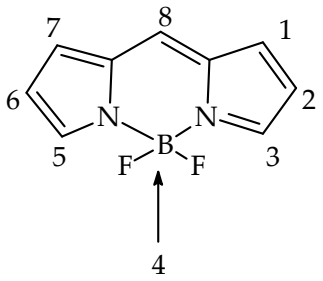

Figura 6. Estructura básica y numeración de las posiciones de los anillos heterocíclicos en los colorantes BODIPY.

Los fluoróforos Alexa Fluor son otro tipo de moléculas orgánicas que han sido utilizados como marcadores de biomoléculas en diferentes ensayos analíticos. La fotoestabilidad es una de las principales características de este tipo de colorantes, por lo que se han utilizado para mejorar las técnicas de captura de imagen celular y en ensayos analíticos con detectores fluorescentes [104, 105].

Los fluoróforos ATTO son otra familia de compuestos que presentan fluorescencia en una amplia región del espectro, en la que algunos compuestos como el ATTO 647 presentan fluorescencia a larga longitud de onda. Algunas de sus características son su elevada capacidad de absorción, alto rendimiento cuántico, una buena solubilidad en agua y un comportamiento fluorescente independiente del pH en un amplio intervalo, en algunos casos, de 2 a 11. Una limitación de estos colorantes es su estrecho desplazamiento Stokes, lo que podría originar fenómenos de dispersión de la radiación. La principal utilidad de estos fluoróforos está orientada al desarrollo de métodos basados en FRET [106].

Por último, cabe destacar otro grupo de LWFs muy utilizados en Química Analítica, como son los complejos de rutenio, los cuales muestran una luminiscencia con un tiempo de vida similar a los fluoróforos orgánicos. La principal ventaja que presentan es la posibilidad de usar diferentes ligandos que permiten modificar las propiedades químicas y espectroscópicas de estos complejos, mostrando máximos de emisión entre 610 y 650 nm. El uso analítico de estos compuestos se ha orientado principalmente para el desarrollo de nuevos sensores [107 - 109].

En los últimos años, los LWFs han sido bastante utilizados en análisis de alimentos con matrices complejas debido, principalmente, a la selectividad espectral que presentan. Por ejemplo, se han empleado como reactivos derivatizantes para la determinación de moléculas endógenas de los alimentos, como son los flavonoides, mediante cromatografía [110], o bien para la determinación de proteínas de soja en bebidas mediante inmunoextracción [111]. También se ha descrito el uso combinado de AuNPs, la enzima laccasa y verde de indocianina para la determinación de compuestos polifenólicos en muestras de zumo y té mediante la técnica de mezcla de flujo detenido [112].

Además de los fluoróforos de larga longitud de onda indicados, se han descrito nuevos polímeros capaces de emitir en la zona del infrarrojo cercano, característica que ha sido fundamental para el desarrollo de nuevos sensores, como es el caso de un sensor para la determinación de Cu(II) y cuya aplicabilidad se ha demostrado mediante el análisis de té [113]. También se han propuesto nanomateriales que emiten a longitudes de onda relativamente largas para utilizarlos en análisis de alimentos. Por

ejemplo, los QDs descritos anteriormente se han utilizado para la determinación de vitamina B1 en suplementos alimenticios [114].

4. Técnicas de inmunoensayo y su uso en análisis de alimentos

Los inmunoensayos son técnicas analíticas basadas en la elevada selectividad que presentan las reacciones antígeno-anticuerpo, siendo ampliamente utilizados en análisis clínico, ambiental y agroalimentario. Desde un punto de vista general, los inmunoensayos pueden dividirse en dos grandes grupos, directos e indirectos o con reactivos marcados.

Los inmunoensayos directos se basan en la medida de una propiedad físico-química del medio que se modifica al reaccionar el analito con el inmunoreactivo. Dentro de los inmunoensayos directos, los más utilizados han sido la inmunoturbidimetría y la inmunonefelometría [115, 116], basadas en la medida de la dispersión de la radiación al formarse el inmunocomplejo. Estas técnicas se utilizan para la determinación de macromoléculas, principalmente proteínas. Su principal limitación es la posible señal de fondo debida a la capacidad dispersante de componentes de la muestra, como pueden ser lipoproteínas y agregados de proteínas, dando lugar a límites de detección relativamente altos.

Los inmunoensayos indirectos ofrecen mayor versatilidad que los anteriores y se basan en el uso de un reactivo adicional, denominado marcador o trazador. Este reactivo es un antígeno o un anticuerpo, según el tipo de inmunoensayo, unido a una sustancia, denominada "label" (L) en la terminología inglesa, que presenta una propiedad como radioactividad,

fluorescencia o actividad enzimática, entre otras, cuya medida se relaciona con la concentración del analito. Estos inmunoensayos se clasifican en dos grandes grupos en función del formato que utilicen, homogéneos y heterogéneos [117].

En el inmunoensayo homogéneo, la unión del antígeno y el anticuerpo da lugar a un cambio en la propiedad del marcador que se relaciona con la concentración de analito. En este caso no es necesario eliminar la matriz de la muestra para realizar la medida, por lo que el ensayo es muy rápido, pero la presencia de la señal de la matriz de la muestra da lugar a límites de detección mayores que el inmunoensayo heterogéneo.

En el inmunoensayo heterogéneo el marcador no modifica su propiedad al intervenir en la inmunoreacción, por lo que es necesario inmovilizar algún reactante en un soporte sólido para conseguir la separación de las fracciones enlazada y libre del marcador. Este inmunoensayo es más versátil que el homogéneo, obteniéndose además, como se ha indicado, mejores límites de detección. Sin embargo, se requiere un mayor número de etapas por lo que los ensayos son más lentos. A continuación se describen sucintamente algunos de los distintos tipos incluidos en cada formato.

4.1 Inmunoensayo homogéneo

Normalmente es competitivo, es decir, se considera que el anticuerpo no distingue entre el analito y el marcador y ambos compiten

por enlazarse al anticuerpo, el cual se encuentra en defecto. Existen dos posibilidades:

1) La propiedad que presenta el marcador se anula al enlazarse al anticuerpo, por lo que la señal medida sólo corresponde al marcador que queda libre, siendo directamente proporcional a la concentración de analito.
2) El marcador sólo presenta la propiedad medida cuando se enlaza al anticuerpo, de forma que la señal disminuye al aumentar la concentración de analito.

Estos ensayos se aplican básicamente a la determinación de moléculas pequeñas tales como fármacos, drogas y plaguicidas. Como ejemplos de estos ensayos se describen a continuación los más representativos:

- EMIT (Enzyme multiplied immunoassay technique): Fue el primer enzimoinmunoensayo que se describió mediante el uso de una enzima unida al hapteno como marcador. Este marcador presenta actividad enzimática y la pierde al enlazarse al anticuerpo, por lo que se mide la actividad del marcador libre mediante la adición del sustrato adecuado [118].
- CEDIA (Cloned enzyme donor immunoassay): Es un tipo especial de ensayo homogéneo, patentado por Microgenics. Como se muestra en el Figura 7, utiliza dos fragmentos inactivos de la enzima β-galactosidasa, a los que se les denomina dador (ED) y aceptor (EA) enzimáticos, y que al unirse forman la enzima activa. El ensayo se realiza en una etapa

mezclando la muestra que contiene el analito con dos reactivos: 1) Reactivo 1, formado por el anticuerpo y el fragmento EA de la enzima, y 2) Reactivo 2, que contiene al marcador formado por el fragmento ED unido al hapteno y el sustrato de la enzima. Después de incubar, sólo el fragmento ED del marcador libre puede unirse al fragmento EA formando la enzima, mientras que ésta no se forma con el fragmento ED del marcador unido al anticuerpo. Por tanto, la señal originada por el producto de la reacción enzimática será debida al marcador libre y directamente proporcional a la concentración de analito [119].

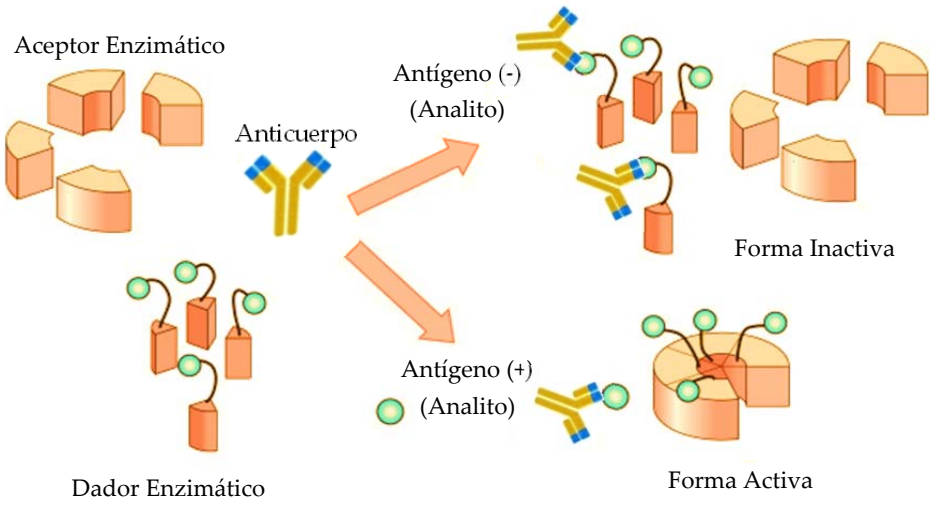

Figura 7. Esquema del formato CEDIA.

- FETI (Fluorescence resonance energy transfer immunoassay): Se diseñó como una alternativa a los inmunoensayos homogéneos tradicionales y se basa en el proceso de transferencia de energía que tiene

lugar al unirse el antígeno y el anticuerpo, ambos marcados con las moléculas implicadas en este proceso. Puede dar lugar a una emisión por parte del inmunocomplejo a una longitud de onda diferente a la de excitación, o bien, a una inhibición de fluorescencia al producirse la reacción inmunoquímica. Aunque este tipo de inmunoensayo homogéneo aún se utiliza, la tendencia actual es el uso de nanomateriales mediante los formatos homogéneo o heterogéneo [120].

- FPIA (Fluorescence polarization immunoassay): En este sistema se utiliza un hapteno unido a un fluoróforo como marcador y radiación polarizada para la excitación [121, 122]. Esta radiación excita a las moléculas cuyos dipolos de absorción vibran en la misma dirección que el vector eléctrico de dicha radiación. Es decir, si la radiación excitante está polarizada verticalmente, se excitarán las moléculas de marcador que vibran paralelamente a esa dirección. La emisión de radiación polarizada va a depender de la velocidad de rotación de las moléculas y del intervalo de tiempo que transcurre entre la excitación y la emisión. Como muestra la Figura 8, existen dos situaciones:

1) El pequeño tamaño del marcador libre permite que su movimiento rotacional sea más rápido que la duración del estado excitado, de forma que cuando se produce la emisión de fluorescencia ha cambiado su posición por lo que ésta se produce en todas las direcciones.
2) El marcador unido al anticuerpo tiene un movimiento rotacional más lento, debido al elevado tamaño de éste, por lo que la emisión de fluorescencia se produce cuando su posición prácticamente no

ha cambiado. Por tanto, si se ha excitado con radiación polarizada verticalmente, emitirá radiación polarizada en la misma dirección.

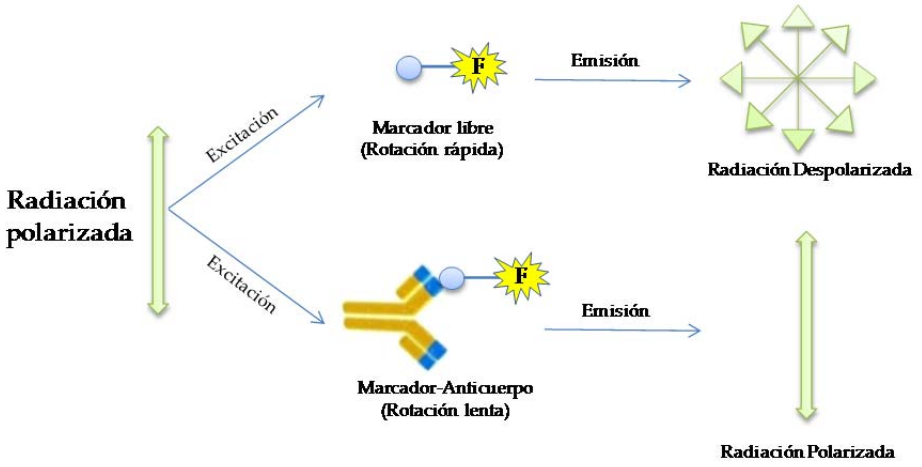

Figura 8. Esquema del formato FPIA.

4.2 Inmunoensayo heterogéneo

Estos inmunoensayos tienen mayor versatilidad ya que mediante formatos competitivos y no competitivos o sándwich pueden determinarse haptenos, antígenos macromoleculares y anticuerpos.

Puesto que, como se ha indicado anteriormente, la propiedad del marcador no se modifica al producirse la reacción inmunoquímica, en cualquier inmunoensayo heterogéneo es imprescindible la inmovilización de algún reactante en un soporte sólido para conseguir la separación de las fracciones enlazada y libre del marcador. Este tipo de inmunoensayo ha sufrido una continua evolución a lo largo del tiempo. La tendencia actual

se centra en el uso de nanomateriales, ya que ofrecen una gran superficie útil para la inmovilización, aumentando la eficacia de las interacciones entre analitos y reactivos, y, con ello, la sensibilidad de los diferentes métodos. Además, la utilización de nanopartículas magnéticas facilita su separación mediante un imán.

Los diferentes inmunoensayos heterogéneos pueden clasificarse a su vez en dos formatos básicos en función del diseño del ensayo, competitivo y no competitivo o sándwich:

- Inmunoensayo heterogéneo competitivo (Figura 9): Este formato puede ser directo con captura de antígeno o indirecto con captura de anticuerpo. En el primer caso, el formato es similar al del ensayo homogéneo, pero el anticuerpo es inmovilizado en un soporte sólido. El analito y el marcador compiten por enlazarse al anticuerpo y, después de incubar y lavar, se mide la señal del marcador enlazado, la cual será inversamente proporcional a la concentración de analito. Normalmente, se utiliza para determinar haptenos ya que sólo se necesita un determinante antigénico.

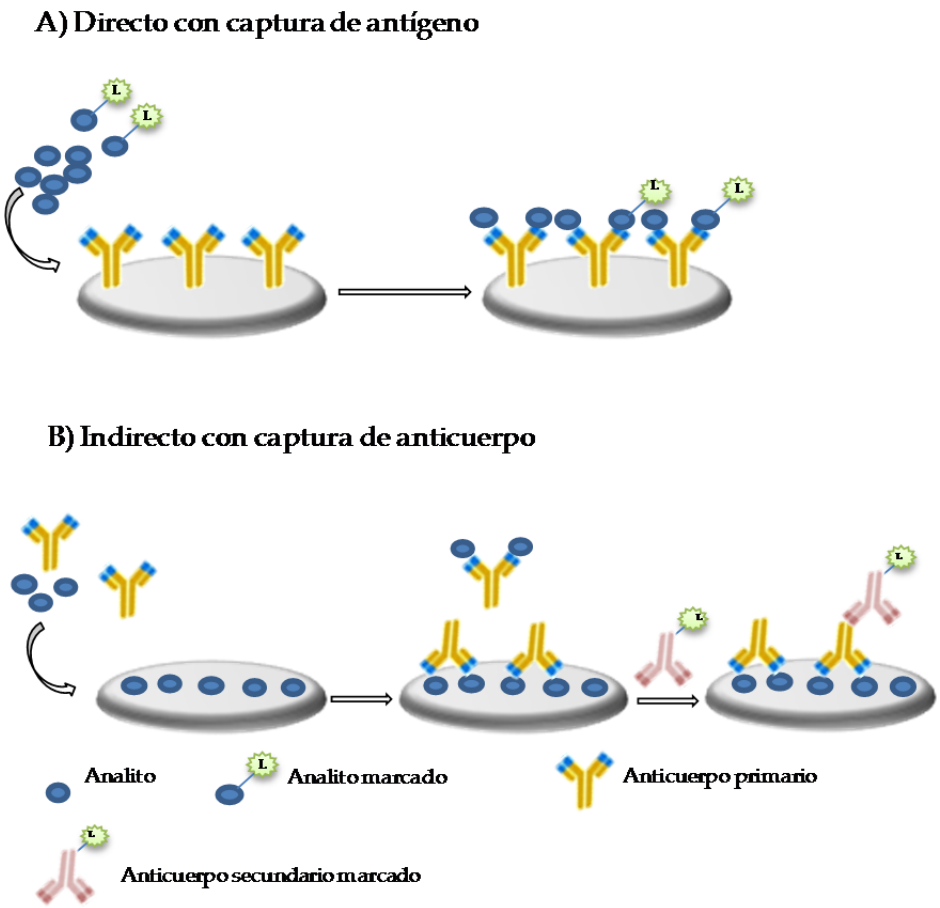

Figura 9. Formatos competitivos: A) con captura de antígeno y B) con captura de anticuerpo.

En el ensayo indirecto con captura de anticuerpo se inmoviliza el antígeno y se adiciona el analito y el anticuerpo. Se incuba, se lava y se adiciona el marcador formado por un anticuerpo inespecífico frente al anticuerpo primario (anticuerpo secundario). Es decir, si el anticuerpo primario se ha obtenido de un individuo de una especie animal dada, por ejemplo un ratón, el anticuerpo secundario se ha obtenido inmunizando un

individuo de otra especie animal, por ejemplo una oveja, con suero de ratón. Este marcador puede utilizarse como reactivo general para determinar distintos analitos siempre que los correspondientes anticuerpos primarios procedan de la misma especie animal. Como alternativa a este marcador, podría usarse directamente el anticuerpo del analito marcado, reduciendo así el número de etapas del ensayo, pero se necesitaría un marcador distinto para cada determinación, aumentado su coste. Este formato se aplica preferentemente a analitos macromoleculares, ya que deben disponer de grupos adecuados para enlazarse al soporte y al anticuerpo.

- Inmunoensayo heterogéneo no competitivo: Estos ensayos, denominados también sándwich, son más adecuados para determinar especies macromoleculares, ya sean antígenos o anticuerpos. La determinación de antígenos, esquematizada en la Figura 10, implica la inmovilización del anticuerpo, denominado primario, el cual se encuentra en cantidad suficiente para que reaccione todo el analito. Después de incubar y lavar, existen dos posibilidades según se utilice el formato directo o el indirecto. En el primer caso, se adiciona el marcador formado por un anticuerpo, denominado secundario, frente al analito. En el formato indirecto, se adiciona el anticuerpo secundario y el marcador formado por un anticuerpo inespecífico frente a este anticuerpo secundario, al igual que se ha descrito anteriormente.

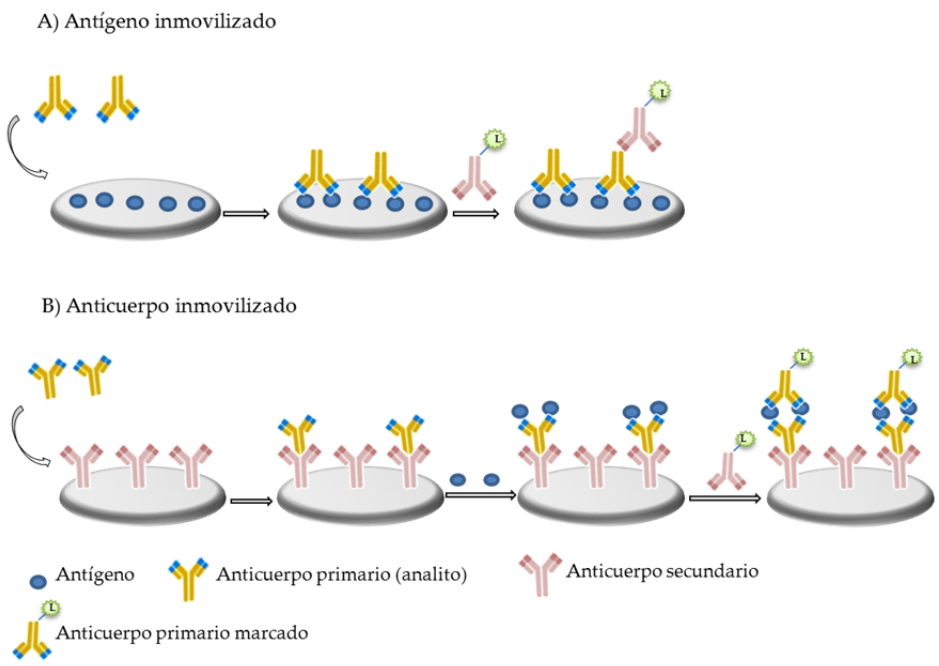

Figura 10. Formatos no competitivos, A) directo y B) indirecto, con captura de antígeno.

El formato sándwich implica que el analito debe tener, al menos, dos determinantes antigénicos para que se enlacen a los correspondientes anticuerpos. Teniendo en cuenta que los anticuerpos son macromoléculas, es preferible que el analito también sea macromolecular, de forma que no exista impedimento estérico y puedan enlazarse adecuadamente los dos anticuerpos. Este formato, utilizado normalmente para determinar proteínas antigénicas, ofrece mayor selectividad que el formato competitivo, ya que se usan dos anticuerpos frente al analito.

El ensayo sándwich también se utiliza para determinar anticuerpos frente a un antígeno y, al igual que en el caso anterior, la determinación puede realizarse de dos formas. Como muestra la Figura 11, se puede

llevar a cabo inmovilizando el antígeno o un anticuerpo inespecífico frente al anticuerpo a determinar. En el primer caso, si la muestra contiene el anticuerpo que se va a determinar, éste quedará retenido en la superficie sólida. Después de lavar, se adiciona el marcador formado por otro anticuerpo. En el segundo caso, se inmoviliza un anticuerpo secundario en la superficie sólida y se adiciona la muestra. Tras incubar y lavar, se adiciona el antígeno específico frente al anticuerpo a determinar y, finalmente, se añade el marcador, formado por un anticuerpo específico frente al antígeno.

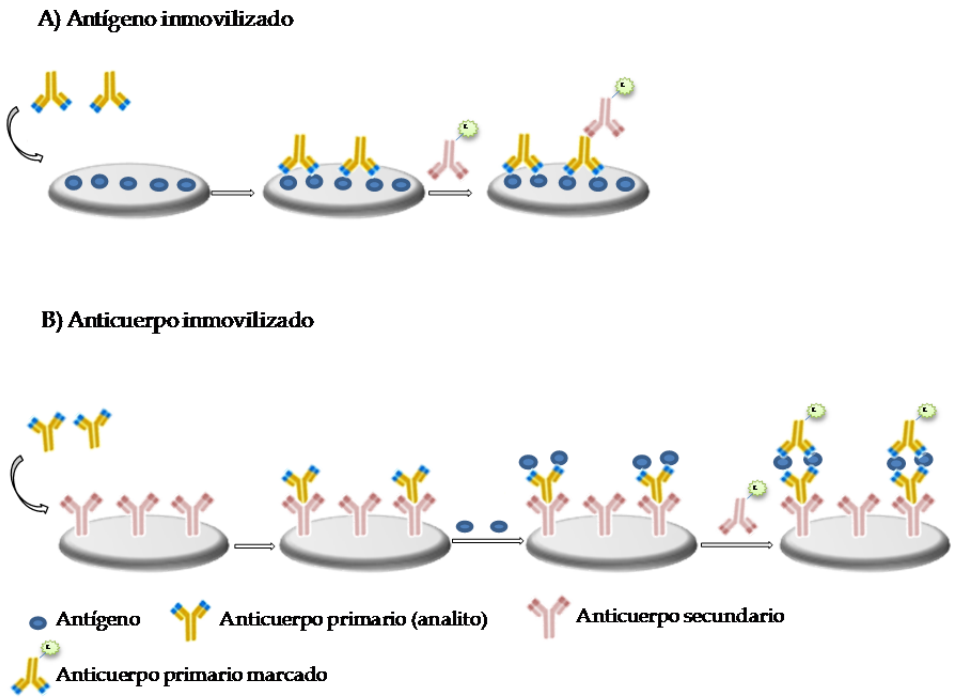

Figura 11. Formatos no competitivos para la determinación de anticuerpos: A) con antígeno inmovilizado y B) con anticuerpo inmovilizado.

Los diferentes inmunoensayos heterogéneos también pueden ser clasificados en función de la propiedad que se mide del marcador. Entre ellos, cabe citar:

- RIA (Radioimmunoassay): Fue el primero en desarrollarse mediante el uso de isótopos radiactivos unidos a biomoléculas para formar el marcador. Este ensayo presenta gran versatilidad, bajos límites de detección, elevada precisión y ausencia de interferencias bien ambientales, tales como las debidas al pH, temperatura o fuerza iónica, o bien debidas a la matriz de la muestra. Sin embargo, también presenta limitaciones, siendo el principal inconveniente el uso de materiales radioactivos con sus posibles riesgos para la salud, necesidad de permisos y recintos exclusivamente preparados para ello, así como la gestión especial de los residuos, lo que encarece el ensayo y limita su uso a laboratorios de referencia [123 - 125].

- FIA (Fluoroimmunoassay): Es una alternativa al uso de material radiactivo en los inmunoensayos heterogéneos. El procedimiento es muy similar al utilizado en RIA pero se utilizan moléculas fluorescentes para formar el marcador. Dentro de estos fluoroinmunoensayos (FIA) cabe citar el sistema DELFIA (Dissociation-Enhanced Lanthanide Fluorescent Immunoassay) [126, 127]. Se trata de un tipo particular de FIA de tiempo resuelto, que utiliza quelatos de europio, samario o terbio y se basa en el principio de intensificación disociativa de la fluorescencia (Figura 12). Uno de los aspectos clave de este ensayo es el uso de una disolución ácida compuesta por una β-diketona (por ejemplo, 2-naftoiltrifluoroacetona, NTA), óxido de tri-n-octilfosfina (TOPO) y Tritón X-100. El agente

quelatante (NTA) forma un complejo muy fluorescente con el ion lantánido, el TOPO elimina las moléculas de agua de la esfera de coordinación mientras que el Tritón X-100 crea un medio micelar que protege al complejo. Este tipo de ensayos presentan límites de detección similares al RIA sin el inconveniente del uso de material radiactivo.

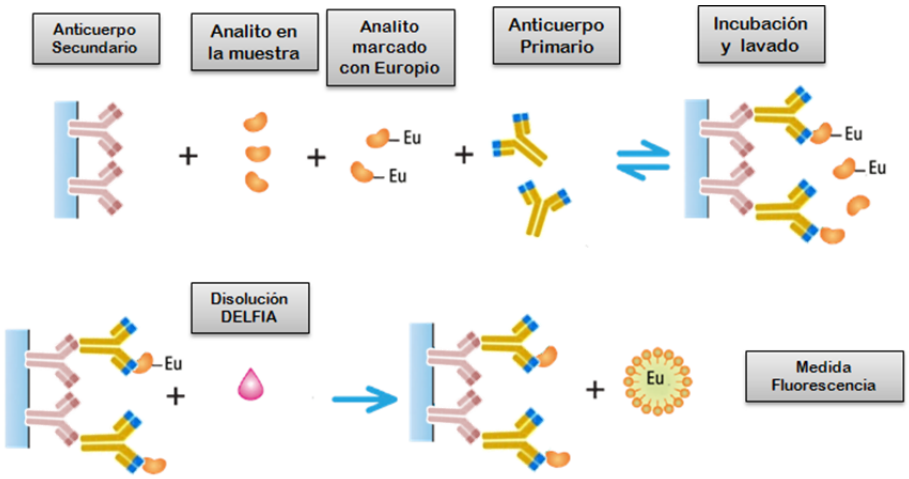

Figura 12. Esquema del sistema DELFIA.

- ELISA (Enzyme linked immunosorbent assay): Puede considerarse el inmunoensayo heterogéneo más utilizado en análisis clínico, ambiental y agroalimentario. En este caso, el marcador es sintetizado a partir de una enzima que, en presencia del sustrato correspondiente, cataliza una reacción, dando lugar a cambios medibles normalmente mediante fotometría o fluorimetría. Las enzimas más utilizadas para formar el marcador son β-galactosidasa, fosfatasa alcalina y peroxidasa de rábano, las cuales necesitan su correspondiente sustrato para llevar a cabo la detección [128 - 131].

- Inmunosensores: Constituyen un tipo de sensores muy selectivos basados en la inmovilización de un antígeno o un anticuerpo en la zona de reconomiento del sensor. Hasta hace unos años, estos inmunosensores presentaban problemas de sensibilidad, ya que los cambios de señal apenas podían ser recogidos por el transductor. En cambio, la utilización de los nanomateriales ha provocado una revolución en estos dispositivos. La inmovilización de NPs sobre la superficie del sensor proporciona un aumento de la superficie específica del mismo y, en consecuencia, de la cantidad de reactivo inmovilizado, consiguiendo mayores cambios de señal y una mejora de la sensibilidad del método.

Los inmunosensores pueden ser clasificados en diferentes grupos en función de la señal originada al unirse el analito a la superficie del sensor (Figura 13).

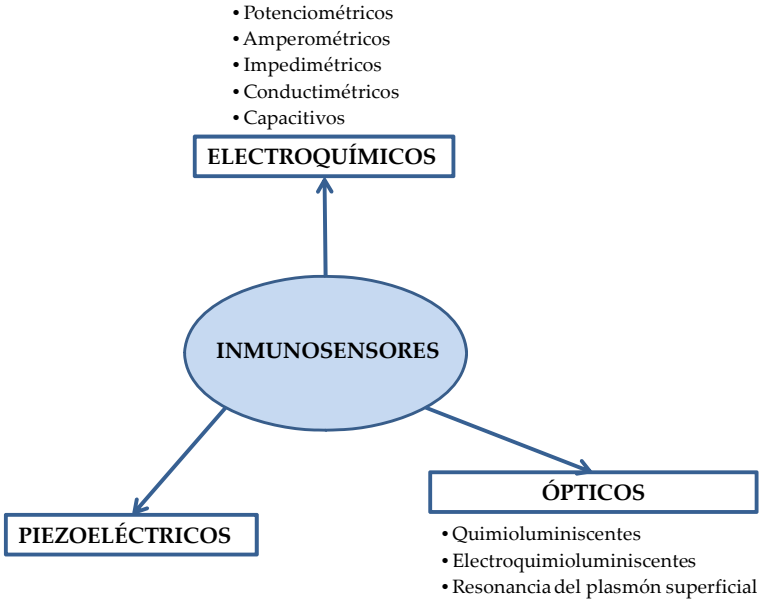

Figura 13. Clasificación de los inmunosensores.

A continuación, se describen sucintamente los distintos tipos:

Los inmunosensores electroquímicos se caracterizan por presentar buena sensibilidad (desde la inclusión de los nanomateriales), bajo coste y fácil automatización. Como se muestra en la clasificación, los inmunosensores electroquímicos están divididos en varios subgrupos, en función del tipo de señal que se origina. Así, los potenciométricos registran el cambio de potencial en la superficie del sensor, los amperométricos recogen la corriente eléctrica generada, los conductimétricos miden los cambios en la conductividad, los sensores de impedancia miden la resistencia al paso de corriente eléctrica y los sensores de capacitancia se basan en los cambios de la constante dieléctrica del sensor al unirse el analito a su superficie [132 - 146].

Los inmunosensores ópticos se basan en la medida de la absorción o emisión producida tras llevarse a cabo la inmunoreacción en la superficie del sensor. Estos inmunosensores son muy utilizados en bioanálisis gracias a las ventajas que presentan: modo de trabajo no destructivo y rápida generación de la señal. Al igual que ocurre con los inmunosensores electroquímicos, los inmunosensores ópticos han experimentado una revolución gracias al uso de nanopartículas. Los nanomateriales utilizados van desde SiO_2NPs dopadas con fluoróforos, AuNPs, QDs, CNTs, hasta los recientemente utilizados UCPs. Estos inmunosensores ópticos, como muestra el esquema anterior, se pueden dividir en sensores quimioluminiscentes (se recoge la intensidad luminiscente generada por una reacción química), electroquimioluminiscentes (implican la formación de especies que, tras una transferencia electrónica, emiten radiación

luminiscente) e inmunosensores de resonancia de plasmón superficial (fenómeno producido al interaccionar la radiación con los electrones superficiales de finas películas metálicas) [147 – 153].

Otro tipo de inmunosensores son los inmunosensores piezoeléctricos, basados en el uso de la microbalanza de cristal de cuarzo (QCM) que registra cambios en la frecuencia de resonancia de un osciloscopio acoplado al sistema, la cual es directamente proporcional a la masa que se une a la superficie. Aunque esta técnica presenta una buena sensibilidad, su utilización es más restringida debido a problemas de selectividad, ya que cualquier molécula que se una a la superficie de forma no específica, originará una respuesta en el detector [154, 155].

Un tipo especial de inmunosensores lo constituyen los basados en ensayos de flujo lateral o inmunocromatografía. Esta técnica utiliza un dispositivo muy simple, portátil y no requiere un sistema de detección costoso ya que en ciertos casos, es visual (cualitativo) y, en otros, solo se necesita un refractómetro o un fluorímetro (cuantitativo). El ejemplo típico de este sistema es el test de embarazo comercialmente asequible. Este dispositivo está fabricado con un material poroso capaz de transportar la muestra líquida por capilaridad a lo largo de las diferentes secciones que lo componen. Como puede observarse en la Figura 14, sobre algunas de estas secciones se inmovilizan antígenos o anticuerpos marcados para que sean arrastrados por la muestra líquida y proporcionen dos señales visibles, una línea de control y otra de ensayo. La línea de control se forma por captura del marcador libre, comprobando así que el ensayo se ha realizado correctamente. En cambio, la línea de ensayo se forma por el enlace del

marcador unido al analito, indicando la presencia del analito en la muestra [156 - 160].

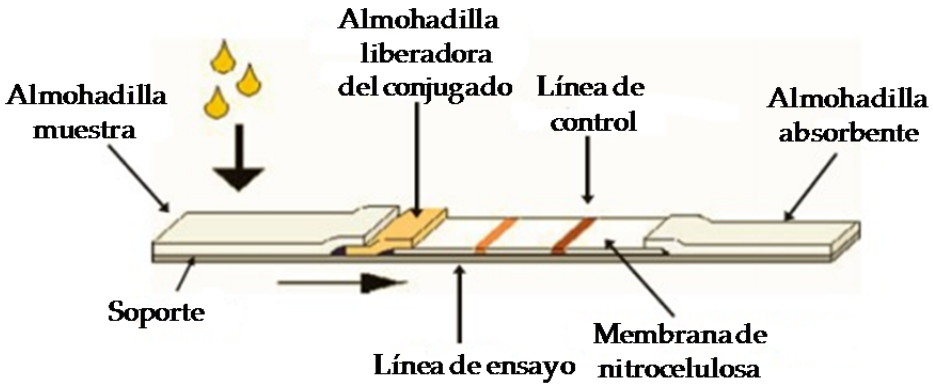

Figura 14. Esquema de ensayo de flujo lateral.

4.3. Uso del inmunoensayo en análisis de alimentos

Aunque las técnicas de inmunoensayo tienen su principal campo de aplicación en análisis clínico, su uso se ha ido consolidando también en análisis de alimentos, como lo demuestra el número relativamente elevado de kits de ensayos comerciales actualmente disponibles. La Figura 15 muestra la distribución de los artículos publicados en los últimos años sobre esta área. Puede observarse que, aunque la mayoría de las técnicas anteriormente descritas se han aplicado al análisis de alimentos, ELISA ha sido y actualmente sigue siendo la más utilizada. Algunas de las razones que justifican su elección inciden en los bajos límites de detección, fácil uso y coste relativamente bajo que presentan los métodos basados en esta técnica.

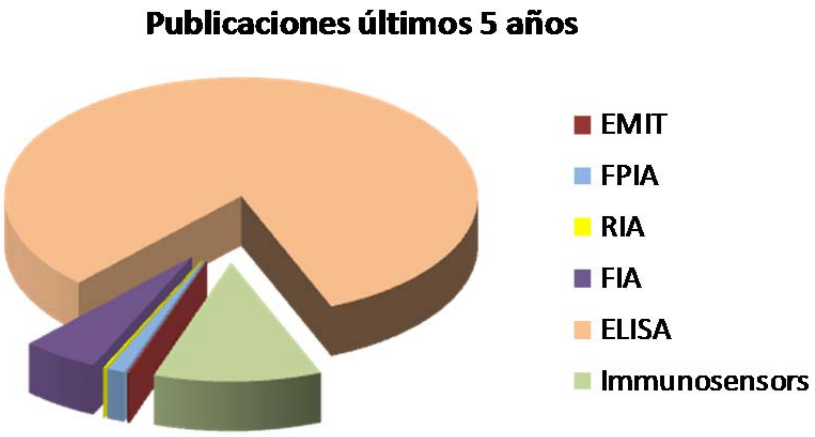

Figura 15. Distribución del número de artículos dedicados al inmunoensayo en análisis de alimentos según la técnica utilizada (base de datos: Scopus).

En la Tabla 1 se recogen algunos ejemplos de los métodos descritos utilizando distintos inmunoensayos [161 – 171]. Como puede observarse, se han desarrollado determinaciones para diversos analitos tales como micotoxinas, plaguicidas, residuos de antibióticos y hormonas aplicables al análisis de alimentos destinados al consumo humano y de alimentos para animales. Cabe destacar que, aunque ELISA sigue siendo la técnica más extendida en esta área, existe una clara tendencia al desarrollo de inmunosensores, principalmente electroquímicos y ópticos [172], aunque su comercialización hasta la fecha ha sido prácticamente nula.

Tabla 1. Ejemplos representativos de inmunoensayos aplicados al análisis de alimentos

Tipo de Inmunoensayo	Fundamento	Analito	Muestra	Ref.
Homogéneo	FRET homogéneo por fluorescencia intrínseca de los anticuerpos	Micotoxinas	Cebada	[161]
Homogéneo	Dispersión de la radiación con AuNPs	Proteínas de soja	Zumo de frutas y yogur con soja	[162]
Homogéneo	FPIA	Micotoxinas	Grano	[163]
Homogéneo	FPIA	Plaguicidas órgano-fosforados	Vegetables y agua ambiental	[164]
Heterogéneo	ELISA	Fluoro-quinolonas	Pescados y mariscos	[165]
Heterogéneo	ELISA	Dodecilciclo-butanona	Ternera	[166]
Heterogéneo	ELISA	Fenil-etanolamina A	Piensos y carne	[167]
Heterogéneo	DELFIA	β-Estradiol	Suero bovino	[168]
Heterogéneo	Ensayo flujo lateral	Residuos de clembuterol y raptomina	Orina de cerdo	[169]
Inmunosensor	Sensor amperométrico	Residuos de sulfonamida y tetraciclina	Leche	[170]
Inmunosensor	Sensor electroquimio-luminiscente	Clembuterol	Carne de cerdo	[171]

Bibliografía

(1) D. Knopp, D. Tang, R. Niessner. Review: Bioanalytical applications of biomolecule-functionalized nanometer-sized doped silica particles. *Anal. Chim. Acta* **(2009)** *647,* 14 – 30.

(2) W. Wei, M.Wei, S. Liu. Silica nanoparticles as a carrier for signal amplification. *Reviews Anal. Chem.* **(2012)** *31*, 163 – 176.

(3) S. W. Bae, W. Tan, J. I. Hong. Fluorescent dye-doped silica nanoparticles: new tolos for bioapplications. *Chem. Commun.* **(2012)** *48*, 2270 – 2282.

(4) W. Stöber, A. Fink. Controlled growth of monodisperse silica spheres in the micron size range. *J. Colloid Interf. Sci.* **(1968)** *26*, 62 – 69.

(5) H. Yamauchi, T. Ishikawa, S. Kondo. Surface characterization of ultramicro spherical particles of silica prepared by W/O microemulsion method. *Colloid Surface.* **(1989)** *37*, 71 – 80.

(6) N. Gan, J. Hou, F. Hu, Y. Cao, T. Li, Z. Guo, J. Wang. A renewable and ultrasensitive electrochemiluminescence immunosensor based on magnetic RuL @ SiO_2-Au~RuL-Ab2 sandwich-type nano-immunocomplexes. *Sensors* **(2011)** *11*, 7749 – 7762.

(7) M. Zhang, S. Ge, W. Li, M. Yan, X. Song, J. Yu, W. Xu, J. Huang. Ultrasensitive electrochemiluminescence immunoassay for tumor marker detection using functionalized Ru-Silica@nanoporous gold composite as labels. *Analyst* **(2012)** *137*, 680 – 685.

(8) N. P. Sardesai, K. Kadimisetty, R. Faria, J. F. Rusling. A microfluidic electrochemiluminescent device for detecting cancer biomarker proteins. *Anal. Bioanal. Chem.* **(2013)** *405*, 3831 – 3838.

(9) N. P. Sardesai, J. C. Barron, J. F. Rusling. Carbon nanotube microwell array for sensitive electrochemiluminescent detection of cancer biomarker proteins. *Anal. Chem.* **(2011)** *83*, 6698 – 6703.

(10) Q. Sun, X. Zhang. Electrochemiluminescence DNA sensor based on $Ru(bpy)_3^{2+}$ -doped silica nanoparticles labeling and proximity-dependent surface hybridization assay. *J. Solid State Electr.* **(2012)** *16*, 247 – 252.

(11) Z. Chen, X. He, Y. Wang, K. Wang, Y. Du, G. Yan. Ru (II) encapsulated phosphorylate-terminated silica nanoparticles-based electrochemiluminescent strategy for label-free assay of protein kinase activity and inhibition. *Biosens. Bioelectron.* **(2013)** *41*, 519 – 525.

(12) S. Peng, J. Li., X. Zhang. Electrogenerated chemiluminescence sensor for glutathione with $Ru(bpy)_3^{2+}$ -doped silica nanoparticles. *J. Solid State Electr.* **(2013)** *17*, 795 – 803.

(13) Y. Wang, S. R. Nugen. Development of fluorescent nanoparticle-labeled lateral flow assay for the detection of nucleic acids. *Biomed. Microdevices.* **(2013)** *15*, 751 – 758.

(14) M. Zhang, L. Ge, S. Ge, M. Yan, J. Yu, J. Huang, S. Liu. Three-dimensional paper-based electrochemiluminescence device for simultaneous detection of Pb^{2+} and Hg^{2+} based on potential-control technique. *Biosens. Bioelectron.* **(2013)** *41*, 544 – 550.

(15) W. Qi, D. Wu, J. Zhao, Z. Liu, W. Zhang, L. Zhang, G. Xu. Electrochemiluminescence resonance energy transfer based on $Ru(phen)_3^{2+}$-doped silica nanoparticles and its application in "Turn-on" detection of ozone. *Anal. Chem.* **(2013)** *85*, 3207 – 3212.

(16) Y. Zhou, X. Xia, Y. Xu, W. Ke, W. Yang, Q. Li. Application of europium (III) chelates-bonded silica nanoparticle in time-resolved immunofluorometric detection assay for human thyroid stimulating hormone. *Anal. Chim. Acta* **(2012)** *722*, 95 – 99.

(17) L. Zhang, T. Tian, Z. Ye, B. Song, J. Yuan. Preparation of visible-light-excited europium biolabels for time-resolved luminescence cell imaging application. *Talanta* **(2013)** *108*, 143 – 149.

(18) J. Wang, H. Han, X. Jiang, L. Huang, L. Chen, N. Li. Quantum dot-based near-infrared electrochemiluminescent immunosensor with gold nanoparticle-graphene nanosheet hybrids and silica nanospheres double-assisted signal amplification. *Anal. Chem.* **(2012)** *84*, 4893 – 4899.

(19) B. Liu, F. Zeng, G. Wu, S. Wu. Nanoparticles as scaffolds for FRET-based ratiometric detection of mercury ions in water with QDs as donors. *Analyst* **(2012)** *137*, 3717 – 3724.

(20) F. Gao, Q. Ye, P. Cui, L. Zhang. Efficient fluorescence energy transfer system between CdTe-doped silica nanoparticles and gold nanoparticles for Turn-On fluorescence detection of melamine. *J. Agric. Food Chem.* **(2012)** *60*, 4550 – 4558.

(21) Y. Wu, P. Xue, Y. Kang, K. M. Hui. Highly specific and ultrasensitive graphene-enhanced electrochemical detection of low-abundance tumor cells using silica nanoparticles coated with antibody-conjugated quantum dots. *Anal. Chem.* **(2013)** *85*, 3166 – 3173.

(22) F. Liu, Y. Zhang, S. Ge, J. Lu, J. Yu, X. Song, S. Liu. Magnetic grapheme nanosheets based electrochemiluminescence immunoassay of cancer biomarker using CdTe quantum dots coated silica nanospheres as labels. *Talanta* **(2012)** *99*, 512 – 519.

(23) Y. Li, L. Deng, C. Deng, Z. Nie, M. Yang, S. Si. Simple and sensitive aptasensor based on quantum dot-coated silica nanospheres and the gold screen-printed electrode. *Talanta* **(2012)** *99*, 637 – 642.

(24) J. Qian, C. Zhang, X. Cao, S. Liu. Versatile immunosensor using a quantum dot coated silica nanosphere as a label for signal amplification. *Anal. Chem.* **(2010)** *82*, 6422 – 6429.

(25) J. Qian, H. Dai, X. Pan, S. Liu. Simultaneous detection of dual proteins using quantum dots coated silica nanoparticles as labels. *Biosens. Bioelectron.* **(2011)** *28*, 314 – 319.

(26) K. Zhang, H. Zhou, Q. Mei, S. Wang, G. Guan, R. Liu, J. Zhang, Z. Zhang. Instant visual detection of trinitrotoluene particulates on various surfaces by ratiometric fluorescence of dual-emission quantum dots hybrid. *J. Am. Chem. Soc.* **(2011)** *133*, 8424 – 8427.

(27) X. Kong, Q. Yu, X. Zhang, X. Du, H. Gong, H. Jiang. Synthesis and application of surface enhanced Raman scattering (SERS) tags of Ag@SiO_2 core/shell nanoparticles in protein detection. *J. Mater. Chem.* **(2012)** *22*, 7767 – 7774.

(28) F. Wang, R. G. Widejko, Z. Yang, K. V. T. Nguyen, H. Chen, L. P. Fernando, K. A. Christensen, J. N. Anker. Surface-enhanced raman scattering detection of pH with silica-encapsulated 4-

mercaptobenzoic acid-functionalized silver nanoparticles. *Anal. Chem.* **(2012)** *84*, 8013 – 8019.

(29) P. Devi, P. Reddy, S. Arora, S. Singh, C. Ghanshyam, M. L. Singla. Sensing behavior study of silica-coated Ag nanoparticles deposited on glassy carbon toward nitrobenzene. *J. Nanopart. Res.* **(2012)** *14*, 1172.

(30) M. Veerapandian, Y. T. Seo, H. Shin, K. Yun, M. H. Lee. Functionalized graphene oxide for clinical glucose biosensing in urine and serum samples. *Int. J. Nanomed.* **(2012)** *7*, 6123 – 6136.

(31) M. Li, J. Zhang, S. Suri, L. J. Sooter, D. Ma, N. Wu. Detection of adenosine triphosphate with an aptamer biosensor based on surface-enhanced raman scattering. *Anal. Chem.* **(2012)** *84*, 2837 – 2842.

(32) V. L. Schmit, R. Martoglio, K. T. Carron. Lab-on-bubble surface enhanced raman indirect immunoassay for Cholera. *Anal. Chem.* **(2012)** *84*, 4233 – 4236.

(33) C. Ma, G. Xie, W. Zhang, M. Liang, B. Liu, H. Xiang. Label-free sandwich type of immunosensor for hepatitis C virus core antigen based on the use of gold nanoparticles on a nanostructured metal oxide surface. *Microchim. Acta* **(2012)** *178*, 331 – 340.

(34) X. Liu, L. Xie, H. Li. Electrochemical biosensor on reduced grapheme oxide and Au nanoparticles entrapped in chitosan/silica sol-gel hybrid membranes for determination of dopamine and uric acid. *J. Electroanal. Chem.* **(2012)** *682*, 158 – 163.

(35) B. Liu, B. Zhang, Y. Cui, H. Chen, Z. Gao, D. Tang. Multifunctional gold-silica nanostructures for ultrasensitive electrochemical immunoassay of streptomycin residues. *ACS Appl. Mater. Interfaces* **(2011)** *3*, 4668 – 4676.

(36) J. Lu, S. Liu, S. Ge, M. Yan, J. Yu, X. Hu. Ultrasensitive electrochemical immunosensor based on Au nanoparticles dotted carbon nanotube-graphene composite and functionalized mesoporous materials. *Biosens. Bioelectron.* **(2012)** *33*, 29 – 35.

(37) S. Hou, Z. Ou, Q. Chen, B. Wu. Amperometric acetylcholine biosensor based on self-assembly of gold nanoparticles and

acetylcholinesterase on the sol-gel/multi-walled carbon nanotubes/choline oxidase composite-modified platinum electrode. *Biosens. Bioelectron.* **(2012)** *33*, 44 – 49.

(38) J. Lin, P. Chu, Z. Wei. A New Dual Immunoassay for tumor markers based on chemiluminescence signal amplification by magnetic mesoporous silica and enzyme modified gold nanoparticles. *Anal. Sci.* **(2012)** *28*, 21 – 25.

(39) J. Zhou, N. Gan, T. Li, H. Zhou, X. Li, Y. Cao, L. Wang, W. Sang, F. Hu. Ultratrace detection of C-reactive protein by a piezoelectric immunosensor based on Fe_3O_4@SiO_2 magnetic capture nanoprobes and HRP-antibody co-immobilized nano gold as signal tags. *Sens. Actuat. B: Chem* **(2013)** *178*, 494 – 500.

(40) A. Venkatanarayanan, K. Crowley, E. Lestini, T. E. Keyes, J. R. Rusling. High sensitivity carbon nanotube based electrochemiluminescence sensor array. *Biosens. Bioelectron.* **(2012)** *31*, 233 – 239.

(41) W. Zhao, Y. Fang, Q. Zhu, K. Wang, M. Liu, X. Huang, J. Shen. A novel glucose biosensor based on phosphonic acid-functionalized silica nanoparticles for sensitive detection of glucose in real samples. *Electrochim. Acta* **(2013)** *89*, 278 – 283.

(42) L. Chen, Z. Zhang, X. Zhang, A. Fu, P. Xue, R. Yan. A novel chemiluminescence immunoassay of staphylococcal enterotoxin B using HRP-functionalised mesoporous silica nanoparticle as label. *Food Chem.* **(2012)** *135*, 208 – 212.

(43) J. Lu, W. Wie, L. Yin, Y. Pu, S. Liu. Flow injection chemiluminescent immunoassay of microcystin-LR by using PEI-modified magnetic beads as capturer and HRP-functionalized silica nanoparticles as signal amplifier. *Analyst* **(2013)** *138*, 1483 – 1489.

(44) H. Zhou, G. Xu, A. Zhu, Z. Zhao, C. Ren, L. Nie, X. Kan. A multiporous electrochemical sensor for epinephrine recognition and detection based on molecularly imprinted polypyrrole. *RSC Advances* **(2012)** *2*, 7803 – 7808.

(45) H. Qiu, L. Fan, X. Li, L. Li, M. Sun, C. Luo. A microflow chemiluminescence sensor for indirect determination of dibutyl

phatalate by hydrolyzing based on biological recognition materials. *J. Pharm. Biomed. Anal.* **(2013)** *75*, 123 – 129.

(46) P. Zhao, J. Hao. Ter-butylhydroquinone recognition of molecular imprinting electrochemical sensor based on core-shell nanoparticles. *Food Chem.* **(2013)** *139*, 1001 – 1007.

(47) P. Bakthavathsalam, V. K. Rajendran, U. Saran, S. Chatterjee, B. M. J. Ali. Immunomagnetic nanoparticle based quantitative PCR for rapid detection of *Salmonella*. *Microchim. Acta* **(2013)** *180*, 1241 – 1248.

(48) X. Huang, Z. P. Aguilar, H. Li, W. Lai, H. Wei, H. Xu, Y. Xiong. Fluorescent $Ru(phen)_3^{2+}$-doped silica nanoparticles-based ICTS sensor for quantitative detection of enrofloxacin residues in chicken meat. *Anal. Chem.* **(2013)** *85*, 5120 – 5128.

(49) W. Xu, X. Chen, X. Huang, W. Yang, C. Liu, W. Lai, H. Xu, Y. Xiong. Ru $(phen)_3^{2+}$ doped silica nanoparticles based immunochromatographic strip for rapid quantitative detection of β-agonist residues in swine urine. *Talanta* **(2013)** *114*, 160 – 166

(50) W. Denk, J. H. Strickler, W. W. Web. Two-photon laser scanning fluorescent microscopy. *Science* **(1990)** *248*, 73 – 76.

(51) F. Wang, X. Liu. Recent advances in the chemistry of lanthanide-doped upconversion nanocrystals. *Chem. Soc. Reviews* **(2009)** *38*, 976 – 989.

(52) J. C. Bünzli, C. Piguet. Taking advance of luminescent lanthanide ions. *Chem. Soc. Reviews* **(2005)** *34*, 1048 – 1077.

(53) J. F. Suyver, D. Biner, P. Gerner, J. Grimm, S. Heer, K. Krämer, C. Reinhard, H. U. Güdel. Novel materials doped with trivalent lanthanides and transition metal ions showing near-infrared to visible photon upconversion. *Opt. Mater.* **(2005)** *27*, 1111 – 1130.

(54) J. F. Suyver, J. Grimm, M. K. van Veen, D. Biner, K. W. Krämer, H. U. Güdel. Upconversion spectroscopy and properties of $NaYF_4$ doped with Er^{3+}, Tm^{3+} and/or Yb^{3+}. *J. Luminesc.* **(2006)** *117*, 1 – 12.

(55) N. Bogdan, F. Vetrone, G. A. Ozin, J. A. Capobianco. Synthesis of ligand-free colloidally stable wáter dispersible brightly luminiscent

lanthanide-doped upconverting nanoparticles. *Nano Lett.* **(2011)** *11*, 835 – 840.

(56) L. Wang, R. Yan, Z. Huo, L. Wang, J. Zeng, J. Bao, X. Wang, Q. Peng, Y. Li. Fluorescence resonant energy transfer biosensor based on upconversion luminescent nanoparticles. *Ang. Chem. Int. Ed.* **(2005)** *44*, 6054 – 6057.

(57) T. Rantanen, H. Päkkilä, L. Jämsen, K. Kuningas, T. Ukonaho, T. Lövgren, T. Soukka. Tandem dye acceptor used to enhance upconversion fluorescence resonance energy transfer in homogeneous assays. *Anal. Chem.* **(2007)** *79*, 6312 – 6318.

(58) M. Wang, W. Hou, C.-C. Mi, W.-X. Wang, Z.-R. Xu, H. H. Teng, C.-B. Mao, S.-K. Xu. Immunoassay of goat antihuman immunoglobulin G antibody based on luminescence resonance energy transfer between $NaYF_4$:Yb, Er upconversion fluorescent nanoparticles and gold nanoparticles. *Anal. Chem.* **(2009)** *81*, 8783 – 8789.

(59) C. Liu, Z. Wang, H. Jia, Z. Li. Efficient fluorescence resonance energy transfer between upconversion nanophosphors and graphene oxide: a highly sensitive biosensing platform. *Chem. Commun.* **(2011)** *47*, 4661 – 4663.

(60) T. Ukonaho, T. Rantanen, L. Jämsen, K. Kuningas, H. Päkkilä, T. Lövgren, T. Soukka. Comparison of infrared-excited up-converting phosphors and europium nanoparticles as labels in a two-site immunoassay. *Anal. Chim. Acta* **(2007)** *596*, 106 – 115.

(61) P. L. Corstjens, S. Li, M. Zuiderwijk, K. Kardos, W. R. Abrams, R. S. Niedbala, H. J. Tanke. Infrared up-converting phosphors for bioassays. *IEE Proceedings Nanotech.* **(2005)** *152*, 64 – 72.

(62) K. Kuningas, T. Rantanen, U. Karhunen, T. Lövgren, T. Soukka. Simultaneous use of time-resolved fluorescence and anti-stokes photoluminescence in bioaffinity assay. *Anal. Chem.* **(2005)** *77*, 2826 – 2834.

(63) L. Li, L. Zhou, Y. Yu, Z. Zhu, C. Lin, C. Lu, R. Yang. Development of up-converting phosphors technology-based lateral-flow assay

for rapidly quantitative detection of hepatitis B surface antibody. *Diagn. Micr. Infec. Dis.* **(2009)** *63*, 165 – 172.

(64) Q. Qu, Z. Zhu, Y. Wang, Z. Zhong, J. Zhao, F. Qiao, X. Du, Z. Wang, R. Yang, L. Huang, Y. Yu, L. Zhou, Z. Chen. Rapid and quantitative detection of *Brucella* by up-converting phosphors technology-based lateral-flow assay. *J. Microbiol. Meth.* **(2009)** *79*, 121 – 123.

(65) C. Liu, X. Qiu, S. Ongagna, D. Chen, Z. Chen, W. R. Abrams, D. Malamud, P. L. Corstjens, H. H. Bau. A timer-actuated immunoassay cassette for detecting molecular markers in oral fluids. *Lab on a Chip* **(2009)** *9*, 768 – 776.

(66) D. Chen, M. Mauk, X. Qiu, C. Liu, J. Kim, S. Ramprasad, S. Ongagna, W. R. Abrams, D. Malamud, P. L. Corstjens, H. H. Bau. An intregrated, self-contained microfluidic cassette for isolation-amplification, and detection of nucleic acid. *Biomed. Microdevices.* **(2010)** *12*, 705 – 719.

(67) D. E. Achatz, R. J. Meier, L. H. Fischer, O. S. Wolfbeis. Luminescent sensing of oxygen using a quenchable probe and upconverting nanoparticle. *Ang. Chem. Int. Ed.* **(2011)** *50*, 260 – 263.

(68) H. S. Mader, O. S. Wolfbeis. Optical ammonia sensor based on upconverting luminescent nanoparticles. *Anal. Chem.* **(2010)** *82*, 5002 – 5004.

(69) L. Aguilar-Vázquez, M.P. Aguilar-Caballos, A. Gómez-Hens. Development of an automatic high-throughput assay for tetracycline determination by using Eu_2O_3 nanoparticles and dry-reagent technology. *Talanta.* (2014) *119*, 111 – 115.

(70) M. Seydack. Nanoparticle labels in immunosensing using optical detection methods. *Biosens. Bioelectron.* **(2005)** *20*, 29 – 43.

(71) C. Cháfer-Pericás, A. Maquieira, R. Puchades. Functionalized inorganic nanoparticles used as labels in solid-phase immunoassays. *Trends Anal. Chem*. **(2012)** *31*, 144 – 156.

(72) J. Feng, G. Shan, A. Maquieira, M.E. Koivunen, B. Guo, B.D. Hammock, I.M. Kennedy. Functionalized europium oxide

nanoparticles used as a fluorescent label in an immunoassay for atrazine. *Anal. Chem*. **(2003)** *75*, 5282-5286.

(73) M.L. Castillo-García, M.P. Aguilar-Caballos, A. Gómez-Hens. Application of Tb_4O_7 nanoparticles for lasalocid and salicylate determination in food analysis. *J. Agric. Food Chem*. **(2012)** *60*, 11741 – 11747.

(74) G. P. C. Drummen. Fluorescent probes and fluorescence (microscopy) techniques –illuminating biological and biomedical research. *Molecules* **(2012)** *17*, 14067 – 14090.

(75) A. Gómez-Hens, M. P. Aguilar-Caballos. Long-wavelength fluorophores: new trend in their analytical use. *Trends Anal. Chem.* **(2004)** *23*, 127 – 136.

(76) V. J. Pansare, S. Hejazi, W. J. Faenza, R. K. Prud´homme. Review of long-wavelength optical and NIR imaging materials: contrast agents, fluorophores, and multifunctional nano carriers. *Chem. Mat.* **(2012)** *24*, 812 – 827.

(77) M. Haase, H. Schäfer. Upconverting nanoparticles. *Ang. Chem. Int. Ed.* **(2011)** *50*, 5808 – 5829.

(78) T. B. Deligeorgiev, N. I. Gadjev, I. I. Timtcheva, V. A. Maximova, H. E. Katerinopoulos, E. Foukaraki. Synthesis of homodimeric monomethine cyanine dyes as noncovalent nucleic acid labels and their absorption and fluorescence spectral characteristics. *Dyes Pigments* **(2000)** *44*, 131 – 136.

(79) M. Koresawa, K. Kikuchi, S. Mizukami, H. Kojima, Y. Urano, T. Higuchi, T. Nagano. Development of a time-resolved fluorometric detection system using diffusion-enhanced energy transfer. *Anal. Chem.* **(2000)** *72*, 4904 – 4907.

(80) E. M. McCorquodale, C. L. Colyer. Indocyanine green as a noncovalent, pseudofluorogenic label for protein determination by capillary electrophoresis. *Electrophoresis* **(2001)** *22*, 2403 – 2408.

(81) L. Tarazi, A. George, G. Patonay, L. Strekowski. Spectral characterization of a novel near-infrared cyanine dye: a study of its complexion with metal ions. *Talanta* **(1998)** *46*, 1413 – 1424.

(82) J. M. Serrano, M. Silva. Trace analysis of aminoglycoside antibiotics in bovine milk by MEKC with LIF detection. *Electrophoresis* **(2006)** *27*, 4703 – 4710.

(83) K. E. Sapsford, C. R. Taitt, S. Fertig, M. H. Moore, M. E. Lassman, C. M. Maragos, L. C. Shriver-Lake. Indirect competitive immunoassay for detection of aflatoxin B_1 in corn and nut products using the array biosensors. *Biosens. Bioelectron.* **(2006)** *21*, 2298 – 2305.

(84) M. Tadatsu, S. Ito, N. Muguruma, Y. Kusaka, T. Bando, Y. Tadatsu, K. Okamoto, K. Li, Y. Nagao, S. Sano, H. Taue. A new infrared fluorescent-labeling agent and labeled antibody for diagnosing microcancers. *Bioorg. Med. Chem.* **(2003)** *11*, 3289 – 3294.

(85) S. Miki, T. Kaneta, T. Imasaka. Capillary electrophoresis immunoassay based on an on-column immunological reaction. *J. Chromatogr. A* **(2005)** *1066*, 197 – 203.

(86) J-P. Song, Y-J. Guo, Q. Zhao, S-M. Shuang, C. Dong, M. M. F. Choi. Assemblies of brilliant cresyl violet to DNA in the presence of ϒ-cyclodextrin. *Talanta* **(2010)** *82*, 681 – 686.

(87) M. L. Sánchez-Martínez, M. P. Aguilar-Caballos, A. Gómez-Hens. Long-wavelength homogeneous enzyme immunoassay for the determination of amikacin in wáter samples. *Talanta* **(2009)** *78*, 305 – 309.

(88) J. Madsen, I. Canton, N. J. Warren, E. Thermiston, A. Blanazs, B. Ustbas, X. Tion, R. Pearsson, G. Battaglia, A. L. Lewis, S. P. Armes. Nile blue-based nanosized pH sensors for simultaneous far-red and near-infrared live bioimaging. *J. Am. Chem. Soc.* **(2013)** *135*, 14863 – 14870.

(89) D. Kul, M. E. Ghica, R. Pauliukaite, C. M. A. Brett. A novel amperometric sensor for ascorbic acid based on poly(Nile blue A) and functionalized multi-walled carbon nanotube modified electrodes. *Talanta* **(2013)** *111*, 76 – 84.

(90) S. S. Mortazavi, H. Noorizadeh, R. Hushmandfar, A. Farmany. Ultra-sensitive quantification of sub-nanomolar levels of iodine in

blood serum samples by kinetic-spectro photometric method. *Biol. Trace El. Res.* **(2011)** *144*, 1430 – 1436.

(91) X. Wang, C. Boschetti, M. J. Ruedas-Rama, A. Tunnacliffe, E. A. H. Hall. Ratiometric pH-dot ANSors. *Analyst* **(2010)** *135*, 1585 – 1591.

(92) T. Kaneta, Y. Saito, T. Imasaka. Indirect detection of amino-substituted polycyclic aromatic hydrocarbons in cyclodextrin-modified micellar electrokinetic chromatography combined with diode laser-induced fluorometry. *J. Chromatogr.* **(1999)** *831*, 285 – 292.

(93) G. Sivaraman, T. Anand, D. Chellappa. Turn-on fluorescent chemosensor for Zn (II) *via* ring opening of rhodamine spirolactam and their live cell imaging. *Analyst* **(2012)** *137*, 5881 – 5884.

(94) W-D. Chen, W-T. Gong, Z-Q. Ye, Y. Lin, G-L. Ning. FRET-based ratiometric fluorescent probes for selective Fe^{3+} sensing and their applications in mitochondria. *Dalton Trans.* **(2013)** *42*, 10093 – 10096.

(95) B. Hu, L-L. Hu, M-L. Chen, J-H. Wang. A FRET ratiometric fluorescence sensing system for mercury detection and intracellular colorimetric imaging in live Hela cells. *Biosens. Bioelectron.* **(2013)** *49*, 499 – 505.

(96) H-S. Lv, S-Y. Huang, B-X. Zhao, J-Y. Miao. A new rhodamine B-based lysosomal pH fluorescent indicator. *Anal. Chim. Acta* **(2013)** *788*, 177 – 182.

(97) R. Zekavati, S. Safi, S. J. Hashemi, T. Rahmani-Cherati, M. Tabatabaei, A. Mohsenifar, M. Bayat. Highly sensitive FRET-based fluorescence immunoassay for aflatoxin B1 using cadmium telluride quantum dots. *Microchim. Acta* **(2013)** *180*, 1217 – 1223.

(98) V. C. Özalp, U. S. Zeydanli, A. Lunding, M. Kavruk, M. T. Öz, F. Evidoqan, L. F. Olsen, H. A. Öktem. Nanoparticle embedded enzymes for improved lateral flow sensors. *Analyst* **(2013)** *138*, 4255 – 4259.

(99) E.-O. Ganbold, T. Kang, K. Lee, S. Y. Lee, S.-W. Joo. Aggregation effects of gold nanoparticles for single-base mismatch detection in influenza A (H1N1) DNA sequences using fluorescence and Raman measurements. *Colloids Surf. B: Biointerf.* **(2012)** *93*, 148 – 153.

(100) B. T. Glaser, J. P. Malerich, S. J. Duellman, J. Fong, C. Hutson, R. M. Fine, B. Keblansky, M. J. Tanga, P. B. Madrid. A high-throughput fluorescence polarization assay for inhibitors of gyrase B. *J. Biomol. Screen.* **(2011)** *16*, 230 – 238.

(101) M. Baruah, W. Qin, N. Basaric, W. M. de Borgraeve, N. Boens. BODIPY-Based Hydroxyaryl Derivatives as Fluorescent pH Probes. *J. Organ. Chem.* **(2005)** *70*, 4152 – 4157.

(102) E. J. Park, K. R. Reid, W. Tang, R. T. Kennedy, R. Kopelman. Ratiometric fiber optic sensors for the detection of inter- and intra-cellular dissolved oxygen. *J. Mat. Chem.* **(2005)** *15*, 2913 – 2919.

(103) D. Marushchak, S. Kalinin, I. Mikhalyov, N. Gretskaya, L. B-A. Johansson. Pyrromethene dyes (BODIPY) can form ground state homo and hetero dimers: Photophysics and spectral properties. *Spectrochim. Acta Part A* **(2006)** *65*, 13 – 122.

(104) M. O. Noor, U. J. Krull. Paper-based solid-phase multiplexed nucleic acid hybridization assay with tunable dynamic range using immobilized quantum dots as donors in fluorescence resonance energy transfer. *Anal. Chem.* **(2013)** *85*, 7502 – 7511.

(105) S. Ding, X. Qiao, J. Suryadi, G. S. Marrs, G. L. Kucera, U. Bierbach. Using fluorescent post-labeling to probe the subcellular localization of DNA-targeted platinum anticancer agents. *Ang. Chem. Int. Ed.* **(2013)** *52*, 3350 – 3354.

(106) E. Lerner, G. Hilzenrat, D. Amir, E. Tauber, Y. Garini, E. Haas. Preparation of homogeneous samples of double-labelled protein suitable for single-molecule FRET measurements. *Anal. Bioanal. Chem.* **(2013)** *405*, 5983 – 5991.

(107) R. Zhang B. Song, Z. Dai, Z. Ye, Y. Xiao, Y. Liu, J. Yuan. Highly sensitive and selective phosphorescent chemosensors for hypochlorous acid based on ruthenium (II) complexes. *Biosens. Bioelectron.* **(2013)** *50*, 1 – 7.

(108) Y. He, Y. Chai, R. Yuan, H. Wang, L. Bai, Y. Cao, Y. Yuan. An ultrasensitive electrochemiluminescence immunoassay based on supersandwich DNA structure amplification with histidine as a co-reactant. *Biosens. Bioelectron.* **(2013)** *50*, 294 – 299.

(109) Y. Lui, M. Luo, J. Yan, X. Xiang, X. Ji, G. Zhou, Z. He. An ultrasensitive biosensor for DNA detection based on hybridization chain reaction coupled with the efficient quenching of a ruthenium complex to CdTe quantum dots. *Chem. Commun.* **(2013)** *49*, 7424 – 7426.

(110) A. Andreu-Navarro, J. M. Fernández-Romero, A. Gómez-Hens. Long-wavelength fluorescence detection of flavonoids in orange juices by LC. *Chromatographia* **(2010)** *72*, 1115 – 1120.

(111) M. Á. Molina-Delgado, M. P. Aguilar-Caballos, A. Gómez-Hens. Determination of soy protein in food samples by dispersive solid-phase immunoextraction and dynamic long-wavelength fluorometry. *Microchim. Acta* **(2013)** *180*, 1279 – 1286.

(112) A. Andreu-Navarro, J. M. Fernández-Romero, A. Gómez-Hens. Determination of polyphenolic content in beverages using laccase, gold nanoparticles and long wavelength fluorimetry. *Anal. Chim. Acta* **(2012)** *713*, 1 – 6.

(113) L. Sun, D. Hao, W. Shen, Z. Qian, C. Zhu. Highly sensitive fluorescent sensor for copper (II) based on amplified fluorescence quenching of a water-soluble NIR emiting conjugated polymer. *Microchim. Acta* **(2012)** *177*, 357 – 364.

(114) Y. Li, P. Wang, X. Wang, M. Cao, Y. Xia, C. Cao, M. Liu, C. Zhu. An immediate luminescence enhancement method for determination of vitamin B_1, using long-wavelength emitting water-soluble CdTe nanorods. *Microchim. Acta* **(2010)** *169*, 65 – 71.

(115) H. W. Zhao, C. Z. Huang, Y. F. Li. Immunoassay by detecting enhanced resonance light scattering signals of immunocomplex using a common spectrofluorometer. *Talanta* **(2006)** *70*, 609 – 614.

(116) P. Montagne, P. Varcin, M. L. Cuillière, J. Duheille. Microparticle-enhanced nephelometric immunoassay with microsphere-antigen conjugates. *Bioconjug. Chem.* **(1992)** *3*, 187 – 193.

(117) A. Gómez-Hens, M. P. Aguilar-Caballos. Trends in Immunoassay Techniques. *Encyclopedia of Analytical Chemistry* **(2010)** a9180, Wiley.

(118) K. Huynh, G. Wang, C. Moore, R. Barhate, C. Coulter, W. Rodrigues, P. Catbagan, J. Soares. Development of a homogeneous

immunoassay for the detection of zolpidem in urine. *J. Anal. Toxicol.* **(2009)** *33*, 486 – 490.

(119) T. Tachi, N. Kaji, M. Tokeshi, Y. Baba. Microchip-based homogeneous immunoassay using a cloned enzyme donor. *Anal. Sciences* **(2009)** *25*, 149 – 151.

(120) R. Zekavati, S. Safi, S. J. Hashemi, T. Rahmani-Cherati, M. Tabatabaei, A. Mohsenifar, M. Bayat. Highly sensitive FRET-based fluorescence immunoassay for aflatoxin B1 using cadmium telluride quantum dots. *Microchim. Acta* **(2013)** *180*, 13 – 14.

(121) J. Tian, L. Zhou, Y. Zhao, Y. Wang, Y. Peng, X. Hong, S. Zhao. The application of CdTe/CdS in the detection of carcinoembryonic antigen by fluorescence polarization immunoassay. *J. Fluoresc.* **(2012)** *22*, 1571 – 1579.

(122) J. Tian, L. Zhou, Y. Zhao, Y. Wang, Y. Peng, S. Zhao. Multiplexed detection of tumor markers with multicolor quantum dots based on fluorescence polarization immunoassay. *Talanta* **(2012)** *92*, 72 – 77.

(123) N. Kaddar, N. Bendridi, C. Harthé, M. Rolland de Ravel, A. L. Bienvenu, C. Y. Cuilleron, E. Mappus, M. Pugeat, H. Déchaud. Development of a radioimmunoassay for the measurement of Bisphenol A in biological samples. *Anal. Chim. Acta* **(2009)** *645*, 1 – 4.

(124) J. H. Sloan, B. J. Ackermann, M. O´Dell, R. R. Bowsher, R. A. Dean, R. J. Konrad. Development of a novel radioimmunoassay to detect autoantibodies to amyloid beta peptides in the presence of a cross-reactive therapeutic antibody. *J. Pharm. Biomed. Anal.* **(2011)** *56*, 1029 – 1034.

(125) K. M. Sallam, R. R. Sheha, A. A. El-Zahhar. Development of solid phase radioimmunoassay system using new polymeric magnetic micro-spheres. *J. Radioanal. Nucl. Chem.* **(2011)** *290*, 339 – 345.

(126) H. Siitari, I. Hemmilä, E. Soini, T. Lövgren. Detection of hepatitis B surface antigen using time-resolved fluoroimmunoassay. *Nature* **(1983)** *301*, 258 – 260.

(127) T. Valta, E. M. Puputti, I. Hyppänen, J. Kankare, H. Takalo, T. Soukka. Ligand enabling visible wavelength excitation of

europium (III) for fluoroimmunoassays in aqueous micellar solutions. *Anal. Chem.* **(2012)** *84*, 7708 – 7712.

(128) M. M. Vdovenko, A. S. Stepanova, S. A. Eremin, N. V. Cuong, N. A. Uskova, I. Y. Sakharov. Quantification of 2,4-dichlorophenoxyacetic acid in oranges and mandarins by chemiluminescent ELISA. *Food Chem.* **(2013)** *141*, 865 – 868.

(129) Z. Chao, M. Tan, M. K. Paudel, S. Sakamoto, L. Ma, K. S. Tabata, H. Tanaka, Y. Shoyama, L. Xuan, S. Morimoto. Development of an indirect competitive enzyme-linked immunosorbent assay (icELISA) using highly specific monoclonal antibody against paclitaxel. *J. Nat. Med.* **(2013)** *67*, 512 – 518.

(130) M. M. Vdovenko, C. T. Hung, I. Y. Sakharov, F. Y. Yu. Determination of okadaic acid in shellfish by using a novel chemiluminescent enzyme-linked immunosorbent assay method. *Talanta* **(2013)** *116*, 343 – 346.

(131) Z. J. Liu, X. Yan, X. Y. Xu, M. H. Wang. Development of a chemiluminescence enzyme-linked immunosorbent assay for the simultaneous detection of imidaclothiz and thiacloprid in agricultural samples. *Analyst* **(2013)** *138*, 3280 – 3286.

(132) Q. Xue, C. Bian, J. Tong, J. Sun, H. Zhang, S. Xia. A micro potentiometric immunosensor for hemoglobin-A1c level detection based on mixed SAMs wrapped nano-spheres array. *Biosens. Bioelectron.* **(2011)** *26*, 2689 – 2693.

(133) R. Liang, H. Peng, J. Qu. Fabrication, characterization, and application of potentiometric immunosensor based on biocompatible and controllable three-dimensional porous chitosan membranes. *J. Colloid Interf. Sci.* **(2008)** *320*, 125 – 13.

(134) H. Yin, Y. Zhou, Z. Xu, M. Wang, S. Ai. Ultrasensitive electrochemical immunoassay for DNA methyltransferase activity and inhibitor screening based on methyl binding domain protein of MeCP2 and enzymatic signal amplification. *Biosens. Bioelectron.* **(2013)** *49*, 39 – 45.

(135) H. Kanso, L. Barthelmebs, N. Inguimbert, T. Noguer. Immunosensors for estradiol and ethinylestradiol based on new

synthetic estrogen derivatives: application to wastewater analysis. *Anal. Chem.* **(2013)** *85*, 2397 – 2404.

(136) X. Liu, Z. Yanq, Y. Zhanq, R. Yu. A novel electrochemical immunosensor for ochratoxin A with hapten immobilization on thionine/gold nanoparticle modified glassy carbon electrode. *Analytical Methods* **(2013)** *5*, 1481 – 1486.

(137) Y. Hou, T. Li, H. Huang, H. Quan, X. Miao, M. Yang. Electrochemical immunosensor for the detection of tumor necrosis factor α based on hydrogel prepared from ferrocene modified amino acid. *Sens. Actuat. B: Chem.* **(2013)** *182*, 605 – 609.

(138) K. Mao, D. Wu, Y. Li, H. Ma, Z. Ni, H. Yu, C. Luo, Q. Wei, B. Du. Label-free electrochemical immunosensor based on graphene/methylene blue nanocomposite. *Anal. Biochem.* **(2012)** *422*, 22 – 27.

(139) T. Yu, W. Cheng, Q. Li, C. Luo, L. Yan, D. Zhang, Y. Yin, S. Ding, H. Ju. Electrochemical immunosensor for competitive detection of neuron specific enolase using functional carbon nanotubes and gold nanoprobe. *Talanta* **(2012)** *93*, 433 – 438.

(140) Q. Gao, J. Han, Z. Ma. Polyamidoamine dendrimers-capped carbón dots/Au nanocrystal nanocomposites and its application for electrochemical immunosensor. *Biosens. Bioelectron.* **(2013)** *49*, 323 – 328.

(141) X. Cao, S. Liu, Q. Feng, N. Wang. Silver nanowire-based electrochemical immunoassay for sensing immunoglobulin G with signal amplification using strawberry-like ZnO nanostructures as labels. *Biosens. Bioelectron.* **(2013)** *49*, 256 – 262.

(142) X. Wang, L. Chen, X. Su, S. Ai. Electrochemical immunosensor with graphene quantum dots and apoferritin-encapsulated Cu nanoparticles double-assisted signal amplification for detection of avian leucosis virus subgroup J. *Biosens. Bioelectron.* **(2013)** *47*, 171 – 177.

(143) Q. Zu, Y. Chai, R. Yuan, Y. Zhuo, J. Han, Y. Li, N. Liao. Amperometric immunosensor for simultaneous detection of three analytes in one interface using dual functionalized graphene sheets

integrated with redox-probes as tracer matrixes. *Biosens. Bioelectron.* **(2013)** *43*, 440 – 445.

(144) A. Montrose, S. Cargou, F. Nepveu, R. Manczak, A. M. Gué, K. Reybier. Impedimetric immunosensor for the detection of curculating pro-inflammatory monocytes as infection markers. *Biosens. Bioelectron.* **(2013)** *49*, 305 – 311.

(145) L. Zhang, M. Wang, C. Wang, X. Hu, G. Wang. Label-free impedimetric immunosensor for sensitive detection of 2,4-dichlorophenoxybutyric acid (2,4-DB) in soybean. *Talanta* **(2012)** *101*, 226 – 232.

(146) S. Samanman, P. Kantharana, P. Asawatreratanakul, P. Thavarungkul. Characterization and application of self-assembled layer by layer gold nanoparticles for highly sensitive label-free capacitive immunosensing. *Electrochim. Acta* **(2012)** *80*, 202 – 212.

(147) C. Zong, J. Wu, C. Wang, H. Ju, F. Yan. Chemiluminescence imaging immunoassay of multiple tumor markers for cancer screening. *Anal. Chem.* **(2012)** *84*, 2410 – 2415.

(148) Y. Liebes, L. Amir, R. S. Marks, M. Banai. Immobilization strategies of *Brucella* particles on optical fibers for use in chemiluminescence immunosensors. *Talanta* **(2009)** *80*, 338 – 345.

(149) X. Jiang, Y. Chai, R. Yuan, Y. Cao, Y. Chen, H. Wang, X. Gan. An ultrasensitive luminol cathodic electrochemiluminescence immunosensor based on glucose oxidase and nanocomposites: Graphene-carbon nanotubes and gold-platinum alloy. *Anal. Chim. Acta* **(2013)** *783*, 49 – 55.

(150) Z. Guo, T. Hao, S. Du, B. Chen, Z. Wang, X. Li, S. Wang. Multiplex electrochemiluminescence immunoassay of two tumor markers using multicolor quantum dots as labels and grapheme as conducting bridge. *Biosens. Bioelectron.* **(2013)** *44*, 101 – 107.

(151) Y. R. Kim, H. J. Seo, J. W. Oh, H. Lim, T. H. Kim, H. Kim. Immunosensor based on electrogenerated chemiluminescence using $Ru(bpy)_3^{2+}$-doped silica nanoparticles and calix[4]crown-5 self-assembled monolayers. *Electroanalysis* **(2013)** *25*, 1056 – 1063.

(152) D. E. P. Souto, J. V. Silva, H. R. Martins, A. B. Reis, R. C. S. Luz, L. T. Kubota, F. S. Damos. Development of a label-free immunosensor based on surface plasmon resonance technique for the detection of anti-*Leishmania infantum* antibodies in canine serum. *Biosens. Bioelectron.* **(2013)** *46*, 22 – 29.

(153) J. Zhang, Y. Sun, B. Xu, H. Zhang, Y. Gao, H. Zhang, D. Song. A novel surface plasmon surface resonance biosensor based on grapheme oxide decorated with gold nanorod-antibody conjugates for determination of transferrin. *Biosens. Bioelectron.* **(2013)** *45*, 230 – 236.

(154) S. Xiulan, Z. Yinzhi, S. Jingdong, S. Liyan, Q. He, Z. Weijuan. A quartz crystal microbalance-based immunosensor for shrimp allergen determination in food. *Eur. food Res. Tech.* **(2010)** *231*, 563 – 570.

(155) D. Tang, Q. Li, J. Tang, B. Su, G. Chen. An enzyme-free quartz crystal microbalance biosensor for sensitive glucose detection in biological fluids based on glucose/dextran displacement approach. *Anal. Chim. Acta* **(2011)** *686*, 144 – 149.

(156) C. C. Liu, C. Y. Yeung, P. H. Chen, M. K. Yeh, S. Y. Hou. *Salmonella* detection using 16S ribosomal DNA/RNA probe-gold nanoparticles and lateral flow immunoassay. *Food Chem.* **(2013)** *141*, 2526 – 2532.

(157) X. Mao, W. Wang, T. E. Du. Dry-reagent nucleic acid biosensor based on blue dye doped latex beads and lateral flow strip. *Talanta* **(2013)** *114*, 248 – 253.

(158) Y. K. Wang, Y. X. Yan, W. H. Ji, H. Wang, S. Q. Li, Q. Zou, J. H. Sun. Rapid simultaneous quantification of zearalenone and fumonisin B1 in corn and wheat by lateral flow dual immunoassay. *J. Agric. Food Chem.* **(2013)** *61*, 5031 – 5036.

(159) C. S. Pantaleón, J. Wichers, A. A. Somovilla, A. Van Amerongen, A. A. Fuentes. Development of an immunochromatographic assay based on carbon nanoparticles for the determination of the phytoregulator forchlorfenuron. *Biosens. Bioelectron.* **(2013)** *42*, 170 – 176.

(160) A. N. Berlina, N. A. Taranova, A. V. Zherdev, Y. Y. Vengerov, B. B. Dzantiev. Quantum dot-based lateral flow immunoassay for detection of chloramphenicol in milk. *Anal. Bioanal. Chem.* **(2013)** *405*, 4997 – 5000.

(161) T. Li, J-Y. Byun, B. B. Kim, Y-B. Shin, M-G. Kim. Label-free homogeneous FRET immunoassay for the detection of mycotoxins that utilizes quenching of the intrinsic fluorescence of antibodies. *Biosens. Bioelectron.* **(2013)** *42*, 403 – 408.

(162) M. L. Sánchez-Martínez, M. P. Aguilar-Caballos, A. Gómez-Hens. Homogeneous immunoassay for soy protein determination in food samples using gold nanoparticles as labels and light scattering detection. *Anal. Chim. Acta* **(2009)** *636*, 58 – 62.

(163) A. P. Bondarenko, S. A. Eremin. Determination of zearalenone and ochratoxin A mycotoxins in grain by fluorescence polarization immunoassay. *J. Anal. Chem.* **(2012)** *67*, 790 – 794.

(164) Z-L. Xu, Q. Wang, H-T. Lei, S. A. Eremin, Y-D. Shen, H. Wang, R. C. Beier, J-Y. Yang, K. A. Maksimova, Y-M. Sun. A simple, rapid and high-throughput fluorescence polarization immunoassay for simultaneous detection of organophosphorus pesticides in vegetable and environmental water samples. *Anal. Chim. Acta* **(2011)** *708*, 123 – 129.

(165) X. Tao, M. Chen, H. Jiang, J. Shen, Z. Wang, X. Wang, X. Wu, K. Wen. Chemiluminescence competitive indirect enzyme immunoassay for 20 fluoroquinolone residues in fish and shrimp based on a single-chain variable fragment. *Anal. Bioanal. Chem.* **(2013)** *405*, 7477 – 7484.

(166) Y. Zhao, F. Wang, W. Li, Y. Ha. Development of a competitive indirect enzyme-linked immunosorbent assay based on monoclonal antibodies for the detection of 2-dodecylcyclobutanone in irradiate beef. *J. Agric. Food Chem.* **(2013)** *61*, 7749 – 7753.

(167) B. Cao, G. He, H. Yang, H. Chang, S. Li, A. Deng. Development of a highly sensitive and specific enzyme-linked immunosorbent assay (ELISA) for the detection of phenylethanolamine A in tissue and

feed samples and confirmed by liquid chromatography tandem mass spectrometry (LC-MS/MS). *Talanta* **(2013)** *115*, 624 – 630.

(168) D. Scalas, S. Squadrone, M. Gili, D. Marchis, M. Prearo, M. C. Abete. Validation of a dissociation enhanced lanthanide fluorescence immunoassay for the screening of 17 β-estradiol in bovine serum according to European Union decision 2002/657/EC. *J. AOAC Int.* **(2007)** *90*, 1427 – 1431.

(169) M-Z. Zhang, M-Z. Wang, Z-L. Chen, J-H. Fang, M-M. Fang, J. Liu, X-P. Yu. Development of a colloidal gold-based lateral-flow immunoassay for the rapid simultaneous detection of clenbuterol and raptopamine in swine urine. *Anal. Bioanal. Chem* **(2009)** *395*, 2591 – 2599.

(170) F. Conzuelo, S. Campuzano, M. Gamella, D. G. Pinacho, A. J. Reviejo, M. P. Marco, J. M. Pingarrón. Integrated disposable electrochemical immunosensors for the simultaneous determination of sulfonamide and tetracycline antibiotics residues in milk. *Biosens. Bioelectron.* **(2013)** *50*, 100 – 105.

(171) X. Pao, P. Yan, Q. Tang, A. Deng, J. Li. Quantum Dots based electrochemiluminescent immunosensor by coupling enzymatic amplification for ultrasensitive detection of clenbuterol. *Anal. Chim. Acta* **(2013)** *798*, 82 – 88.

(172) F. Ricci, G. Volpe, L. Micheli, G. Palleschi. A review on novel developments and applications of immunosensors in food analysis. *Anal. Chim. Acta* **(2007)** *605*, 111 – 129.

CAPÍTULO 1

Herramientas analíticas

En el desarrollo experimental de la presente Tesis Doctoral se han empleado diferentes herramientas analíticas para llevar a cabo las distintas investigaciones realizadas. En este capítulo de la Memoria de la Tesis Doctoral se enumeran dichas herramientas y se profundiza en sus características y aspectos más relevantes de su utilización.

Materiales y reactivos

1- Materiales nanoestructurados

En la siguiente Tabla se relacionan los diferentes nanomateriales no sintetizados en el laboratorio y necesarios para desarrollar los trabajos experimentales descritos en esta Memoria, sus diámetros medios y la fuente de suministro.

Tipo de Nanomaterial	Tamaño	Distribuidor
$NaYF_4$:Yb(III), Er(III)	10 – 20 nm	Departamento de Química de los Materiales y Análisis Químico. Universidad de Turku (Finlandia)
$NaYF_4$:Yb(III), Tm(III)	10 – 20 nm	Departamento de Química de los Materiales y Análisis Químico. Universidad de Turku (Finlandia)
$NaYF_4$:Yb(III), Ho(III)	10 – 20 nm	Departamento de Química de los Materiales y Análisis Químico. Universidad de Turku (Finlandia)
Tb_4O_7	< 100 nm	Aldrich
Eu_2O_3	< 150 nm	Aldrich
Diamante	< 10 nm	Aldrich
Ag	10 nm	Aldrich

2- Precursores de sílice

En la siguiente Tabla se relacionan los diferentes precursores de sílice utilizados para la síntesis de nanopartículas de sílice y el recubrimiento de los upconverting phosphors, así como la funcionalización de la superficie de ambos materiales.

Precursor de sílice	Función	Distribuidor
Tetraetoxisilano (TEOS)	Estructura de sílice	Aldrich
(3-Aminopropil)trietoxisilano (APS)	Introducción grupos amino	Aldrich
3-(Trihidroxisilil)propil metilfosfonato (THPMP)	Introducción grupos fosfonato	Aldrich
(N-(3-(trimetoxisilil)propil)etilen diamino	Introducción grupos amino	Aldrich

3- Fluoróforos

En la siguiente Tabla se relacionan los diferentes fluoróforos, así como sus respectivas longitudes de onda de excitación y emisión, utilizados en las diferentes investigaciones presentadas en esta Memoria.

Fluoróforo	$\lambda_{excitación}$ (nm)	$\lambda_{emisión}$ (nm)	Distribuidor
Violeta de cresilo	585	620	Sigma
Azul nilo	620	680	Sigma
Fluoresceína sódica	485	520	Sigma
Ácido 8-(hidroxipireno-1,3,6-trisulfónico (HPTS)	455	510	Sigma-Aldrich
Azure A	632	645	Sigma
Azure B	648	662	Sigma
2-[4-(Dimetilamino)styryl]-1-metilpiridinio yoduro (2-Di-1-ASP)	465	505	Aldrich
Styryl 7	565	620	Sigma-Aldrich
Azul de toluidina	620	638	Sigma
β-ficoeritrina (BPE)	550	575	Cyanotech Corp
R-ficoeritrina (RPE)	565	575	Cyanotech Corp
Alexa Fluor 488	495	520	Molecular Probes Invitrogen Paysley
Alexa Fluor 546	556	570	Molecular Probes Invitrogen Paysley
Alexa Fluor 680	680	702	Molecular Probes Invitrogen Paysley
ATTO 495	495	525	Spa-BioSpa

4- Tensoactivos

Se han utilizado los siguientes tensoactivos neutros, aniónicos y catiónicos: Tritón X-100 (Sigma), Tween 20 (Sigma), dodecil sulfato sódico (SDS) (Sigma-Aldrich) y bromuro de hexadeciltrimetilamonio (CTAB) (Fluka).

5- Disolventes orgánicos

Se han utilizado diferentes disolventes orgánicos como medio de reacción, eliminación de reactantes y preparación de disoluciones de etanol (Panreac), acetona (Panreac), ciclohexano (Panreac), 1-hexanol (Merck), metanol (Panreac), dimetilformamida (Sigma-Aldrich) y acetonitrilo (Panreac).

6- Anticuerpos

Se han utilizado varios tipos de anticuerpos para llevar a cabo los diferentes formatos de inmunoensayo de esta tesis: Anticuerpos policlonales anti-proteína de soja producidos en conejo (Sigma), anticuerpos IgG anti-conejo producidos en cabra (Sigma-Aldrich), anticuerpos policlonales anti-monensín producidos en oveja (Abcam) y anticuerpos IgG anti-oveja producidos en conejo (Sigma-Aldrich).

7- Estándares

En la siguiente Tabla se relacionan los compuestos químicos utilizados para preparar estándares de los analitos y de los potenciales interferentes utilizados en las diferentes investigaciones experimentales recogidas en

esta Tesis Doctoral, su pureza y las casas comerciales que los han suministrado.

Analito	Pureza	Distribuidor
Proteína de soja	90 %	Doscadesa
Monensín	90 – 95 %	Sigma
Trolox	97 %	Sigma-Aldrich
Ácido cafeico	≥ 98 %	Sigma
Ácido málico	≥ 99,5 %	Merck
Ácido gálico	97,5 – 102,5 %	Sigma
Glucosa	≥ 99,8 %	Sigma-Aldrich
Ácido ascórbico	≥ 99 %	Sigma-Aldrich
Sacarosa	≥ 99 %	Fluka
Ácido cítrico	≥ 99,5 %	Sigma
Sulfito sódico	≥ 98 %	Merck
Biotina	≥ 99 %	Sigma-Aldrich

8- Otros reactivos

Para llevar a cabo las investigaciones realizadas a lo largo de esta Memoria se han usado disoluciones reguladoras preparadas a partir de sus correspondientes sales, ácidos y bases, así como otros reactivos los cuales se relacionan a continuación junto con la casa comercial donde fueron adquiridos: Hidróxido amónico (Panreac), albúmina de suero bovino (Sigma-Aldrich), borohidruro sódico (Sigma-Aldrich), acetato sódico (Sigma-Aldrich), ácido sulfúrico (Panreac), additol (Surface Specialities), carbonato sódico (Sigma-Aldrich), tetraborato sódico (Panreac), anhídrido

glutárico (Sigma), monohidrógeno fosfato potásico (Merck), vainillina (Aldrich), metaperyodato sódico (Scharlau), ácido clorhídrico (Merck), N-(3-dimetilaminopropil)-N´-etilcarbodiimida (EDAC) (Sigma-Aldrich), diclorhidrato 2,2´-azobis(2-metilpropionamida) (AAPH) (Aldrich), piridina (Sigma), sulfo-N-hidroxisuccinimida (sulfo-NHS) (Sigma-Aldrich), glutaraldehido (Sigma), disolución DELFIA (Perkin Elmer life and Analytical Sciences, enzima laccasa (Sigma), nitrato de terbio (Aldrich), tampón ensayo para reacciones de bioafinidad y disolución de lavado para placas de ensayos de bioafinidad (Innotrac diagnostic Oy), cloruro sódico (Sigma-Aldrich) y reactivo de Folin-Ciocalteau (Sigma-Aldrich).

Instrumentación

En el desarrollo experimental de esta Memoria se ha utilizado la siguiente instrumentación:

- Lector de microplacas 1420 Multilabel Counter Victor ^{3}V (Perkin Elmer and Analytical Sciences, Wallac Oy, Turku, Finlandia).
- Espectrofluorímetro SLM Aminco modelo 8100 (Urbana, IL, USA) equipado con una lámpara de arco de xenón de 450 W y un tubo fotomultiplicador R928.
- Plate Chameleon (Hidex Oy, Turku) equipped with a 200mW infrared laser module (Roithner Lasertechnik) and RG-850 nm long-pass excitation filter (Andover Corp., Salem, NH). The photomultiplier tube in the plate fluorometer was replaced with Hamamatsu R4632 (Hamamatsu Photonics K.K.).

- Microscopio electrónico de transmisión Philips CM-10, resolución 0,5 nm x 0,34 nm, y equipado con una cámara digital megaview III. Rejillas de cobre (200C-FC) recubiertas con unas película de carbono Formvar® 200 mesh, suministradas por Aname (Madrid, España).
- Espectrofotómetro Lambda 35 UV/VIS (Perkin Elmer, Reino Unido).

Programas informáticos

Se emplearon diferentes programas informáticos para el cálculo estadístico y elaboración de las diferentes representaciones gráficas: Origin 7,0 (ORIGIN LAB), Statgraphics 5.1, Microsoft Excel y Sigma Plot 7.0.

CAPÍTULO 2

CHAPTER 2

Síntesis y caracterización de nanopartículas de sílice con fluorescencia a larga longitud de onda y su aplicación al análisis de alimentos

Synthesis and characterization of long-wavelength fluorescent silica nanoparticles and their application to food analysis

Este capítulo recoge las investigaciones realizadas para desarrollar nuevos métodos de análisis utilizando conjuntamente las prestaciones que ofrecen la nanotecnología y la fluorimetría de larga longitud de onda. Se describe la síntesis y caracterización de nanopartículas de sílice (SiO_2NPs) dopadas con oxazinas y se demuestra su utilidad en análisis de alimentos mediante inmunoensayo heterogéneo. Los estudios realizados han dado lugar a los siguientes artículos:

- Synthesis and characterization of oxazine-doped silica nanoparticles for their potential use as stable fluorescent reagents. J. Godoy-Navajas, M.P. Aguilar-Caballos, A. Gómez-Hens, Journal of Fluorescence, 20 (2010) 171-180.

- Heterogeneous immunoassay for soy protein determination using nile blue-doped silica nanoparticles as labels and front-surface long-wavelength fluorimetry. J. Godoy-Navajas, M.P. Aguilar Caballos, A. Gómez-Hens. Analytica Chimica Acta, 701 (2011) 194-199.

- Determination of monensin in milk samples by front-surface long-wavelength fluoroimmunoassay using nile blue-doped silica nanoparticles as labels. J. Godoy-Navajas, M. P. Aguilar-Caballos, A. Gómez-Hens, Talanta, 94 (2012) 195-200.

Cabe indicar que las investigaciones desarrolladas han tenido dos objetivos: 1) Estudiar la potencial versatilidad de estas NPs con

fluorescencia a larga longitud de onda para aplicarlas a la determinación de macromoléculas y moléculas pequeñas; y 2) Demostrar que los marcadores basados en SiO_2NPs dopadas con oxacinas pueden constituir una alternativa útil frente a los marcadores enzimáticos. Para alcanzar estos objetivos se han seleccionado las proteínas de soja y el antibiótico monensin debido a que un porcentaje elevado de los métodos descritos para la determinación de estos analitos en alimentos utiliza técnicas de inmunoensayo, principalmente enzimoinmunoensayo [1,2]. Aunque posteriormente se discutirán los resultados obtenidos, se ha demostrado que las nuevas NPs pueden utilizarse satisfactoriamente para determinar ambos tipos de analitos y que los correspondientes inmunoensayos desarrollados presentan menores límites de detección que los basados en el uso de marcadores enzimáticos, siendo también menor la duración de los ensayos.

Otro aspecto a destacar es la contribución de las investigaciones realizadas a expandir el uso de las SiO_2NPs dopadas con fluoróforos en análisis de alimentos, poniendo de manifiesto la utilidad del efecto protector de las NPs en las propiedades fluorescentes del reactivo encapsulado. Como se ha indicado en la Introducción general de esta Memoria, dentro de los escasos antecedentes descritos, cabe citar el uso reciente de SiO_2NPs dopadas con un quelato de rutenio para la determinación de residuos del antibiótico enrofloxacina en carne de pollo utilizando inmunocromatografía en membranas desechables de nitrocelulosa [3].

BIBLIOGRAFÍA

(1) D.L. Brandon, M. Friedman. Immunoassays of soy proteins. *J. Agric. Food Chem*. (**2002**) *50*, 6635-6642.

(2) A.C. Huet, M. Bienenmann-Ploum, U. Vincent, P. Delahaut. Screening methods and recent developments in the detection of anticoccidials. *Anal. Bioanal. Chem*. (**2013**) *405*, 7733-7751.

(3) X. Huang, Z. P. Aguilar, H. Li, W. Lai, H. Wei, H. Xu, Y. Xiong. Fluorescent $Ru(phen)_3^{2+}$-doped silica nanoparticles-based ICTS sensor for quantitative detection of enrofloxacin residues in chicken meat. *Anal. Chem.* **(2013)** *85*, 5120 – 5128.

This chapter contains the investigations performed to develop new analytical methods by combining the benefits of nanotechnology and long-wavelength fluorometry. The synthesis and characterization of silica nanoparticles (SiO_2NPs) doped with oxazine dyes is described and their usefulness in food analysis by the development of heterogeneous immunoassays is shown. These investigations have given rise to the following articles:

- Synthesis and characterization of oxazine-doped silica nanoparticles for their potential use as stable fluorescent reagents. J. Godoy-Navajas, M.P. Aguilar-Caballos, A. Gómez-Hens, Journal of Fluorescence, 20 (2010) 171-180.

- Heterogeneous immunoassay for soy protein determination using nile blue-doped silica nanoparticles as labels and front-surface long-wavelength fluorimetry. J. Godoy-Navajas, M.P. Aguilar Caballos, A. Gómez-Hens. Analytica Chimica Acta, 701 (2011) 194-199.

- Determination of monensin in milk samples by front-surface long-wavelength fluoroimmunoassay using nile blue-doped silica nanoparticles as labels. J. Godoy-Navajas, M. P. Aguilar-Caballos, A. Gómez-Hens, Talanta, 94 (2012) 195-200.

The investigations performed had two main objectives: 1) To study the potential versatility of the synthesized long-wavelength fluorescent

NPs to be applied to the determination of macromolecules and low-molecular weight compounds; and 2) To demonstrate that the tracers based on oxazine-doped SiO_2NPs can be a useful alternative to enzyme tracers. To achieve these goals, soy proteins and the antibiotic monensin have been selected as analytes owing to the fact that a high percentage of analytical methods reported for their determination are based on immunoassays, and more specifically, on enzyme immunoassays [1,2]. Although the results obtained will be discussed below, it is worth to mention that the new NPs can be satisfactorily used to determine both types of analytes and the immunoassays developed feature lower detection limits and shorter analysis times than those based on the use of enzyme tracers.

Another salient aspect of these investigations is their contribution to expand the use of SiO_2NPs doped with fluorophores in food analysis, where the protecting role of NPs on the fluorescent properties of the encapsulated reagent has been shown. As it has been already mentioned in the Introduction of this Dissertation, there are a scarce number of applications of these NPs in food analysis. A recent example is the use of SiO_2NPs doped with a ruthenium chelate to determine enrofloxacin antibiotic residues in chicken muscle using immunochromatography on disposable nitrocellulose membranes [3].

LITERATURE

(1) D.L. Brandon, M. Friedman. Immunoassays of soy proteins. *J. Agric. Food Chem*. (**2002**) *50*, 6635-6642.

(2) A.C. Huet, M. Bienenmann-Ploum, U. Vincent, P. Delahaut. Screening methods and recent developments in the detection of anticoccidials. *Anal. Bioanal. Chem*. (**2013**) *405*, 7733-7751.

(3) X. Huang, Z. P. Aguilar, H. Li, W. Lai, H. Wei, H. Xu, Y. Xiong. Fluorescent $Ru(phen)_3^{2+}$-doped silica nanoparticles-based ICTS sensor for quantitative detection of enrofloxacin residues in chicken meat. *Anal. Chem.* **(2013)** *85*, 5120 – 5128.

Journal of Fluorescence (2010) 20:171-180

Synthesis and characterization of oxazine-doped silica nanoparticles for their potential use as stable fluorescent reagents

J. Godoy-Navajas, M.P. Aguilar-Caballos, A. Gómez-Hens
Department of Analytical Chemistry. University of Córdoba. Campus of Rabanales. Marie-Curie Annex building. 14071-Córdoba

Abstract

The synthesis process to obtain silica nanoparticles (NPs) doped with two oxazine dyes, nile blue and cresyl violet, has been investigated using a modification of the reverse micelle microemulsion method and a procedure based on the Stöber method. A micellar medium provided by the non-ionic surfactant Triton X-100 in a hexanol:water mixture and an ethanol:water mixture, have been used to provide the synthesis medium in each case. Tetraethoxysilane has been used as the initiator of the polymerization and condensation reactions after its hydrolysis in basic medium using ammonium hydroxide. Dye-silane precursor NPs have been also synthesized in order to compare their potential advantages against the NPs obtained by the direct encapsulation of the oxazine dyes.

Size distribution and fluorescence of the synthesized NPs, which were monitored using Transmision Electron Microscopy (TEM) and a microplate reader, respectively, depend on the molar ratio and total concentration of the reagents involved in the synthesis. NPs obtained using the developed synthesis procedures had sizes below 400 nm in most instances and the best luminescent properties were observed for NPs with sizes ranging from 100 to 300 nm. Lower sizes result in a decrease in the fluorescence intensities of these nanomaterials. Parameters related with the luminescence features of these NPs were calculated in order to compare the feasibility of both synthesis approaches. The repeatability of the reverse-micelle microemulsion procedure performed in different days gave a relative standard deviation of 10% for the fluorescence intensity values.

Keywords: Dye-doped silica nanoparticles; cresyl violet; nile blue; long-wavelength fluorescence

1. Introduction

The use of nanomaterials is having a huge impact in the bioanalysis field [1-9], being their composition and physicochemical properties the main factors to choose the detection system best suited for each assay. The use of silica NPs as labels is interesting in bioassays with optical detection because of the transparency of silica to visible light. Other desirable properties are: 1) silica polymerization chemistry is well known, 2) silica material is not microbiologically degraded, and 3) porosity or swelling changes of silica NPs do not happen at moderate pH variations. However, the porosity of these materials can originate drawbacks in their performance as labels due to losses of the encapsulated substances as it will be discussed below.

Different silica precursors, such as tetramethoxysilane (TMOS) and tetraethoxysilane (TEOS) are commonly used to synthesize silica NPs. These precursors undergo hydrolysis and polycondensation reactions, which result in the formation of monodisperse spherical silica particles [10]. There are two general routes to synthesize silica NPs, namely reverse-micelle microemulsion and Stöber methods. The reverse-micelle microemulsion method relies on the formation of a water-in-oil microemulsion formed by a small amount of water, an organic solvent and a surfactant. Water nanodroplets inside the reverse micelles act as reactors in which the growth of silica NPs takes place. The Stöber method involves the hydrolysis of the silica precursor in an alcohol/water mixture and the silicic acid formed nucleates and condenses to give rise to spherical monodisperse NPs. The choice of every synthesis approach depends on the physicochemical properties of the species to be encapsulated [2, 4, 6]. In

general, hydrophobic and hydrophilic dyes can be encapsulated by using the Stöber method whereas the reverse-micelle microemulsion method has been mainly used for the synthesis of metal-chelate doped silica NPs [2, 4]. An advantage of the reverse-micelle microemulsion method is that usually provides NPs with narrower size distributions than those obtained by the Stöber method[2].

A common issue to both synthesis approaches is the probability of dye leakage, especially for organic dyes. This phenomenon can be minimized or avoided by coupling the organic fluorophor to hydrophilic species with high molecular weight, such as dextrans [11] or proteins [12], for two reasons: 1) the resulting derivative is hydrophilic as the silica matrix, and 2) the large size of the macromolecule can prevent the diffusion through silica matrix pores. Another option is the synthesis of precursors by covalent linking of the dye or a derivative, usually containing carboxyl [13], sulfonyl chloride [14] and isothiocyanate [15] groups, to a silane precursor, previously to the synthesis of silica NPs.

Metal chelates and organic dyes have been traditionally used as labels in bioassays with luminescent detection [7]. Conventional fluorophores, such as fluorescein isothiocyanate, fluorescamine or umbelliferone derivatives, provide the achievement of relatively low detection limits, but these compounds suffer from photobleaching processes due to the relatively high energy of their incident excitation wavelengths. However, this drawback can be minimized by embedding these dyes into a silica matrix, which protects them from environmental factors that would affect their fluorescence [2, 6]. Another limitation of conventional fluorophores is that their emission can be overlapped by static background fluorescence

signals from sample matrix, which usually happens at short wavelengths. An alternative is the use of long-wavelength fluorophores, such as organic dyes (cyanines, oxazines, alexa dyes) and lanthanide and ruthenium chelates [16-18].

The work presented here encompasses different approaches to synthesize long-wavelength emitting silica NPs doped with cresyl violet acetate and nile blue chloride for the first time. Two different sol-gel methods, based on the modification of the reverse-micelle microemulsion and Stöber approaches and on the use of the silane precursor TEOS and ammonium hydroxide, have been developed for the direct encapsulation of the fluorophore. The fluorescence of the NPs obtained by the first method has been improved in the absence of cyclohexane, which is used in the conventional procedure. The reverse-micelle microemulsion method has been also applied to the encapsulation of a newly synthesized silane precursor from nile blue chloride using glutaraldehyde and 3-aminopropyl triethoxysilane (APS). The influence of the different reagents on the features of the NPs formed in both synthesis procedures has been studied and optimized by measuring the fluorescence intensity using a microplate reader and the NP size by Transmission Electron Microscopy (TEM). The luminescent features of the NPs synthesized by both methods have been compared in order to select the synthesis procedure more suitable to obtain nanomaterials useful as stable fluorescent reagents for analytical purposes, such as labels in fluoroimmunoassays. Some properties of these long-wavelength emitting NPs, such as photodegradability, chemical stability and dye leakage are also discussed.

2. Experimental

2.1. Instrumentation

A 1420 Multilabel counter Victor ^{3}V microplate reader (Perkin Elmer and Analytical Sciences, Wallac Oy, Turku, Finland) was used to perform fluorescence measurements. Different filters (nominal wavelength/passband) were used to select the excitation (531/25 nm and 590/7 nm for cresyl violet, 620/8 nm for nile blue) and emission (620/8 nm for cresyl violet, 680/10 nm for nile blue) wavelengths of the doped NPs. An SLM-Aminco (Urbana, IL, USA), Model 8100 photon-counting spectrofluorimeter, equipped with a 450 W xenon arc source and a R928 photomultiplier tube, was used to perform fluorescence excitation and emission scans of pure dyes and synthesized NPs, as well as photobleaching experiments. Size characterization was performed by Transmision Electron Microscopy (TEM), using a CM10 Philips Microscope. Copper grids (200C-FC) coated with a Formvar® carbon film 200 mesh supplied by Aname (Madrid, Spain) were used as support in TEM experiments.

2.2. Reagents

All reagents were of analytical grade. 3-Aminopropyl triethoxysilane (APS) was obtained from Aldrich (Aldrich, Milwaukee, USA), and tetraethoxysilane (TEOS) and Triton X-100 from Fluka (Buch, Switzerland). Cresyl violet acetate, nile blue chloride and 25% glutaraldehyde aqueous solution (Grade II) were supplied by Sigma (St Louis, MO, USA) and absolute ethanol, acetone and ammonium hydroxide (25% as NH_3) by Panreac (Castellar del Vallès, Spain). Cyclohexane was

supplied by Probus (Badalona, España) and 1-hexanol by Merck (Schuchardt, Germany). Cresyl violet and nile blue solutions (1 x 10^{-3} M) were prepared by dissolving the appropriate amount of each dye in the minimum amount of methanol and then, raised up with distilled water until a final concentration of methanol of 10%, and stirring the mixture for 24 h.

2.3. Procedures

2.3.1. Synthesis of cresyl violet and nile blue-doped silica NPs by a modified reverse micelle microemulsion method

The synthesis was performed according to the following procedure: an amount of Triton X-100 (510 – 530 mg or 0.79 – 0.82 mmol) was dissolved in 9.6 ml (0.53 mol) of distilled water by stirring vigorously this mixture for 5 min. Then, a volume of 100 μl (0.44 mmol) of TEOS was added and the solution was stirred for 5 min. A volume (1.8 ml) of 10^{-3} M (1.8 μmol) cresyl violet or nile blue was added and the mixture stirred again for 5 min. Afterwards, 3 ml (0.024 mol) of hexanol were added and the microemulsion formed was stirred for 15 min. Concentrated ammonium hydroxide (70 μl, 0.9 mmol) was then added and the mixture stirred for 5 min to start the TEOS hydrolysis and condensation reactions. The mixture was then placed in a thermostated tank at 35 °C for 7.5 h in the dark.

The reaction mixture of each fluorophore-doped NPs, which was composed by two phases clearly differenciated, was centrifuged for 5 min at 2.000 rpm to complete the separation of two phases. The upper phase, which was strongly colored, was extracted and 5 – 7 ml of acetone were

added to break the microemulsion formed, and the precipitate was separated by centrifugation for 20 min at 3000 rpm. Then, NPs were washed with ethanol using ultrasound sonication for 30 s to desorb the fluorophore from the NP surface and then centrifuged for 5 min at 10000 rpm to get rid of unreacted precursors and the excess of surfactant and fluorophore. The washing process was repeated several times with ethanol and distilled water until the fluorescence signal of the supernatant was the same as the blank signal. NPs were finally re-dispersed in 1 ml of distilled water.

2.3.2. Synthesis of cresyl-violet doped NPs using a Stöber method-based procedure

To a volume of 25 ml of ethanol (0.43 mol) were added 500 μl of 10^{-3} M (0.5 μmol) cresyl violet. Then, 1 ml (4.4 mmol) of TEOS and 1.5 ml (19.5 mmol) of concentrated ammonium hydroxide solution were added. The mixture was stirred for 1 hour at room temperature. After this time, it was centrifuged at 3.000 rpm for 10 minutes. The NPs synthesized were purified by washing them with ethanol and water for several times as mentioned above for the reverse micelle microemulsion method.

2.3.3. Synthesis of NPs using nile blue-APS precursor as fluorophore

A volume (12 ml) of 8.9×10^{-4} M (10 μmol) nile blue solution was mixed with 100 μl of 1% glutaraldehyde (10 μmol) aqueous solution and, immediately after, 20 μl (85 μmol) of APS were added and the mixture stirred for 5 min before its use in the reverse-micelle microemulsion method above described. A volume (1.2 ml) of the reaction mixture,

without any additional purification step, was added to the mixture instead of the unchanged fluorophore.

2.3.4. Characterization of cresyl violet- and nile blue-doped silica NPs

Synthesized NPs were characterized by TEM and fluorescence intensity measurements. TEM experiments were carried out by spotting 10-μl drops of NP suspensions in ethanol onto the copper grids, which were placed above a filter paper and let to dry at room temperature for several minutes. Fluorescence measurements were obtained by dispensing aliquots of 200 μl of NP suspensions onto microwells in triplicate and using the filters above described to choose the adequate excitation and emission wavelengths.

2.3.5. Fluorescence stability of oxazine-doped silica NPs

Silica NPs were divided in five 1-ml aliquots in Eppendorf tubes. All of them were washed several times with ethanol and water until the supernatants presented a fluorescence intensity corresponding to the blank signal and, then, NPs were stored at 4 °C. At the time of the performance of the fluorescence measurements, each aliquot was sonicated for 30 s and then centrifuged at 10.000 rpm for 5 min to remove the supernatant. Then, they were again reconstituted and re-dispersed in water. A volume (200 μl) of the NP suspension was added to a microwell plate and the fluorescence intensity was measured in triplicate.

2.3.6. Photobleaching study of oxazine-doped silica NPs

Free organic dye solution or dye-doped NP dispersion was placed in a quartz cuvette and the fluorescence intensity was measured at the corresponding maximum excitation and emission wavelengths by continuosly irradiating the cuvette with light from the 450 W xenon arc lamp of the photon counting spectrofluorimeter. Fluorescence intensity measurements were monitored at room temperature for 1 h, with an integration time of 1.0 min.

3. Results and Discussion

3.1. Synthesis of cresyl-violet- and nile blue-doped silica NPs

Both synthesis approaches were optimized by using mainly the univariate method although, in some instances, the influence of variable ratios of the reagents was also studied.

3.1.1 Optimization of reverse micelle microemulsion method

As indicated above, the formation of microemulsions involves the use of a surfactant, an aqueous solution and an organic solvent. Depending on the relative amounts of the components, water-in-oil microemulsions (rich in organic solvent) or oil-in-water microemulsions (rich in water) can be formed. In the first case, a co-surfactant, generally a medium or long hydrocarbon chain alcohol, is often incorporated in the micelles. Cyclohexane, n-hexanol, Triton X-100 and water were chosen to develop the reverse-micelle microemulsion method, according to the procedures previously reported [2, 4, 6, 12-14]. These approaches involve continuous mechanical stirring to originate stable water-in-oil microemulsions.

However, the use of the experimental conditions previously described did not give rise to satisfactory results for the synthesis of the oxazine-doped silica NPs. The study of the stirring conditions showed that, after mixing the reagents in the addition order described in the procedure and then leaving the mixture to stand, two phases appeared: an upper phase (rich in organic solvent) and a lower phase (rich in water). The upper phase, which was strongly coloured, was a stable water-in-oil microemulsion containing the brightest NPs.

Studies carried out about the microemulsion composition revealed that NPs can be synthesized in the absence of cyclohexane, yielding NPs with similar features (number, size) but with slightly higher fluorescence intensity than that obtained using cyclohexane. Figure 1 shows TEM images of the NPs obtained in the presence of different volumes of cyclohexane. The water volume was also modified to keep constant the total volume. As can be seen, the amount and sizes of NPs synthesized in the absence of cyclohexane (Figure 1a) were comparable to those achieved using 7.5 ml of cyclohexane (Figure 1c). However, the use of intermediate volumes of cyclohexane (Figure 1b) provided larger NPs with wider size distributions. According to these results, the use of cyclohexane was precluded and only water, Triton X-100 and 1-hexanol were the main components of the microemulsion.

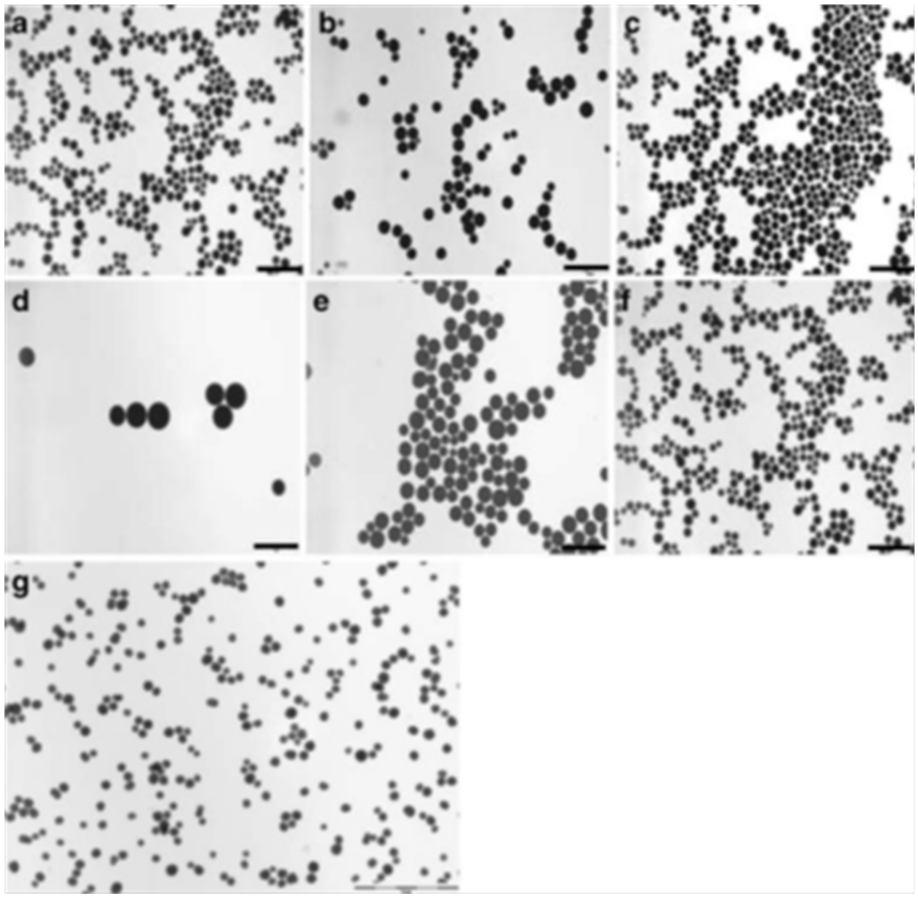

Figure 1. TEM images of nile blue-doped NPs synthesized using different cyclohexane volumes (**a**, **b** and **c**), different Triton X-100 concentrations (**d**, **e**, **f**) and those for nile-blue-APS doped silica NPs (**g**). Experimental conditions: 100 μl (0.44 mmol) TEOS, 0.2 ml of 1 x 10^{-3} M (0.2 μmol) nile blue, 3 ml (0.024 mol) hexanol, 70 μl (0.9 mmol) NH_4OH. In (**Figure 1a-c**): 510-520 mg (0.79-0.82 mmol) Triton X-100. In Fig. 1a 11.3 ml (0.63 mol) water, 0 ml cyclohexane, in **Figure 1b**, 7.5 ml (0.42 mol) water, 3.75 ml (0.034 mol) cyclohexane, in **Figure 1c** 3.8 ml (0.21 mol) water, 7.5 ml (0.068 mol) cyclohexane. In **Figure 1d-f** 11.3 ml (0.63 mol) of water, in **Figure 1d** 0 mg, in **Figure 1e** 310.9 mg (0.48 mmol), in **Figure 1f** 510.9 (0.79 mmol) of Triton X-100. Scale bar: 1 μm. In **Figure 1g** Experimental conditions: 510-520 mg (0.79-0.81 mmol) of Triton X-100, 10.3 ml (0.57 mol) of water, 100 μl (0.44 mmol) TEOS, 1.2 ml precursor reaction mixture, 3 ml (0.024 mol) hexanol, 70 μl (0.9 mmol) of NH_4OH. Scale bar: 2 μm.

The phases obtained were separated by centrifugation of the mixture at 2.000 rpm for 5 min. A precipitate appeared in the botton of the lower phase at reagent concentrations higher than the optimum values, which indicated the saturation of the upper phase. The analysis by TEM of the re-suspended solid revealed that it was mainly constituted by large size particles.

The distribution of the reagents in both phases is related with the total volume of solution, the volume of hexanol and the amount of surfactant used. The reduction of the water volume from 11.5 ml to 5 ml, keeping constant the amount of the other components, resulted in the no appearance of NPs after breaking the microemulsion, which would be ascribed to the change of the effective reagent concentrations.

The influence of water amount was studied by keeping constant the total mixture volume, and hence, the final concentrations of the synthesis components. Water volume was decreased from 12.5 ml to 7.3 ml, increasing hexanol volumes from 1.8 ml to 7 ml. The number of NPs decreased and their sizes were higher than 200 nm when the hexanol volume was higher than 3 ml, choosing this value as optimum.

The influence of the amount of Triton X-100 (Figure 2) showed that the number of nile blue-doped NPs increases and their size decreases as Triton X-100 amount increases. The best results were obtained using 510-520 mg of Triton X-100 (Figure 1f), because lower amounts gave NPs of sizes higher than 200 nm (Figure 1d and e). Very small and partially aggregated nanoparticles were obtained when the Triton X-100 amount was close to 1.0 g. It was also checked that the Triton X-100/hexanol ratio is a critical variable, as Figure 2 shows. As it can be seen, a ratio of 170 mg

Triton X-100/ml hexanol gave the maximum fluorescence intensity of the synthesized material. The amount of the surfactant used is relatively high, but is in agreement with the fact that the critical microemulsion concentration of a non-ionic surfactant in water-in-oil microemulsions is higher [10] than the critical micelle concentration of the same surfactant in water.

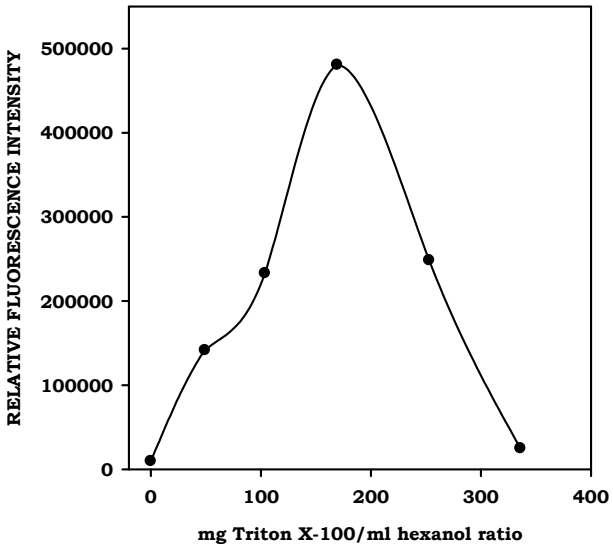

Figure 2. Influence of Triton X-100/hexanol ratio on the fluorescence intensity of nile blue-doped NPs. Experimental conditions: 11.3 ml (0.63 mol) of water, 100 μl (0.44 mmol) TEOS, 0.2 ml of 1 x 10^{-3} M (0.2 μmol) nile blue, 3 ml (0.024 mol) hexanol, 70 μl (0.9 mmol) NH_4OH.

The fluorescence intensity and the size of the NPs were evaluated modifying the temperature and the reaction time. Figure 3 shows the influence of these variables in the fluorescence intensity of nile blue-doped NPs, finding that the fluorescence increased from 25 to 35 °C, but it decreased at 45 °C. Although the fluorescence intensity was higher after 9 h

of reaction, the size of the NPs obtained also increased so, a time of 7.5 h was chosen as optimum. The NP sizes slightly decreased with increasing temperatures in the range of 25 – 45 °C. This study was also performed for cresyl violet doped-NPs finding similar results.

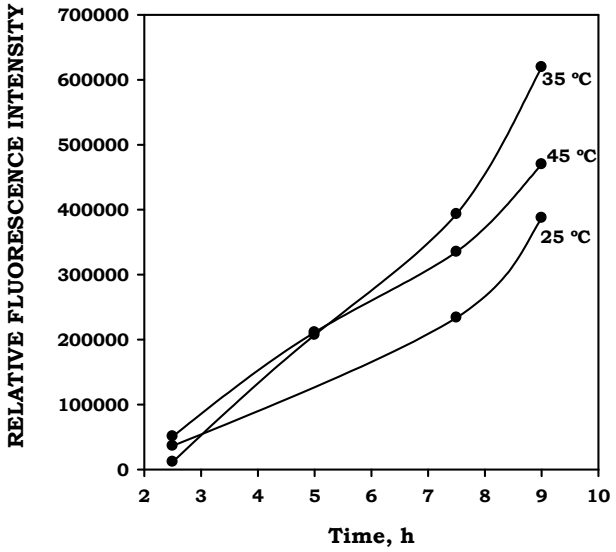

Figure 3. Influence of reaction time and temperature on the fluorescence intensity of nile blue-doped NPs. Experimental conditions: 510-520 mg (0.79-0.81 mmol) of Triton X-100, 11.3 ml (0.63 mol) of water, 100 μl (0.44 mmol) TEOS, 0.2 ml of 1 x 10^{-3} M (0.2 μmol) nile blue, 3 ml (0.024 mol) hexanol, 70 μl (0.9 mmol) NH_4OH.

The features of nile blue-doped NPs obtained after a reaction time of 7.5 h and at 35 °C are compared in Table 1 with the features of similar NPs obtained after 24 h at 25 °C. Some parameters were calculated in a similar way as described elsewhere [19] using 200 μl of 0.1 mg/ml NP dispersions in each well. The number of NPs was obtained by dividing the amount of NPs into the weight of one particle, which was calculated from

the volume of one particle (assuming that it is a perfect sphere and expressing the volume in mm^3) and multiplying this volume by the specific gravity of silica (2.3).

The intensity/particle ratio is defined as the fluorescence intensity divided by particle amount, and the specific intensity is the intensity/particle ratio divided by the volume of one particle. An increase in the synthesis time yields larger NPs, which are more luminescent, since the specific intensity, which is independent on the particle volume, is about 1.6 times higher than that of NPs obtained at 7.5 h and 35 °C.

Table 1. Comparison of the properties of nile blue-doped silica nanoparticles obtained at two reaction time and temperature values by the modified reverse-micelle microemulsion method

Conditions	**24 h, 25 °C**	**7.5 h, 35 °C**
Concentration	0.1 mg/ml	0.1 mg/ml
Amount (mg)	0.02	0.02
Mean diameter, nm	323	170
Particle volume, mm^3	1.76×10^{-11}	2.57×10^{-12}
Particle number	4.92×10^{8}	3.38×10^{9}
Intensity[a]	180927	111708
Intensity/particle ratio	3.67×10^{-4}	3.3×10^{-5}
Specific intensity	2.09×10^{7}	1.29×10^{7}

[a]Measurements performed in microplates (200 μl) using excitation and emission filters of 620/8 and 680/10 nm, respectively

The influence of ammonium hydroxide was studied in the range of 35 – 140 μl of a commercial concentrated solution (0.45 – 1.8 mmol). The number of nile blue-NPs formed was scarce at the limits of the assayed interval, being also the fluorescence intensity obtained quite low (Figure 4a). The size of the NPs obtained increased in the range of 70 – 610 nm of diameter as NH_4OH was increased. The decrease in the fluorescence intensity at high NH_4OH values would be ascribed to the partial degradation of the fluorofore in the alkaline medium, as it has been reported elsewhere for a cyanine dye [20]. The volume chosen as optimum was 70 μl (0.9 mmol).

The influence of TEOS was evaluated for nile blue NPs in the range of 50-800 μl (0.22 – 3.52 mmol). Increasing TEOS volumes, the size of NPs increased from 140 to 300 nm, obtaining sizes larger than 200 nm above 100 μl. These results were obtained under the optimal experimental conditions, excepting for the fluorophore amount, which was ten times lower than the optimum value. As it was found that the fluorescence intensity also increased with the TEOS amount, a compromised solution was adopted and 100 μl (0.44 mmol) of TEOS was chosen as the optimum value to obtain intermediate sizes and intensities.

The amount of fluorophore used is a critical variable. The volume of 1×10^{-3} M aqueous nile blue solution was varied from 100 μl to 7.2 ml by adjusting the total volume of the aqueous phase to 11.5 ml with distilled water, in order to keep constant the initial concentrations of the other reagents. The influence of this variable on the fluorescence intensity is shown in Figure 4b, in which can be seen that the maximum value was obtained using 1.8 μmol of nile blue. The decrease in the fluorescence

intensity at higher values is ascribed to the appearance of a coloured precipitate in the tube bottom after the centrifugation process, which was mainly formed by large size particles. The formation of fluorophore aggregates can also contribute to this behaviour as they are less fluorescent than their monomers [6].

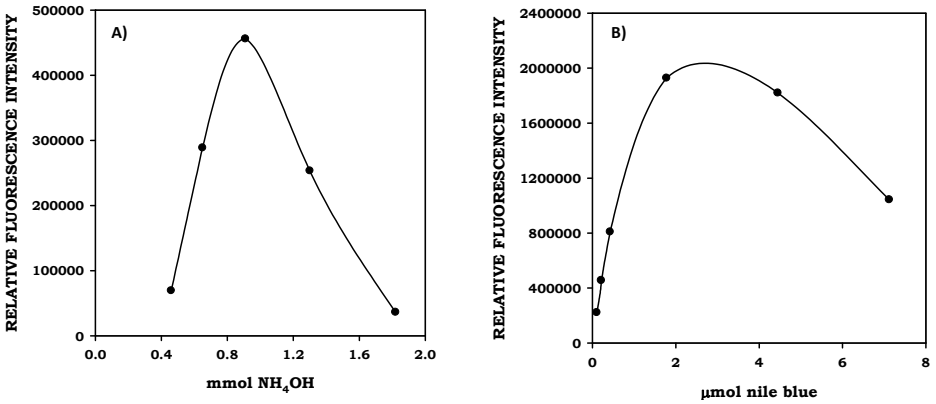

Figure 4. Influence of the amount of ammonium hydroxide (**A**) and nile blue (**B**) added on the fluorescence intensity of nile blue-doped NPs. Experimental conditions: 510-520 mg (0.79-0.81 mmol) of Triton X-100, 11.3 ml (0.63 mol) of water, 100 µl (0.44 mmol) TEOS, 3 ml (0.024 mol) hexanol. In **A**) 0.2 ml of 1 x 10^{-3} M (0.2 µmol) nile blue, in **B**) 70 µl (0.9 mmol) of NH_4OH.

The fluorophore concentration also affects the size of the NPs, which decreases until the amount of nile blue is 0.43 µmol, from which their diameter remains constant, with a mean value of about 170 nm. A similar behaviour was observed for cresyl violet-doped NPs.

The synthesis of precursors involving the covalent linking of the primary amino groups of the fluorophore and the silane derivative APS was assayed to obtain NPs less susceptible to dye leakage. It was found

that the use of equimolar ratios of nile blue and glutaraldehyde, and APS in an 8.5-fold molar excess, gave the best results in terms of fluorescence intensity of the NPs obtained. The time of reaction of the mixture was studied in the interval of 0 – 10 min, and 5 min were found to be enough, since larger irregular particles were obtained at longer reaction times. This mixture was used for the NP synthesis without any further purification step. The influence in the fluorescence intensity of the precursor volume added to the synthesis procedure was studied in the range of 0.6 – 2.4 ml, providing 1.2 ml of precursor the highest value. The mean size of the NPs synthesized by using 1.2 ml of precursor mixture was 150 nm, decreasing the size at higher volumes. Figure 1g shows the aspect of the NPs obtained using 1.2 ml of precursor, which are not completely spherical, although they have a uniform size with a relative standard deviation around 10%.

3.1.2. Optimization of the synthesis by the Stöber method

The approach used was similar to previously described methods for the encapsulation of a fluorescein-silane precursor and a ruthenium chelate [19, 21], which encompassed the use of an ethanol:water mixture as the medium for the hydrolysis and condensation of silane reagent. The application of this method has been carried out using cresyl violet as fluorophore, with the aim of comparing the features of the NPs obtained with those of the NPs obtained with the above described method.

Ethanol volume was assayed in the range of 10-25 ml (0.17 – 0.43 mol), obtaining the best fluorescence intensity values with the highest ethanol amount. This would be ascribed to the increase in the effective

fluorophore concentration at low volumes of ethanol, which gives rise to the formation of the non-fluorescent fluorophore dimers above mentioned.

The influence of water was studied in the range of 0.5-25 ml, yielding sizes below 180 nm, which increased (300-350 nm) when the water volume was 5-10 ml. This behaviour could be explained bearing in mind that the TEOS hydrolysis, which would be the limiting step at low water volumes, should be favoured by an increase in water volumes leading to faster NP synthesis and larger NP sizes. The use of 25 ml of water provided a lower amount of NPs, owing to the dilution of the reagents involved in the synthesis.

The optimization of the fluorophore amount, performed from 0.5 to 10 ml of 1 x 10^{-3} M (0.5 – 10 μmol) cresyl violet at a fixed water volume of 0.5 ml, showed that the best results were obtained for 0.5 μmol of fluorophore. The influence of TEOS was assayed in the range of 0.1 – 10 ml finding that NPs obtained at low TEOS volumes (0.1 – 2 ml) were practically monodisperse whereas those synthesized at higher TEOS volumes (5 – 10 ml) were quite irregular in shape and in size distribution.

Table 2 shows the comparison of the cresyl violet-doped silica NPs obtained by the modified reverse-micelle microemulsion and the Stöber methods. The excitation filter used for cresyl violet was 531/25 nm, which is an excitation wavelength shorter than the maximum, in order to minimize scattering phenomena. The specific intensity of the NPs obtained by the modified microemulsion method was about 12 times higher than that obtained by the Stöber procedure. This would be ascribed to the fact that cresyl violet is less degraded by the alkaline conditions owing to the protection that micelles can confer.

Table 2. Comparison of the properties of cresyl violet-doped NPs obtained by the proposed reverse-micelle microemulsion and Stöber methods

	Reverse micelle microemulsion method	**Stöber method**
Concentration, mg/ml	0.1	0.1
Particle amount, mg	0.02	0.02
Diameter, nm	178	133
Particle number	2.94×10^{9}	7.06×10^{9}
Intensity[a]	125563	10138
Intensity/particle ratio	4.27×10^{-5}	1.44×10^{-6}
Specific intensity	1.45×10^{7}	1.17×10^{6}

[a]Measurements were performed using microplates (200 μl) and excitation and emission filters of 531/25 and 620/8 nm, respectively

3.2. Fluorescence spectra of cresyl violet- and nile blue- silica NPs

The spectral features of the synthesized NPs were compared to those showed by pure dyes and by bare silica NPs. Figure 5 shows the emission spectra obtained at the maximum excitation wavelength of each fluorophore, in which can be seen that there is not appreciable fluorescent signal from bare silica NPs. The emission bands of the oxazine-doped silica NPs show a slight shift of approximately 9 nm towards shorter wavelengths. This behaviour is in accordance to the results obtained after encapsulating other fluorophores, such as fluorescein isothiocyanate or ruthenium dyes [6], which experienced shifts towards shorter and longer wavelengths, respectively. This fact could be ascribed to the interaction of the dyes, which are cationic, with the negatively charged silanol groups from the silica matrix. Figure 5 also shows that the emission spectrum for

nile blue-APS-doped NPs is practically the same as that obtained for nile blue-doped silica NPs.

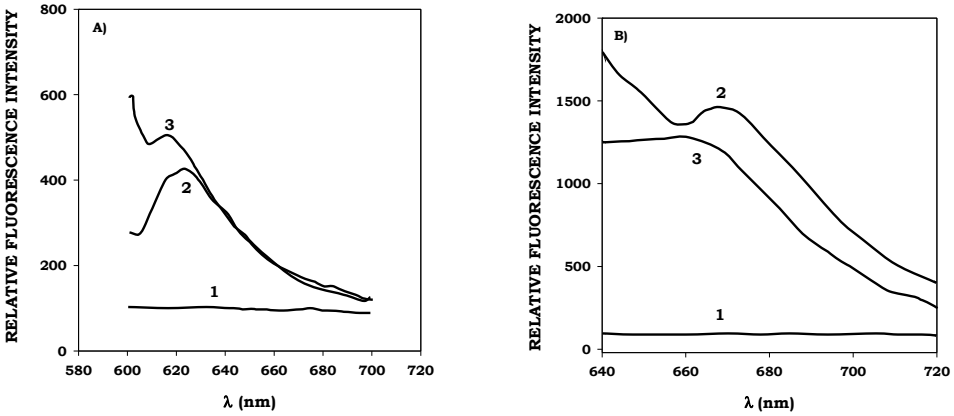

Figure 5. Emission spectra in distilled water of: bare silica NPs (**A.1, B.1**), 0.07 μM pure cresyl violet **(A.2**) and 0.5 μM nile blue (**B.2**) dye solutions, and cresyl violet-(**A.3**) and nile blue-doped (**B.3**) NPs, respectively.

3.3. Fluorescence stability of NPs

The suspensions of cresyl violet and nile blue NPs were divided in five aliquots of 1 ml each, which were stored at 4 °C. At the assay time, NPs were washed, centrifuged and re-dispersed in water. The fluorescence intensity was measured the same day that NPs were synthesized and 1, 2, 5 and 9 days later, using in all instances the same number of washes to each aliquot (three times with 1 ml of ethanol and four times with distilled water), until supernatant fluorescence close to blank signal. Under these conditions, the fluorescence intensity remained almost constant for at least 9 days without appreciable changes in the fluorescence intensity caused by dye leakage. The fluorescence intensity from nile blue- and nile blue-APS-doped NPs decreased after the seven washes, being the decrease of the first

NPs two fold that of the second ones, which would be ascribed to the covalent binding of the fluorophore to the silane reagent, which minimizes dye leakage.

Once the NPs were totally purified (supernatant fluorescence close to blank signal), they were subjected to additional subsequent washes with 1 ml of distilled water to study the potential dye leakage from the core of NPs, finding that the fluorescence of both nile blue- and nile blue-APS-doped NPs remained almost constant. The stability of nile blue-doped NPs could be ascribed to the abovementioned fact that nile blue is a cationic dye and would interact with the negative silanol groups from silica matrix. In this way, dye leakage would be less favoured than for anionic dyes, such as Cy5, which are more prone to repulsion forces with the silanol groups from silica matrix [12].

3.4. Photostability experiments

To investigate the potential photobleaching of the synthesized NPs in aqueous solution, they were irradiated for 1 h and the results were compared to those obtained for pure dye solutions (Figure 6). The intensity of pure cresyl violet (Figure 6a, curve 1) and nile blue (Figure 6b, curve 1) dropped until the 72% and the 65%, respectively, of the initial intensity. However, the fluorescence intensity of both cresyl violet NPs (Figure 6a, curve 2) and nile blue-doped NPs (Figure 6b curve 2) remained almost constant and the NPs prepared by using the nile blue-APS precursor (Figure 6b, curve 3) experienced a decrease by a 10% of the initial intensity. Similar results have been reported in recently synthesized NPs containing

Cy5 [12] and fluorescein [19], which confirm the increased photostability of encapsulated dyes due to the protection that silica matrix confers them.

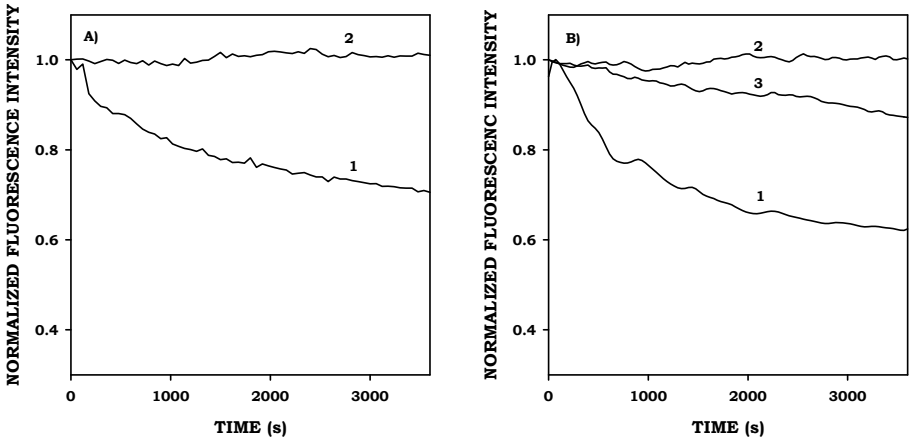

Figure 6. Photobleaching experiments for pure cresyl violet (**A.1**) and nile blue (**B.1**) solutions, respectively; cresyl violet (**A.2**) and nile blue-doped (**B.2**) NPs, respectively; and nile blue-APS-doped NPs (**B.3**).

4. Conclusions

The work presented here reports the synthesis of cresyl violet- and nile blue-doped silica NPs for the first time. The emission at long wavelengths of these NPs is a useful option to avoid the potential interferences of static background signals from sample matrix. The systematic study of the experimental variables involved in the synthesis process has given rise to the achievement of NPs with homogeneous size and high and stable fluorescence intensity. The modified reverse microemulsion method proposed precludes the use of cyclohexane as organic solvent, which is replaced by 1-hexanol. The use of the oxazine dye and the APS precursor to obtain the NPs has shown that the second one

reduces dye leakage in the purification process. The comparison of the luminescent properties of cresyl violet-doped NPs synthesized by microemulsion and Stöber methods has shown the usefulness of the first one to obtain more luminescent NPs.

The increased photostability of the synthesized NPs with respect to the pure dye proves the succesful dye encapsulation and the protection that silica matrix confers them. The features of the synthesized NPs seem to make them suitable as analytical reagents in fluoroimmunoassays after their functionalization, which is currently under research.

Acknowledgments

Authors gratefully acknowledge the financial support from the Spanish Ministerio de Educación y Ciencia (Grant No. CTQ2006-03263) and from the Autonomous Andalusian Government (Grant No. P06-FQM1356). They also acknowledge the technical assistance of the Electron Microscopy Section of the Central Service of Support to Research (SCAI) from the University of Cordoba.

References

(1) A. Gómez-Hens, J. M. Fernández-Romero, M. P. Aguilar-Caballos. Nanostructures as analytical tools in bioassays. *Trends Anal. Chem*. **(2008)** *27*, 394–406.

(2) J. Yan, M. C. Estévez, J. E. Smith, K. Wang, X. Ho, L. Wang, W. Tan. Dye-doped nanoparticles for bioanalysis. *Nanotoday* (**2007**) *2*, 44–50.

(3) M. Seydack. Nanoparticles labels in immunosensing using optical detection methods. *Biosens. Bioelectron*. **(2005)** *20*, 2454–2469.

(4) N. C. Tansil, Z. Gao. Nanoparticles in biomolecular detection. *Nanotoday* (**2006**) *1*, 28-37.

(5) G. Liu, Y. Lin. Nanomaterial labels in electrochemical immune-sensors and immunoassays. *Talanta* (**2007**) *74*, 308–317.

(6) G. Yao, L. Wang, G. Wu, J. Smith, J. Xu, W. Zhao, E. Lee, W. Tan. FloDots: luminescent nanoparticles. *Anal. Bioanal. Chem.* (**2006**) *385*, 518–524.

(7) F. Wang, W. B. Tan, Y. Zhang, X. Fan, M. Wang. Luminescent nanomaterials for biological labelling. *Nanotechnology* (**2006**) *17*, R1–R13.

(8) V. Wiwanitkit, A. Seereemaspun, R. J. Rojanathanes. Increasing the agglutination reaction in slide test for weak B blood group by gold nanoparticle solution: the first world report. *J. Immunol. Methods* (**2007**) *328*, 201–203.

(9) B. Du, Z. Li, Y. Cheng. Homogeneous immunoassay based on aggregation of antibody-functionalized gold nanoparticles coupled with light scattering detection. *Talanta* (**2008**) *75*, 959–964.

(10) F. J. Arriagada, K. Osseo-Asare. Synthesis of nanosize silica in a nonionic water-in-oil microemulsion: effects on the water/surfactant molar ratio and ammonia concentration. *J. Colloid Interf. Sci.* (**1999**) *211*, 210–220.

(11) X. Zhao, R. P. Bagwa, W. Tan. Development of organic-dye-doped silica nanoparticles in a reverse microemulsion. *Adv. Mater.* (**2004**) *16*, 173–176.

(12) X. He, J. Chen, K. Wang, D. Qin, W. Tan. Preparation of luminescent Cy5 doped core-shell SFNPs and its application as a near-infrared fluorescent marker. *Talanta* (**2007**) *72*, 1519–1526.

(13) X. L. Chen, J. L. Zou, T. T. Zhao, Z. B. Li. Preparation and fluoro-immunoassay application of new red-region fluorescent silica nanoparticles. *J. Fluoresc*. (**2007**) *17*, 235–241.

(14) W. Yang, C. G. Zhang, H. Y. Qu, H. H. Yang, J. G. Xu. Novel fluorescent silica nanoparticle probe for ultrasensitive immune-assays. *Anal. Chim. Acta* **(2004)** *503*, 163–169.

(15) S. R. Hu, J. M. Liu, T. L. Yang, H. Z. Lin, J. L. Huang, Q. W. Lin, G. H. Zhu, X. M. Huang. Determination of human alpha-fetoprotein (AFP) by solid substrate room temperature phosphorescence enzyme-linked immune response using luminescent nanoparticles. *Microchim. Acta* (**2005**) *152*, 53–59.

(16) A. Gómez-Hens, M. P. Aguilar-Caballos. Long-wavelength fluoro-phores: new trends in their analytical use. *Trends Anal. Chem.* (**2004**) *23*, 127–136.

(17) I. Hemmilä, V. Laitala. Progress in lanthanides as luminescent probes. *J. Fluoresc*. (**2005**) *15*, 529–542.

(18) A. Gómez-Hens, M. P. Aguilar-Caballos. Terbium-sensitized luminescence: a selective and versatile analytical approach. *Trends Anal. Chem.* (**2002**) *21*, 131–141.

(19) N. Nakamura, M. Shono, K. Ishimura. Synthesis, characterization, and biological applications of multifluorescent silica nanoparticles. *Anal. Chem.* (**2007**) *79*, 6507–6514.

(20) J. F. Bringley, T. L. Penner, R. Wang, J. F. Harder, W. J. Harrison, L. Buonemani. Silica nanoparticles encapsulating near-infrared emissive cyanine dyes. *J. Colloid Interf. Sci.* (**2008**) *320*, 132–139.

(21) L. M. Rossi, L. Shi, F. H. Quina, Z. Rosenzweig. Stöber synthesis of monodispersed luminescent silica nanoparticles for bioanalytical assays. *Langmuir* (**2005**) *21*, 4277–4280.

Analytica Chimica Acta 701 (2011) 194–199

Contents lists available at ScienceDirect

Analytica Chimica Acta

journal homepage: www.elsevier.com/locate/aca

Heterogeneous immunoassay for soy protein determination using nile blue-doped silica nanoparticles as labels and front-surface long-wavelength fluorimetry

J. Godoy-Navajas, M.P. Aguilar Caballos, A. Gómez-Hens

Department of Analytical Chemistry, Institute of Fine Chemistry and Nanochemistry (IAQFN). Campus of Rabanales. Marie Curie Building (Annex). University of Cordoba. 14071-Cordoba. Spain.

Abstract

A long-wavelength fluoroimmunoassay for the determination of soy protein is reported for the first time using a conjugate composed of anti-soy protein antibodies bound to nile-blue doped silica nanoparticles (NPs). These NPs have been synthesized by a reverse-micelle microemulsion method and functionalized by using 3-(aminopropyl)triethoxysilane (APS) and 3-(trihydroxysilyl)propyl methylphosphonate (THPMP) to avoid NP aggregation. The tracer has been obtained by linking the functionalized NPs with anti-soy protein antibodies previously oxidised with sodium periodate. The immunoassay has been developed in 96-well microplates using a heterogeneous competitive format with antibody capture. Soy proteins are immobilised onto the wells and bovine serum albumin is added to block the surface, thus minimising nonspecific binding. After washing, the microplates can be stored ready to use. At the analysis time, soy protein standards or sample and tracer are added and incubated and, after the corresponding washing and drying steps, the fluorescence is measured onto the solid surface at λ_{ex} 620 and λ_{em} 680 nm. The method features a dynamic range of 0.1 – 10 mg L^{-1} and a detection limit of 0.05 mg L^{-1}. The precision of the method has been assayed at 0.5 and 5 mg L^{-1} protein concentrations, obtaining the values of relative standard deviation of 9.6% and 6.1 %, respectively. This new immunoassay has been applied to the analysis of food containing soy protein and the results obtained have been compared to those provided by a commercial ELISA kit with no statistically differing results. Also, a recovery study has been performed, providing percentages in the range of 81.5 – 111.0 %.

Keywords: soy protein, food samples, long-wavelength fluorimetry, heterogeneous immunoassay, nile blue-doped silica nanoparticles

1. Introduction

In recent years, the global consumption of soy foodstuffs has increased because of their reported beneficial effects on nutrition and health, such as a decrease of the plasma cholesterol, prevention of cancer, diabetes and obesity, and protection against bowel and kidney disease [1]. Soybean proteins are used as additives in human foodstuffs, thus being marketed as different commercial formulations, such as soy flour, protein concentrates and isolates. These formulations are used to obtain better mechanical properties in soy milks, drinks, tofu and vegetarian meat substitutes and a number of new food varieties is being developed. However, soybeans contain proteins that can produce allergic responses in some people. The safe choice of processed foods free from soy proteins may become more critical for these patients because these proteins and their derivatives have been increasingly incorporated in a number of processed foods. The allergenicity of these proteins largely depends on the food processing, e.g. high temperature treatments and conjugation to some organic compounds, such as polysaccharides [2], among others.

Native soy proteins are globular proteins, mainly constituted by 7S and 11S (glycinin and conglycinin) fractions [3], which have been characterized and determined by liquid chromatography [4], electrophoresis [5] and immunoblotting [6]. Also, a number of enzyme-linked immunosorbent assays (ELISA) methods have been described for soy protein determination in different food samples [7-11], thus existing some commercial kits developed for this purpose [11]. Only few alternative approaches to the use of enzymes as labels have been reported for soy protein determination. A commercial four-channel optical biosensor based

on surface plasmon resonance (Biacore 3000) has been applied to the determination of several non-milk proteins, including soy proteins, in milk products [12]. An advantage of this method is that proteins are directly detected, avoiding the use of a label, but the relatively high cost of the instrument hinders its generalized use. Also, a more complex immunoassay has been described using an expensive flow analyzer (Luminex), fluorescent microspheres and a fluorophore (Alexa 532) as label of the proteins [13]. The use of nanoparticles (NPs) as labels for soy protein determination has been previously described in a homogeneous immunoassay in which the tracer, formed by gold NPs-soy protein antibodies, reacts with the analyte increasing the light scattering intensity of the solution [14].

The method presented here is a long-wavelength fluorimetric heterogeneous immunoassay using nile blue (NB)-doped silica NPs as label, which have been obtained by a relatively simple reverse-micelle microemulsion method [15]. This procedure has been slightly changed to achieve NP surface modification with amino- groups to be further linked to soy protein antibodies in order to develop the long-wavelength luminescent tracer. The use of silica NPs as labels in immunoassays with optical detection has very interesting features: 1) transparency of silica to visible light, 2) almost negligible photobleaching phenomena of encapsulated organic dyes, 3) stability of silica matrix at medium-term since it is not susceptible to microbiological degradation, and 4) porosity or swelling changes do not happen at moderate pH variations. An additional advantage of the use of NPs as labels is the decreased number of steps needed to perform this heterogeneous immunoassay compared to those

required for the development of ELISA assays, since the use of the enzyme conjugate and substrate solutions is avoided. To date, a limited number of immunoassays have been described which make use of biofunctionalized dye-doped silica nanoparticles [16]. These assays mainly involve the encapsulation of fluorescein and rhodamine derivatives, and ruthenium and lanthanide chelates to obtain luminescent silica NPs. The results obtained in these methods have shown that the sensitivity is greatly increased when compared with the corresponding immunoassays performed with direct fluorophore labeling.

To the best of our knowledge, the method reported here is the first heterogeneous immunoassay described for soy protein determination in food samples using NPs as labels. Two competitive formats involving antibody and antigen capture were assayed, but only the first one, in which soy proteins were immobilised on the wells of a microplate, gave rise to satisfactory results.

The method has been applied to the analysis of fruit and soy juice, soy yoghourt and milk samples and the results obtained have been compared to those provided by a commercial ELISA with no statistically relevant differences. Also, the detection limit using the reported method is about 10 times lower than the afforded by the commercial ELISA.

2. Experimental

2.1. Instrumentation

A 1420 Multilabel counter Victor ^{3}V microplate reader (Perkin Elmer and Analytical Sciences, Wallac Oy, Turku, Finland) was used to perform fluorescence measurements. Two filters (nominal

wavelength/passband) were used to select the excitation (620/8 nm) and emission (680/10 nm) wavelengths of the doped NPs. Fluorescence mesurements were performed using the stabilized energy mode of the instrument with an integration time of 1 s. NP size characterization was performed by transmission electron microscopy (TEM), using a CM10 Philips Microscope. Copper grids (200C-FC) coated with a Formvar® carbon film 200 mesh supplied by Aname (Madrid, Spain) were used as support for TEM experiments. Both 300-µL well Opti-plate and 100-µL well black and shallow Proxy-plate 96-well microplates (Perkin Elmer) were assayed as supports for the development of the heterogeneous immunoassay method.

2.2. Reagents

All the reagents were of analytical grade and used as supplied by the manufacturer. Tetraethyl orthosilicate (TEOS) and Triton X-100 were obtained from Fluka (Germany). Nile Blue chloride, 3-(trihydroxysilyl)propyl methyl-phosphonate monosodium salt, bovine serum albumin (BSA), polyclonal anti-soy protein antibodies (raised in rabbits), sodium borohydride, sodium acetate and sodium carbonate were supplied by Sigma-Aldrich (USA), and (3-aminopropyl)-triethoxysilane (APS) by Aldrich (Germany). 1-Hexanol and di-potassium hydrogen phosphate were acquired from Merck (Germany). Ammonium hydroxide (25% in NH_3), acetone and absolute ethanol were obtained from Panreac (Spain), sodium metaperiodate from Scharlau (Spain) and soy protein isolate, PROTEINA SUPRO 500E (90% protein content), was kindly gifted by DOSCADESA (Spain). Phosphate (0.02 M, pH 7.5), acetate (0.1 M, pH

5.5 and pH 4.8), and carbonate (0.05 M, pH 9.5) buffer solutions were prepared by dissolving the appropriate amount of these salts and adjusting the pH with either hydrochloric acid or sodium hydroxide when appropriate. A commercial ELISA kit (ELISA SYSTEMS, Windsor, Australia) for the determination of soy protein[11] was used for comparative purposes.

2.3. Procedures

2.3.1. Synthesis of amino-functionalized NB-doped silica NPs

The procedure used to synthesize NB-doped silica NPs is similar to a reverse-micelled microemulsion method previously reported [15], but it has been modified in the last step to provide the doped silica NP surface with amino groups to be linked to anti-soy protein antibodies, in order to give rise to the conjugate used as tracer.

Briefly, an amount of Triton X-100 (510-530 mg or 0.79-0.82 mmol) was dissolved in 9.6 mL (0.53 mol) of distilled water by stirring vigorously this mixture for 5 min. Then, a volume of 100 μL (0.44 mmol) of TEOS was added and the solution was stirred for 5 min. A volume (1.8 mL) of 10^{-3} M (1.8 μmol) NB solution was added and the mixture stirred again for 5 min. Afterwards, 3 mL (0.024 mol) of hexanol were added and the microemulsion formed was stirred for 15 min. Concentrated ammonium hydroxide (70 μL, 0.9 mmol) was then added and the mixture stirred for 5 min to start the TEOS hydrolysis and condensation reactions. The mixture was then placed in a thermostated tank at 25 °C for 24 h in the dark and, afterwards, it was centrifuged for 5 min at 2000 rpm to separate the phases involved. The upper phase (about 3 mL) was transferred to a 10-mL beaker

and 40 μL of APS and 80 μL of THPMP were added. This mixture was magnetically stirred during 1.5 h in a water bath to keep the temperature at 25 °C. Afterwards, the microemulsion was broken by adding 10 mL of acetone and stirring for 5 min. The supernatant was discarded and NPs were recovered from the bottom with 8 - 10 mL of distilled water. The mixture was centrifuged for 5 min at 10000 rpm and the NP precipitate was washed with ethanol and water until the fluorescence intensity of supernatants was similar to the blank. Finally, the NPs were re-dispersed in 1 mL of phosphate buffer solution.

2.3.2. Preparation of the NB-doped silica nanoparticles anti-soy protein antibody conjugate

A volume (50 μL) of anti-soy protein were diluted with 0.1 M sodium acetate solution (pH 5.5) until a volume of 2 mL, and 200 μL of 0.1 M sodium metaperiodate solution were added to this volume. The mixture was incubated for 20 min in the freezer at 0 °C and the reaction volume was layered on a HiTrap Desalting Column (GE Healthcare) equilibrated with 25 mL 0.1 M sodium acetate - 0.5 M sodium chloride solution (pH 4.8), at a 5 mL min^{-1} flow rate, and 300-μL fractions were taken. Their absorbance was monitored at 280 nm and the anti-soy protein was recovered from the first seven fractions, accounting for about 2 mL of solution. This volume was added to the amino-modified NB-doped silica NPs, which had been previously centrifuged to remove phosphate buffer solution. The mixture was incubated for 20 h at 4 °C, in a similar way as previously described elsewhere [17]. Then, 50 μL of 0.66 M $NaBH_4$ solution were added to the dispersion and allowed to react for 20 min at 4 °C.

Afterwards, the reaction mixture was centrifuged and the NP-anti-soy protein conjugate obtained was washed with phosphate buffer solution. Finally, NPs were re-dispersed in 1 mL of the same phosphate buffer solution and stored at 4 °C for further use.

2.3.3. Preparation of soy standard

The procedure used involves a denaturation-renaturation process, according to the procedure indicated by the anti-soy protein antibody supplier, as follows: an amount of soy protein isolate (50 mg) was placed in a glass test tube and mixed with 3 g of urea, 1 mL of 0.001 M TRIS-HCl buffer solution of pH 8.6, 0.1 mL of 2-mercaptoethanol and water. The total volume of the reaction mixture did not exceed 5 mL. The test tube was sealed with a cap and aluminum foil and the tube was placed in a boiling water bath for 2 h. After this time, the tube was cooled for 5 min in cold water and the reaction mixture was diluted to 10 mL with distilled water. This solution can be stored at 4 °C in the fridge for a month. Working standard solutions were daily prepared by diluting this stock solution in phosphate buffer solution.

2.3.4. Determination of soy protein

A volume (80 μL) of a 5 mg L^{-1} soy protein solution prepared in carbonate buffer solution was added to each well, and the microplate was incubated overnight at 4 °C. Afterwards, wells were washed three times with distilled water and then, 80 μL of a 0.01 % BSA solution prepared in phosphate buffer were added to each well. The microplate was stirred for 1

h at room temperature, it was washed for three times with phosphate buffer solution and then, it was stored at 4 °C until use.

To perform the immunoassay, a volume (60 μL) of a pre-incubated mixture, prepared by mixing 75 μL of NB-doped silica NPs-labeled anti-soy protein antibody (20 nM) in phosphate buffer solution (0.02 M, pH 7.5), and 225 μL of soy protein standard or sample solution (0.1-10 μg mL^{-1}) were added to each well. The microplate was incubated for 1.5 h at 37 °C, the wells were washed three times with the same phosphate buffer solution, and the plate was dried for 10 min at room temperature. Then, the measurements were directly performed onto the solid surface of the well.

2.3.5. Determination of soy protein in food samples

An amount (0.85 mL or g of soy milk and yoghourt, respectively, and 1.7 g of fruit and soy juice) of food sample was treated in the same way as described above for soy protein standards.

The sample extracts were diluted (1:2000) in phosphate buffer solution and 225 μL of this solution were analysed following the above mentioned procedure for soy protein determination.

3. Results and discussion

3.1. Choice and optimization of the immunoassay system

The synthesis and optical properties of NB-doped silica NPs used to obtain the tracer have been recently described [15]. These NPs feature low photobleaching phenomena because of the protection that silica matrix confers them and good stability owing to the interaction of the fluorophor NB with silica matrix. However, the surface functionalization to introduce

reactive groups to couple these NPs to either analytes or antibodies, is described here for the first time. The NP surface was functionalized with amino groups using APS as reagent, which has been previously described for this purpose [18]. This process can lead to aggregation phenomena because of the accumulation of positive charges at physiological pH onto their surface. Thus, the amine-modified silica NPs can back bond to residual silanol groups, as it has been reported elsewhere [19], leading to a very low charge in the surface, which originates NP aggregation. The use of a silane reagent containing phosphonate groups, such as THPMP, can partially or totally avoid this effect since more electrostatic repulsions are created among NPs, which contribute to their dispersion. Thus, at the end of the synthesis of NPs once the phase separation was performed, the upper layer, which is rich in NB and hexanol, was taken and different mixtures of APS and THPMP were assayed. Volumes ranging from 10 to 40 μL of APS and from 20 to 160 μL of THPMP, in volume ratios in the range of 1:1 to 1:16, were used. It was found by TEM that the addition of these reagents in an 1:2 APS:THPMP volume ratio gave rise to non-aggregated silica NPs. Several volumes at the 1:2 APS:THPMP ratio were assayed to check out which volumes would give rise to a suitable amount of amino groups, and the confirmation of their presence was followed by a fluorescamine method [20]. The highest fluorescence intensity was obtained using 40 μL of APS and 80 μL of THPMP, being these volumes chosen to perform the functionalization.

The temperature of the functionalization was assayed in the range of 0 - 37 °C. Temperatures above 25 °C increase the hydrolysis rate of APS and can lead to aggregation phenomena, thus selecting 25 °C for the

development of the reaction. The reaction time was also studied from 30 min to 2 h, finding that 1.5 h provided a silica shell incorporating enough amino groups to perform the further conjugation chemistry. Under these conditions, the NB-doped silica NPs obtained featured a mean diameter of 257 nm, measured by TEM (Figure 1).

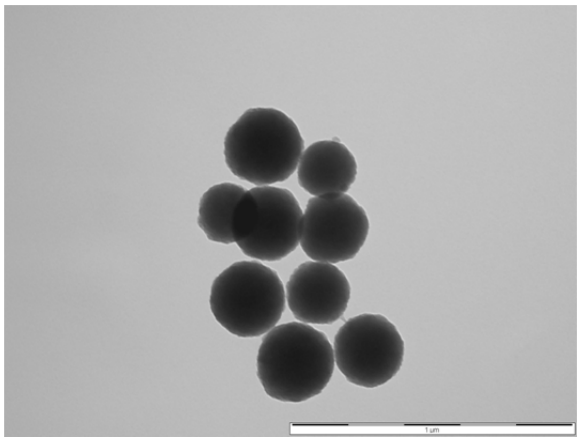

Figure 1. TEM image of functionalized NB-doped-silica NPs.

These NPs were coupled to soy protein and to anti-soy protein antibodies to study the potential use of the corresponding tracers for the development of two different heterogeneous competitive formats: with antigen capture and with antibody capture. The first involved the immobilisation of anti-soy protein antibodies onto the wells, after the previous immobilisation of anti-rabbit IgG antibodies, and the use of the tracer composed of soy protein linked to NB-doped silica NPs. Although the well surface was coated with BSA at different concentrations, there were still non-specific interactions of the tracer with anti-rabbit IgG

antibodies. To overcome this problem, the use of the antibody capture format was assayed. Thus, soy proteins were immobilised first onto the wells, and the remaining sites of the well were blocked with BSA. Then, a preincubated mixture of soy protein standards or sample together with a conjugate anti-soy protein-NB-doped silica NPs (tracer) was added, competing both immobilised and in solution soy proteins for the active sites of the conjugate. After washing, the fluorescence from bound tracer fraction was measured. The performance of fluorescence measurements onto the well surface was investigated assaying 100-μL proxy-plate and conventional 300-μL Optiplate microplates. The signal obtained using proxy-plates was slightly better, which could be ascribed to that well bottom can be more easily approached by the detection system using these plates. Also, an additional advantage is the use of lower volumes, which considerably reduces immunoassay costs.

The synthesis of the tracer encompassed the previous oxidation of carbohydrate moieties of antibody molecule to give rise to aldehyde moieties, which react to NP surface amino groups giving rise to Schiff bases that can be further reduced using sodium borohydride [17].

After the oxidation of the antibody with sodium metaperiodate, it is necessary to perform a purification step using commercial desalting columns to remove the excess of oxidant in order to proceed with the next step, taking 300-μL fractions. These fractions were selected by measuring their absorbance at 280 nm. Once the antibody and NPs were coupled, the reaction mixture was purified by subsequent washing and centrifugation steps with phosphate buffer solution, being finally stored in this buffer.

The optimisation of the system was carried out by modifying the experimental conditions at different soy protein concentrations. The concentration of immobilized soy protein onto the wells is an important variable on the system, which influences the assay sensitivity, since immobilised and in solution soy protein compete for the active sites of the tracer. The influence of this variable was assayed in the range of 1 to 50 mg L^{-1}, finding that 5 mg L^{-1} provided the best results as the dynamic range obtained for the calibration curve was wider and the sensitivity obtained was also better than those obtained at higher or lower concentrations. BSA has been used to block the remaining free sites of plate surface after soy protein immobilization. The influence of BSA concentration was checked out in the range of 0.001 - 0.1%, finding that 0.01% BSA was enough at the incubation conditions assayed (1 h, room temperature) (Figure 2A).

BSA concentrations above 0.01% led to a sensitivity decrease, whereas some non-specific interactions with the well surface were observed at lower BSA concentrations, since a higher background signal was obtained for high analyte concentrations.

The sensitivity of the assay also depends on the tracer concentration, as Figure 2B shows, being the best results obtained at 20 nM. Although the signals obtained at concentrations above 20 nM were higher, the assays were less sensitive, since the dynamic range was shifted to soy protein concentrations higher than 0.1 mg L^{-1}.

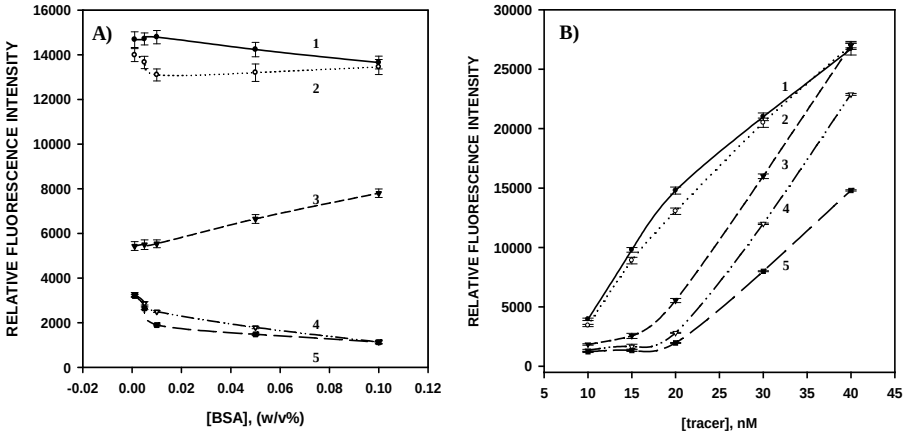

Figure 2. Influence of BSA (**A**) and tracer (**B**) concentrations on the assay in the presence of different soy protein concentrations (mg L^{-1}): 1) 0.0; 2) 0.1; 3) 1.0; 4) 5.0; 5) 10.0. [tracer] = 20 nM in (**A**). [BSA] = 0.01% in (**B**). Other experimental conditions in both (**A**) and (**B**) are: [immobilized soy protein] = 5 mg L^{-1}, assay incubation time = 1.5 h, temperature = 37 °C.

The study of incubation temperature influence showed that the assay sensitivity was better at 37 °C. The incubation time was investigated from 15 min to 3 h, finding that 1.5 h was enough to achieve an adequate signal. Although the signal increased slightly at longer times, the results were less reproducible, which could be ascribed to a higher probability of nonspecific interactions with the plate.

3.2 Analytical features

Fluorescence intensity measurements were performed by selecting the most appropriate filters to fix the maximum excitation and emission wavelengths for the tracer, λ_{ex} 620 and λ_{em} 680 nm. The method presented a dynamic range of 0.1 - 10 mg L^{-1} (Figure 3).

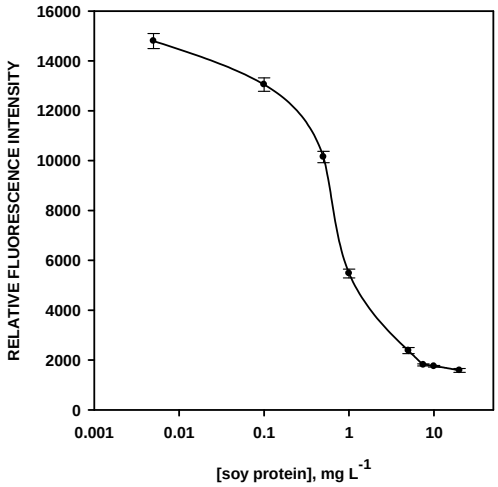

Fig. 3. Calibration curve obtained under optimum conditions.

The calibration curve was adjusted to a 4-parameter sigmoidal curve using the software Sigma Plot 2001, which equation is:

$$y = y_0 + \left(\frac{a}{1 + e^{\frac{-(x - x_0)}{b}}}\right),$$

where y is the fluorescence intensity and x is the decimal logarithm of soy protein concentration expressed in mg L^{-1}. The values of the regression parameters a, b, x_0 and y_0 were (1.12 ± 0.04) x 10^4, -0.17 ± 0.02, -0.13 ± 0.02, and (1.9 ± 0.2) x 10^3, respectively. The value of the regression coefficient was 0.9989. The detection limit, calculated according to IUPAC recommendations [21], was 0.05 mg L^{-1}, which is about ten times lower than that provided by the ELISA kit used as reference method [11]. The precision, expressed as the percentage of relative standard deviation and assayed at two different soy protein concentrations, 0.5 and 5 mg L^{-1}, gave values of 9.6% and 6.1 %, respectively.

The selectivity of the method mainly depends on anti-soy protein antibodies selectivity. According to the antibody specification sheet, these antibodies present some cross-reactivity towards hot urea extracts of wheat and ovalbumin, but no cross-reactivity is observed in extracts from meat, corn or casein, and rice or potato flour.

Additionally, in a previous work that involved the use of the same anti-soy protein antibodies [14], it was found that bovine serum albumin , γ-globulins, myoglobin and hemoglobin were tolerated in excess higher than 80-fold the analyte concentration.

3.3 Applications

The method was applied to the analysis of milk, yoghourt and fruit juice samples containing soy proteins. The sample treatment includes the same procedure used for soy protein standard preparation to obtain soy protein with a suitable conformation to be recognized by the antibody. Similar procedures have been used for the treatment of some food samples in immunoassays intended for soy protein determination [22]. These samples were also analysed using a commercial ELISA kit [11], thus being extracted using a commercial extraction solution for samples containing polyphenols, according to the protocol given by the manufacturer.

Table 1 shows the soy protein content found by the reported immunoassay and the ELISA method, which were compared by a paired *t*-test carried out at a 95% significance level, finding that there were not statistically relevant differences between them.

Table 1. Determination of soy protein content in food samples

Sample	Reported method[a, b]	Commercial ELISA[a, b]
Soy milk	74 ± 6	84 ± 3
Fruit and soy juice	8.4 ± 0.7	10.5 ± 0.3
Soy yoghourt	64 ± 4	60 ± 3

[a]Mean ± SD (n =3)

[b]Units: fruit and soy juice, soy yoghourt are expressed in g kg^{-1}, soy milk units are g L^{-1}

A recovery study was also carried out to validate the method (Table 2). It was performed by adding three different amounts of soy protein to each sample and subtracting the results obtained from similarly treated non spiked samples. The values obtained ranged from 81.5 and 111.0 %.

Table 2. Recovery of soy protein added to food samples

Sample	Added[a, b]	Found[a, b]	Recovery (%)
Soy milk	24	27 ± 2	111.0
	72	69 ± 4	95.7
	123	110 ± 10	89.4
Fruit and soy juice	2.7	2.2 ± 0.2	81.5
	8.1	7.7 ± 0.6	95.1
	13.5	12 ± 1	88.9
Soy yoghourt	23	21 ± 2	91.3
	65	61 ± 4	93.2
	113	95 ± 7	84.1

[a]Mean ± SD (n =3)

[b]Units: fruit and soy juice, soy yoghourt are expressed in g kg^{-1}, soy milk units are g L^{-1}

4. Conclusions

The reported method can be regarded as a useful alternative to enzyme-linked immunosorbent assays , since the use of enzyme conjugate and substrate solutions are avoided, thus decreasing the number of steps required. In addition, the detection limit achieved with the reported method is lower than that provided by some ELISA assays described for this purpose [11]. The use of the 96-well format ensures the automation of the assay together with a relatively high sample throughput compared to other methods, which include sequential operations. Proxy-plates allow the use of lower sample and tracer volumes than conventional 300-µL wells, which contribute to minimize the costs associated to the immunoassay.

The results obtained for the analysis of real food samples using the reported method are in accordance with those provided by an ELISA method used as a reference, which indicates the practical usefulness of the developed method.

Acknowledgements

Authors gratefully acknowledge financial support from the MICINN (Grant No. CTQ2009-08621), from the Junta of Andalucia (Grant No. P09-FQM4933) and from the FEDER-FSE Program (Grant No. P09-FQM4933). J. Godoy Navajas thanks the Junta of Andalucia (Grant No. P09-FQM4933) for the financial support of his pre-doctoral fellowship.

References

(1) M. Friedman, D.L. Brandon. Nutritional and health benefits of soy proteins. *J. Agr. Food Chem*. (**2001**) *49*, 1069–1086.

(2) E. F. E. Babiker, A. Hiroyuki, N. Matsudomi, H. Iwata, T. Ogawa, N. Bando, A. Kato. Effect of polysacchraride conjugation or transflutaminase treatment on the allergenicity and functional properties of soy protein. *J. Agr. Food Chem*. (**1998**) *46*, 866–871.

(3) H.D. Belitz, W. Grosch, P. Schieberle, Food Chemistry, 3rd ed., Springer-Verlag, 2004, p.750.

(4) J.H.G. Cordewener, D.M.A.M. Luykx, R. Frankhuizen, M.G.E.G. Bremer, H. Hooijerink, A.H.P. America. Untargeted LC-Q-TOF mass spectrometry method for the detection of adulterations in skimmed-milk powder. *J. Sep. Sci*. (**2009**) *32*, 1216–1223.

(5) M. De Angelis, R. Di Cagno, F. Minervini, C.G. Rizzello, M. Gobbetti. Two-dimensional electrophoresis and IgE-mediated food allergy. *Electrophoresis* (**2010**) *31*, 2126–2136.

(6) H.B. Krishnan, W.S. Kim, M.S. Kerley. All three subunits of soybean β-Conglycinin are potential food allergens. *J. Agr. Food Chem*. (**2009**) *57*, 938–943.

(7) D.L. Brandon, M. Friedman. Immunoassays of soy proteins. *J. Agr. Food Chem*. (**2002**) *50*, 6635–6642.

(8) J.M. Yeung, P.G. Collins. Determination of soy proteins in food products by enzyme immunoassay. *Food Technol. Biotechnol*. **(1997)** *35*, 209 - 214.

(9) L. Sánchez, M.D. Puyol, M. Calvo, G. Brett, T.M.P. Cattaneo, W. Haasnoot, R. López-Fandino, M.A. Manso, L. Mata, P. Razquín, A.

Sánchez, C. Svenning, G.E. Vegarud. Determination of vegetal proteins in milk powder by enzyme-liked immunosorbent assay: Interlaboratory study. *J. AOAC Int*. (**2002**) *85*, 1390–1397.

(10) A.F. González-Córdova, A.M. de la Barca, M. Cota, B. Vallejo-Córdoba. Immunochemical detection of adulteration of pork chorizo sausage with soy protein. *Food Sci. Technol. Int.* (**1998**) *4*, 257–262.

(11) L. L'Hocine, J.I. Boye, C. Munyana. Detection and quantification of soy allergens in food: study of two commercial enzyme-linked immunosorbent assays. *J. Food Sci*. (**2007**) *72*, C145–C153.

(12) W. Haasnoot, K. Olieman, G. Cazemier, R. Verheijen. Direct biosensor immunoassays for the detection of nonmilk proteins in milk powder. *J. Agr. Food Chem*. (**2001**) *49*, 5201–5206.

(13) W. Haasnoot, J.G. Du Pré. Luminex-based triplex immunoassay for the simultaneous detection of soy, pea, and soluble wheat proteins in milk powder. *J. Agr. Food Chem*. (**2007**) *55*, 3771–3777.

(14) M.L. Sánchez-Martínez, M.P. Aguilar-Caballos, A. Gómez-Hens. Homogeneous immunoassay for soy protein determination in food samples using gold nanoparticles as labels and light scattering detection. *Anal. Chim. Acta* (**2009**) *636*, 58–62.

(15) J. Godoy-Navajas, M.P. Aguilar-Caballos, A. Gomez-Hens. Synthesis and characterization of oxazine-doped silica nanoparticles for their potential use as stable fluorescent reagents. *J. Fluoresc*. (**2010**) *20*, 171–180.

(16) D. Knopp, D. Tang, R. Niessner. Review: bioanalytical applications of biomolecule-fuctionalized nanometer-sized doped silica particles. *Anal. Chim. Acta* (**2009**) *647*, 14–30.

(17) V.S. Prisyaznoy, M. Fusek, Y.B. Alakhow. Synthesis of high-capacity immunoaffinity sorbents with oriented immobilized immunoglobulins or their F_{ab} fragments for isolation of proteins. *J. Chromatogr*. (**1988**) *424*, 243–253.

(18) J. Yan, M. C. Estévez, J. E. Smith, K. Wang, X. He, L. Wang and W. Tan. Dye-doped nanoparticles for bioanalysis. *NanoToday* (**2007**) *2*, 44–50.

(19) R.P. Bagwe, L.R. Hilliard, W. Tan. Surface modification of silica nanoparticles to reduce aggregation and nonspecific binding. *Langmuir* (**2006**) *22*, 4357–4362.

(20) T. Bantan-Polak, M. Kassai, K.B. Grant. A comparison of fluorescamine and naphthalene-2,3-dicarboxaldehyde fluorogenic reagents for microplate-based detection of amino acids. *Anal. Biochem*. (**2001**) *297*, 128–136.

(21) G.L. Long, J.D. Winefordner. Limit of detection: a closer look at the IUPAC definition. *Anal. Chem*. (**1983**) *55*, 712A - 724A.

(22) J. Belloque, M.C. García, M. Torre, M.L. Marina. Analysis of soyabean proteins in meat products: a review. *Crit. Rev. Food Sci. Nutr*. (**2002**) *42*, 507 - 532.

Determination of monensin in milk samples by front-surface long-wavelength fluoroimmunoassay using nile blue-doped silica nanoparticles as labels

Juan Godoy-Navajas, Maria Paz Aguilar-Caballos, Agustina Gómez-Hens
Department of Analytical Chemistry. Institute of Fine Chemistry and Nanochemistry (IQFN). Campus of Rabanales. Annex to Marie Curie (C-3) Building. University of Cordoba.14071-Cordoba. Spain.

Abstract

A heterogeneous immunoassay for monensin determination in milk samples using a tracer formed by anti-monensin antibodies bound to nile blue (NB)-doped silica nanoparticles (NPs), 96-well microplates as solid supports and long-wavelength fluorescence measurements is described for the first time. The assay relies on the competition of the monensin present in the samples with a monensin-bovine serum albumin conjugate, which was immobilized onto the well surface, for the active sites of anti-monensin antibodies. After subsequent incubation and washing steps, the fluorescence of the bound tracer fraction is measured onto the dry surface of the well. An antigen capture format was also assayed by immobilizing anti-sheep IgG previously to the incubation of sheep anti-monensin antibodies and using a tracer formed by monensin bound to nile blue-doped silica NPs, which competes with the analyte for binding the immobilized antibody. Although the fluorescence signal obtained in both formats can be correlated to the analyte concentration, better results were obtained using the antibody capture format. After the optimization of the system using this format, the method features a detection limit of 0.015 μg L^{-1} and a dynamic range from 0.05 to 5 μg L^{-1}. The precision, assayed at two different analyte concentrations, 0.2 and 1 μg L^{-1}, and expressed as relative standard deviation, gave values of 5.9% and 4.0%, respectively. The method was satisfactorily applied to the analysis of milk samples, which only required a simple extraction step in order to remove the proteins from samples, giving recoveries in the range 83.3 - 107.5%.

Keywords: monensin; milk samples; long-wavelength front-surface fluorescence; immunoassay; nile-blue-doped silica nanoparticles

1. Introduction

Monensin is a veterinary drug polyether ionophore produced by *Streptomyces cinnamonensis* that exhibits both antibacterial and anticoccidial activities and has been traditionally used to prevent coccidiosis in poultry [1]. This antibiotic has been considered as a growth-promoter, since this disease prevents the growth of poultry owing to the bloody diarrhea and weight loses associated. Although the use of many veterinary antibiotics as growth promoters has been banned since 2006, they can be still administered to some species according to the EU Regulation 1831/2003/EC [2]. Also, the treatment with monensin has been extended to calves for which the EU has set maximum residue limits (MRL) of 2 $\mu g\ kg^{-1}$ in bovine muscle, kidney and milk, 10 $\mu g\ kg^{-1}$ in fat and 30 $\mu g\ kg^{-1}$ in liver, the residues being determined in all the samples as unchanged monensin, as stated in the 37/2010/EC regulation [3].

The concern on food safety has led to the search for reliable analytical methods to screen and confirm the presence of antibiotic residues in foodstuffs to reduce the increasing bacterial resistance to antibiotics. The determination of polyether ionophore antibiotics has been traditionally performed using liquid chromatographic methods with UV and fluorometric detection after their derivatization [4, 5]. This step is required owing to the lack of suitable chromophore and/or fluorophore groups in their structure, except for lasalocid, which has been determined by measuring its intrinsic fluorescence [4].

Nowadays, several LC-MS/MS methods have been developed for the determination of cocciodiostats [6 - 10] and for multiclass residue analysis including the ionophore class [11 - 13]. These confirmatory

methods require the availability of a sophisticated and expensive technique and, sometimes, are time-consuming owing to the extraction and further clean-up procedures involved. For this reason, the use of screening methods plays two essential roles: in one hand, the number of samples subjected to confirmatory analysis is lower and, on the other, the cost of the analysis is reduced. Immunoassays, whenever used in a quantitative or semi-quantitative way, have shown their usefulness as screening methods for antimicrobial residues in foodstuffs [14 - 21]. Several commercial and non-commercial enzyme-linked immunosorbent assays (ELISAs) have been described for the determination of monensin in biological [14 - 18] and environmental [19] samples. Most of these methods involve the use of photometric measurements, reaching detection limits close to 1 ng mL^{-1}, but a lower detection limit (0.06 ng mL^{-1}) has been reported using chemiluminescence detection [18]. Also, time-resolved fluoroimmunoassays involving the use of an europium (III) chelate as label have been described for monensin determination [20, 21], but the detection limit reached is very similar to those obtained using ELISA with photometric detection.

The use of functionalized inorganic matrix nanoparticles (NPs) as alternative labels in immunoassay is a relatively new trend justified by their versatile physicochemical properties which allow the improvement of the features of these assays [22 - 25]. Among these NPs, doped silica NPs are a useful option owing to their chemical and thermal stability, fine dispersion in aqueous solution, transparency to visible light, capability to encapsulate a wide variety of compounds and relatively inert environmental behavior, in addition to their large surface area and easy

surface functionalization [25]. These properties have given rise to a great variety of immunoassay methods, which have been mainly devoted to the determination of macromolecules, such as tumor markers [23, 24].

The immunoassay reported here shows the usefulness of nile blue (NB)-doped silica NPs as labels for the determination of monensin in milk samples using long-wavelength fluorescence measurements, which provide the spectral selectivity required to avoid interferences from the sample matrix. The synthesis and optical properties of these NPs have been recently reported [26]. Although a limitation of dye-doped silica NPs is the potential dye leakage, owing to the porosity of silica material, NB-doped silica NPs show an excellent stability, which is ascribed to the interaction of the cationic dye with the negative silanol groups from silica matrix. These NPs have been used as labels in a heterogeneous immunoassay for soy protein determination in several food samples [27], reaching a detection limit about 10 times lower than the afforded by a commercial ELISA kit available for the determination of these proteins.

To the best of our knowledge, the method proposed here is the first immunoassay for monensin determination using NPs as labels, which shows their capability to improve the analytical features, such as the detection limit, of the immunoassays previously described for the determination of this drug [14 - 18, 20, 21]. Although most of these assays are applied to the analysis of plasma and liver samples, milk samples have been chosen in this instance because they are easily obtained and allow a non-invasive detection of monensin for its safe use in milk producing animals. The sample treatment is quite simple as it only requires a deproteinization step and a suitable dilution.

2. Experimental

2.1. Instrumentation

A 1420 Multilabel counter Victor ^{3}V microplate reader (Perkin Elmer and Analytical Sciences, WallacOy, Turku, Finland) was used to perform fluorescence measurements. Two filters (nominal wavelength/passband) were used to select the excitation (620/8 nm) and emission (680/10 nm) wavelengths of the doped NPs. An additional filter (531/25 nm) was used to perform absorbance measurements using the Komarowsky reaction in order to calculate monensin concentrations. Fluorescence measurements were performed using the constant voltage mode of the instrument with an integration time of 1 s. NP size characterization was performed by TEM as described elsewhere [26, 27]. Black and shallow 100-μL well proxy-plate 96-well microplates (Perkin Elmer) were assayed as support for the development of the heterogeneous immunoassay method.

2.2. Reagents and solutions

All the reagents were of analytical grade and were used as supplied by the manufacturer. Triton X-100, NB chloride, sodium acetate, sodium chloride, sodium borohydride, monensin sodium salt, anhydrous N-dimethylformamide (DMF), N-hydroxysulfosuccinimide sodium salt (sulfo-NHS), N-(3-dimethylaminopropyl)-N′-ethylcarbodiimide hydrochloride (EDAC), bovine serum albumin (BSA) and sodium carbonate were obtained from Sigma-Aldrich (USA). Tetraethyl orthosilicate (TEOS), (3-aminopropyl)-triethoxysilane (APS), 3-(trihydroxysilyl)propylmethylphosphonate monosodium salt (THPMP) and vanillin were supplied by

Aldrich (Germany). 1-Hexanol and di-potassium hydrogen phosphate were acquired from Merck (Germany). Acetone, absolute ethanol, sodium tetraborate, sulphuric acid and methanol were obtained from Panreac (Spain), sodium metaperiodate from Scharlau (Spain) and sheep polyclonal antibody to monensin was supplied by Abcam (United Kingdom).

NB solution was prepared in distilled water according to the aforementioned procedures [26, 27]. A 1.0 g L^{-1} stock solution of monensin was prepared by dissolving the appropriate amount of monensin sodium salt in ethanol. Intermediate and working monensin solutions were prepared by further dilution in phosphate buffer solution (0.015 M, pH 8.0). Phosphate (0.015 M, pH 8.0), acetate (0.1 M, pH 5.5 and pH 4.5), and carbonate (0.05 M, pH 9.0) buffer solutions were prepared by dissolving the appropriate amount of these salts and adjusting the pH with either hydrochloric acid or sodium hydroxide when appropriate. The Komarowsky reagent solution [5, 28] was prepared by dissolving vanillin (4 g) in methanol, adding 2 mL of concentrated sulphuric acid to adjust the pH and raising the mixture to 100 mL with methanol. This solution was freshly prepared whenever used.

2.3. Procedures

2.3.1. Synthesis and functionalization of NPs

The procedure used to synthesize NB-doped silica NPs is similar to a reverse-micelle microemulsion method previously reported [26, 27]. Briefly: an amount of Triton X-100 (510 - 530 mg or 0.79 - 0.82 mmol) was dissolved in 9.6 mL (0.53 mol) of distilled water by stirring vigorously this mixture for 5 min. Then, a volume of 100 μL (0.44 mmol) of TEOS was

added and the solution was stirred for 5 min. A volume (1.8 mL) of 10^{-3} M (1.8 μmol) NB was added and the mixture stirred again for 5 min. Afterwards, 3 mL (0.024 mol) of hexanol were added and the microemulsion formed was stirred for 15 min. Concentrated ammonium hydroxide (70 μL, 0.9 mmol) was then added and the mixture stirred for 5 min to start the TEOS hydrolysis and condensation reactions. The mixture was then placed in a thermostated tank at 25 °C for 24 h in the dark and, afterwards, it was centrifuged for 5 min at 537 x g to separate the phases involved. The upper phase (about 3 mL) was transferred to a 10-mL beaker and 40 μL of APS and 80 μL of THPMP were added to introduce amino groups onto NP surface. This mixture was magnetically stirred during 1.5 h in a water bath at 25 °C. Afterwards, the microemulsion was broken by adding 10 mL of acetone and stirring for 5 min. The supernatant was discarded and NPs were recovered from the bottom with 8 - 10 mL of distilled water. The mixture was centrifuged for 5 min at 9300 x g to separate the NPs from unreacted reagents. Then, the NP precipitate was washed with ethanol and water until the fluorescence intensity of supernatants was similar to the blank and, finally, the NPs were re-dispersed in 1 mL of phosphate buffer solution.

2.3.2. Preparation of tracers using nile blue-doped silica NPs

NB-doped silica NPs were coupled to either anti-monensin antibodies or monensin to obtain the tracers required to study the potential determination of this drug using antibody or antigen capture format, respectively. The synthesis of the NPs-anti-monensin antibodies tracer involves an oxidation step of carbohydrate moieties of the antibody

molecule to give rise to aldehyde groups capable of reacting to amino groups of the NP surface. Firstly, 200 μL of 1.2 μM anti-monensin antibody solution prepared in 0.1 M phosphate buffer solution at pH 7.5, were diluted with 0.1 M sodium acetate buffer solution (pH 5.5) until a volume of 2 mL, and 200 μL of 0.1 M sodium metaperiodate solution were added to this volume. The mixture was let to stand for 20 min at 0 °C, layered on a HiTrap Desalting Column (GE Healthcare) equilibrated with 25 mL acetate buffer solution (pH 4.5), at a 5 mL/min flow-rate, and 400-μL fractions were taken. Their absorbance was monitored at 280 nm and the anti-monensin protein was recovered from fractions 7 to 11, accounting for about 2 mL of solution. This volume was added to the amino-modified NP-doped silica NPs, which had been previously centrifuged to remove phosphate buffer solution. The mixture was incubated for 5 min at room temperature and then, 50 μL of 0.66 M $NaBH_4$ solution were added to the dispersion and allowed to react for 20 h at 4 °C. Afterwards, the reaction mixture was centrifuged and the NP-anti-monensin protein conjugate obtained was washed with phosphate buffer solution (0.015 M, pH 8.0). Finally, the tracer was re-dispersed in 1 mL of the same phosphate molar concentration solution and stored at 4 °C for further use.

The synthesis of the NPs-monensin tracer was performed using a carbodiimide reaction in which 200 μl of a 2 g L^{-1} monensin solution in DMF were mixed with the same volume of a 0.2 M EDAC solution prepared in 0.05 M 2-(N-morpholino)-ethanesulphonic acid (MES) at pH 6.2 and 21.6 mg of sulfo-NHS were then added, being the mixture raised to 2 mL with the same MES buffer solution and incubated at room temperature for 15 min. Then, 40 μL of 1 M 2-mercaptoethanol were added

and the mixture was left to stand for 10 min. An appropriate volume (50 μL) of this mixture was mixed together with the amino-functionalized NB-doped silica NPs and 950 μL of phosphate saline buffer were added and the resulting mixture was incubated for 2 h at room temperature. After this time, the synthesized tracer was washed using absolute ethanol and phosphate buffer solution, reconstituted in 1 mL of the same phosphate molar concentration solution and stored at 4 °C until use.

2.3.3. Synthesis of BSA-monensin conjugate

The use of a BSA-monensin conjugate was required to immobilize monensin onto the wells. The coupling of monensin to BSA molecule was performed via a carbodiimide reaction [29] using the following procedure: an amount of monensin (0.2 mmol) was dissolved in 1 mL of dry DMF, then sulfo-NHS (23.0 mg, 0.1 mmol) and EDAC (41.2 mg, 0.2 mmol) were added in order to activate the carboxylic acid group of monensin. The mixture was stirred at room temperature for 4 h, and then was centrifuged to remove the precipitate from the acylisourea derivative formed. An aliquot (250 μL) of the activated hapten solution was added dropwise to a stirred BSA solution prepared by dissolving BSA (50 mg) in 5 mL of 0.05 M borate buffer (pH 7.8) and DMF (1.05 mL). The synthesized conjugate was purified using a HiTrap Desalting column (GE Healthcare) by a similar procedure to that described above for the synthesis of NP-anti monensin conjugate.

The concentration of monensin in the conjugate was determined using the Komarowsky reaction [5, 28] by reacting 500 μL aliquots of monensin standard or BSA-monensin conjugate dilutions prepared in

methanol to 1 mL of Komarowsky reagent in glass test tubes. These tubes were sealed and placed in a water bath at 80 °C for 5 min. The red-purple color indicative of monensin presence was measured at 520 nm immediately after cooling the tubes to room temperature. The BSA concentration in the synthesized conjugate was calculated from the absorbance of the protein measured at 280 nm. As a convention, the concentration of the conjugate will be given in terms of the monensin concentration found by using the abovementioned Komarowsky reaction.

2.3.4. Determination of monensin

The competitive heterogeneous immunoassay with antibody capture involves the previous immobilization of the BSA-monensin conjugate in the well, which was performed by adding 60 μL of a 10 mg L^{-1} BSA-monensin conjugate prepared in carbonate buffer solution (0.05 M, pH 9.0) to each well, and incubating the microplates overnight at 4 °C. Afterwards, wells were washed three times with phosphate solution (0.015 M, pH 8.0) and the plates were stored at 4 °C until use.

To perform the immunoassay, a volume (60 μL) of a pre-incubated mixture, prepared by mixing 75 μL of NB-doped silica NPs-labeled anti-monensin antibody (10 nM) in phosphate molar concentration solution (0.015 M, pH 8.0), and 225 μL of monensin antibiotic standard or sample solution (0.05 - 5 μg L^{-1}) were added to each well. The microplate was incubated for 1.5 h at 37 °C, the wells were washed for three times with the same phosphate buffer solution, and dried for 10 min at room temperature. Then, fluorescence measurements were directly performed at λ_{ex} 620 and λ_{em} 680 nm onto the solid surface of the well.

2.3.5. Analysis of milk samples

The sample preparation involved the deproteinization of food samples using a slight modification of a previously described procedure [21]: 0.4 g of milk sample was acidified with 0.1 mL of 0.1 M hydrochloric acid and mixed with 1.6 mL of pure acetonitrile in order to quantitatively precipitate all proteins. Then, the mixture was vigorously mixed during 30 min and centrifuged (2722 x g, 10 min, 10 °C). The supernatant was collected in an Eppendorf tube® and was evaporated to dryness under a gentle stream of nitrogen at 65 °C in order to achieve a medium compatible with the immunoassay. Then, the samples were reconstituted in 3 mL of phosphate buffer solution 0.015 M pH 8.0.

Spiked samples were prepared by adding suitable amounts of monensin standard to 10 g of skimmed milk, semi skimmed milk and whole milk and allowing sample matrix and standards to equilibrate for 1.5 h. Aliquots of 0.4 g were treated as described above for non-spiked samples.

3. Results and discussion

3.1. Choice and optimization of the immunoassay system

Two heterogeneous competitive immunoassays, involving antibody or antigen capture format, were assayed to choose the best option for monensin determination using NB-doped silica NPs as labels. The first format was based on the immobilization of a BSA-monensin conjugate and the use of an anti-monensin antibody-NP tracer, which was synthesized by a similar procedure to that described in an immunoassay for soy protein determination [27]. The second assay needed a monensin-NP tracer,

synthesized via a carbodiimide reaction using EDAC, and the immobilization of anti-monensin antibodies by coating the wells with anti-sheep IgG. Preliminary assays performed using both formats showed that the difference in the fluorescence signals obtained for 0.0 and 0.2 μg L^{-1} monensin standard using the antibody-capture format was about 3-fold higher than that obtained using the analyte-capture assay, so the first format was chosen to develop the new immunoassay for monensin determination.

Since monensin is a hapten, its immobilization required the use of a protein-hapten conjugate to avoid potential steric hindrance that would prevent its reaction with the tracer. BSA was chosen to produce the conjugate via a carbodiimide reaction with the carboxylic acid of monensin, which also allows the simple immobilization of monensin by passive adsorption onto the well surface. It was found that under the reaction conditions, one molecule of BSA was coupled to approximately one molecule of monensin, by calculating the BSA concentration by measuring the absorbance at 280 nm and the monensin concentration by the Komarowsky reaction [5, 28]. A study of the potential non-specific adsorption of the tracer using this format was performed by assaying the system in the absence and presence of BSA-monensin at different monensin concentrations (Figure 1).

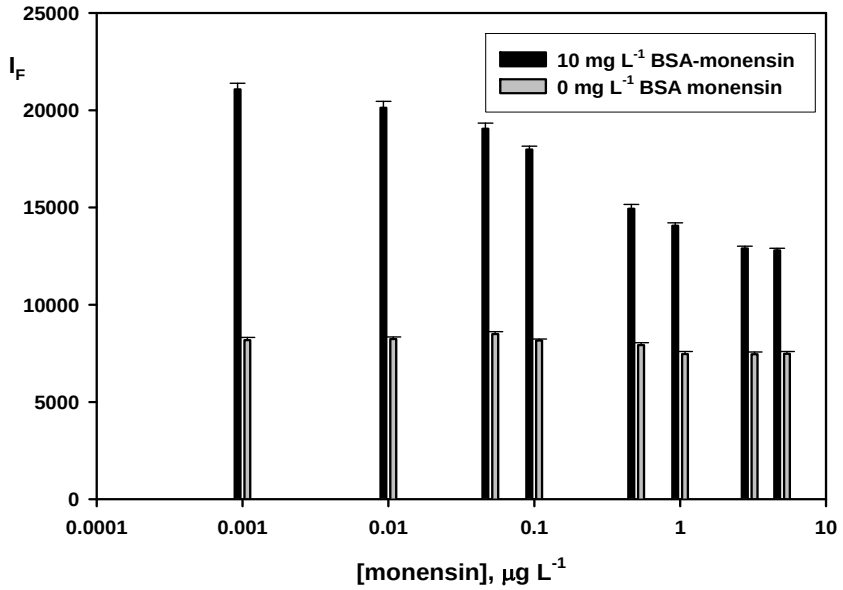

Figure 1. Fluorescence intensity signals obtained using 0 and 10 mg L^{-1} BSA-monensin conjugate at different monensin concentrations. [Tracer] = 10 nM; [phosphate] = 0.015 M; pH = 7.5.

In the presence of BSA-monensin conjugate, the signal can be correlated to monensin concentration, as a result of the competition between monensin and BSA-monensin conjugate. The results obtained in the absence of BSA-monensin conjugate showed that the signal obtained was almost constant at all the monensin concentrations assayed and lower than the signal obtained at the highest analyte concentration assayed. These results show that the tracer concentration being attached to the well in the absence of BSA-monensin conjugate is almost negligible and, thus, non-specific adsorption does not occur.

The optimization of the system was carried out by modifying the experimental conditions at different monensin concentrations. The

concentration of the immobilized BSA-monensin conjugate on the well surface is an important variable on the system, which influences the sensitivity of the assay, since immobilized and in solution monensin compete for the active sites of the tracer. The influence of this variable was assayed in the range of 0 - 60 mg L^{-1} (expressed as monensin concentration) finding that 10 mg L^{-1} provided the best results as the dynamic range obtained for the calibration curve was wider and the sensitivity obtained was also better than those obtained at concentrations below and above (Figure 2A).

Another important variable that influences the sensitivity and working range of the assay is the tracer concentration (Figure 2B), which was assayed in the range from 5 to 12.5 nM, finding that a 10 nM concentration provided the best sensitivity for the assay.

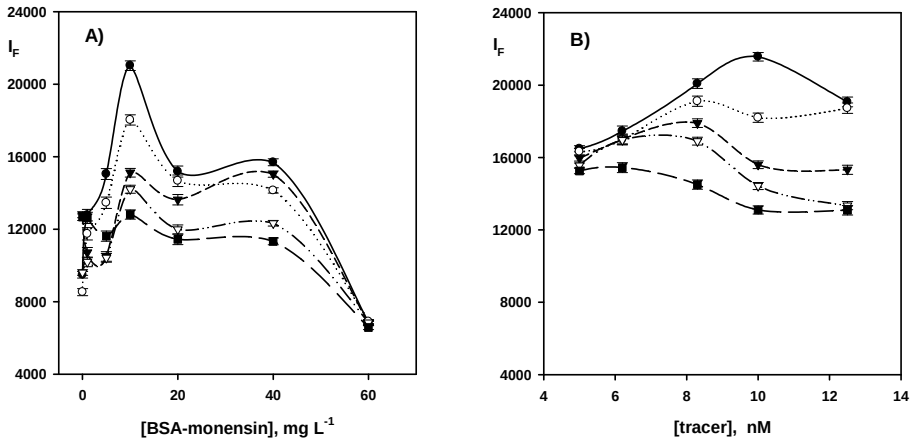

Figure 2. Influence of BSA-monensin (**A**) and tracer (**B**) concentration on the assay in the presence of different monensin concentrations (μg L^{-1}): 1) 0.0; 2) 0.1; 3) 0.5; 4) 1.0; 5) 5.0. [tracer] = 10 nM in figure A. [BSA-monensin] = 10 mg L^{-1} in figure B. Other experimental conditions in both figures are: [phosphate] = 0.015 M, pH 7.5, assay incubation time = 1.5 h, temperature = 37 ˚C.

The influence of pH and phosphate molar concentration on the system was also studied to optimize the reaction conditions. The pH was investigated in the range of 6.0 - 8.5, finding that there was an increase in the signal at pH values above 7.0, being the best results obtained at pH 8.0, from which a slight decrease in the fluorescence signal was observed. The study of buffer concentration showed that the assay sensitivity remained independent on this variable in the range of 0.01 - 0.03 M, being a 0.015 M concentration chosen as the optimum value. The incubation temperature and time were studied in the ranges 25 - 40 °C and 30 min - 2 h, respectively, choosing 37 °C and 1.5 h as optimum values.

3.2. Analytical features

Figure 3 shows the calibration curve obtained for monensin under optimal experimental conditions and measuring the fluorescence signals at λ_{ex} 620 and λ_{em} 680 nm.

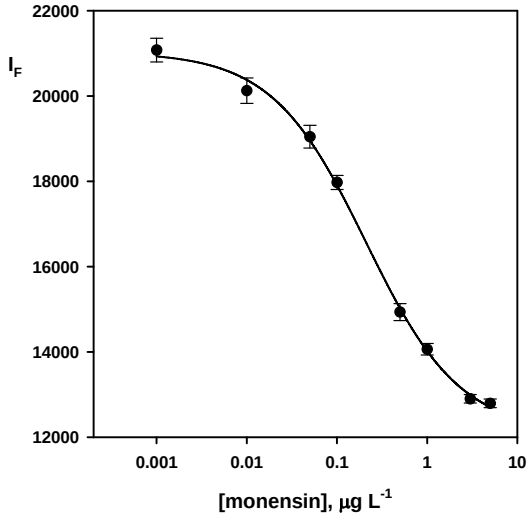

Figure 3. Calibration curve obtained under optimum conditions.

The method presents a dynamic range of 0.05 - 5 μg L^{-1}. The calibration curve was adjusted to a 4-parameter logistic curve using the Sigma Plot 2001software, which equation is:

$$y = y_{\circ} + \left(\frac{a}{1+\left(\frac{x}{x^{\circ}}\right)^{b}} \right),$$

where y is the fluorescence intensity and x is the concentration of monensin expressed in μg L^{-1}. The values of the regression parameters a, b, x_0 and y_0 were (8.9 ± 0.4) x 10^3, 0.83 ± 0.08, 0.21 ± 0.03, and (1.21 ± 0.03) x 10^4 respectively, and the regression coefficient was 0.9992. The detection and quantification limits, calculated according to IUPAC recommendations [30], were 0.015 and 0.05 μg L^{-1}, respectively, which would correspond to 0.12 and 0.40 μg kg^{-1} in the milk samples. The latter value is about 5 times lower than the MRL set by the 37/2010/EC Commission Regulation [3] for monensin in milk samples. Also, the detection limit is four times lower than that reported using ELISA with chemiluminescence detection [18]. The precision, expressed as the percentage of relative standard deviation and assayed at two different monensin antibiotic concentrations, 0.2 and 1 μg L^{-1}, gave values of 5.8 and 4.0 % respectively.

The selectivity of the system was studied by assaying different antibiotics of veterinary use belonging to the ionophore group, such as lasalocid, or to other antibiotic groups such as aminoglycosides, tetracyclines and fluoroquinolones, which can be used for therapeutic purposes in animals. Neomycin, oxytetracycline and enrofloxacin were

chosen as representative components of these groups. A compound was considered not to interfere at a given concentration when the analytical signal obtained in the presence of this substance was within one standard deviation of the value obtained in its absence. The maximum concentration tested for all these compounds was 200 μg L^{-1} using a 0.2 μg L^{-1} monensin concentration, finding that all of them were tolerated at this 1000:1 concentration ratio. This result agrees with the results already reported for other monensin immunoassays [15 - 17, 20, 21], which shows the good selectivity of anti-monensin antibodies.

3.3. Applications

The method was applied to the analysis of skimmed, semi skimmed and whole milk samples. The sample treatment was quite simple and consisted in a deproteinization step after which the solvent was evaporated owing to the lack of compatibility of the organic solvent with the immunoassay performance. This compatibility was studied using methanol and ethanol and they proved to decrease the fluorescence signal at percentages above 3% of each solvent. These extraction and evaporation steps are common to those required by immunoassays for monensin determination in sample extracts of feedstuff [15, 16] and foodstuff [21] samples. The monensin concentration in the milk samples was determined according to the procedure above described. A recovery study was also carried out to validate the method (Table 1), obtaining values in the range of 83.3 – 107.5%.

Table 1. Recoveries obtained for monensin added to milk samples

	Monensin		
Sample	Added/ μg kg^{-1}	Found[a/] μg kg^{-1}	Recovery (%)
Skimmed milk	1.5	1.6 ± 0.1	106.7
	2	1.96 ± 0.09	98.0
	4	4.1 ± 0.2	102.5
Semi-skimmed milk	1.5	1.5 ± 0.1	100.0
	2	2.0 ± 0.1	100.0
	4	3.4 ± 0.3	85.0
Whole milk	1.5	1.25 ± 0.07	83.3
	2	1.7 ± 0.1	85.0
	4	4.3 ± 0.3	107.5

[a]Mean ± SD (n = 3)

4. Conclusions

The results obtained have shown the usefulness of NB-doped silica NPs as labels for the determination of monensin using immunoassay, reporting a lower detection limit than those previously reported using other labels [14 - 18, 20, 21]. Also, the number of steps of the assay is lower than those required using an enzyme as label. The development of the assay in 96-well microplates, using 100-μL proxy-plate, allows the automation of the method together with a relatively high sample throughput, and reduces the sample and tracer volumes required in comparison with the conventional 300-μL wells, which contribute to minimize the costs associated to the immunoassay.

The low quantification limit of this method allows the determination of monensin at levels below its MRL for milk samples. The use of these samples to control the potential presence of monensin in foodstuffs is a useful alternative to the analysis of other biological samples, since they can be easily obtained.

Acknowledgments

Authors gratefully acknowledge financial support from the MICINN (grant no. CTQ2009-08621), from the Junta of Andalucia (grant no. P09-FQM4933) and from the FEDER-FSE Program (grant no.P09-FQM4933). J. Godoy-Navajas thanks the Junta of Andalucia (grant no. P09-FQM4933) for the financial support of his pre-doctoral fellowship.

References

(1) Opinion of the Scientific Panel on Contaminants in the Food Chain. *EFSA J* (**2008**) *592*, 1–40.

(2) Regulation (EC) No 1831/2003 of the European Parliament and of the Council of 22 September 2003 on additives for use in animal nutrition. *Off. J. Eur. Union* (**2003**) *L268*, 29–43.

(3) Commission Regulation (EU) No 37/2010 on pharmacologically active substances and their classification regarding maximum residue limits in foodstuffs of animal origin. *Off. J. Eur. Union* (**2010**) *L15*, 1–72.

(4) C.T. Elliot, D.G. Kennedy, W.J. McCaughey. Methods for the detection of polyether ionophore residues in poultry. *Analyst* (**1998**) *123*, 45R–56R

(5) M. Sokolic, M. Pokorny. Comparative determination of salinomycin by high-performance liquid chromatography, microbiological and colorimetric methods in testing production processes and animal feed preparations. *J. Pharm. Biomed. Anal.* (**1991**) *9*, 1047–1053.

(6) R. Galarini, L. Fioroni, S. Moretti, L. Pettinacci, G. Dusi. Development and validation of a multi-residue liquid chromatography-tandem mass spectrometry confirmatory method for eleven coccidiostasts in eggs. *Anal. Chim. Acta*, (**2011**) *700*, 167–176.

(7) M. Cronly, P. Behan, B. Foley, E. Malone, P. Shearan, L. Regan. Determination of eleven coccidiostats in animal feed by liquid chromatography-tandem spectrometry at cross contamination levels. *Anal. Chim. Acta* (**2011**) *700*, 26–33.

(8) U. Vincent, Z. Ezerskis, M. Chedin, C. von Holst. Determination of ionophore coccidiostats in feeding stuffs by liquid chromatography-tandem mass spectrometry. Part II. Application to cross-contamination levels and non-targeted fee. *J. Pharm. Biomed. Anal.* (**2011**) *54*, 526–534.

(9) T.S. Thompson, D.K. Noot, J.D. Kendall. Determination of ionophores in raw bovine milk using LC—MS/MS: Application to residue surveillance. *Food Chem*. (**2011**) *127*, 321–326.

(10) M. Olejnik, T. Szprengier-Juzskiewicz, P. Jedziniak. Multi-residue confirmatory method for the determination of twelve coccidiostats in chicken liver using liquid chromatography tandem mass spectrometry. *J. Chromatogr. A* (**2009**) *1216*, 8141–8148.

(11) G. Stubbings, T. Bigwood. The development and validation of a multiclass liquid chromatography tandem mass spectrometry (LC-MS/MS) procedure for the determination of veterinary drug residues in animal tissue using a QuEChERS (Quick, Easy, Cheap, Effective, Rugged and Safe) approach. *Anal. Chim. Acta* (**2009**) *637*, 68–78.

(12) B. Ferraz Spisso, R. Gomes Ferreira, M. Ulberg Pereira, M. Alves Monteiro, T. Ávila Cruz, R. Pinto da Costa, A.M. Belém Lima, A. Wanderley da Nóbrega. Simultaneous determination of polyether ionophores, macrolides and lincosamides in hen eggs by liquid chromatography-electrospray ionization tandem mass spectrometry using a simple solvent extraction. *Anal. Chim. Acta* (**2010**) *682*, 82–92.

(13) A. Boscher, C. Guignard, T. Pellet, L. Hoffmann, T. Bohn. Development of a multi-class method for the quantification of veterinary drug residues in feedingstuffs by liquid chromatography-tandem mass spectrometry. *J. Chromatogr. A* (**2010**) *1217*, 6394–6404.

(14) H. Watanabe, A. Satake, M. Matsumoto, Y. Kido, A. Tsuji, K. Ito, M. Maeda. Monoclonal-based enzyme-linked immnosorbent assay and immunochromatographic rapid assay for monensin. *Analyst* (**1998**) *123*, 2573–2578.

(15) Monensin ELISA kit (Cat # KA1422 V.01), http://www.abnova.com/.

(16) Monensin ELISA. Enzyme-linked Immunosorbent Assay for the Determination of Monensin in Feed and Contaminated Samples, *http://www.abraxiskits.com/*.

(17) S.R.H. Crooks, I.M. Traynor, C.T. Elliott, W.J. McCaughey. Detection of monensin residues in poultry liver using an enzyme immunoassay. *Analyst* (**1997**) *122*, 161–163.

(18) M.A.J. Godfrey, M.F. Luckey, P. Kwasowski. IAC/cELISA detection of monensin elimination from chicken tissues, following oral therapeutic dosing. *Food Addit. Contam*. (**1997**) *14*, 281–286.

(19) H. Dolliver, K. Kumar, S. Gupta, A. Singh. Application of enzyme-linked immunosorbent assay analysis for determination of monensin in environmental samples. *J. Environ. Qual*. (**2008**) *37*, 1220–1226.

(20) S.R.H. Crooks, T.L. Fodey, G.R. Gilmore, C.T. Elliott. Rapid screening for monensin residues in poultry plasma by a dry reagent dissociation enhanced lanthanide fluoroimmunoassay. *Analyst* (**1998**) *123*, 2493–2496.

(21) V. Hagren, P. Peippo, M. Tuomola, T. Lövgren. Rapid time-resolved fluoroimmunoassay for the screening of monensin residues in eggs. *Anal. Chim. Acta* (**2006**) *557*, 164–168.

(22) C. Cháfer-Pericás, A. Maquieira, R. Puchades. Functionalized inorganic nanoparticles uses as labels in solid-phase immunoassays. *Trends Anal. Chem*. (**2012**) *31*, 144–156.

(23) A. Gómez-Hens, J.M. Fernández-Romero, M.P. Aguilar-Caballos. Nanostructures as analytical tolos in bioassays. *Trends Anal. Chem*. (**2008**) *27*, 394–406.

(24) A. Gómez-Hens, J.M. Fernández-Romero, M.P. Aguilar-Caballos. Control of tumor markers using nanotechnology. *Mini-Rev. Med. Chem*. (**2009**) *9*, 1064–1074.

(25) D. Knopp, D. Tang, R. Niessner. Review: Bioanalytical applications of biomolecule-functionalized nanometer-sized doped silica particles. *Anal. Chim.Acta* (**2009**) *647*, 14–30.

(26) J. Godoy-Navajas, M.P. Aguilar-Caballos, A. Gómez-Hens. Synthesis and characterization of oxazine-doped silica nanoparticles for their potential use as stable fluorescent reagents. *J. Fluoresc*. (**2010**) *20*, 171–180.

(27) J. Godoy-Navajas, M.P. Aguilar-Caballos, A. Gómez-Hens. Heterogeneous immunoassay for soy protein determination using nile blue-doped silica nanoparticles as labels and front-surface long-wavelength fluorimetry. *Anal. Chim. Acta* (**2011**) *701*, 194–199.

(28) M. Blazsek, M. Kubis. HPLC determination of salinomycin and related compounds in fermentation media of Streptomyces albus and premixes. *J. Pharm. Biomed. Anal*. (**2005**) *39*, 564–571.

(29) E. Watanabe, H. Kubo, Y. Kanzaki, H. Nakazawa. Immunoassay based on a polyclonal antibody for sex steroid hormones produced by a heterogeneous hapten-conjugated immunogen: Estimation of its potentiality and antibody characteristics. *Anal. Chim. Acta* **(2010**) *658*, 56–62.

(30) G. Long, J.D. Winefordner. Limit of detection a close look at the IUPAC definition. *Anal. Chem*. (**1983**) *55*, 712–724.

CAPÍTULO 3

CHAPTER 3

Nuevas aportaciones para la determinación de antioxidantes en alimentos

New approaches for the determination of food antioxidants

Este capítulo recoge las investigaciones realizadas para la propuesta de nuevas metodologías analíticas para la determinación de antioxidantes en alimentos. En concreto, se ha trabajado en el desarrollo de un método para la determinación de la capacidad antioxidante de alimentos y, en segundo lugar, se ha abordado la puesta a punto de un método para la determinación de polifenoles en muestras de vinos. Estos estudios han originado dos artículos científicos:

- J. Godoy-Navajas, M.P. Aguilar-Caballos, A. Gómez-Hens. Long-wavelength fluorimetric determination of food antioxidant capacity using nile blue as reagent. Journal of Agriculture and Food Chemistry, 59 (2011) 2235 – 2240.
- J. Godoy-Navajas, M.P. Aguilar-Caballos, A. Gómez-Hens. Automatic determination of polyphenols in wines using laccase and terbium oxide nanoparticles. Food Chemistry, enviado.

El interés de estas determinaciones emana de las numerosas investigaciones realizadas en las últimas décadas sobre el impacto del estrés oxidativo en la salud humana y las causas que lo producen. El estrés oxidativo se define como el desequilibrio entre la producción de especies reactivas de oxígeno (ROS) o de nitrógeno (RNS) y la defensa antioxidante, encontrándose que desempeña un papel fundamental en distintas condiciones patofisiológicas [1]. La existencia de este estrés oxidativo se atribuye a la incapacidad de los antioxidantes endógenos para evitar el daño oxidativo de biomoléculas claves.

Los antioxidantes se han definido como "cualquier sustancia que, cuando se encuentra presente a bajas concentraciones con respecto a un

sustrato oxidable, retrasa significativamente o inhibe la oxidación de dicho sustrato" [2]. Esta definición se modificó más tarde, en 2007, para pasar a definirlos como "cualquier sustancia que retrasa, evita o elimina el daño oxidativo a una molécula diana" [3]. Su relación con las especies reactivas de oxígeno (ROS) se estableció ese mismo año mediante la definición de Khlebnikov y colaboradores [4], en la que se definen los antioxidantes como "cualquier especie que atrapa directamente ROS o indirectamente actúa para regular las defensas antioxidantes o para inhibir la producción de ROS". Después de atrapar las ROS, las sustancias antioxidantes deben ser capaces de formar un nuevo radical estable mediante la formación de puentes de hidrógeno intramoleculares [5]. Los antioxidantes realizan esta actividad de diversas formas: 1) como inhibidores de las reacciones de oxidación que transcurren mediante radicales libres, en las que actúan inhibiendo la formación de radicales libres de lípidos; 2) interrumpiendo la propagación de las reacciones de autoxidación; 3) como inhibidores del oxígeno singlete; 4) mediante acción sinérgica con otros antioxidantes; 5) como agentes reductores que convierten los hidroperóxidos en otras sustancias más estables; 6) como agentes quelatantes de metales que transforman metales pro-oxidantes (derivados de hierro y cobre) en productos estables y, por último, 7) actuando como inhibidores de enzimas pro-oxidantes (p.ej. lipooxigenasas). Actualmente se está trabajando en la determinación de la actividad de los antioxidantes a nivel celular para expandir la definición de sustancias antioxidantes a aquellas sustancias que activan factores de transcripción capaces de inducir la expresión de enzimas con actividad antioxidante [1].

Las sustancias antioxidantes pueden clasificarse en tres grupos: naturales, sintéticas y sustancias con carácter pro-oxidante [6]. Dentro de los antioxidantes naturales, se ha considerado los que actúan sobre la salud humana (Figura 1), que se dividen en un primer nivel en antioxidantes enzimáticos y no enzimáticos.

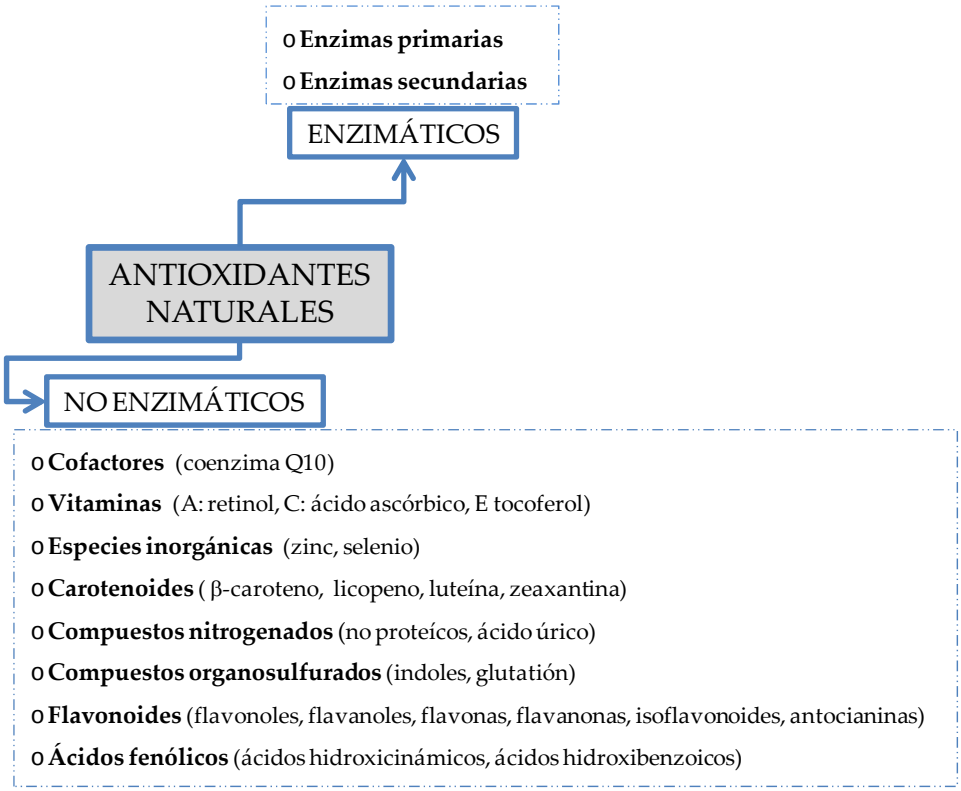

Figura 1. Clasificación de las sustancias antioxidantes naturales.

Las enzimas antioxidantes se clasifican en defensas primarias y secundarias, según neutralicen la presencia de radicales libres o participen en reacciones de regeneración de sustancias antioxidantes, respectivamente. Dentro de los antioxidantes no enzimáticos, se

encuentran las vitaminas, coenzimas, especies inorgánicas, carotenoides, compuestos orgánicos de azufre y de nitrógeno no proteico, flavonoides y, por último, ácidos fenólicos. A pesar de que muchas de estas sustancias antioxidantes se encuentran de forma endógena en nuestro sistema, se necesita un aporte externo mediante la dieta para mantener una baja concentración de radicales libres. Algunos antioxidantes se encuentran en relativamente alta concentración como metabolitos secundarios en las plantas. De esta forma, los zumos naturales, extractos de plantas y vinos, entre otros, presentan contenidos elevados de antioxidantes como vitaminas, especies inorgánicas, flavonoides y ácidos fenólicos [7].

Los antioxidantes sintéticos son compuestos químicos que se adicionan a los alimentos para mantener sus propiedades después de los tratamientos incluidos en el procesado de alimentos y, también, para prolongar su duración. La Figura 2 muestra algunos componentes de esta familia, tales como butilhidroxianisol (BHA), butilhidroxitolueno (BHT), terbutilhidroquinona, ésteres del ácido gálico (más conocidos como galatos) y derivados de otros fenoles como, por ejemplo, el resorcinol. La Autoridad Europea de Seguridad Alimentaria (EFSA) revisó en 2012 las concentraciones máximas permitidas de estos aditivos, que siguen estando en uso a pesar de algunos estudios que indican efectos nocivos en la salud [8].

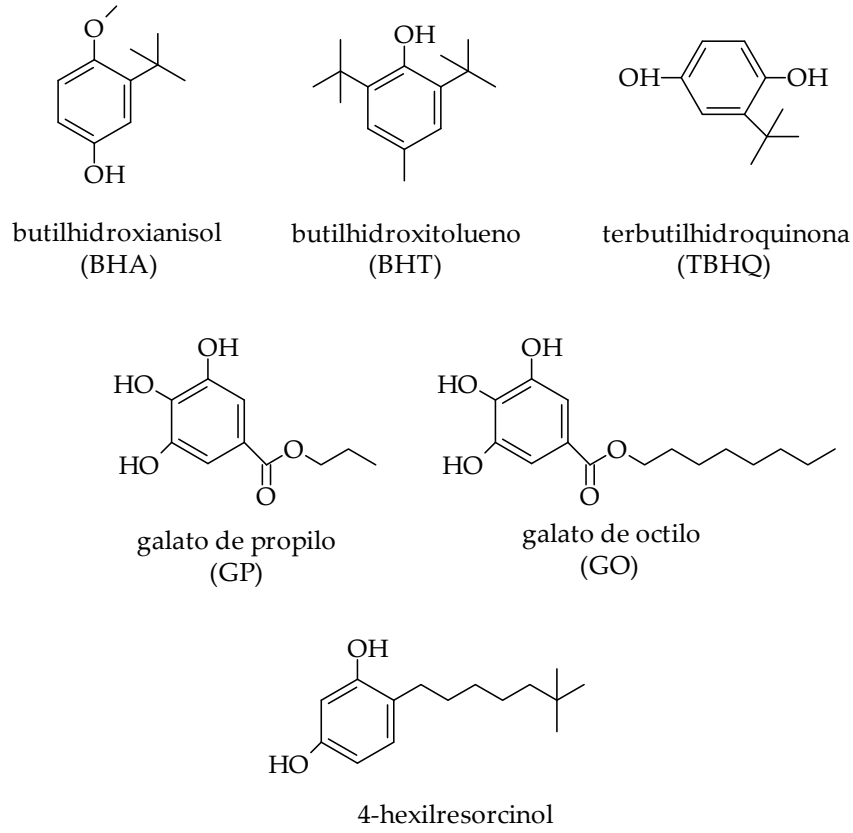

Figura 2. Estructuras químicas de algunos antioxidantes sintéticos.

Las sustancias pro-oxidantes se definen como especies químicas que inducen estrés oxidativo, normalmente mediante la formación de especies reactivas o mediante la inhibición de sistemas antioxidantes. Los radicales libres son conocidos pro-oxidantes, pero las sustancias antioxidantes pueden tener también un comportamiento pro-oxidante [6]. Por ejemplo, la vitamina C es un conocido antioxidante pero, en presencia

de hierro, puede descomponer peróxido de hidrógeno en radicales hidroxilo, lo que le confiere naturaleza pro-oxidante. El comportamiento antioxidante o pro-oxidante depende del antioxidante considerado y de su concentración, siendo el estudio de la relación antioxidante:pro-oxidante un área de investigación muy activa en la actualidad.

La gran variedad de sustancias antioxidantes que pueden existir en los alimentos dificulta la determinación individual de cada una de las especies de este grupo y, por otra parte, el poder antioxidante total de un alimento es una herramienta muy útil para evaluar los efectos beneficiosos de la ingesta de antioxidantes en la salud humana. Cabe distinguir entre dos conceptos que se utilizan a menudo de forma indistinta pero que tienen connotaciones ligeramente diferentes: actividad y capacidad antioxidante. La actividad antioxidante se relaciona con la cinética de una reacción entre un antioxidante y un pro-oxidante o un radical al que reduce o atrapa, mientras que la capacidad antioxidante mide la eficacia de la transformación termodinámica de la reacción de un pro-oxidante con una sustancia antioxidante. Se han desarrollado diversos ensayos para evaluar el poder antioxidante total de un alimento, pero no proporcionan medidas que puedan correlacionarse entre sí, debido fundamentalmente a que no existen métodos normalizados para estas determinaciones [9]. En general, los ensayos químicos de actividad antioxidante se pueden clasificar en dos grandes grupos, atendiendo al tipo de reacción involucrada:

- Ensayos basados en transferencia de átomos de hidrógeno (HAT)
- Ensayos basados en transferencia de electrones (ET)

Los ensayos basados en reacciones HAT miden la capacidad de un antioxidante para inhibir los radicales libres (generalmente radicales peróxido) mediante la cesión de átomos de hidrógeno. El mecanismo por el que se interpreta la acción antioxidante de un compuesto fenólico que transfiere un protón a un radical es el siguiente:

$$ROO^{\cdot} + AH \,/\, ArOH \longrightarrow ROOH + A^{\cdot}/ArO^{\cdot}$$

donde el radical oxiarilo ($ArO^{\cdot}$) formado por la reacción del antioxidante fenólico con el radical peróxido se estabiliza mediante resonancia y las especies AH y ArOH se corresponden con las biomoléculas protegidas y las de antioxidante fenólico, respectivamente. En estos ensayos, se utiliza un fluoróforo que compite con la sustancia antioxidante por los radicales peróxido. La actividad antioxidante se determina mediante medidas de la diferencia en la inhibición de la fluorescencia del fluoróforo en ausencia y presencia de las sustancias antioxidantes. Algunos ensayos basados en HAT son el que mide la capacidad de absorción de radicales de oxígeno (ORAC), el de poder antioxidante total (TRAP) y los ensayos de decoloración de crocina y β-carotenos.

En los ensayos mediante reacciones ET, el antioxidante reacciona con un cromóforo o un fluoróforo con naturaleza oxidante en lugar de reaccionar con los radicales peróxido. Así, la presencia de sustancias antioxidantes origina una variación en la absorbancia o en la fluorescencia del cromóforo y fluoróforo, respectivamente, de forma que estos cambios se pueden correlacionar con la concentración de sustancias antioxidantes presentes en la muestra. Algunos ejemplos de ensayos basados en estas

reacciones son el que mide la capacidad antioxidante total equivalente de Trolox (TEAC), el ensayo DPPH (que utiliza radicales 2,2-difenilpicrilhidracilo), el método de Folin-Ciocalteu, el del potencial antioxidante reductor de iones férricos (FRAP) y la capacidad antioxidante reductora de iones cúpricos (CUPRAC).

Las investigaciones de esta Memoria que abordan el desarrollo de un método para la determinación de la capacidad antioxidante están basadas en la aplicación del método ORAC. Este método utiliza un iniciador azo-bis, como el diclorhidrato de 2,2'-azobis(2-amidinopropano) (AAPH), el cual libera radicales peróxido cuando se calienta con ayuda del oxígeno disuelto [10].

$$R-N=N-R \longrightarrow N_2 + 2ROO^{\cdot}$$

$$ROO^{\cdot} + fluoróforo \longrightarrow ROOH + fluoróforo\ oxidado$$

$$ROO^{\cdot} + AH \longrightarrow ROOH + A^{\cdot}$$

$$ROO^{\cdot} + A^{\cdot} \longrightarrow ROOA$$

Los radicales peróxido liberados reaccionan con un fluoróforo e inhiben su fluorescencia. Los fluoróforos utilizados de forma convencional han sido β-ficoeritrina [11], que se sustituyó posteriormente por fluoresceína y diclorofluoresceína [12], debido a que éstas presentaban mayor fotoestabilidad y una reactividad prácticamente nula con los polifenoles.

El estudio realizado ha estado orientado a investigar la utilidad analítica de los fluoróforos de larga longitud de onda con objeto de mejorar algunas propiedades analíticas del ensayo ORAC, tales como la selectividad espectral, como se discutirá más adelante. Esta mejora es posible ya que las medidas se realizan a longitudes de onda más largas que las que presentan los fluoróforos tradicionalmente utilizados con este fin. Estas innovaciones están en consonancia con las directrices de un informe técnico de la IUPAC [9] publicado recientemente, en el que se proponen las siguientes acciones de mejora:

- Desplazar el foco de atención desde el "screening" al estudio de los mecanismos de reacción de las sustancias antioxidantes.
- Sustituir la fluoresceína por otros fluoróforos que no presenten inhibición de la fluorescencia por irradiación, reacciones o interacciones colaterales.
- Analizar potenciales interferencias mediante el análisis de muestras blanco en las que se analice la contribución de las muestras sin antioxidantes junto con el fluoróforo, en presencia y ausencia del reactivo generador de radicales.
- Ensayar intervalos de concentraciones de antioxidantes para proponer mecanismos de reacción de las sustancias antioxidantes y conocer a partir de qué concentraciones se comportan como pro-oxidantes.
- Obtener información para la normalización de los procedimientos ORAC: relación fluoróforo:generador de radicales para eliminar efectos de auto-inhibición del fluoróforo que oculten la acción del antioxidante, estudio sistemático de la influencia de los niveles de

oxígeno disuelto en la velocidad de reacción, determinación de los niveles de oxígeno disuelto mínimos para que la reacción tenga lugar y desarrollo de métodos para asegurar niveles de oxígeno adecuados, de acuerdo a lo expuesto anteriormente.

- Diseñar métodos para controlar adecuadamente la temperatura.
- Desarrollar normas para el desarrollo de métodos en el formato de microplacas en ensayos de actividad antioxidante y conseguir que los fabricantes diseñen la instrumentación apropiada para tal fin.
- Poner a punto métodos normalizados para el cálculo de áreas bajo la curva.
- Proporcionar datos conjuntos de capacidad antioxidante y de otros parámetros como la concentración total de polifenoles para conocer los perfiles de actividad.
- Conocer la capacidad antioxidante en extractos naturales después de su tratamiento con polivinilpirrolidona para la eliminación de compuestos fenólicos y deducir la contribución de los compuestos no fenólicos a dicho ensayo.

De los dos últimos puntos de mejora del informe técnico anterior se deduce la importancia de proporcionar datos complementarios, tales como la concentración total de antioxidantes fenólicos y la de antioxidantes no fenólicos, íntimamente relacionada con la capacidad antioxidante para conocer los perfiles de actividad antioxidante de cada alimento. En la segunda sección de este capítulo se aborda la determinación de antioxidantes fenólicos mediante el uso de la enzima laccasa en presencia de nanopartículas de óxido de terbio como activador.

Las enzimas de la familia de las laccasas son fenoloxidasas que oxidan las sustancias antioxidantes con ayuda del oxígeno disuelto en el medio. Las enzimas laccasas son activas frente a compuestos antioxidantes que incorporan grupos orto- y para-difenol, aunque presentan mayor afinidad por los compuestos fenólicos sustituidos en para-. Estas enzimas presentan una relativa selectividad por los sustratos, que pueden tener mayor o menor potencial de reducción dependiendo del tipo de laccasa. Las enzimas laccasas catalizan la oxidación de una amplia variedad de sustratos, entre los que se incluyen mono-, di- y polifenoles, aminofenoles, metoxifenoles, aminas aromáticas y ascorbato, con la reducción de oxígeno a agua mediante el intercambio de cuatro electrones.

Estas enzimas pueden obtenerse de diversas fuentes, ya sean plantas, como es el caso de la planta japonesa *Rhus vernicifera*, de la cual se aisló la primera variedad de laccasa, insectos y bacterias [13]. No obstante, la mayoría de las laccasas actualmente utilizadas se obtienen de hongos superiores, como *Trametes versicolor* y *Trametes hirsuta*, entre otros.

Estas enzimas presentan numerosas aplicaciones industriales y analíticas cuando se encuentran inmovilizadas sobre un soporte sólido. Se han revisado recientemente [13] las diversas opciones de inmovilización tales como atrapamiento, adsorción, encapsulamiento, entre otras, para finalmente concluir que no siempre se recupera la actividad enzimática de forma satisfactoria tras el proceso de inmovilización. Las aplicaciones analíticas más destacables de la enzima laccasa han estado orientadas al desarrollo de biosensores con detección electroquímica [14]. El modo de operación de estos biosensores es generalmente secuencial, lo que limita su velocidad de muestreo, a diferencia de otros ensayos que utilizan

microplacas de pocillos donde las medidas se realizan de forma prácticamente simultánea. Éste es un aspecto que se ha estudiado y optimizado en las investigaciones descritas en esta Memoria. En concreto, el segundo apartado de este capítulo ha tenido como objeto el desarrollo de un método de alta velocidad de muestreo para la determinación de polifenoles en vinos con el que se pretende reducir el consumo de enzima con las nanopartículas de óxido de terbio como activador, al mismo tiempo que se acorta el tiempo requerido para las determinaciones analíticas basadas en el uso de esta enzima.

BIBLIOGRAFÍA

(1) B.D. Craft, A.L. Kerrihard, R. Amarowicz, R.B.Pegg. Phenol-based antioxidants and the in vitro methods used for their assessment. *Compr. Rev. Food Sci. Food Safety*. **(2012)** *11*, 148 – 173.

(2) B. Halliwell, J.M. Gutteridge. The definition and measurement of antioxidants in biological systems. *Free Radic. Biol. Med.* **(1995)** *18*, 125 – 126.

(3) B. Halliwell. Biochemistry of oxidative stress. *Biochem. Soc. Trans.* **(2007)** *35*, 1147 – 1150.

(4) A.J. Khlebnikov. I.A. Schepetkin, N.G. Domina, L.N. Kirpotina, M.T. Quinn. Improved quantitative structure-activity relationship models to predict antioxidant activity of flavonoids in chemical, enzymatic, and cellular systems. *Bioorg. Med. Chem.* **(2007)** *15*, 1749 – 1770.

(5) B. Halliwell. How to characterize a biological antioxidant. *Free Radic. Res.* **(1990)** *9*, 1 – 32.

(6) M. Carocho, I.C.F.R. Ferreira. A review on antioxidants, prooxidants and relatived controversy: Natural and synthetic compounds, screening and analysis methodologies and future perspectives. *Food Chem. Tox.* **(2013)** *51*, 15 – 25.

(7) B. Lorrain, I. Kay, L. Pechamat, P.L. Teissedre. Evolution of analysis of polyphenols from grapes, wines and extracts. *Molecules*. **(2013)** *18*, 1076 – 1100.

(8) European Food Safety Authority (EFSA). Statement on the safety assessment of the exposure to butylated hydroxyanisole E320 (BHA) by applying a new exposure assessment methodology. *EFSA J*. **(2012)** *10:2759*, 1 – 16.

(9) R. Apak, S. Gorinstein, V. Böhm, K.M. Schaich, M. Ozyürek, K. Güçlü. Methods of measurement and evaluation of natural antioxidant capacity/activity (IUPAC Technical Report). *Pure Appl. Chem.* **(2013)** *85*, 957 – 998.

(10) R.L. Prior, X. Wu, K. Schaich. Standardized methods for the determination of antioxidant capacity and phenolics in foods and dietary supplements. *J. Agric. Food Chem.* **(2005)** *53*, 4290 – 4294.

(11) G.H. Cao, H.M. Alessio, R.G. Cutler. Oxygen-radical absorbance capacity assay for antioxidants. *Free Radical Biol. Med.* **(1993)** *14*, 303 – 465.

(12) B. Ou, M. Hampsch-Woodill, R.L. Prior. Development and validation of an improved oxygen radical absorbance capacity assay using fluorescein as the fluorescent probe. *J. Agric. Food Chem.* **(2001)** *49*, 4619 – 4621.

(13) M. Fernández-Fernández, M.A. Sanromán, D. Moldes. Recent developments and applications of immobilized laccase. *Biotechnol. Adv*. **(2013)** *31*, 1808-1825.

(14) A. Sánchez-Arribas, M. Martínez-Fernández, M. Chicharro. The role of electroanalytical techniques in analysis of polyphenols in wine. *Trends Anal. Chem.* **(2012)** *34*, 78 – 96.

This chapter contains the investigations performed to develop new analytical methodologies for the determination of antioxidants in food samples. More specifically, these investigations have been focused to the development of a method to determine the antioxidant capacity in food samples, and secondly, on the proposal of a method to determine polyphenols in wines. These studies have given rise to two scientific articles:

- J. Godoy-Navajas, M.P. Aguilar-Caballos, A. Gómez-Hens. Long-wavelength fluorimetric determination of food antioxidant capacity using nile blue as reagent. Journal of Agricultural and Food Chemistry, 59 (2011) 2235 – 2240.
- J. Godoy-Navajas, M.P. Aguilar-Caballos, A. Gómez-Hens. Automatic determination of polyphenols in wines using laccase and terbium oxide nanoparticles. *Food Chemistry*, submitted for publication.

The interest on these determinations comes from the numerous investigations performed in the latest decades on the impact of the oxidative stress on human health and its causes. The oxidative stress can be defined as the unbalance between the production of reactive oxygen (ROS) or nitrogen (RNS) species and the antioxidant defence, finding that it plays a significant role in different pathophysiological conditions [1]. The reason for this oxidative stress is the inability of endogen antioxidants to avoid the oxidative damage of key biomolecules.

Antioxidant substances have been defined as "any substance that at very low concentration can significantly delay or inhibit the oxidation of a

substrate" [2]. This definition was later modified in 2007, to define an antioxidant as "any substance that delays, prevents or removes the oxidative damage to a target molecule" [3]. The relationship of oxidative stress with ROS was established in the same year by Khlebnikov et al. [4], who defined antioxidants as "any species that scavenges ROS directly or indirectly acts to up-regulate antioxidant defences or to inhibit ROS production". After scavenging ROS, proper antioxidant substances must be able to give rise to new stable radicals by means of intramolecular hydrogen bonds [5]. Antioxidants can act in many different ways: 1) as inhibitors of redox reactions happening via free radicals, by mainly inhibiting lipid free radicals; 2) breaking the chain of auto-oxidation reactions; 3) as inhibitors of singlet oxygen; 4) through synergism with other antioxidants; 5) as reducing agents that change hydroperoxides into more stable compounds; 6) as metal chelating agents that convert pro-oxidative metal species (mainly derived from iron and copper) into stable products, and, 7) as inhibitors of pro-oxidant enzymes (e.g. lipooxygenases). Nowadays, an active area of research is the determination of cellular antioxidant activity to expand the definition of antioxidant compounds to those substances that activate transcription factors able to induce the expression of antioxidant enzymes [1].

Antioxidant compounds can be categorized into three different groups: natural, synthetic and pro-oxidant substances [6]. Figure 1 shows the most important natural antioxidants involved in the human system, which can be divided in first instance in enzymatic and non-enzymatic antioxidants.

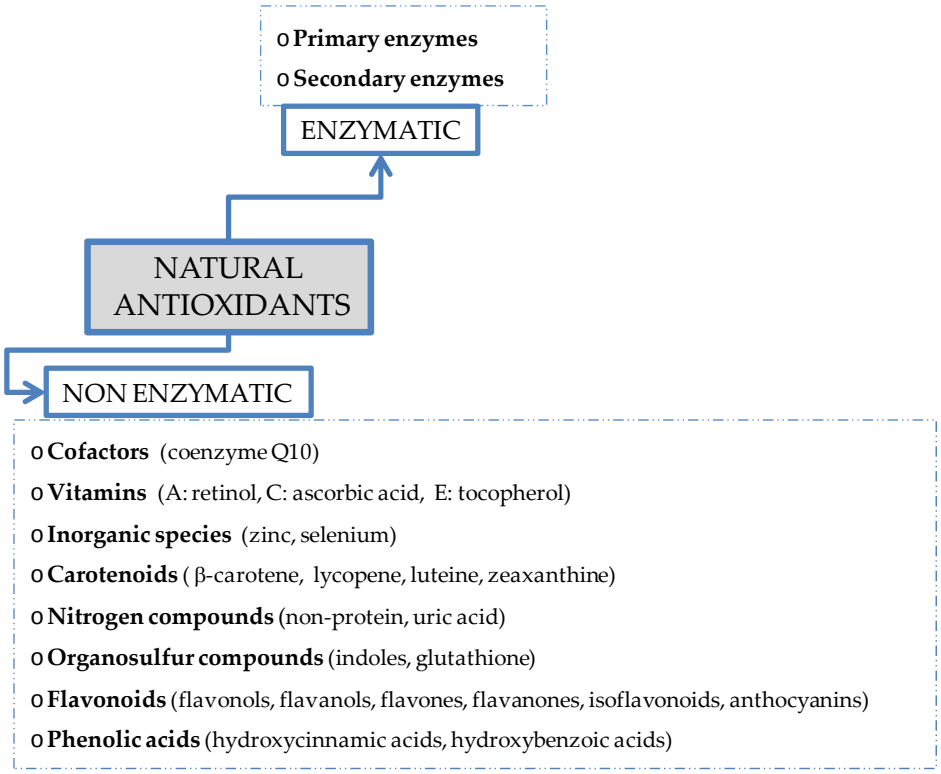

Figure 1. Classification of natural antioxidant substances.

Antioxidant enzymes either classify as primary or secondary defences depending on whether they neutralise the presence of free radicals or they participate in regeneration reactions for antioxidant compounds. Among non-enzymatic compounds, we can find vitamins, coenzymes, inorganic species, carotenoids, organosulfur compounds, non-protein nitrogen compounds, flavonoids and phenolic acids. Although some of them are endogenous substances, an external intake from diet is needed to preserve the free radical concentration at low levels. Some

antioxidant compounds can be found in relatively high concentrations as secondary plant metabolites. Thus, fruit and extract juices and wines, among others, exhibit a high content of some antioxidants as vitamins, inorganic species, flavonoids and phenolic acids [7].

Synthetic antioxidants are chemical compounds that are added to foods to keep them unaltered after food processing and to elongate shelf life. Figure 2 shows some components of this group, such as butylated hydroxyanisole (BHA), butylated hydroxytoluene (BHT), tertbutylhydroquinone, esters of gallic acid (better known as gallates) and some phenol derivatives, such as e.g. resorcinol derivatives.

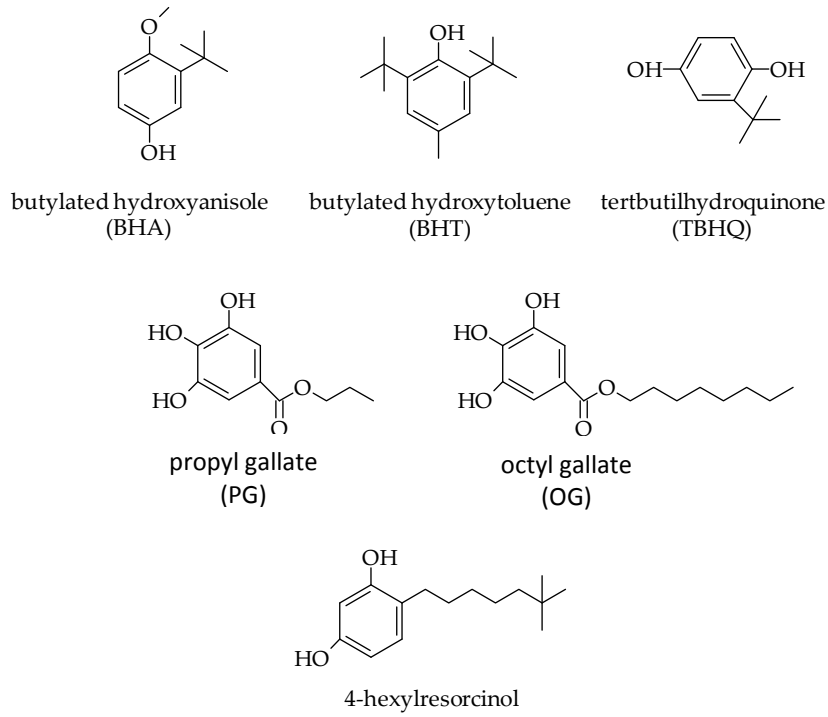

Figure 2. Chemical structures of some synthetic antioxidants.

The European Food Safety Authority (EFSA) revised in 2012 the maximum allowed concentrations for these additives, which are still in use, though the results obtained in some studies indicated they can pose a hazard to human health [8].

Pro-oxidant substances are defined as chemical species that induce oxidative stress, usually by giving rise to the formation of reactive species or by inhibiting antioxidant systems. Free radicals are well known pro-oxidant substances, but antioxidant compounds can also bear a pro-oxidant behavior [6]. For instance, vitamin C is a well known antioxidant that in presence of iron can decompose hydrogen peroxide into hydroxyl radicals, as a pro-oxidative substance would do. The antioxidant or pro-oxidant behavior depends on the antioxidant substance and on the concentration, the study of antioxidant:pro-oxidant ratio for each compound being an active current research area.

The great variety of antioxidant compounds that can exist in food makes it difficult the individual determination of every single species belonging to this family, and on the other hand, the total antioxidant power of a food sample is a very useful tool to assess the beneficial effects of antioxidant intake on human health. There are two terms, which are often indistinctly used, but have slightly different meanings: antioxidant activity and capacity. The antioxidant activity is related to the kinetics of reaction between an antioxidant compound and a pro-oxidant or a radical to which reduces or scavenges, whereas the antioxidant capacity measures the efficiency of the thermodynamic transformation through the reaction of

a pro-oxidant with an antioxidant. Several assays have been developed for the assessment of the total antioxidant power of foods, but they do not provide measurements that correlate mainly owing to the lack of standardized methods [9]. In general, the chemical assays of antioxidant activity can be divided into two main groups according to the type of reaction involved:

- Assays based on hydrogen atom transfer (HAT)
- Assays based on electron transfer (ET)

The assays based on HAT reactions measure the ability of an antioxidant compound to inhibit free radicals (generally peroxyl radicals) by the donation of hydrogen atoms. The mechanism interpreting the antioxidant action of a phenol compound that transfers a proton to a radical is the following:

$$ROO^{\cdot} + AH \,/\, ArOH \longrightarrow ROOH + A^{\cdot}/ArO^{\cdot}$$

where the aryloxy radical ($ArO^{\cdot}$) formed after the reaction of the phenolic antioxidant with the peroxyl radical is stabilized by resonance, and AH and ArOH species are the protected biomolecules and the antioxidant molecules, respectively. In these assays, a fluorophore competes with the antioxidant substance for the peroxyl radicals and the antioxidant activity is determined by measuring the difference in the inhibition of the fluorophore signals obtained in the presence and in the absence of antioxidant compounds. Some HAT-based assays are the oxygen radical

absorbance capacity (ORAC), the total radical antioxidant power (TRAP) and the crocin and β-carotene bleaching assays.

For the ET-based assays, the antioxidant reacts to an oxidant chromophore or fluorophore instead of reacting with peroxyl radicals. Thus, the presence of antioxidant compounds gives rise to a change in the absorbance or the fluorescence of the chromophore or fluorophore, respectively, so that these changes can be correlated to the concentration of antioxidant compounds in the sample. Some assays based on these reactions are the Trolox Equivalent Antioxidant Capacity (TEAC), the DPPH assay (that uses 2,2-diphenylpicrylhydrazyl radical), the Folin-Ciocalteu method, the ferric reducing antioxidant power (FRAP) and cupric reducing antioxidant capacity (CUPRAC).

The investigations of this Dissertation dealing with the development of a method for the determination of antioxidant capacity are based on the application of the ORAC approach. This method involves the use of a bis-azo initiator, such as 2,2′-azobis(2-methylpropionamidine) dihydrochloride (AAPH), which generates peroxyl radicals when heated in the presence of dissolved oxygen [10].

$$R-N=N-R \longrightarrow N_2 + 2ROO^{\cdot}$$

$$ROO^{\cdot} + fluorophore \longrightarrow ROOH + oxidised\ fluorophore$$

$$ROO^{\cdot} + AH \longrightarrow ROOH + A^{\cdot}$$

$$ROO^{\cdot} + A^{\cdot} \longrightarrow ROOA$$

The peroxyl radicals generated react to a fluorophore thus inhibiting its fluorescence. The fluorophores traditionally used have been β-phycoerythrin [11], which was further replaced by fluorescein and dichlorofluorescein [12] owing to the fact that these later presented higher photostability and a practically negligible reactivity toward polyphenols.

The investigations performed have been focused to the study of the analytical usefulness of long-wavelength fluorophores with the aim of improving the spectral selectivity of ORAC assays, as it will be discussed below in this Dissertation. This improvement is possible because the measurements are performed at longer wavelengths than those exhibited by the fluorophores conventionally used for this purpose. These innovations are in agreement with the guidelines of a recently published IUPAC technical report [9], where the following improvement actions are suggested:

- To shift the focus of these assays from screening to elucidation of the antioxidant mechanism.
- To replace fluorescein by other fluorophores insensitive to photobleaching, to side reactions or interactions.
- To analyze potential interferences by the analysis of blank samples where the contribution of samples and fluorophore can be analyzed in the absence and in the presence of the radical generator.
- To test antioxidant concentration ranges to suggest reaction mechanisms of antioxidants and to identify pro-oxidant concentration ranges.

- To obtain information in order to standardize ORAC procedures: fluorophore:radical generator ratio to avoid quenching effects of the fluorophore that can hide the antioxidant action, systematic study of the influence of dissolved oxygen levels on the reaction rate, determination of minimum dissolved oxygen levels to observe the reaction and development of methods to ensure suitable oxygen levels according to the abovementioned.
- To devise methods for suitable temperature monitoring and control.
- To establish standards for the development of microplate-based methods for the determination of antioxidant capacity and to encourage manufacturers to design appropriate instrumentation.
- To develop standardized methods for the calculation of area under the curve.
- To provide data of antioxidant capacity and other parameters, such as for instance, the total polyphenol concentration to know the activity profile.
- To know the capacity profile in natural extracts after their treatment with polyvinylpyrrolidone for the removal of phenolic compounds and to obtain the contribution of non-phenolic compounds to this assay.

From the last two actions described above, it can be seen the significance of complementary data, such as total concentration of phenolic antioxidants and that of non-phenolic antioxidants, intimately related with the antioxidant activity to know the activity profile of each food. The second section of this chapter tackles the determination of phenolic

antioxidant concentration by using laccase enzyme in the presence of terbium oxide nanoparticles as activators.

Laccase enzymes are phenoloxidases that can oxidise antioxidant compounds using dissolved oxygen. These enzymes have activity for antioxidant compounds with ortho- and para-diphenol groups, although their affinity is higher toward para-substituted phenolic compounds. Laccases have a relative selectivity toward their substrates, which have higher or lower reduction potential depending on the laccase type. These enzymes catalyze the oxidation of a wide variety of substrates, such as mono-, di- and polyphenols, aminophenols, methoxyphenols, aromatic amines and ascorbate, with the reduction of oxygen to water by exchanging four electrons.

These enzymes can be obtained from different sources, such as from plants, like the Japanese lacquer tree *Rhus vernicifera*, which the first laccase variety was isolated from, insects and bacteria [13]. However, most laccase currently in use are obtained from higher fungi, such as *Trametes versicolor* and *Trametes hirsuta*, among others.

These enzymes have found a great number of industrial and analytical applications when immobilised onto a solid support. Different immobilisation approaches, such as entrapment, adsorption and encapsulation, among others, have been recently reviewed [13], to finally conclude that the initial enzyme activity cannot be satisfactorily recovered in all instances after these procedures. The most salient analytical applications of laccase enzyme have been focused to the development of electrochemical biosensors [14]. These biosensors often operate sequentially, which limits their sample throughput, unlike other assays

based on the use of well microplates, where measurements are performed almost simultaneously. This is an aspect that has been investigated and optimized in this Dissertation. More specifically, the second section of this chapter has dealt with the development of a high-throughput method for the determination of polyphenols in wines, where the enzyme consumption has been lowered by using terbium oxide nanoparticles as activators. The method also decreases the analysis times required when the enzyme is used in the absence of nanoparticles.

LITERATURE

(1) B.D. Craft, A.L. Kerrihard, R. Amarowicz, R.B.Pegg. Phenol-based antioxidants and the in vitro methods used for their assessment. *Compr. Rev. Food Sci. Food Safety*. **(2012)** *11*, 148 – 173.

(2) B. Halliwell, J.M. Gutteridge. The definition and measurement of antioxidants in biological systems. *Free Radic. Biol. Med.* **(1995)** *18*, 125 – 126.

(3) B. Halliwell. Biochemistry of oxidative stress. *Biochem. Soc. Trans.* **(2007)** *35*, 1147 – 1150.

(4) A.J. Khlebnikov. I.A. Schepetkin, N.G. Domina, L.N. Kirpotina, M.T. Quinn. Improved quantitative structure-activity relationship models to predict antioxidant activity of flavonoids in chemical, enzymatic, and cellular systems. *Bioorg. Med. Chem.* **(2007)** *15*, 1749 – 1770.

(5) B. Halliwell. How to characterize a biological antioxidant. *Free Radic. Res.* **(1990)** *9*, 1 – 32.

(6) M. Carocho, I.C.F.R. Ferreira. A review on antioxidants, prooxidants and relative controversy: Natural and synthetic compounds, screening and analysis methodologies and future perspectives. *Food Chem. Tox.* **(2013)**, *51*, 15 – 25.

(7) B. Lorrain, I. Kay, L. Pechamat, P.L. Teissedre. Evolution of analysis of polyphenols from grapes, wines and extracts. *Molecules*. **(2013)** *18*, 1076 – 1100.

(8) European Food Safety Authority (EFSA). Statement on the safety assessment of the exposure to butylated hydroxyanisole E320 (BHA) by applying a new exposure assessment methodology. *EFSA J*. **(2012)** *10:2759*, 1 – 16.

(9) R. Apak, S. Gorinstein, V. Böhm, K.M. Schaich, M. Ozyürek, K. Güçlü. Methods of measurement and evaluation of natural antioxidant capacity/activity (IUPAC Technical Report). *Pure Appl. Chem.* **(2013)**, *85*, 957 – 998.

(10) R.L. Prior, X. Wu, K. Schaich. Standardized methods for the determination of antioxidant capacity and phenolics in foods and dietary supplements. *J. Agric. Food Chem.* **(2005)**, *53*, 4290 – 4294.

(11) G.H. Cao, H.M. Alessio, R.G. Cutler. Oxygen-radical absorbance capacity assay for antioxidants. *Free Radical Biol. Med.* **(1993)**, *14*, 303 – 465.

(12) B. Ou, M. Hampsch-Woodill, R.L. Prior. Development and validation of an improved oxygen radical absorbance capacity assay using fluorescein as the fluorescent probe. *J. Agric. Food Chem.* **(2001)** *49*, 4619 – 4621.

(13) M. Fernández-Fernández, M.A. Sanromán, D. Moldes. Recent developments and applications of immobilized laccase. *Biotechnol. Adv*. **(2013)** *31*, 1808-1825.

(14) A. Sánchez-Arribas, M. Martínez-Fernández, M. Chicharro. The role of electroanalytical techniques in analysis of polyphenols in wine. *Trends Anal. Chem.* **(2012)** *34*, 78 – 96.

JOURNAL OF AGRICULTURAL AND FOOD CHEMISTRY *J. Agric. Food Chem. 2011, 59, 2235-2240*

Long-Wavelength Fluorimetric Determination of Food Antioxidant Capacity by Using Nile Blue as Reagent

J. Godoy-Navajas, M.P. Aguilar Caballos, A. Gómez-Hens

Department of Analytical Chemistry, University of Cordoba, Campus of Rabanales. Annex to Marie Curie Building. 14071-Cordoba. Spain

ABSTRACT

A method for the determination of the antioxidant capacity by using long-wavelength fluorescence measurements is described for the first time. This method is a modification of the conventional oxygen radical absorbance capacity (ORAC) method that uses fluorescein or phycoerythrin and the generator of peroxyl radicals 2,2′ azo-bis-(2-methylpropionamidine) dihydrochloride (AAPH). The long-wavelength fluorophor nile blue is proposed as an analytical reagent alternative to these conventional fluorophores.

Kinetic curves have been obtained by monitoring the fluorescence variation (λ_{ex} 620, λ_{em} 680 nm) with time, using the 96-well microplate format. The vitamin E analogue 6-hydroxy-2,5,7,8-tetramethylchroman-2-carboxylic acid (Trolox) has been chosen as model analyte, and the normalized area under the decay curve has been used as the analytical parameter. The dynamic range of the calibration curve is 0.8 – 8.0 μM and the detection limit is 0.45 μM. The precision of the method, expressed as relative standard deviation and assayed using 1 and 5 μM Trolox concentrations, was 5.6 and 2.9%, respectively. The method has been applied to the analysis of fruit juices and wines, obtaining results that did not differ significantly from those provided using the ORAC method with fluorescein as reagent.

Keywords: nile blue, antioxidant capacity, long-wavelength fluorimetry, 96-well plate

1. Introduction

Oxidation processes involving free radicals contribute to the development of many types of illnesses, such as, e.g., cardiovascular disease, Alzheimer's disorder, and cancer. This redox phenomenon is produced by reactive oxygen species (ROS), which damage cell membranes, with this effect being reduced by the ingest of antioxidant compounds. The antioxidant capacity of foods is mainly given by polyphenols, such as flavonoids, and vitamins C and E, among others [1]. From an analytical point of view, there are two types of methods for assessing this parameter. The first group involves a single electron-transfer reaction, which can be followed by a change in the colour as the oxidant species is reduced. The second involves the use of hydrogen atom transfer reactions, in which the antioxidant and the substrate compete for the free radicals generated. The oxygen radical absorbance capacity (ORAC) assay is an example of the latter methods. This assay involves the use of 2,2' azo-bis-(2-methylpropionamidine)dihydro-chloride (AAPH) to give rise to peroxyl radicals that directly attack absorbing or fluorescent probes, leading to the quenching of their absorbance or fluorescence, respectively. The dyes β-phycoerythrin [2-4] and fluorescein (FL) [1, 5-14] have been by far the most used fluorescent probes, although Pyrogallol Red has been also described to develop photometric approaches for the determination of the antioxidant capacity in berry extracts [15] and human blood plasma and urine [16]. This assay relies on the performance of photometric measurements of Pyrogallol Red bleaching by action of the peroxyl radical generator, AAPH. It has been reported that this dye allows for the separate estimation of the contribution of ascorbic acid and some polyphenols to the

total antioxidant capacity of fruits with high ascorbic acid concentration, thus allowing for the determination of ascorbic acid in complex samples. The ORAC assay has been also used to assess, e.g., the antioxidant capacity of human milk [14].

Despite the high sensitivity that the above mentioned fluorophores offer, these compounds feature a relatively short Stokes shift (about 27 nm), which favors scattering phenomena. Also, β-phycoerythrin is relatively expensive and suffers from photobleaching, with this fact being the main one responsible for the almost widespread use of FL as probe for the ORAC assay. However, this fluorophor shows a limitation common to organic conventional fluorophores that emit in the 400 – 550 nm range, which is an increased influence of static background signals from the sample matrix. The usefulness of long-wavelength dyes as fluorescent probes to overcome this limitation has been previously demonstrated in several analytical methods [17], but their potential application to the determination of the antioxidant capacity has not been studied up to now.

Nile blue (NB) is a dye from the oxazine group (Figure 1), which emits light in the red region of the spectrum and features a Stokes shift of about 60 nm. This reagent has been previously used for the fluorimetric determination of the synthetic antioxidant butylhydroxyanisole (BHA) [18] and the photometric determination of cerium(IV) [19]. Other recent applications of this fluorophor have been its use in energy- and electron-transfer reactions in covalently functionalized carbon nanotubes [20] and to describe a hydrogen peroxide biosensor by its immobilization, together with horseradish peroxidase [21].

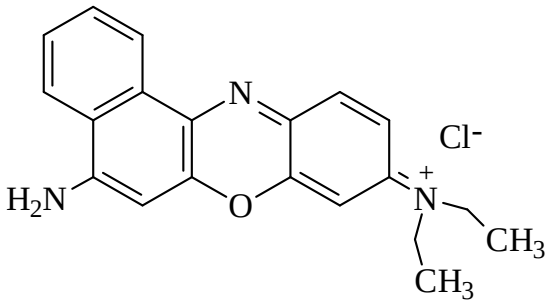

Figure 1. Chemical structure of NB chloride

The work described here involves a modification of the ORAC assay by using NB as the fluorescent probe and 6-hydroxy-2,5,7,8-tetramethylchroman-2-carboxylic acid (Trolox) as the reference standard for antioxidant capacity. The method has achieved its automation by using a microplate reader, which monitored the variation of the fluorescence intensity with time using 620 and 680 nm as excitation and emission wavelengths, respectively. The proposed method has been applied to the analysis of fruit juice and wine samples, and the results obtained have been compared to those provided by the ORAC approach using FL as the reference method, with no statistically relevant differences between the results given by both methods. Also, a recovery study was carried out to validate the usefulness of the proposed method to the analysis of real samples, which has been scarcely reported in the ORAC methods described up to date. These results confirm the usefulness of NB as an analytical reagent for antioxidant capacity determination with better spectral selectivity than the ORAC-FL assay, owing to the use of long-wavelength fluorescence measurements.

2. Materials and methods

2.1. *Instrumentation*

A 1420 Multilabel counter Victor ^{3}V microplate reader (Perkin Elmer and Analytical Sciences, Wallac Oy, Turku, Finland) was used to perform fluorescence measurements. Different filters (nominal wavelength/passband) were used to select the excitation (485/15 nm for FL and 620/8 nm for NB) and emission (535/25 nm for FL and 680/10 nm for NB) wavelengths used to monitor ORAC-FL and ORAC-NB systems, respectively. Each measurement was obtained in 0.5 s, and the subsequent measurements for each well with time were made in 1 min intervals.

2.2. Reagents

All reagents used were of analytical grade. NB chloride was supplied by Sigma (St Louis, MO), and Trolox and AAPH were obtained from Aldrich (Milwaukee, WI, and Steinheim, Germany). Dipotassium hydrogen phosphate was purchased from Merck (Darmstadt, Germany). Phosphate buffer solutions (0.085 M pH 6.9 and 0.075 M pH 7.5) were prepared by dissolving appropriate amounts of dipotassium hydrogen salt and adjusting the pH values with hydrochloric acid to develop ORAC-NB and ORAC-FL methods, respectively. A NB stock solution (29.4 μM) was prepared by dissolving the appropriate amount of the dye in distilled water by magnetic stirring for 24 h and stored at room temperature. Working standard solutions of 89 nM NB were prepared daily by diluting the appropriate volume of the stock solution in phosphate buffer solution (0.085 M at pH 6.9). A stock 4.5 x 10^{-4} M FL solution was prepared by dissolving the appropriate amount of sodium fluorescein in distilled

water, and subsequent dilutions were made daily in phosphate buffer (0.075 M at pH 7.5) to prepare working 70 nM FL solutions. A 0.012 M AAPH solution was also prepared daily in phosphate buffer solution (0.085 M at pH 6.9) and kept at room temperature protected from light to prevent its degradation.

3. Procedures

3.1. Determination of Antioxidant Capacity by the ORAC-NB Method

A volume (20 μL) of standard (0.8 – 8 μM Trolox), wine or juice diluted sample, or blank (0.085 M phosphate buffer at pH 6.9) solutions was added to each well together with 120 μL of 89 nM NB. This mixture was preincubated in sealed plates at 37 °C for 15 minutes, and then, 60 μL of AAPH 0.012 M was added to each well by using an eight-channel electronic micropipet to achieve the simultaneous addition of this reagent. Immediately, the plate was inserted into the microplate reader, and the variation of the fluorescence intensity with time was monitored at 37 °C for 60 min, using the instrumental conditions indicated above. Each measurement was performed in triplicate, and a blank triplicate was recorded at the beginning of each series to control potential changes that may occur, owing to the lack of stability of AAPH, which was kept protected from light at room temperature to ensure identical thermal conditions at time 0 of the reaction. The decay curves were integrated by using Origin software, and then, the normalized net area under the curve (AUC) was calculated by subtracting the blank signal from the signal obtained in the presence of the standard or sample and dividing the result by the blank signal.

3.2. *Determination of the Antioxidant Capacity using the ORAC-FL Method*

The ORAC-FL measurements were done according to the instructions described elsewhere [5], which involve the use of a microplate reader and FL as reagent. Briefly, 20 μL of standard or diluted sample solutions were mixed with 120 μL of 70 nM FL in phosphate buffer (0.075 M, pH 7.4) for 15 min at 37 °C, and then, 60 μL of 0.012 M AAPH were added. The variation of the fluorescence intensity with time was monitored for 60 min using 485 and 535 nm filters to select excitation and emission wavelengths, respectively. The curves obtained were processed in the same way as that described for the ORAC-NB method.

3.3. *Determination of Antioxidant Capacity in Commercial Wine and Fruit Juice Samples*

Several wines (white, semidry and red) and fruit juices (peach, pineapple and apple) were bought in a local market and analysed immediately after they were opened according to the following procedure: A volume (4.5 mL) of sample was treated with 300 μL of 1 M NaOH to increase the pH to neutral values, and it was raised up to 5 mL with phosphate buffer. Then, an adequate dilution (1:500 – 1:10000 dilutions) with the same phosphate buffer was performed to match the dynamic ranges of the calibration curves of either ORAC-FL or ORAC-NB method. A volume (20 μL) of the diluted sample was treated according to the procedures indicated above for both methods.

4. Results and discussion

4.1. Selection of the Long-Wavelength Fluorophor

ROS, such as peroxyl radicals (ROO·), hydroxyl radicals (OH·), superoxide ion ($O_2^{\cdot-}$), and singlet oxygen ($^1O_2$) are involved in the physiology of some diseases. Radical chain-breaking antioxidants convert reactive free radicals into stable and non-aggressive molecules by mechanisms in which AAPH radicals formed in air-saturated solutions react rapidly with molecular oxygen to give rise to peroxyl radicals, ROO·, as described elsewhere [6]. The presence of antioxidant compounds gives rise to the formation of a hydroperoxide and a stable antioxidant radical that breaks the action of peroxide radicals. Although a wide variety of antioxidant compounds can be used as reference standards in ORAC assays [13], such as gallic, caffeic and ascorbic acids, the vitamin E analogue Trolox has been chosen to develop the ORAC-NB method presented here.

The reactions involving the formation of free radicals can be followed by the decrease in the inhibition of the fluorescence from some organic molecules, such as phycoerythrin and FL, in the presence of samples with antioxidant capacity [1-14]. However, the short Stokes shift of these compounds can give rise to light-scattering phenomena that could affect the performance of fluorescence measurements.

Also, *β*-phycoerythrin shows a low photostability, and its price is relatively high. With the aim of studying the potential use of fluorescent dyes that emit in the red region of the spectrum as alternative reagents for this purpose, several oxazine and thiazine dyes, namely NB, azure A and azure B, were assessed. Figure 2 shows the curves obtained for each

fluorophor, in the presence and absence of Trolox, which was used as standard.

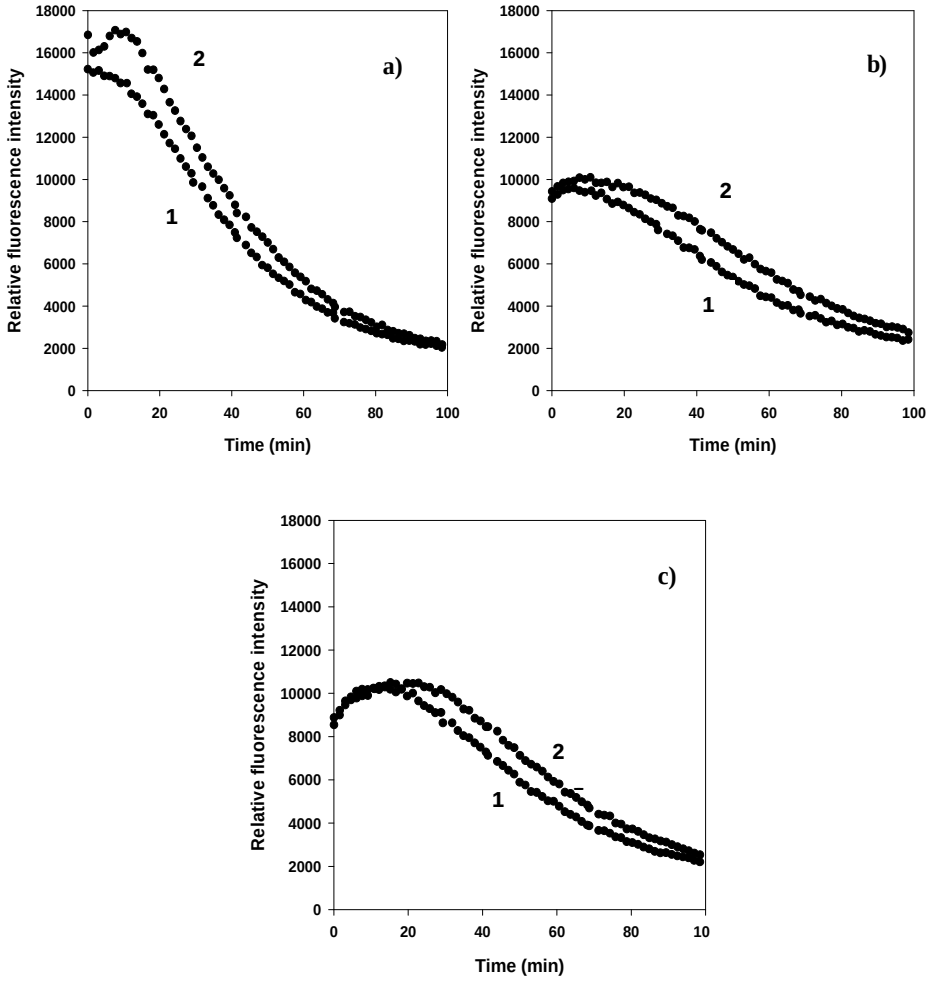

Figure 6: Curves obtained for the ORAC assay using (a) nile blue, (b) azure A, and (c) azure B fluorophores: (a) blank and (2) 2 μM Trolox.

Although it was possible to measure the difference between the blank and standard with all the fluorophors assayed, NB gave the best results. Also, NB was chosen because it has a wider Stokes' shift that the

other two reagents, which avoids potential light-scattering signals. The decay curves obtained in the presence of NB, AAPH, and different Trolox concentrations are shown in Figure 3, in which the AUC increased with the Trolox concentration.

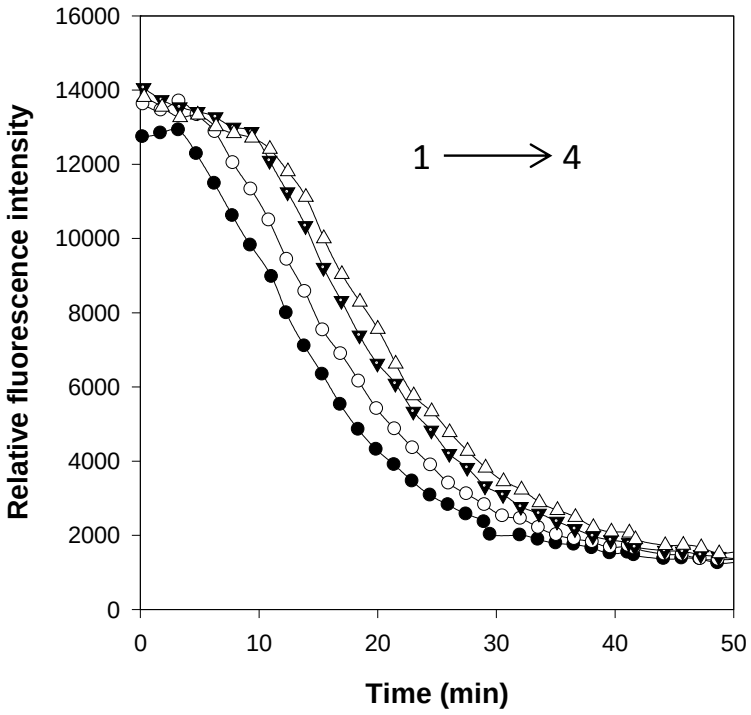

Figure 3. Antioxidant capacity curves obtained at different Trolox concentrations: (**1**) 0 μM, (**2**) 1 μM, (**3**) 2 μM, and (**4**) 4 μM. Experimental conditions: [NB], 89 nM; [AAPH], 0.012 M; pH, 6.9; [phosphate], 0.085; and temperature, 37 °C.

4.2. Optimisation of the ORAC-NB Method

The variables affecting the system were optimised by the univariate method. Each result was the average of three measurements. The analytical

parameter used to optimise the system was the net AUC, calculated as indicated above in the procedure of the ORAC-NB method.

The influence of the pH was investigated in the range of 4 - 11, using 0.075 M acetate, phosphate, borate and, carbonate buffer solutions to keep the pH constant in the buffering region of each solution. As Figure 4A shows, there was not appreciable net AUC at pH values below 5.8 and above 8. The behaviour of the system at low pH values could be ascribed to the fact that the pKa value of Trolox is about 3.89, showing a low solubility at this pH [22]. The solubility increases with the pH, which improves the value of the net AUC, obtaining the best results in the pH range of 6.0 - 7.0. A pH of 6.9 was chosen, which is slightly lower than that required to develop the ORAC-FL method (pH 7.4). The influence of buffer concentration was studied by assaying phosphate concentrations in the range of 0.02 – 0.15 M, finding that a 0.085 M phosphate buffer solution gave the best signal.

NB and AAPH concentrations are two critical variables that are interrelated. The influence of the fluorophor concentration was studied by adding a fixed volume (120 μL) of solutions with NB concentrations ranging from 60 to 370 nM (Figure 4B). The system was practically independent on this variable in the range 80 - 130 nM, choosing 89 nM NB for the development of the method. The influence of the peroxyl radical generator, AAPH, was evaluated in the range of 0.006 - 0.024 M, finding that the AUC signals of both analyte and blank solutions decrease, with the difference also decreasing between both signals, when the AAPH concentration increases. However, the curves obtained at low AAPH concentrations were less defined and showed a low

reproducibility. Thus, a 0.012 M AAPH concentration was chosen.

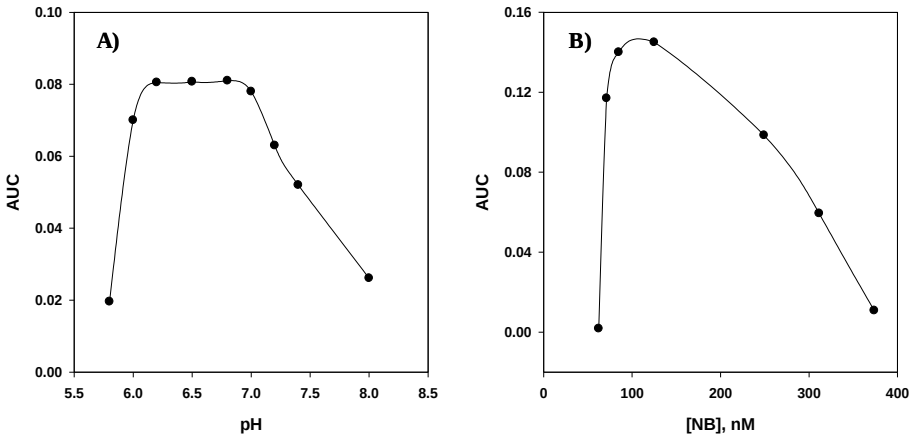

Figure 4. Influence of pH (**A**) and (**B**) NB concentration on the ORAC-NB method. In panel A, [NB], 120 nM; [phosphate], 0.075 M; [AAPH], 0.024 M; [Trolox], 2 μM; and temperature, 27 °C. In panel B, [AAPH], 0.012 M; [Trolox], 2 μM; pH, 6.9; [phosphate], 0.085 M; and temperature, 37 °C.

The temperature is an important variable in kinetic studies, and also, it has a remarkable effect on the decomposition of AAPH [7], mainly at values close to 37 °C. The influence of this variable on the system was studied by mixing NB with Trolox for 15 min at 37 °C and, and after the addition of 60 μL of 0.012 M AAPH, the mixture was kept at different temperatures, in the range 25 °C - 40 °C. The kinetic curves obtained at 25 °C were relatively slow, providing a net AUC value 1.5 times lower than that obtained at 37 °C. This temperature was chosen to develop the method because the curves obtained were also more defined, which could probably be ascribed to the fact that the decomposition reaction of AAPH was not

the limiting step. The method using FL as reagent [8] is also developed at 37 °C.

4.3. Analytical Features

The kinetic curves were obtained under optimum conditions, using λ_{ex} of 620 nm and λ_{em} of 680 nm to monitor the variation of the fluorescence intensity with time for 60 min and the net AUC as the analytical parameter. The dynamic range of the calibration graph was 0.8 - 8 μM Trolox. The regression equation was AUC = (0.02 ± 0.01) + (0.074 ± 0.006) X, where X was the Trolox concentration expressed in micromolar. The regression coefficient (R) is 0.993, which is indicative of a good linearity of the calibration curve. The detection limit, calculated following International Union of Pure and Applied Chemistry (IUPAC) recommendations [23], was 0.45 μM, which is lower [6, 7] or similar [8] to those obtained in other ORAC methods involving FL. The precision of the method was assessed at two different Trolox concentrations, 1 and 5 μM, and expressed as the percentage of relative standard deviation, giving 5.6 and 2.9%, respectively.

4.4. Applications

The proposed method was applied to the analysis of wines, namely, white, semi-dry and red, and commercial fruit juices, namely, pineapple, peach and apple. These samples were analyzed by both ORAC-FL and ORAC-NB methods with a simple sample treatment, which consisted in the adjustment of the pH to neutral values, because the samples featured acidic pH values. Then, the samples were

diluted to accommodate the antioxidant content to the dynamic range of the calibration curve. Figure 5 shows the curves obtained for the blank and those obtained at different sample dilutions for (A) white wine and (B) pineapple juice samples. It can be seen from these curves that the area proportionally increased as the sample dilution decreased. The net AUC of the samples was measured as (AUC_{sample} – AUC_{blank})/AUC_{blank}, and this result was interpolated in the calibration curve obtained for Trolox standards.

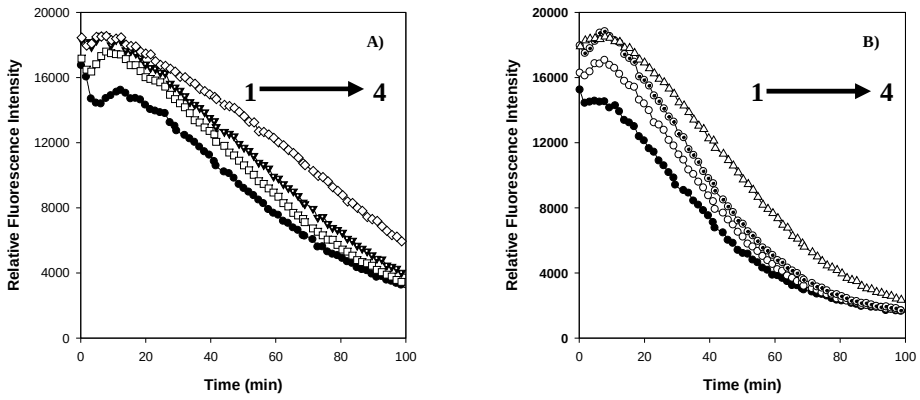

Figure 5. Antioxidant capacity curves obtained in the presence of (**A**) semi-dry white wine and (**B**) pineapple juice samples at different sample dilutions. Experimental conditions are as follow: [NB], 89 nM; [AAPH], 0.024 M, pH, 6.9; [phosphate], 0.085 M; and temperature, 27 °C. In **panel A**, (1) blank and (2, 3 and 4) are 1/4000, 1/2000, and 1/1000 dilutions of the white wine sample, respectively. In **panel B** (1) blank.

After the application of the corresponding dilution factors, the antioxidant content of each analyzed sample, expressed as millimolar Trolox Equivalents of sample, was calculated. Table 1 lists the content

found in the samples using both ORAC-NB and ORAC-FL methods. The paired *t* test was applied to the results at a 95% significance level, and it was found that there were not significant differences in the results provided by both methods, which confirms the practical utility of the proposed ORAC-NB method to the analysis of these food samples.

Table 1. Antioxidant Capacity (Expressed as millimolar Trolox Equivalents of Sample) of Food Samples Analyzed by ORAC-NB and ORAC-FL Methods

Sample	ORAC-NB [a]	ORAC-FL [a]
white wine (manzanilla)	1.50 ± 0.09	1.3 ± 0.2
semidry wine	7.7 ± 0.9	4.4 ± 0.4
red wine	15.3 ± 0.4	10.4 ± 0.9
peach juice	2.222 ± 0.001	1.93 ± 0.09
pineapple juice	2.7 ± 0.3	2.399 ± 0.006
apple juice	2.7 ± 0.3	3.5 ± 0.4

[a]Mean ± standard deviation (SD) (n = 3)

Also, the values found for both types of samples agree with values reported in the literature [9, 10].

A recovery study was also carried out to validate the method. It was performed by adding three different amounts of Trolox to each sample and by subtracting the results obtained from similarly treated unspiked samples. Table 2 shows the recovery percentages, which ranged from 72.7

to 113.6%. The mean recovery values obtained were 92.0 and 92.9 % for wine and juice samples, respectively. This internal validation also confirms the usefulness of the developed ORAC-NB method for the analysis of real samples.

Table 2. Recovery values obtained for the different samples analyzed

	Recovery study		
Sample	Added[a]	Found[a,b]	Recovery (%)
White wine	2.2	2.0 ± 0.2	92.0
	8.9	6.7 ± 0.9	75.2
	11.1	9.2 ± 0.8	82.9
Semi-dry wine	4.4	3.6 ± 0.2	81.8
	8.8	8.1 ± 0.3	92.1
	13.2	12.9 ± 0.6	97.0
Red wine	17.8	18 ± 2	101.1
	35.6	38 ± 4	106.7
	44.4	44 ± 4	99.1
Peach juice	2.2	2.1 ± 0.1	95.5
	4.4	3.5 ± 0.4	79.5
	5.5	4.3 ± 0.2	78.2
Pineapple juice	2.2	2.5 ± 0.2	113.6
	4.4	4.5 ± 0.3	102.3
	5.5	5.8 ± 0.4	105.5
Apple juice	4.4	3.2 ± 0.2	72.7
	8.8	7.9 ± 0.5	89.6
	11.1	11 ± 1	99.1

[a]Units in millimolar Trolox equivalents of sample.
[b] Mean ± SD (n =3).

The results obtained show the feasibility of long wavelength fluorimetry for the determination of antioxidant capacity in foods using the

fluorophor NB for the first time as an analytical reagent. The use of this reagent instead of other fluorophores previously proposed for this purpose, such as FL or β-phycoerythrin, is a useful alternative to avoid potential background signals from the sample matrix, which can appear at lower wavelengths. Also, the relatively wide Stokes shift of NB allows analytical measurements to be free of scattering signals, which can be a limitation when the above-mentioned fluorophores are used. Finally, the probability of photobleaching processes for NB is lower than that for β-phycoerythrin, as well as its cost.

Acknowledgement

The authors gratefully acknowledge financial support from the Ministerio de Ciencia e Innovación (MICINN) (Grant CTQ2009-08621) and from the Junta of Andalucia (Grant P09-FQM4933).

Abbreviations used

AAPH, 2,2′ azo-bis-(2-methylpropionamidine) dihydrochloride; AUC, area under the curve; BHA, butylhydroxyanisole; FL, fluorescein; NB, nile blue; ORAC, oxygen radical absorbance capacity; ROS, reactive oxygen species

References

(1) M. Ciz, H. Cizova, P. Deneb, M. Kratchanova, A. Slavov, A. Lojek. Different methods for control and comparison of the antioxidant properties of vegetables. *Food Control* (**2010)** *21*, 518–523.

(2) M. D. Rivero-Pérez, M. L. González-Sanjosé, M. Ortega Herás, P. Muñiz. Antioxidant potential of single-variety red wines aged in the barrel and in the bottle. *Food Chem.* (**2008)** *111*, 957–964.

(3) E. Sofic, Z. Rimpapa, Z. Kundurovic, A. Sapcanin, I. Tahirovic, A. Rustembegovic, G. Cao. Antioxidant capacity of the neurohormone melatonin. *J. Neural Transm.* (**2005)** *112*, 349–358.

(4) G. Cao, C. P. Verdon, A. H. B. Wu, H. Wang, R. L. Prior. Automated assay of oxygen radical absorbance capacity with the COBAS FARA II. *Clin. Chem.* (**1995**) *41*, 1738–1744.

(5) G. Cao, H. M. Alessie, R. G. Cutler. Oxygen-radical absorbance capacity assay for antioxidants. *Free Radical Bio. Med.* (**1993**) *14*, 303–311.

(6) B. Ou, M. Hampsch-Woodill, R. L. Prior. Development and validation of an improved oxygen radical absorbance capacity assay using fluorescein as the fluorescent probe. *J. Agric. Food Chem.* (**2001**) *49*, 4619–4626.

(7) D. Huang, B. Ou, M. Hampsch-Woodill, J. A. Flanagan, R. L. Prior. High-throughput assay of oxygen radical absorbance capacity (ORAC) using a multichannel liquid handling system coupled with a microplate fluorescence reader in 96-well format. *J. Agric. Food Chem.* (**2002**) *50*, 4437–4444.

(8) A. Dávalos, C. Gómez-Cordovés, B. Bartolomé. Extending applicability of the Oxygen Radical Absorbance Capacity (ORAC-Fluorescein) assay. *J. Agric. Food Chem.* (**2004**) *52*, 48–54.

(9) A. Dávalos, B. Bartolomé, C. Gómez-Cordovés. Antioxidant properties of commercial grape juices and vinegars. *Food Chem.* (**2005**) *93*, 325–330.

(10) W. Mullen, S. C. Marks, A. Crozier. Evaluation of phenolic compounds in commercial fruit juices and fruit drinks. *J. Agric. Food Chem.* (**2007**) *55*, 3148–3157.

(11) J. Tabart, C. Kevers, J. Pincemail, J. O. Defraigne, J. Dommes. Comparative antioxidant capacities of phenolic compounds measured by various tests. *Food Chem.* (**2009**) *113*, 1226–1233.

(12) L. Müller, S. Groyke, A. M. Popken, V. Böhm. Antioxidant capacity and related parameters of different fruit formulations. *Food Sci. Technol.* (**2010**) *43*, 992–999.

(13) N. Nenadis, O. Lazaridou, M. Z. Tsimidou. Use of reference compounds in antioxidant activity assessment. *J. Agric. Food Chem.* (**2007**) *55*, 5452–5460.

(14) A. Tijerina-Sáenz, I. Elisia, S. M. Innis, J. K. Friel, D. D. Kitts. Use of ORAC to assess antioxidant capacity of human milk. *J. Food Compos. Anal.* (**2009**) *22*, 694–698.

(15) E. Atala, L. Vásquez, H. Speisky, E. Lissi, C. López-Alarcón. Ascorbic acid contribution to ORAC values in berry extracts: An evaluation by the ORAC-pyrogallol red methodology. *Food Chem.* (**2009**) *113*, 331–335.

(16) P. Torres, P. Galleguillos, E. Lissi, C. López-Alarcón.

Antioxidant capacity of human blood plasma and human urine: Simultaneous evaluation of the ORAC index and ascorbic acid concentration employing pyrogallol red as probe. *Bioorg. Med. Chem.* (**2008**) *16*, 9171–9175.

(17) A. Gómez-Hens, M. P. Aguilar-Caballos. Long-wavelength fluorophores: new trends in their analytical use. *Trends Anal. Chem.* (**2004**) *23*, 127–136.

(18) M. P. Aguilar-Caballos, A. Gómez-Hens, D. Pérez-Bendito. Simultaneous stopped-flow determination of butylated hydroxyanisole and propyl gallate using a T-format spectrofluorimeter. *J. Agric. Food Chem.* (**2000**) *48*, 312–317.

(19) H. Tavallali, E. Asrari, M. A. Ameri Siahoe. Sensitive kinetic spectrophotometric method for trace determination of cerium (IV) based on decolarization of nile blue by potassium periodate. *Int. J. Chem. Tech Res.* (**2009**) *1*, 359–362.

(20) G. M. do Nascimento, R. C. de Oliveira, N. A. Pradie, P. R. G. Lins, P. R. Worfel, G. R. Martinez, P. Di Mascio, M. S. Dresselhaus, P. Corio. Redox mediator single-wall carbon nanotubes modified with organic dyes: Synthesis, characterization and potential cytotoxic effects. *J. Photochem. Photobiol. A* (**2010**) *211*, 99–107.

(21) A. K. Upadhyay, Y. Y. Peng, S. M. Chen. Immobilization of horseradish peroxidase and nile blue into the ormosil nanocomposite for the fabrication of hydrogen peroxide biosensor based on MWCNT modified glassy carbon electrode. *Sens. Actuat. B* (**2009**) *141*, 557–565.

(22) M. Lúcio, C. Nunes, D. Gaspar, H. Ferreira, J. L. F. C. Lima, S. Reis. Antioxidant activity of vitamin E and Trolox: Understanding of the factors that govern lipid peroxidation studies in vitro. *Food Biophys.* (**2009**) *4*, 312–320.

(23) G. L. Long, J. D. Winefordner. Limit of detection: A closer look at the IUPAC's definition. *Anal. Chem*. (**1983)** *55*, 712A–724A.

Automatic determination of polyphenols in wines using laccase and terbium oxide nanoparticles

J. Godoy-Navajas, M.P. Aguilar Caballos, A. Gómez-Hens
Department of Analytical Chemistry, University of Cordoba, Campus of Rabanales. Annex to Marie Curie Building. 14071-Cordoba. Spain

Abstract

The analytical usefulness of the combined use of laccase, terbium oxide nanoparticles (Tb_4O_7NPs) and 8-hydroxypyrene-3-sulfonate trisodium (HPTS) for the determination of polyphenol compounds in wine samples is described. The system is based on the temporal inhibition by polyphenols on the decrease of the HPTS fluorescence in the presence of laccase and on the activating effect of Tb_4O_7NPs, which increase the reaction rate of the system, shortening analysis times.

The method has been developed in a microplate format using an automatic reader, reaching a sample throughput of 35 samples h^{-1}. The dynamic range of the calibration graph is 0.5 - 12 μM gallic acid, which was chosen as model analyte, and the detection limit is 0.14 μM. Precision data, expressed as relative standard deviation, ranged between 2.5 and 6.3%. The method was applied to the analysis of several wine samples, obtaining recovery values in the range of 80.0-108.3%.

Keywords: Polyphenols, terbium oxide nanoparticles, laccase, fluorometric detection, wine analysis.

1. Introduction

Polyphenols are an important group of natural antioxidant compounds present in the human diet that, after numerous epidemiological and clinical studies, have shown their usefulness in the prevention of various chronic diseases. The interest in the determination of these compounds has given rise to chromatographic (Lorrain, Ky, Pechamat & Teissedre, 2013; Medić-Ŝarić, Rastija & Bojić, 2011) and capillary electrophoretic (Franquet-Griell, Checa, Núñez, Saurina, Hernández-Cassou & Puignou, 2012; Sánchez-Arribas, Martínez-Fernández & Chicharro, 2012) methods for their identification and quantification. However, the high variety of compounds that form this group justifies the development of methods devoted to determine phenol content and antioxidant activity, which is another related parameter that includes non-phenolic antioxidants. Both parameters are widely determined in fruits and beverages such as wines.

The photometric Folin-Ciocalteu method (Magalhães, Segundo, Reis, Lima & Rangel, 2006; Nenadis, Lazaridou & Tsimidou, 2007; Sánchez-Rangel, Benavides, Heredia, Cisneros-Zevallos & Jacobo-Velázquez, 2013) is usually chosen for phenolic content determination, using a polyphenol, such as gallic acid, as calibration standard. However, a limitation of this method is that usually provides an overestimation of these compounds due to interferences from some non-phenolic reducing substances. Several methods involving the measurement of scavenging capacity of antioxidants against a given radical have been described for antioxidant activity determination (Sochor et al., 2010; Dawidowicz, Wianowska & Olszowy, 2012; Nkhili & Prat, 2011; Godoy-Navajas, Aguilar-Caballos &

Gómez-Hens, 2011). Most of these methods use Trolox (6-hydroxy-2,5,7,8-tetramethylchroman-2-carboxylic acid), which is a water-soluble analogue of vitamin E, as calibration standard. Although several studies have been carried out using different wine types to relate the phenol content with the antioxidant activity, the correlation coefficients obtained are usually low (Fernández-Pachón, Villaño, García-Parrilla & Troncoso, 2004; Di Majo, La Guardia, Giammanco, La Neve & Giammanco, 2008; Li, Wang, Li, Li & Wang, 2009), which is the result of the different antioxidant potential of the phenol compounds present in wines.

Laccase is a phenoloxidase enzyme that has been described for the determination of both phenolic content and antioxidant activity, using different experimental conditions. This enzyme catalyzes the oxidation of phenolic compounds to quinones or radicals by reducing the dissolved oxygen to water. Several laccase-based amperometric sensors have been described for polyphenol determination in wines (Gamella, Campuzano, Reviejo & Pingarrón, 2006; Di Fusco, Tortolini, Deriu & Mazzei, 2010; Montereali, Della Seta, Vastarella & Pilloton, 2010) using gallic acid as the polyphenol standard. Although the detection limits of these methods are adequate for their use in routine analysis, they show a limited life time that is ascribed to the adsorption of oxidized products on the surface of the electrode with the consequent negative effect on the enzyme activity. A fluorometric method has been reported for the determination of polyphenol content in juice and tea samples using indocyanine green and positively charged gold nanoparticles (Andreu-Navarro, Fernández-Romero & Gómez-Hens, 2012). The method is based on the temporal inhibition caused by polyphenols on the oxidation of the fluorophore and

the modification of the enzyme activity by its interaction with the nanoparticles. Laccase has also been described for the determination of antioxidant activity using high reactive chromophore substrates, such as 2,2´-azino-bis-(3-ethylbenzothiazolin-6-sulfonic) acid (ABTS) (Kulys & Bratkovskaya, 2007) or syringaldazine (Nugroho-Pratseyo, Kudanga, Steiner, Murkovic, Nyanhongo & Guebitz, 2009; Nugroho-Pratseyo, Kudanga, Steiner, Murkovic, Nyanhongo & Guebitz, 2010), which are oxidized to free radicals that react with the phenolic and non-phenolic antioxidants present in the sample. In addition to the use of laccase in food analysis, this enzyme has been also applied in detoxification procedures of effluents from chemical industries, in which the degradation of some compounds, such as phenol is performed (Wang, Hu, Guo, Huang & Liu, 2012). Also, it has been used in textile industries for dye decolourization and degradation (Benzina et al., 2013; Ashrafi, Rezaei, Foroontanfar, Mahvi & Faramarzi, 2013; Taha, Shwaish, Mohamed, Haider & Stamatis, 2013).

A feature of the methods described for the determination of polyphenol content and antioxidant capability is that measurements are usually performed sequentially, so that the sample throughput is lower than in systems operating simultaneously such as those involving the use of a microplate reader. This approach has been here used for the first time to develop an automatic method for the determination of polyphenols in wines using laccase and the fluorophore 8-hydroxypyrene-1,3,6-trisulfonic acid trisodium salt (HPTS or pyranine) in the presence of Tb_4O_7 nanoparticles (NPs). Other aims of this research were the study of the potential usefulness of HPTS as a laccase substrate and the capacity of these NPs to play a role as laccase activators.

HPTS has been previously used for the evaluation of the antioxidant potential of polyphenols by measuring the bleaching of HPTS by peroxyl radicals using 2,2'-azo-bis(2-amidinopropane) hydrochloride (AAPH) as the free radical source (Campos, Sotomayour, Pino & Lissi, 2004). However, the practical application of this method was not described. A comparative study of the radical-scavenging capacity of red wine has been carried out using the bleaching of HPTS and pyrogallol red induced by free radicals generated from an azo initiator (Omata, Saito, Yoshida & Niki, 2008). This study showed that HTPS has much lower reactivity toward peroxyl radicals than pyrogallol red, which allows antioxidants to inhibit HTPS bleaching almost completely to produce a lag phase, from which the total amounts of free radicals that can be scavenged by antioxidants, may be estimated. The results obtained in the study carried out here have shown the usefulness of HPTS as a laccase substrate for polyphenol determination and the positive effect of Tb_4O_7 NPs to improve the features of the developed method.

2. Experimental

2.1 Instrumentation

A 1420 multilabel counter Victor ^{3}V microplate reader (Perkin-Elmer and Analytical Sciences, Wallac Oy, Turku, Finland) was used to perform fluorescence measurements. Different filters (nominal wavelength/passband) were used to select excitation and emission wavelengths of several fluorophores assayed in the study (Table 1) and each measurement was made in 0.5 s. An SLM-Aminco (Urbana, IL, USA), Model 8100 photon-counting spectrofluorometer, equipped with a 450 W

xenon arc source and a R928 photomultiplier tube, was used to perform fluorescence excitation and emission scans of the different fluorophores in solution and photobleaching experiments. A Lambda 35 UV/VIS spectrometer (Perkin-Elmer, United Kingdom) was used to perform photometric measurements of the Folin-Ciocalteu method. 1/2AreaPlate™ microplates (PerkinElmer, USA) with a total volume of 180 ◎L were used to record the kinetic curves of the system.

2.2 Reagents

All reagents used were of analytical grade. The fluorophores 8-hydroxypyrene-1,3,6-trisulfonic acid trisodium salt (HPTS), 2-[4-(dimethylamino)styryl]-1-methylpyridinium iodide (2-Di-1-ASP), 2-[4-(dimethylaminophenyl]-1,3-butadienyl)-3-ethylbenzothiazolium p-toluenesulfonate salt (Styryl 7), nile blue chloride, azure B chloride and toluidine blue O were provided by Sigma-Aldrich (St. Louis, Mo, USA), as well as Tween 20, laccase enzyme (*Trametes Versicolor,* EC Number 1.10.3.2, 2.05 U/mg), and caffeic acid. The surfactants Triton X-100 and hexadecyl-trimethylammonium bromide (CTAB) were purchased from Fluka (Buchs, Switzerland). Europium (III) oxide nanoparticles (Eu_2O_3 nanopowder, <150 nm), diamond nanoparticles (<10 nm particle size) and gallic acid were acquired from Sigma. Terbium oxide nanopowder (TEM <150 nm), silver nanoparticles (10 nm, in aqueous buffer containing citrate as stabilizer), terbium nitrate pentahydrate and sodium chloride were purchased for Sigma-Aldrich and fluorescein sodium was purchased for Fluka**.** Ascorbic acid was acquired from Sigma-Aldrich while citric acid and sulfuric acid were purchased from Panreac (Barcelona, Spain). Glucose and sucrose

were purchased from Sigma-Aldrich and Fluka, respectively. Di-potassium hydrogen phosphate, tris(hydroxymethyl)-aminomethane (TRIS), sodium sulfite, malic acid and sodium hydroxide were purchased from Merck (Darmstadt, Germany). Sodium carbonate, sodium acetate and sodium dodecyl sulfate (SDS), Folin-Ciocalteu´s phenol reagent (2N) and 6-hydroxy-2,5,7,8-tetramethylchromane-2-carboxylic acid (Trolox) were provided from Sigma-Adrich.

Phosphate buffer solution (0.4 M pH 7.0) was prepared by dissolving an appropriate amount of dipotassium hydrogen phosphate salt (Merck) in distilled water and adjusting the pH with hydrochloric acid. A HPTS stock solution (890 μM) was prepared by dissolving the appropriate amount of the fluorophore in distilled water by magnetic stirring for several minutes and stored at room temperature. Working solutions (10 μM HPTS) were prepared daily by diluting the appropriate volume of the stock solution in the phosphate buffer solution. A 10 mM stock solution of gallic acid was prepared daily by dissolving the appropriate amount of the reagent in distilled water and the different standards solutions were prepared diluting the appropriate volume of the stock solution in distilled water. A 4 mg/mL stock Tb_4O_7 NPs dispersion was prepared daily by dispersing the appropriate amount of nanopowder in distilled water by using an ultrasound bath. Working solutions were prepared by diluting the stock dispersion in the phosphate buffer solution. A laccase stock solution (4 U/mL) was prepared daily by sonication for 10 s and let overnight to stand before use. Working laccase solutions were prepared by diluting the appropriate volume of the stock solution in the phosphate buffer solution.

2.3. Procedures

2.3.1. Determination of polyphenols using the laccase-Tb_4O_7 NP method

A volume (75 μL) of zero standard, gallic acid standards (0.5 – 12 μM) or diluted wine sample was firstly added to each well of the microplate together with 15 μL of 10 μM HPTS. This mixture was kept for 15 minutes at 37 ^{o}C to reach constant temperature and, then, a volume (60 μL) of a mixture containing 1 mg/mL Tb_4O_7 NPs and 1 U/mL laccase in phosphate buffer solution was added to each well by using an electronic multichannel micropipette. Immediately after, the microplate was inserted into the microplate reader, and the variation of the fluorescence intensity of HPTS with time was monitored at 37 ^{o}C for 36 min, using nominal excitation and emission wavelength filters of 450 and 535 nm, respectively. Normalized decay curves were obtained by dividing the fluorescence signals obtained at each time by the fluorescence signal obtained at time zero for each curve. These curves were later integrated using Origin software, and then, the net normalized area under the curve (AUC) was calculated by subtracting the AUC for the blank from the AUC obtained in the presence of gallic acid.

2.3.2. Analysis of wine samples

Wine samples (red, white and sweet wine samples) were bought at a local supermarket and analyzed immediately after they were opened. Samples were diluted according to their content to match the dynamic range of the calibration curve. The dilutions were in the ranges of 1:4000 -

1:8000 for red, 1:100 – 1:500 for white and 1:500 – 1:2000 for sweet wine samples.

2.3.3. Folin-Ciocalteu method

This method was performed as described elsewhere (Magalhães et al., 2006). Briefly, a volume (2.5 mL) of gallic acid standard (15-150 μM prepared in distilled water) or diluted wine sample was mixed with 500 μL of Folin-Ciocalteu reagent (heteropolyphosphotungstate- molybdate) and 5 mL of sodium carbonate (60 g/L). This mixture was kept at room temperature for 2 h and, afterwards, the absorbance was measured at 760 nm.

3. Results and Discussion

3.1. Study of the system

This study was carried out to choose the experimental conditions that allow the development of a fast and automatic fluorometric method for the determination of polyphenol compounds using laccase. The study was carried out in an automatic system involving the use of microplates with a volume of 180 μL for each well, so that the sample and reagent consumption was lower than in conventional microplates (350-400 μL).

Several potential fluorescent laccase substrates (Styryl 7, 2-Di-1-ASP, azure B chloride, toluidine blue O, nile blue chloride, sodium fluorescein and HPTS) (Table 1) were assayed to study their capability to compete with phenolic antioxidants for the active sites of the enzyme. Although indocyanine green has been described as a laccase substrate (Andreu-Navarro et al., 2012), it was not assayed because its long

excitation and emission wavelengths were not adequate for the microplate reader used in this study.

Table 1. Fluorophores assayed as potential substrates of laccase enzyme in this study

Fluorophore	Excitation filter	Emission filter
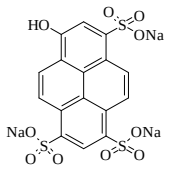 8-Hydroxypyrene-1,3,6-trisulfonic acid trisodium salt (HPTS)	450/6	535/25
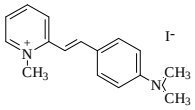 2-[4-(Dimethylamino)styryl]-1-methylpyridinium iodide (2-Di-1-ASP)	485/15	535/25
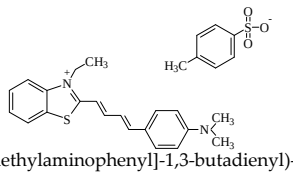 2-[4-(Dimethylaminophenyl]-1,3-butadienyl)-3-ethyl benzothiazolium p-toluenesulfonate salt (Styryl 7)	531/25	680/10
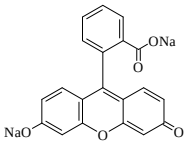 Sodium fluorescein	485/15	535/25
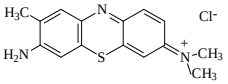 Toluidine blue O	620/8	680/10
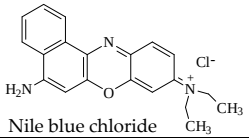 Nile blue chloride	620/8	680/10
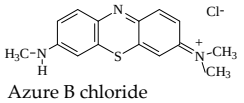 Azure B chloride	620/8	680/10

Figure 1 shows the behavior of some of the fluorophores assayed on the system, in which can be seen that only HPTS shows a relatively fast decrease in its fluorescence intensity. These results could be ascribed to the fact that HPTS has a phenol group, unlike the other fluorophores assayed, allowing its enzymatic oxidation by dissolved oxygen. Another feature of HPTS that could be related with its behavior in the presence of laccase is that this compound is a weak acid in the ground state, with a pK of 7.4, but this value decreases up to 0.4 in the excited state (Mondal, Ghosh, Sahu, Sen & Battacharyya, 2007), behaving as a strong acid when fluorescence measurements are obtained.

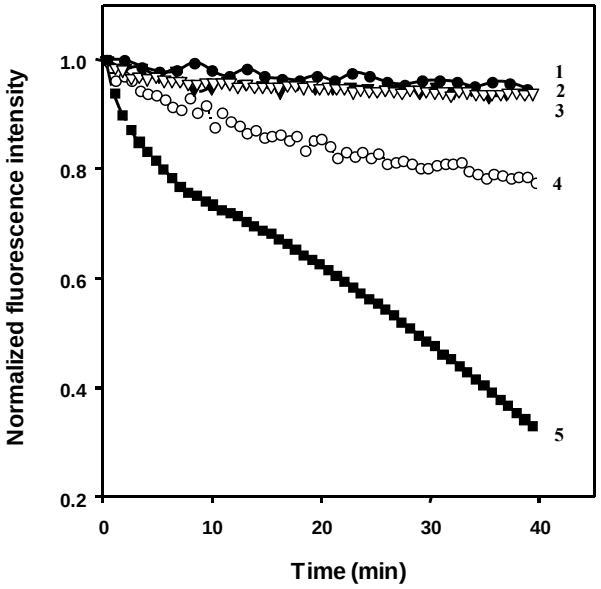

Figure 1. Behavior of different fluorophores in the presence of laccase. 1) azure B chloride, 2) sodium fluorescein, 3) toluidine blue O, 4) 2-Di-1-ASP, 5) HPTS. Experimental conditions: In 1), 3) and 4) [fluorophore] = 5 μM, [laccase] = 0.2 U/mL. In 2) and 5) [fluorophore] = 1 μM, [laccase] = 0.1 U/mL. All the assays were carried out using phosphate buffer solution (0.2 M, pH 7.0).

The presence of gallic or caffeic acid on the system caused a delay on the fluorescence decrease of HPTS, ascribed to the sequential catalytic effect of laccase, which acts over the fluorophore when the polyphenol has been oxidized. Figure 2 shows the kinetic curves obtained in the absence and in the presence of gallic acid.

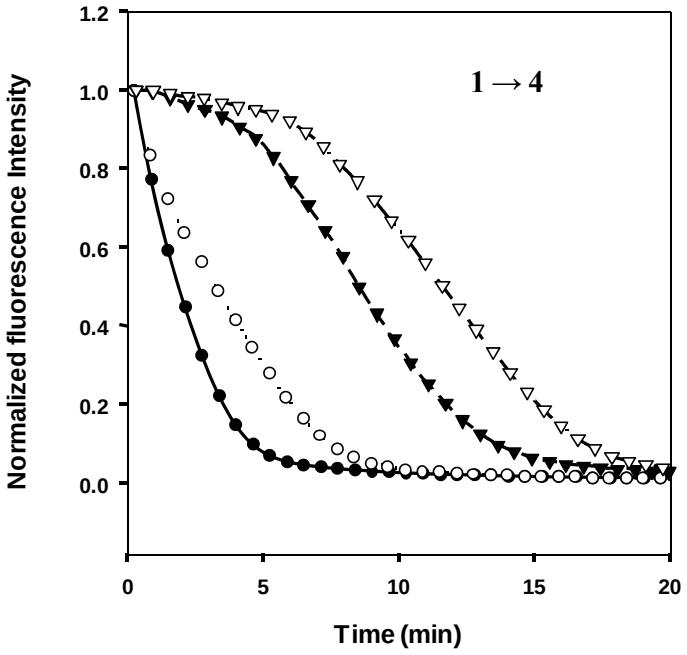

Figure 2. Kinetic curves obtained for the HPTS-laccase system in the absence (curves 1 and 2) and in the presence (curves 3 and 4) of 2 μM gallic acid, and in the presence (curves 1 and 3) and in the absence (curves 2 and 4) of 1 mg/ml Tb_4O_7 NPs. [HPTS] = 10 μM, [laccase] = 1 U/mL, pH = 7.0, [phosphate] = 0.4 M, temperature 37 °C.

Another assay carried out to improve the features of the system was the study of the potential activator effect of different NPs on the catalytic behavior of laccase. The positive effect of copper oxide NPs on the degrading activity of laccase has been previously described using syringaldazine, but the activation mechanism of these NPs has not been elucidated (Mukhopadhyay, Dasgupta & Chakrabarti, 2013). Although Cu(II) in solution also caused an activation effect, it was lower than that obtained in the presence of the NPs. Several NPs, such as diamond, Eu_2O_3, Tb_4O_7, magnetic-gold NPs and silver NPs (AgNPs) were assayed in the range of 0.1-2 mg/mL, finding that only Tb_4O_7 NPs notably increased the reaction rate of the system. Both blank and analyte AUC decreased, but the net AUC difference was better than in the absence of the NPs, as can be seen in Figure 2. Also, the effect of Tb_4O_7 NPs on the system was checked in the absence of laccase, finding that the NPs did not modify the fluorescence of HPTS. Diamond and magnetic-gold NPs caused the fluorescence quenching of HPTS and AgNPs inhibited the catalytic effect of laccase, while no change on the kinetic behavior of the system was found in the presence of Eu_2O_3 NPs. Terbium(III) ions in solution were assayed at equivalent concentrations than Tb_4O_7 NPs, obtaining lower net AUC values than using the NPs. These results show the usefulness of these NPs as activators of the enzymatic system. Terbium(III) in solution has been recently described as an activator of deoxyribozymes, which are DNA catalysts (Javadi-Zarnaghi & Höbartner, 2013), but the use of Tb_4O_7 NPs as a catalyst activator has not been described up to date.

The effect of cationic (CTAB), anionic (SDS) and non-ionic (Triton X-100 and Tween 20) surfactants on the system was assayed below and

above their critical micellar concentration. The strong interaction of HPTS with CTAB, which has been previously described (Pramanik, Banerjee & Bhattacharya, 2007), gave rise to a decrease of the reaction rate of the system, which made difficult to develop an assay with a suitable sample throughput. The presence of SDS and Triton X-100 caused a decrease in the fluorescence intensity of HPTS, decreasing also the AUC values obtained in the absence and the presence of the analyte. Finally, the fluorescence of HPTS and the reaction rate of the system were not affected in the presence of Tween 20. According to these results, surfactants were not used for the development of the system.

3.2. Optimization of the system

The variables affecting the system were optimized by the univariate method using the net AUC as the analytical parameter, which was calculated as indicated in the procedure. However, it was necessary to find a compromised solution between this parameter and the time required to obtain each measurement, in order to avoid the excessive duration of the procedure. Each result was the average of three measurements.

The influence of the pH on the system was studied in the range of 4.0-9.0 using different buffers solutions, such as acetic acid/acetate, phosphate and carbonate at a 0.2 M concentration. The fluorescence of HPTS was very low at pH 4.0 in the presence of acetate ions and it remained constant without undergoing any oxidation reaction with laccase. HPTS showed a high fluorescence at pH values in the range of 8.0-9.0, but it was not modified in the presence of laccase. However, appropriate net AUC values were obtained at pH 7.0 - 7.5. Hexamine,

imidazole and phosphate buffer solutions were assayed to adjust the pH within this range, obtaining the best net AUC in the presence of phosphate buffer solution in the concentration range of 0.2 – 0.5 M. The influence of the HPTS concentration was studied adding a fixed volume (15 μL) of solutions with HPTS concentrations ranging from 2.5 to 20 μM, obtaining that the system was independent of this variable in the range of 8-12 μM HPTS concentration.

Laccase activity and Tb_4O_7 NPs concentration are two critical variables that have a remarkable effect on both the net AUC and the duration of the kinetic curve. Both variables were studied in the ranges of 0.5 - 2 U/mL and 0.2 - 2 mg/mL for laccase activity and Tb_4O_7NP concentration, respectively. High values of both variables gave rise to very high reaction rates and low net AUC, which has a negative effect on the sensitivity of the method. Several assays were carried out using different values of these variables, obtaining appropriate net AUC and duration of the process in the presence of 1 U/mL laccase and 1 mg/mL NPs. As Figure 2 shows, the activation effect of the NPs on the catalytic action of laccase is demonstrated under these experimental conditions. The temperature was studied in the range of 20 - 40 °C, and the best results were obtained at 37 °C.

3.3. Analytical features

The net AUC values were obtained from the normalized kinetic curves, monitored at λ_{ex} 450 nm and λ_{em} 535 nm under the optimum experimental conditions for different gallic acid concentrations (Figure 3). The dynamic range of the calibration graph was 0.5 – 12 μM gallic acid and

the regression equation was: AUC = (0.40 ± 0.05) + (2.4 ± 0.6)X, in which X is the gallic acid concentration expressed as micromolar. The regression coefficient (R) was 0.996, which is indicative of the good linearity of the calibration curve. The limit of detection (LOD), calculated according to IUPAC recommendations (Long & Winefordner, 1983), was 0.14 μM, while the value obtained in the absence of Tb_4O_7 NPs was 0.4 μM, which shows the positive effect of the NPs on the method.

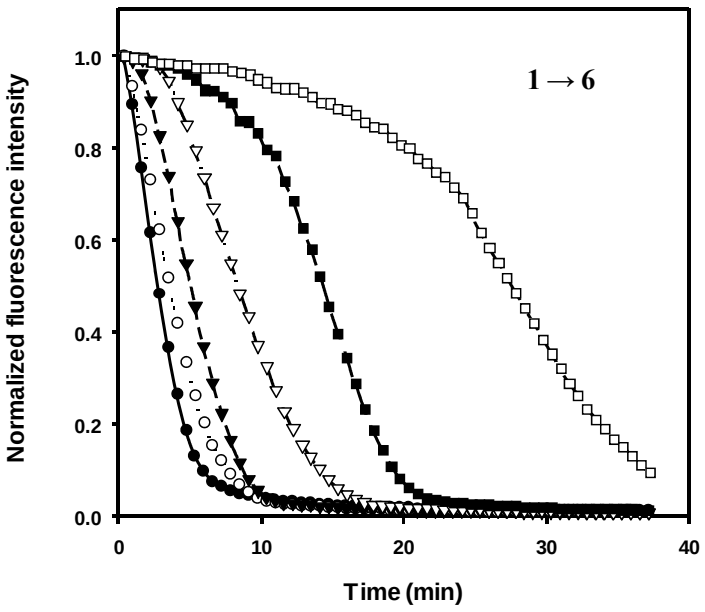

Figure 3. Kinetic curves obtained for different gallic acid concentrations: 1) 0 μM, 2) 0.5 μM, 3) 1 μM, 4) 2 μM, 5) 5 μM and 6) 10 μM. [HPTS] = 10 μM, [laccase] = 1 U/mL, [Tb_4O_7 NPs] = 1 mg/mL, pH = 7.0, [phosphate] = 0.4 M, temperature = 37 °C.

The LOD reached in the presence of the NPs is lower than those described for gallic acid using some amperometric biosensors (Di Fusco et al., 2010; Montereali et al., 2010). Although a LOD of 0.04 μM has been obtained for gallic acid using indocyanine green (Andreu-Navarro et al., 2012), this method involves the sequential analysis of each sample, requiring about 15 min to carry out each measurement. However, the automation of the measurements using a microplate reader allows a sample throughput of 35 samples h^{-1} (three measurements for each sample) in the new method. The precision of the method, expressed as the percentage of relative standard deviation, was assessed at 0.7 and 5 μM gallic acid concentrations, providing values of 6.3 and 2.5 %, respectively.

The selectivity of the method was checked by assaying some non-phenolic reducing substances, which could be present in wines. A compound was considered not to interfere if the analytical signal obtained in its presence was within one standard deviation the signal obtained in its absence. Table 2 shows the results obtained after assaying different potential interfering compounds. The most serious interference was caused by ascorbic acid, which was tolerated at the same molar concentration than that of the analyte. However, this interference would be negligible because the maximum limit allowed for ascorbic acid when used as an additive in wine is 0.85 mM ("Oxford companion to wine", Robinson J. (Ed.), 2006), which is lower than the usual content of polyphenols in wines. Sulfites were tolerated in a concentration 20-fold of the analyte. Although this interference could be removed using a pre-treatment step (Montereali et al., 2010), it was not necessary as the presence of sulfites in wines is controlled according to their total content in reducing substances

(Organisation Internationale de la Vigne et du Vin (OIV), 2011). Thus, the maximum limit of sulfur dioxide is 2.5 mM for red wine, 3.3 mM for white wine and 6.3 mM for sweet wine samples, when they contain up to 4 g/l of reducing substances. According to these limits and the values for phenolic antioxidant concentration found in literature (Gamella et al., 2006; Di Fusco et al., 2010), the new method can be directly applied to the analysis of wines since the concentration of polyphenols is higher than those of ascorbic acid and sulfites. Trolox, which is usually the standard used for the determination of the antioxidant activity, as indicated above, was also assayed in the concentration range of 0.4 – 10 μM, but the curves obtained were similar to that obtained for the blank sample. These results show that the new method is suitable for the determination of polyphenols, but it does not allow the determination of antioxidant activity.

Table 2. Influence of some reducing agents on the proposed determination of phenolic antioxidants at 2 μM gallic acid

Compound	**Maximum tolerated interferent/analyte ratio***
Malic acid	100
Citric acid	100
Sucrose	100
Glucose	25
Sodium sulfite	20
Ascorbic acid	1

*Maximum ratio assayed was 100

3.4. Applications

The proposed method was applied to the analysis of red, white and sweet wines. The sample treatment only consisted in the dilution of the samples to match the dynamic range of the calibration curve, using gallic acid standards and the net AUC as analytical parameter. Table 3 shows the content of antioxidants found in these samples analyzed by the proposed method and by the Folin-Ciocalteu method. The values found by using the new method agree with those reported in the literature (Gamella et al., 2006; Di Fusco et al., 2010). As it can be seen from the table, the values provided by Folin-Ciocalteu method were higher in all instances than those provided by the laccase method, which is ascribed to the capability of the later to also detect non-phenolic substances. A recovery study was performed by adding three different amounts of gallic acid to each sample and subtracting the results obtained from similarly treatment unspiked samples (Table 3). The recovery percentages obtained ranged from 81.0 to 108.3 % and the mean recoveries for red, white and sweet wines were 90.9, 92.4 and 99.5 %, respectively.

Table 3. Antioxidant concentration found and recovery study for the wine samples analyzed

sample	Folin-Ciocalteu method	Proposed method			
	content[a,b]	content[a,b]	added[a]	found[a,b]	recovery (%)
Red wine (La Rioja)	11.5 ± 0.1	7.0 ± 0.4	4	4.3 ± 0.5	108.3
			12	10.0 ± 0.5	84.1
			20	16 ± 1	81.0
Red wine (Cuenca)	14.04 ± 0.18	9.5 ± 0.5	4	3.2 ± 0.2	80.0
			12	11.7 ± 0.3	97.4
			20	18.9 ± 0.8	94.5
White wine (Rueda)	1.92 ± 0.04	1.00 ± 0.06	0.25	0.24 ± 0.03	97.2
			0.75	0.77 ± 0.04	102.8
			1.25	1.08 ± 0.03	86.7
White wine (Valdepeñas)	2.028 ± 0.005	1.00 ± 0.03	0.25	0.23 ± 0.03	92.0
			0.75	0.70 ± 0.04	92.2
			1.25	1.0 ± 0.1	83.3
Sweet wine (Córdoba)	3.64 ± 0.05	1.27 ± 0.09	1	1.01 ±0.09	101.5
			3	3.0 ± 0.3	102.0
			5	4.7 ± 0.3	95.0

[a]Units: mM gallic acid equivalents of sample

[b]Mean ± SD (n=3)

4. Conclusions

An automated method has been reported for the determination of polyphenols in wine samples using HPTS as a new fluorescent laccase substrate and Tb_4O_7 NPs as activators of laccase. The presence of these NPs on the system allows shorter analysis times and lower enzyme consumption. The microplate reader enables the simultaneous processing of 96 tests, reaching an overall sample throughput of about 35 samples h^{-1}, when analysed in triplicate. Also, the use of wells with a total volume of 180 μL, in spite of conventional microplates with volumes of 350-400 μL per well, is cost-effective, since the reagent consumption is lower.

The analytical usefulness of the proposed method for the determination of polyphenols in wine samples has been demonstrated and the results have been compared with those provided by the Folin-Ciocalteu method, which was used as reference. The results obtained for all samples analyzed by the new method were lower owing to its better selectivity compared to the reference method, which is a common aspect for other laccase-based enzyme methods previously described for wine analysis (Gamella et al., 2006; Di Fusco et al., 2010).

Acknowledgements

Authors gratefully acknowledge financial support from the Spanish Ministerio de Economía y Competitividad MINECO (Grant No. CTQ2012-32941), the Junta de Andalucía Program (Grant No. P09- FQM4933) and the FEDER-FSE program.

References

Andreu-Navarro, A., Fernández-Romero, J. M. & Gómez-Hens, A. (2012). Determination of polyphenolic content in beverages using laccase, gold nanoparticles and long wavelength fluorimetry. *Analytica Chimica Acta*, *713*, 1-6.

Ashrafi, S D., Rezaei, S., Forootanfar, H., Mahvi, A. H. & Faramarzi, M.A. (2013). The enzymatic decolorization and detoxification of synthetic dyes by the laccase from a soil-isolated ascomycete, Paraconiothyrium variabile. *International Biodeterioration and Biodegradation*, *85*, 173 - 181.

Benzina, O., Daâssi, D., Zouari-Mechichi, H., Frikha, F., Woodward, S., Belbahri, L., Rodríguez-Couto, S. & Mechichi, T. (2013). Decolorization and detoxification of two textile industry effluents by the laccase/1-hydroxybenzotriazole system. *Environmental Science and Pollution Research*, *20*, 5177 - 5187.

Campos, A. M., Sotomayor, C. P., Pino, E. & Lissi, E. (2004). A pyranine based procedure for evaluation of the total antioxidant potential (TRAP) of polyphenols. A comparison with closely related methodologies *Biological Research, 37*, 287 - 292.

Dawidowicz, A. L., Wianowska, D. & Olszowy, M. (2012). On practical problems in estimation of antioxidant activity of compounds by DPPH method (Problems in estimation of antioxidant activity). *Food Chemistry*, *131*, 1037-1043.

Di Fusco, M., Tortolini, C., Deriu, D. & Mazzei, F. (2010). Laccase-based biosensor for the determination of polyphenol index in wine. *Talanta*, *81*, 235 - 240.

Di Majo, D., La Guardia, M., Giammanco, S., La Neve, L. & Giammanco, M. (2008) The antioxidant capacity of red wine in relationshipwith its polyphenolic constituents. *Food Chemistry*, *111*, 45 - 49.

Fernández-Pachón, M. S., Villaño, D., García-Parrilla, M. C. & Troncoso, A. M. (2004). Antioxidant activity of wines and relation with their polyphenolic composition. *Analytica Chimica Acta*, *513*, 113 - 118.

Franquet-Griell, H., Checa, A., Núñez, O., Saurina, J., Hernández-Cassou, S. & Puignou, L. (2012). Determination of polyphenols in spanish wines by capillary zone electrophoresis. Application to wine characterization by using chemometrics. *Journal of Agricultural and Food Chemistry*, *60*, 8340 - 8349.

Gamella, M., Campuzano, S., Reviejo, A. J. & Pingarrón, J. M. (2006). Electrochemical estimation of the polyphenol index in wines using a laccase biosensor. *Journal of Agricultural and Food Chemistry*, *54*, 7960 - 7967.

Godoy-Navajas, J., Aguilar-Caballos, M. P. & Gómez-Hens, A. (2011). Long-wavelength fluorimetric determination of food antioxidant capacity using nile blue as reagent. *Journal of Agricultural and Food Chemistry*, *59*, 2235-2240.

Javadi-Zarnaghi, F. & Höbartner, C. (2013). Lanthanide cofactors accelerate DNA-catalyzed synthesis of branched RNA. *Journal of the American Chemical Society, 135*, 12839 - 12848.

Kulys, J. & Bratkovskaya, I. (2007). Antioxidants determination with laccase. *Talanta*, *72*, 526 – 531.

Li, H. H., Wang, X., Li, Y., Li, P. & Wang, H. (2009). Polyphenolic compounds and antioxidant properties of selected China wines. *Food Chemistry*, *112*, 454 - 460.

Long, G. L. & Winefordner, J. D. (1983). Limit of detection. A closer look at the IUPAC definition. *Analytical Chemistry*, *55*, 712A - 724A.

Lorrain, B., Ky, I., Pechamat, L. & Teissedre, P. L. (2013). Evolution of analysis of polyphenols from grapes, wines, and extracts. *Molecules*, *18*, 1076 - 1100.

Magalhães, L. M., Segundo, M. A., Reis, S., Lima, J. L. F. C. & Rangel, A. O. S. S. (2006). Automatic method for the determination of Folin-Ciocalteu reducing capacity in food products. *Journal of Agricultural and Food Chemistry*, *54*, 5241 - 5246.

Medić-Ŝarić, M., Rastija, V. & Bojić, M. (2011). Recent advances in the application of high performance liquid chromatography in the analysis of polyphenols in wine and propolis. *Journal of AOAC International*, *94*, 32 - 42.

Mondal, S. K., Ghosh, S., Sahu, K., Sen, P. & Bhattacharyya, K. (2007). Excited state proton transfer from pyranine to acetate in methanol. *Journal of Chemical Sciences*, *119*, 71 - 76.

Montereali, M.R., Della Seta, L., Vastarella, W. & Pilloton, R. (2010). A disposable Laccase-Tyrosinase based biosensor for amperometric detection of phenolic compounds in wine. *Journal of Molecular Catalysis B: Enzymatic*, *64*, 189 - 194.

Mukhopadhyay, A., Dasgupta, A. K. & Chakrabarti, K. (2013). Thermostability, pH stability and dye degrading activity of a bacterial

laccase are enhanced in the presence of Cu_2O nanoparticles. *Bioresource Technology*, *127*, 25 - 36.

Nenadis, N., Lazaridou, O. & Tsimidou, M. Z. (2007). Use of reference compounds in antioxidant activity assessment. *Journal of Agricultural and Food Chemistry*, 55, 5452 - 5460.

Nkhili, E. & Brat, P. (2011). Reexamination of the ORAC assay: effect of metal ions. *Analytical and Bioanalytical Chemistry*, *400*, 1451 - 1458.

Nugroho Prasetyo, E., Kudanga, T., Steiner, W., Murkovic, M., Nyanhongo, G. S. & Guebitz, G. M. (2010). Laccase-generated tetramethoxy azobismethylene quinone (TMAMQ) as a tool for antioxidant activity measurement. *Food Chemistry*, *118*, 437 - 444.

Nugroho Prasetyo, E., Kudanga, T., Steiner, W., Murkovic, M., Nyanhongo, G. S. & Guebitz, G. M. (2009). Antioxidant activity assay based on laccase-generated radicals. *Analytical and Bioanalytical Chemistry*, *393*, 679 - 687.

Omata, Y., Saito, Y., Yoshida, Y. & Niki, E. (2008). Simple assessment of radical scavenging capacity of beverages. *Journal of Agricultural and Food Chemistry*, *56*, 3386 - 3390.

Organisation Internationale de la Vigne et du Vin (OIV). Maximum acceptable limits of various substances contained in wine. *Compendium of International Methods of Analysis*, OIV-MA-C1-01:R2011.

Pramanik, S., Banerjee, P. & Bhattacharya, S.C. (2007). Interaction of 8-hydroxypyrene-1,3,6-trisulphonate in alkyltrimethylammonium bromide (CnTAB) micellar medium. *Journal of Photochemistry and Photobiology A: Chemistry*, *187*, 384 - 388.

Robinson, J. (Ed.) "Oxford companion to wine" 3rd edition. (2006) 35 – 36.

Sánchez-Arribas, A., Martínez-Fernández, M. & Chicharro, M. (2012). The role of electroanalytical techniques in analysis of polyphenols in wine. *Trends in Analytical Chemistry*, *34*, 78 - 96.

Sánchez-Rangel, J. C., Benavides, J., Heredia, J. B., Cisneros-Zevallos, L. & Jacobo-Velázquez, D. A. (2013). The Folin–Ciocalteu assay revisited: improvement of its specificity for total phenolic content determination. *Analytical Methods*, *5*, 5990 - 5999.

Sochor, J., Ryvolova, M., Krystofova, O., Salas, P., Hubalek, J., Adam, V., Trnkova, L., Havel, L., Beklova, M., Zehnalek, J., Provaznik, I. & Kizek, R. (2010). Fully automated spectrometric protocols for determination of antioxidant activity: advantages and disadvantages. *Molecules*, *15*, 8618 - 8640.

Taha, A.A., Shwaish, I.I., Mohamed, A.H., Haider, A. J. & Stamatis, H. (2013). Production of a laccase from Botrytis cinerea (DSMZ 877) and application for textile phenolic dye decolorization. *Energy Procedia*, *36*, 862 – 871.

Wang, F., Hu, Y, Guo, C., Huang, W. & Liu, C.Z. (2012). Enhanced phenol degradation in coking wastewater by immobilized laccase on magnetic mesoporous silica nanoparticles in a magnetically stabilized fluidized bed. *Bioresource Technology*, *110*, 120 - 124.

CAPÍTULO 4

CHAPTER 4

Innovaciones en ensayos de afinidad mediante el uso de “upconverting phosphors” y fenómenos de transferencia de energía resonante luminiscente

Innovations in affinity assays by using upconverting phosphors and luminescence resonance energy transfer

Este capítulo aborda un estudio sistemático del uso de *"upconverting phosphors"* (UCPs) en ensayos homogéneos de afinidad con detección de la luminiscencia basada en transferencia de energía resonante luminiscente (LRET). Estas investigaciones se realizaron durante la estancia de tres meses en el Departamento de Biotecnología de la Universidad de Turku (Finlandia) bajo la supervisión del Prof. Tero Soukka. Con esta visita se cumple uno de los requisitos para optar a la Mención de Doctorado Internacional. El estudio realizado ha dado origen a un artículo científico en vías de redacción:

- J. Godoy-Navajas, T. Riuttamäki, T. Soukka. Evaluation of different donor-acceptor pairs for the development of homogeneous bioaffinity assays using upconversion luminescence resonance energy transfer.

La transferencia de energía resonante (RET) o transferencia de energía electrónica (EET) es un proceso que tiene lugar entre dos moléculas o materiales. Una de estas moléculas actúa como dador, emitiendo energía a una determinada longitud de onda, mientras que la otra molécula actúa como aceptor, absorbiendo la energía emitida. Cuando las dos moléculas son fluorescentes, a este mecanismo se le conoce como transferencia de energía resonante de fluorescencia (FRET) o de luminiscencia (LRET). No obstante, la energía no siempre se transmite por fluorescencia y no necesariamente el aceptor emite fluorescencia ya que pueden utilizarse también inhibidores de fluorescencia. Para que este proceso tenga lugar se tiene que cumplir una serie de requisitos: (1) la molécula dadora debe tener un elevado rendimiento cuántico; (2) debe existir un solapamiento

sustancial entre el espectro de emisión del dador y el espectro de absorción del aceptor; (3) es necesario un adecuado alineamiento entre los momentos de transición de la absorción y la emisión; y (4) la distancia que separa al dador del aceptor debe ser muy corta, normalmente menor de 10 nm [1].

Los UCPs han sido usados para el desarrollo de diferentes ensayos basados en la tecnología LRET utilizando fluoróforos con una longitud de onda de absorción similar a la emisión del UCP en cuestión. Por ejemplo, los UCPs se han usado como dadores, mientras que el fluoróforo Oyster 556 se utilizó como aceptor para el desarrollo de un inmunoensayo homogéneo para la determinación de estradiol [2]. Utilizando otros tipos de fluoróforos, como son las ficobiliproteínas (Figura 1), se ha descrito un ensayo de transferencia de energía con los UCPs como dadores mediante el sistema de afinidad biotina-estreptavina [3]. En estos estudios de afinidad, los UCPs se unen a estreptavidina (SA) para formar un conjugado SA-UCP que actúa como dador y un fluoróforo orgánico se enlaza a biotina para que actúe como aceptor. Cuando el dador y el aceptor interaccionan, se produce la transferencia de energía, cuya intensidad se utiliza como parámetro analítico. Esta metodología LRET permite excitar en la zona del infrarrojo cercano (para los UCPs dopados con Yb(III), la excitación ocurre a 980 nm). En esta zona del espectro, la probabilidad de interferencias debidas a la matriz de la muestra es relativamente baja, lo que contribuye a disminuir las señales de fondo y, por tanto, a mejorar los límites de detección. La emisión ocurre en la zona del visible, sobre 600 nm, si se utiliza β-ficoeritrina como aceptor. Los ensayos de afinidad desarrollados por el grupo del Prof. Soukka, basados en metodologías LRET, han implicado el uso de UCPs dopados con Er(III) para formar el dador [2,3]

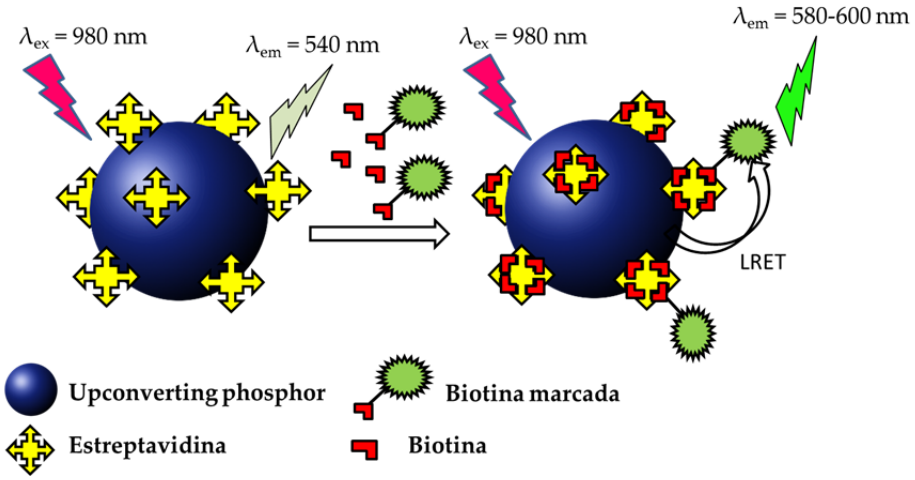

Figura 1. Fenómeno de transferencia de energía resonante de luminiscencia (LRET) donde el dador es un UCP, el aceptor es un fluoróforo y la interacción entre ambos se lleva a cabo mediante el sistema de afinidad biotina-estreptavidina.

Más recientemente, se ha diseñado un biosensor basado en el fenómeno LRET usando UCPs como dadores y nanoesferas de poli-m-fenilendiamina (PMPD) como aceptores para la determinación de ADN en muestras de suero humano [4]. Por otro lado, estos nanocristales pueden combinarse con otro tipo de nanomaterial para obtener una eficiente transferencia de energía. La transferencia de energía entre los UCPs y nanopartículas de carbono ha sido la base para el diseño de un nuevo biosensor homogéneo en la determinación de 2-metaloproteinasa en sangre [5].

El estudio que se incluye pretende expandir la aplicabilidad de UCPs dopados con Ho(III) y Tm(III), susceptibles de ser utilizados individualmente o en ensayos multiplex donde puedan funcionar como

dadores, además de los convencionalmente utilizados, que son nanocristales dopados con Er(III). Por otra parte, se han ensayado diversos fluoróforos orgánicos pertenecientes a los ATTO y los Alexa Fluor, para investigar su uso como potenciales aceptores.

BIBLIOGRAFÍA

(1) J. Fan, M. Hu, P. Zhan, X. Peng. Energy transfer cassettes based on organic fluorophores: construction and applications in ratiometric sensing. *Chem. Soc. Reviews* **(2013)** *42*, 29 – 43.

(2) K. Kuningas, T. Ukonaho, H. Päkkilä, T. Rantanen, T. Lövgren, T. Soukka. Upconversion fluorescence resonance energy transfer in a homogeneous immunoassay for estradiol. *Anal. Chem*. **(2006)** *78*, 4690 – 4696

(3) K. Kuningas, T. Rantanen, T. Ukonaho, T. Lövgren, T. Soukka. Homogeneous assay technology based on upconverting phosphors. *Anal. Chem*. **(2005)** *77*, 7348 – 7355

(4) Y. Wang, Z. Wu, Z. Liu. Upconversion fluorescence resonance energy transfer biosensor with aromatic polymer nanospheres as the label-free energy acceptor. *Anal. Chem*. **(2013)** *85*, 258 – 264

(5) Y. Wang, P. Shen, C. Li, Y. Wang, Z. Liu. Upconversion fluorescence resonance energy transfer based biosensor for ultrasensitive detection of matrix metalloproteinase-2 in blood. *Anal. Chem*. **(2012)** *84*, 1466 – 1473.

This chapter tackles a systematic study of the usefulness of *"upconverting phosphors"* (UCPs) in homogeneous affinity assays with detection of luminescence resonance energy transfer (LRET). These investigations were performed during the three-month stay at the Department of Biotechnology of the University of Turku (Finland) under the supervision of Prof. Tero Soukka. This is one of the requisites for the International Doctorate Mention. The study performed has given rise to a scientific article currently in preparation:

- J. Godoy-Navajas, T. Riuttamäki, T. Soukka. Evaluation of different donor-acceptor pairs for the development of homogeneous bioaffinity assays using up-conversion luminescence resonance energy transfer.

The resonance energy transfer energy (RET) or electron energy transfer (EET) is a process that happens between two molecules or materials. One of these molecules acts as donor, which emits energy at a specific wavelength, whereas the other molecule acts as acceptor, thus absorbing the emitted energy. When both molecules are fluorescent, this phenomenon is known as fluorescence or luminescence resonance energy transfer (FRET or LRET). However, the energy is not always transferred as fluorescence and the acceptor does not necessarily emit fluorescence, since fluorescence quenchers can also be used. Some requisites need to be met for this process to occur: (1) the donor molecule should have a high quantum yield; (2) both donor emission

and acceptor absorption spectra have to overlap in a high extent; (3) an adequate alignment of absorption and emission transition moments is required; and (4) the distance that separates donor from acceptor needs to be very short, usually lower than 10 nm [1].

The UCPs have been used to develop different assays based on LRET using fluorophores with an absorption wavelength similar to the UCP emission wavelength. For instance, the UCPs have been used as donors, while the Oyster 556 fluorophore was used as acceptor to develop a homogeneous immunoassay for the determination of estradiol [2]. Another energy transfer assay has been reported using other types of fluorophores, such as phycobiliproteins as acceptors (Figure 1) and UCPs as donors, using the biotin-streptavidin affinity system [3]. In these studies, the UCPs bind streptavidin (SA) to give rise to a SA-UCP conjugate, which acts as a donor and an organic fluorophore bound to biotin is the acceptor. When donor and acceptor interact, the energy transfer process occurs, which intensity is used as analytical parameter. This LRET methodology allows the excitation in the near IR region of the spectrum (Yb(III)-doped UCPs are excited at 980 nm). In this region of the spectrum, the probability of interferences owing to sample matrix is relatively low, which contributes to decrease background signals, and hence, to improve detection limits. When β-phycoerythrin is used as acceptor, the emission happens in the visible region, at about 600 nm. The affinity assays based on LRET methodologies developed by the research team of Prof. Soukka have involved the use of Er(III)-doped UCPs to give rise to the donor [2,3]

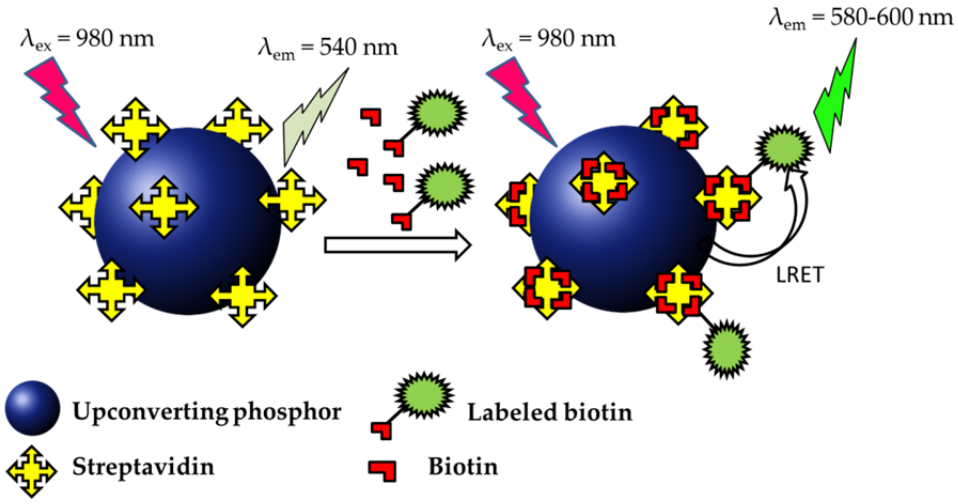

Figure 1. Luminescence resonance energy transfer (LRET) where the UCP acts a donor and the fluorophor is the acceptor, their interaction occurring by means of biotin-streptavidin affinity system.

More recently, a biosensor based on the LRET phenomenon that involves the use of UCPs as donors and nanospheres of poly-m-phenylenediamine (PMPD) as acceptors for the DNA determination in human serum [4] has been designed. On the other hand, these nanocrystals can combine other types of nanomaterials to give rise to an efficient energy transfer. The energy transfer between UCPs and carbon nanoparticles has been the basis for the design of a new homogeneous biosensor for the determination of 2-metalloproteinase in blood [5].

The study included in this Dissertation is aimed to expand the applicability of Ho(III)- and Tm(III)-doped UCPs, which can be used individually or in multiplexed assays as donors together with the conventionally used Er(III)-doped UCPs. On the other hand, several

organic fluorophores belonging to ATTO and Alexa Fluor families have been assayed in order to investigate their potential use as acceptors.

LITERATURE

(1) J. Fan, M. Hu, P. Zhan, X. Peng. Energy transfer cassettes based on organic fluorophores: construction and applications in ratiometric sensing. *Chem. Soc. Reviews* **(2013)** *42*, 29 – 43.

(2) K. Kuningas, T. Ukonaho, H. Päkkilä, T. Rantanen, T. Lövgren, T. Soukka. Upconversion fluorescence resonance energy transfer in a homogeneous immunoassay for estradiol. *Anal. Chem*. **(2006)** *78*, 4690 – 4696

(3) K. Kuningas, T. Rantanen, T. Ukonaho, T. Lövgren, T. Soukka. Homogeneous assay technology based on upconverting phosphors. *Anal. Chem*. **(2005)** *77*, 7348 – 7355

(4) Y. Wang, Z. Wu, Z. Liu. Upconversion fluorescence resonance energy transfer biosensor with aromatic polymer nanospheres as the Label-free energy acceptor. *Anal. Chem*. **(2013)** *85*, 258 – 264

(5) Y. Wang, P. Shen, C. Li, Y. Wang, Z. Liu. Upconversion fluorescence resonance energy transfer based biosensor for ultrasensitive detection of matrix metalloproteinase-2 in blood. *Anal. Chem*. **(2012)** *84*, 1466 – 1473.

Evaluation of different donor-acceptor pairs for the development of homogeneous bioaffinity assays using upconversion luminescence resonance energy transfer

J. Godoy-Navajas[a], T. Riuttamäki[b], T. Soukka[b]

[a]Department of Analytical Chemistry. Research Institute on Fine Chemistry. Campus Rabanales. Annex to Marie Curie Building. 14071-Córdoba. Spain

[b]Department of Biotechnology. University of Turku. Biocity 6A. 20520-Turku. Finland

Abstract

A systematic study on the suitability of different donor-acceptor pairs for the development of affinity assays with biotin as model analyte is reported. Upconversion luminescence resonance energy transfer (LRET) has been measured for several streptavidin-coated up-converting phosphors (UCPs) (donors) with different biotinylated fluorescent acceptors. The donors assayed were streptavidin-coated UCPs of different chemical composition, such as $NaYF_4$, Yb(III)Er(III); $NaYF_4$, Yb(III)Ho(III) and $NaYF_4$, Yb(III)Tm(III). Biotinylated derivatives of suitable fluorescent acceptors, namely β-phycoerythrin (BPE), R-phycoerythrin (RPE), Alexa Fluor 488 (AF488), Alexa Fluor 546 (AF546), Alexa Fluor 680 (AF680) and ATTO 495, were assayed.

The results obtained show that the LRET intensity depends on the UCP considered. The brightest luminescence was obtained with Er(III)-doped UCP, but the sensitivity of the assays, in terms of biotin IC50 values, was not influenced by UCP composition. The use of Tm(III) provides good opportunity to develop LRET assays using biotinylated R-phycoerythrin (bio-RPE) as the acceptor. Thus, the present study opens the possible use of UCPs other than Er(III)-doped ones to develop sensitive LRET affinity assays.

Keywords: homogeneous affinity assays, upconversion luminescence, resonance energy transfer assays, nanosphosphors.

Introduction

The analytical applications of anti-Stokes luminescence have experienced a huge increase in the last decade, with the advent of lanthanide upconverting phosphors (UCPs). These phosphors are composed of inorganic host lattices, where $NaYF_4$ is one of the most commonly used, although the use of Gd and La lattices has also been reported [1-7]. These inorganic matrices are usually doped with the infrared emitting Yb(III) ion together with other lanthanide ions, such as Er(III), Ho(III) and Tm(III), among others.

The phenomenon of anti-Stokes luminescence happens by irradiating these nanophosphors with a laser source in the infrared region, generally at 980 nm, and measuring thereafter the emission of the other lanthanide ions in the green to red region of the spectrum. This effect constitutes an advantage compared to Stokes luminescence since many undesirable phenomena that usually affect the performance of photoluminescence emission techniques, such as the autofluorescence coming from sample matrix when excited at short wavelengths in the UV-visible region, are avoided. Sample matrices do not absorb at the long excitation wavelength used to excite UCPs, so a high spectral selectivity is attained. Another advantage of using these nanophosphors is the excellent photostability owing to their inorganic nature and to the low power required for their excitation, thus being these laser sources much cheaper than the powerful lasers required for two-photon excitation. Also, some excellent properties that are common to conventional Stokes lanthanide sensitized luminescence, such as narrow emission peaks, long luminescence lifetime

and their low toxicity make them especially suitable for bioanalytical and biomedical applications [2,8]. Some applications describe their use as labels in heterogeneous assays to determine prostate specific antigen (PSA) [8] and biotin [9,10]. However, many analytical applications of UCPs have been focused on the development of luminescence resonance energy transfer (LRET) assays [11-14], which have opened new possibilities for homogeneous binding assays. LRET phenomenon relies on the nonradiative energy transfer from one fluorescent molecule (donor) to an acceptor, which is also a fluorophore.

The excellent features of UCPs above mentioned have enabled the avoidance the influence of background signals from biological samples, and hence, to obtain relatively low detection limits using homogeneous assays. The use of UCPs in bioanalysis requires these nanocrystals to be biocompatible and readily dispersed in water, owing to their hydrophobic shell, e.g. of oleic acid, after some synthesis procedures [1,2]. Thus, the use of functionalization procedures is needed, among which ligand exchange [11-14] and silanization [1,2] have been used for this purpose. Ligand exchange procedures are simple to perform but it has been reported that the ligands attached to the surface can be finally lost. The stability of silica-encapsulated UCPs is better, although it has been observed in some cases a decrease in the luminescence intensity, which has been ascribed to the remaining free amino groups on the surface and to a subsequent decrease in the quantum yield [15]. Furthermore, the performance of LRET assays relies on the use of streptavidin-coated UCPs donors and biotinylated acceptors, where similar functionalization procedures to those above mentioned are needed. However, the comparison of the performance of

LRET assays using different UCP functionalization procedures has not been performed, although this can be a factor influencing the sensitivity of the homogeneous assays developed.

The work presented here reports a systematic study of the behaviour of different UCPs according to the dopant element (Er(III), Ho(III) and Tm(III)). Er(III)-doped UCPs have already proven to give rise to very luminescent donors in LRET assays. However, the use of Ho(III) and Tm(III) may provide good options for multiplexing or to expand the application field of UCP technology, since the emission wavelength of Tm(III) is much shorter than those of Er(III) and Ho(III) phosphors and it is closer to the maximum excitation wavelength of many organic acceptors. Bearing this in mind, the performance of several donor-acceptor pairs has been evaluated, using streptavidin coated nanophosphors doped with either Er(III), Ho(III) and Tm(III) as the donors and organic dyes as the acceptors. Phycobiliprotein dyes have been used as acceptors in some LRET assays [11,13]. Although these compounds show an intense fluorescence, they are also relatively expensive, so the potential usefulness of other fluorophores, such as Alexa Fluor or ATTO dyes has been checked. Also, the influence of UCP functionalization procedures based on silylation and on ligand exchange has been studied for Er(III) and Ho(III)-doped UCPs. This study was carried out to elucidate which is the most adequate for the development of homogeneous LRET assays and whether the treatment depends on the chemical composition of the UCP.

2. Experimental procedures

2.1. Reagents

Different infrared to visible nanosized UCPs, which were doped with Er(III), Ho(III) and Tm(III) and obtained by a re-precipitation method [16], were used to perform all the experiments. Fluorescent phycobiliproteins, such as β-phycoerythrin and R-phycoerythrin (BPE) were purchased from Cyanotech Corp (Kailua-Kona, HI), supplied in 100 mM sodium phosphate buffer, pH 7.0, containing 60% ammonium sulphate and 0.02% (w/v) sodium azide, with protein concentration of 10 mg/mL. Alexa Fluor 488, Alexa Fluor 546 and Alexa Fluor 680 succinimidyl esters were purchased from Molecular Probes Invitrogen Paysley, UK) and ATTO 495 succinimidyl ester was obtained from Sigma. Streptavidin was purchased from Spa-BioSpa (Milan, Italy). Biotinamidohexanoic acid N-hydroxysuccinimide ester (bio-LC-NHS) was from Pierce (Rockford, IL). Fluorescent protein (bio-BPE) was biotinylated with a 25-fold molar excess of NHS-LC-biotin according to a previously described procedure [11]. A freshly prepared solution of NHS-LC-biotin in dimethylformamide was added into protein solution containing 8.5 mg/mL phycobiliproteins in 50 mM carbonate buffer, pH 9.3. The reaction mixture, with a total volume of 500 μL and containing about 2% (v/v) DMF, was incubated in rotation at 17 rpm (Rotamix RK, Heto-Holten A/S, Allerod, Denmark) protected from light for 3 h at room temperature. Finally, it was purified using NAP-5 and NAP-10 columns (Amersham Biosciences, Uppsala, Sweden). Polyacrylic acid ammonium salt, Additol XW330 (MW 30000 – 50000) (Surface

Specialities) was used to prepare 5% Additol solutions in doubly de-ionized water to coat UCPs.

Cyclohexane, n-hexanol, N-(3-trimethoxysilyl)propyl)ethylene diamine (TMED, 97% purity) and 3-(trihydroxysilyl)propyl methylphosphonate (THPMP, purity 42%) (Sigma Aldrich), Triton X-100 and tetraethyl orthosilicate (TEOS, 98% purity) (Acros Organics), were used for the silylation of UCPs. Ammonium hydroxide, acetone and absolute ethanol were used to purify the conjugated UCPs. Glutaric anhydride (95% purity, Sigma-Aldrich) and dry pyridine were used to change amino- groups of silica-UCPs into carboxyl- groups. N-(3-dimethylamino)propyl)-N′-ethylcarbodiimide hydrochloride (EDAC) and N-hydroxysulfosuccinimide sodium salt (sulfo-NHS) (Fluka) and a buffer solution of morpholino ethanesulfonic acid (MES) (20 mM, pH 6.1) were used for conjugation reactions by using carbodiimide mediated synthesis. Streptavidin-coated normal-capacity microtitration wells, assay buffer (50 mM Tris-HCl, pH 7.8, containing 9 g/L NaCl, 0.5 g/L NaN3, 5 g/L BSA, 0.1 g/L bovine ϒ-globulin and 20 μM DTPA), and wash solution (5 mM Tris-HCl, pH 7.8, containing 9 g/L NaCl, 0.05 g/L Tween 20, and 1 g/L Germal II) were obtained from Innotrac Diagnostics Oy (Turku). Delfia enhancement solution (DES) and enhancer solution (DE) were purchased from PerkinElmer Life and Analytical Sciences (Wallac Oy, Turku).

2.2. Instrumentation

A Plate Chameleon (Hidex Oy, Turku) equipped with a 200 mW infrared laser module (Roithner Lasertechnik) and RG-850 nm long-pass excitation filter (Andover Corp., Salem, NH) was used. The

photomultiplier tube in the plate fluorometer was replaced with Hamamatsu R4632 (Hamamatsu Photonics K.K.). Emission light coming from donor and acceptor at their corresponding wavelengths was collected for 2000 ms under continuous laser excitation at 980 nm. Anti-Stokes photoluminescence emission from Ho(III) and Er(III) doped UCPs was measured at 550 nm employing a band-pass emission filter of 535/50 nm (center wavelength 535 nm, half-width 50 nm; peak transmittance ≥ 60%; Bk Interferezoptik Electronik, Nabburg, Germany), combined with an absorptive neutral density filter (optical density 2.0; i.e. average transmittance 1%; Thorlabs, Newton, NJ). The LRET sensitized emission was measured at 600 nm for 1000 ms, by using a band-pass emission filter of 600/40 nm (peak transmittance ≥ 80%; Chroma Technology Corp.). For Tm(III)-doped UCPs, LRET was measured using a emission filter of 555/20 nm.

2.3. Measurement of $NaYF_4$:Yb(III), Er(III)-, Ho(III)-, and Tm(III) luminescence intensity

An amount of UCP (ca. 1 mg) is placed in an Eppendorf tube and a volume of 0.75% acetic acid is added to reach a UCP concentration of 6 mg/mL. The tube is sonicated for 20 cycles, then, doubly-deionized water is added to dilute the dispersion up to 2 mg/mL and the tube is placed in a thermal block at 77 °C at the maximum power for 1 h and it is vortexed once during incubation. After this, it is incubated for 30 minutes under continuous rotation at room temperature and sonicated again. A volume of this dispersion was diluted 10 times with the measurement buffer and 150 μL were dispensed in triplicate onto Maxisorp microplates and the

luminescence was measured using Chameleon 5 instrument fitted with the appropriate filters for each UCP composition.

2.4. Measurement of UCP concentration

The preparation of UCP standards and UCP samples was done by diluting the phosphor in the measurement buffer and by sonicating them for 1 min. Then, a duplicate analysis was done in duplicate by adding 150 μL to each well. The measurements were obtained for 2 s by using a 550 nm for Er(III) and Ho(III) doped UCPs and 470 nm for Tm(III)-doped UCPs.

2.5. UCP suspension and pre-precipitation

The dispersion of the synthesized nanophosphors is made more reproducible in size by a suspension and pre-precipitation method to get a more colloidal form of these UCPs and to remove the largest aggregates in order to discard them prior to the functionalization step. The suspension was performed by weighing 15 mg of UCP in an Eppendorf tube and 930 μL of 50% diethyleneglycol in doubly de-ionized water were added. The suspension was vortexed and sonicated using 20 + 20 cycles with 100% amplitude. The bath was left in swirl for 3 min and the dispersion was vortexed again and sonicated with 20 + 20 cycles. The Eppendorf tube was incubated again in rotation at 60 °C for 1 h and then, sonicated in swirl until the UCP was totally dispersed, and incubated for 1 h at room temperature. The mixture was vortexed and sonicated for 20 + 20 cycles again and incubated on rotation overnight.

The pre-precipitation process was done just before coating and the UCP suspension was let to stand for 30 min and 870 μL of the suspension was taken from the top and transferred to another tube and the rest of the dispersion, which contained large particles, was discarded.

2.6. Functionalization of the surface with carboxylic acid groups

- *Coating with poly(acrylic acid)*: An amount of pre-precipitated UCPs (5 mg, 390 μL), was taken and mixed with Additol 0.1% and the reaction mixture was left to react overnight at 35 °C in rotation. Afterwards, the Additol excess was removed by centrifugating first for 7 min at 8000 rpm, then, the supernatant was replaced with Milli-Q water and the dispersion vortexed and sonicated for 1 min and subjected to centrifugation again. This process was repeated four times, leaving the third wash aliquot for 45 min at room temperature and rotation. The wash process was ended by suspending UCPs in Milli-Q water, until a final volume of 300 μL.

- *Coating with glutaric anhydride after UCP silylation*: An amount of pre-precipitated UCPs (6 mg, 470 μL) was taken for silylation. The process was done by using a reverse micelle microemulsion method, which was performed first by mixing 11.25 mL of cyclohexane, 2.66 mL of Triton X-100 and 2.7 mL of n-hexanol. The mixture was divided in two different microemulsion fractions A (7.5 mL) and B (the rest of the microemulsion). The tube with microemulsion A was mixed with 435 μL UCP suspension and 90 μL of ammonium hydroxide were added and the tube was sonicated in a bath for 10 min. To the tube with microemulsion B, 350 μL of water were added to give rise to a water-in-oil microemulsion, 9.4 μL of

TEOS, 37.5 μL of TMED and 37.5 μL of THPMP were subsequently added and the mixture vortexed after each addition. Both tubes A and B were combined, vortexed and incubated for 2 h at room temperature with sonication in the first 10 min and the rest of the time with continuous vortexing. Afterwards, a volume (2.25 mL) of acetone was added to break the microemulsion and precipitate the UCPs, which were collected after centrifugation at 2860 rpm for 1 min. The supernatant was transferred to another tube and acetone was added to reach a total volume of 20 mL and centrifuged again (2860 rpm, 3 min), the supernatant was discarded and the UCP-pellet was suspended in a small volume (400 μL) of doubly-deionized water. The UCP particles obtained after the two precipitation processes were combined in a single 2-mL Eppendorf tube. The precipitate was washed twice with ethanol and twice with doubly-deionized water, by sonicating each washing for 1 min and centrifugating at 8000 rpm for 7 min. The pellet was finally suspended in doubly-deionized water to obtain a final volume of 500 μL. These functionalized UCPs were stored at room temperature in rotation and the concentration of the silica-functionalized NPs was measured following the procedure described in section 2.4. The next step was to change the amino-functionalized UCPs into carboxylic-functionalized UCPs.

The introduction of carboxylate groups was done by reacting the silylated amino UCPs with glutaric anhydride. The UCPs obtained in the above mentioned procedure were centrifuged (12000 rpm, 7 min), the supernatant liquid was discarded and 150 μL of dry pyridine was added. Then, glutaric anhydride was added in a 10-fold mass ratio compared to UCP mass, after being dissolved in 120 μL of pyridine. The mixture was

vortexed and sonicated for 5 min and later transferred to a bath for 2.5 h at 50 °C. Afterwards, another batch of glutaric anhydride was diluted and added and the process was repeated as for the first batch. At the end, a volume (400 μL) of ethanol was added and centrifuged at 12000 rpm for 7 min. Finally, the pellet was washed twice with doubly-deionized water, suspended in 450 μL of doubly-deionized water and stored at room temperature in slow rotation.

2.7. Conjugation of –COOH functionalized UCPs with streptavidin

The conjugate of streptavidin (SA) with the functionalized UCPs was synthesized by using a carbodiimide reaction in the presence of sulfo-NHS and EDC. To start the process, functionalized UCPs were washed with 1 mL of MES buffer (pH 6.1, 20 mM) and then, they were re-suspended in 500 μL. On the other hand, 20 mM EDC and 30 mM sulfo-NHS were dissolved by weighing the appropriate amount brought to room temperature. Afterwards, a volume (10 μL) of sulfo-NHS and a volume (10 μL) of EDC were added to the UCP dispersion and the resulting mixture was incubated for 45 min at room temperature in rotation. After this time, the dispersion was washed with MES buffer, centrifuged at 12000 rpm for 7 min and the dispersion was reconstituted with MES buffer. To the synthesized sulfo-succinimidyl ester, 33 μL of streptavidin (30 mg/mL) were added to the mixture and incubated for 2.5 h at room temperature and in rotation. The reaction was stopped by adding 12.8 mL of 2 M glycine, pH 11, and the mixture was allowed to react for 30 min with rotation. The conjugate obtained was purified by washing twice with borate buffer (10 mM, pH 8.5) containing 0.1% Tween 20 and one with

storage buffer, which consisted of borate buffer (5 mM, pH 8.5), 0.2% Tween 85, 0.5% BSA and 0.05%NaN_3. The conjugate was stored at room temperature in an Eppendorf tube in rotation and its concentration was determined as described in the procedure for the measurement of UCP concentration.

The amount of total SA and free SA was calculated by using a heterogeneous competitive binding for streptavidin using a biotin-Tb-chelate conjugate [11]. Unconjugated SA was separated from UCP suspension by centrifugation and collection of the supernatant. In the assay, 0-50 ng of streptavidin in 75 μL of assay buffer, or appropriate dilutions of phosphor suspension and supernatant, were mixed with 75 μL of 4 nM biotin conjugate of Tb-chelate and the reactions were incubated for 30 min at room temperature with slow shaking to capture all unbound biotin conjugates of Tb-chelate. Finally, the wells were washed twice and the signal was developed and measured similarly to the heterogeneous biotin-binding assay.

2.8. Homogeneous acceptor titration

The amount of biotin-acceptor concentration necessary to saturate SA-UCP binding sites was found using a homogeneous acceptor titration, which involves the use of biotin as the analyte, a donor (a SA-conjugate) and an acceptor (biotinylated fluorophores). The microtiter plates used were black half area 96-well plates.

The assay was performed as follows: a volume (32 μL) of biotin 12.5 μM or same volume of reaction buffer was added to 24 μL of a SA-UCP (0.05 mg/mL, 0.015mg/ml in the final reaction mixture). The mixture

was incubated for 15 min at 23 °C and at 900 rpm using a plate tape to protect the plate from light and the luminescence was measured with the Chameleon 5 instrument, using an emission filter of 550 nm, for 2000 ms. Afterwards, biotinylated-acceptor at different concentrations (0.25, 0.74, 2.2, 7, 20 nM in the final reaction mixture) was added and the incubation was performed at 23 °C at 900 rpm. Luminescence measurements were taken at 45 min using 600 and 550 nm as emission filters for 2000 ms in the case of Er(III) and Ho(III)-doped UCPs, and of 555 and 470 nm for Tm(III)-doped UCPs. Signals were treated as described previously elsewhere [11].

2.9 Homogeneous LRET affinity assay for D-biotin

The homogeneous competitive format for biotin determination was also assayed using D-biotin concentrations in the range of 0 – 12.5 μM in the assay tube. The concentration of SA-UCP was 0.015 mg/mL for Er(III) and Ho(III) donors and 0.03 mg/mL for Tm(III) donor. The acceptor concentrations used were 0.2 and 0.4 nM, for bio-BPE, 1.33 nM for bio-RPE and 4 nM for AF680. A 12.5 μM biotin concentration was used to verify the background level.

3. Results and Discussion

3.1. Luminescent features of donor-acceptor pairs

The LRET study presented has been carried out using the streptavidin-biotin affinity system, as model assay. Streptavidin was coated to UCP donors, whereas biotin was coupled to fluorescent acceptors. Figure 1 shows a typical scheme for this system, in which can be seen that after UCP excitation, there is an energy transfer process from the

donor to the acceptor, thus resulting in acceptor emission. This process is subject to the following two conditions: 1) The excitation spectrum of the acceptor has to overlap donor emission, and 2) The distance between donor and acceptor follows Förster equation.

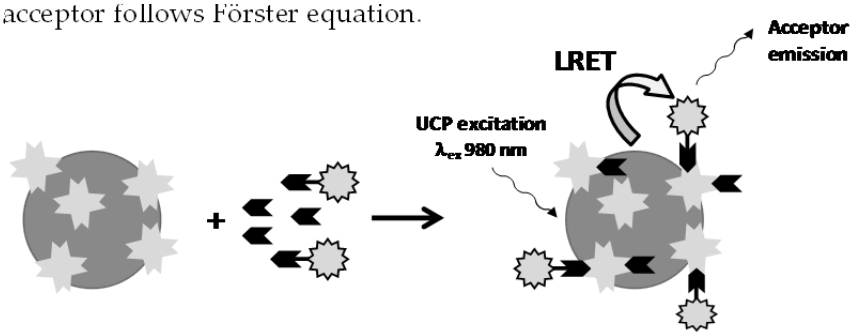

Figure 1. General scheme of a homogeneous up-conversion LRET affinity assay (streptavidin coated UCP (donor), biotin D, biotinylated-fluorophore (acceptor)

Figure 2 shows the excitation and emission spectra of the different donor-acceptor pairs used in this study. Figure 2.A shows the up-conversion emission spectra of the Er(III)-doped-UCP (donor) when excited at 980 nm and the excitation and emission spectra of β-phycoerythrin (BPE) (acceptor). As it can be seen, the overlap of UCP emission and BPE excitation is complete. A critical aspect to enhance FRET emission is the selection of the appropriate wavelengths of the emission filter to measure acceptor emission without collecting the signal coming from acceptor self-excitation. For this reason, although maximum emission of BPE happens at 575 nm, a 600/40 nm filter was chosen to measure LRET intensity. The UCP emission at 550 nm was measured by using 535/50 nm filter. This combination of donor-acceptor pairs has been previously used for the development of several affinity assays [11, 13] and homogeneous immunoassays [12] to determine estradiol. Other fluorescent acceptors,

such as AF546 (λ_{ex} 556, λ_{em} 570 nm) and AF680 (λ_{ex} 680, λ_{em} 702 nm), were also assayed. As it can be observed in Fig. 2.B) the 600/40 nm filter is still appropriate for the Er(III)-doped UCP-AF546 pair, while a 750/40 nm filter is used when AF680 is used as acceptor. A 665/10 nm filter was used in this instance to collect UCP emission.

Similar luminescence spectra were also recorded for Ho(III)-doped (Fig 2.D and 2.E) and Tm(III)-doped (Figs 2.F-2.H) UCPs as donors using different fluorescent acceptors. For Ho(III)-doped-UCPs, BPE and AF546 were assayed as potential acceptors, using in both cases 600/40 nm filters to measure the LRET intensity. This is possible owing to the fact that Ho(III)-doped UCPs have their maximum emission at 535 nm. In a similar way as for Er(III)-doped UCPs, the wide excitation spectra of BPE allows its efficient excitation. The excitation of AF546 is less favoured because only the emission of the donor matches the excitation of the acceptor at 50% of its maximum intensity. However, its emission wavelength enables the use of 600/40 to measure LRET with minimum background.

Tm(III)-doped UCPs have a lower emission wavelength than Er(III) and Ho(III) centered at 472 nm (Figs. 2.F-2.H). Although the best overlap is obtained for the Tm(III)-doped UCP and AF488 pair, compared to the use of RPE and ATTO495. Regarding the filters used to measure LRET, the use of 600/40 nm filter seems to be the best option to collect the emission from RPE, although some emission from acceptor self-excitation could still happen. For AF488, several filters such as 520/10, 555/20 and 600/40, could be used to collect emission. As it can be seen, the emission intensity at 600/40 is really poor. The best option for ATTO495 seemed to be the filter

555/20, since the intensity obtained was about three times higher than that obtained with the 600/40 nm filter.

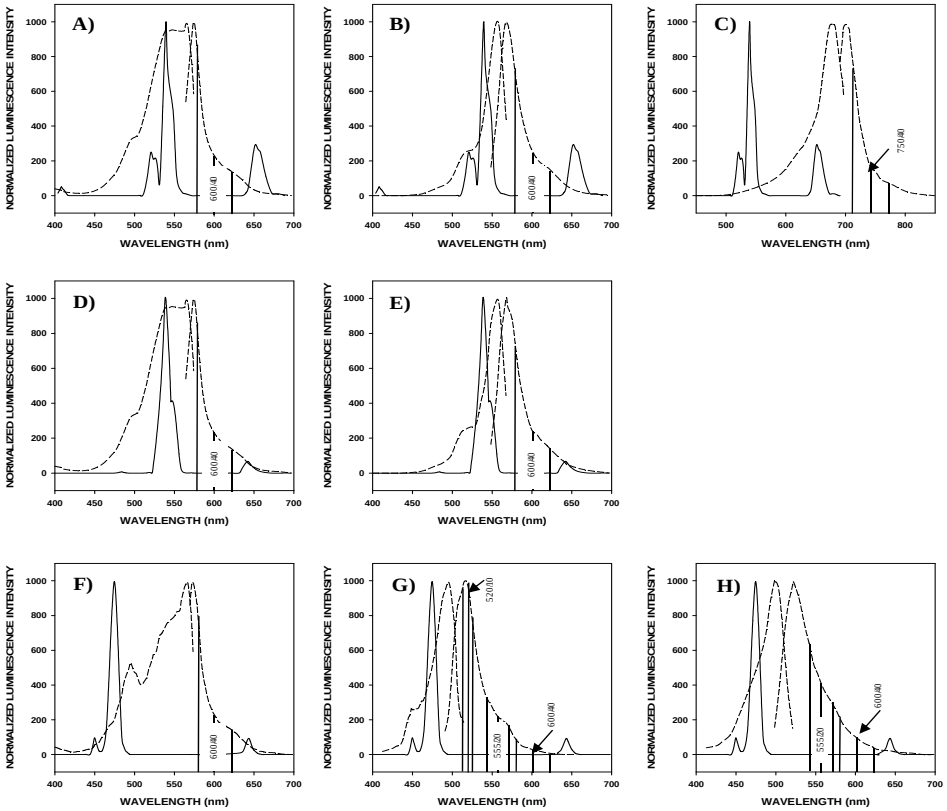

Figure 2. Emission spectra obtained for different UCPs (solid line) and excitation and emission spectra of different acceptors (dashed lines). In 2.A-2.C, Er(III)-doped UCP emission spectra together with BPE (2.A), AF546 (2.B) and AF680 (2.C). In 2.D and 2.E, Ho(III)-doped UCPs with BPE (2.D) and AF546 (2.E). In 2.F-2.H, Tm(III)-doped UCPs with RPE (2.F), AF488, (2.G) and ATTO495 (2.H).

3.2. Homogeneous acceptor titration experiments

The aim of these titration assays is to find the amount of biotinylated acceptor required to saturate the binding sites of the UCPs. The lower the concentration of biotinylated acceptor, the more sensitive the

homogeneous LRET determination will be. These experiments were performed for biotinylated UCPs of different chemical composition. In order to make the different measurements comparable, the streptavidin-coated UCPs (SA-UCPs) were diluted to be at the same final UCP concentration. The influence of surface functionalization procedure was studied by performing the titration of SA-coated UCP donors composed by the same UCP that had been functionalized according to different procedures, with the same acceptor. It has been previously described that bio-BPE provides excellent LRET signals with SA-Er(III)-doped UCPs as donors [11-14]. For this reason, Er(III)-doped UCPs and Ho(III)-doped UCPs functionalized with Additol and those encapsulated with a silica layer were assayed as potential donors, at an equivalent UCP concentration of 0.015 mg/mL with varying bio-BPE concentrations (Figure 3). As can be seen, the best luminescence intensity was obtained for a bio-BPE concentration lower than 1 nM and the highest values were obtained for SA-Er(III)-doped UCPs. It can be also seen that the functionalization procedure did not affect the final LRET intensity, although it was observed for both types of UCPs that the acceptor concentration required for UCPs coated with Additol was lower than that for those encapsulated into a silica shell. A possible explanation of this fact could be that SA-silica-Er(III) doped UCP contained about 2-fold streptavidin molecules attached to the surface than SA-Additol-Er(III)-coated UCP donor. As it can be seen, the LRET intensity when SA-Ho(III)-doped donors were used was much lower, so the feasibility of using other SA-Ho(III)-doped UCP concentrations was explored in a further experiment.

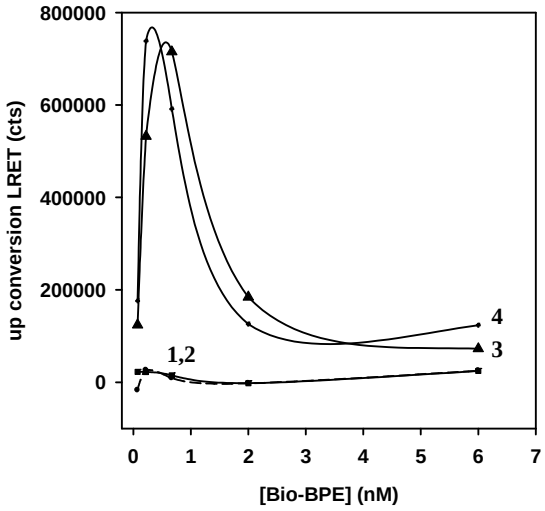

Figure 3. Homogeneous acceptor titrations for streptavidin-Er(III) and streptavidin-Ho(III) doped UCP donors obtained by ligand exchange with Additol (2,4) and by silylation (1,3). In 1,2 [Ho(III)-doped UCP] = 0.015 mg/mL. In (3,4) [Er(III)-doped UCP] = 0.015 mg/mL. LRET signals were calculated by subtracting the background signal of the assay (excess of D-biotin) from the maximum signal (absence of D-biotin), cts: counts.

In an attempt to increase the signal exhibited by SA-Ho(III)-doped-UCPs, higher equivalent UCP concentrations (0.03 and 0.045 mg/mL) were assayed, using bio-BPE as acceptor (Figure 4). However, the LRET signals obtained were 5-times lower than those obtained for SA-Er(III)-doped UCP donors. A 0.4 nM bio-BPE and 0.03 mg/mL SA-Er(III)-UCP were chosen to perform homogeneous assays for biotin determination, since they provide an adequate LRET signal with a bio-BPE concentration relatively low, reaching an adequate sensitivity.

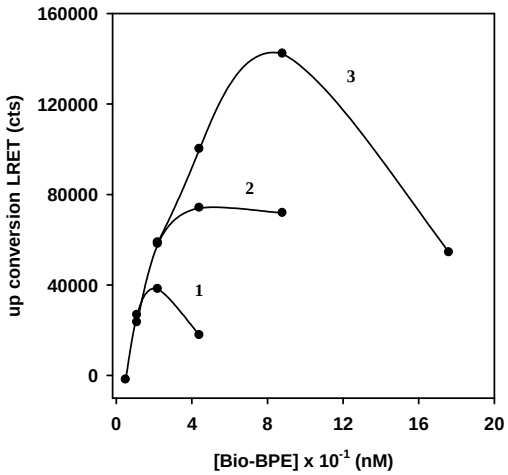

Figure 4. Influence on the concentration of Ho(III)-doped UCP on the luminescence and on the sensitivity of homogeneous acceptor titration curves. [donor] are: (1) 0.015 mg/mL, in (2) 0.03 mg/mL in (3) 0.045 mg/mL. LRET signals were calculated as indicated in Figure 3.

As indicated above, the UCP silylation can produce more stable SA-UCP donors. Several assays were carried out to optimize this process using a reverse-micelle microemulsion procedure for the formation of the silica shell. The concentration of surfactant used and the addition order of the reagents can affect the shape and the thickness of silica shell [17]. The functionalization was performed by assaying three surfactant concentrations and modifying the addition order of the microemulsion components. Figure 5 shows the different curves obtained for the homogeneous acceptor titration with the SA-UCP donors. As it can be seen, the addition order is a critical variable, which could be explained by a different structure of the silica layer with no apparent changes in the final amount of SA-Er(III)-doped UCP. It has also been described that the free

amino groups from silica layer can modify UCP intensity [15], which could explain the different LRET intensity obtained for identical donor and acceptor concentrations. The use of silica to encapsulate UCPs seems to be a good alternative to the use of Additol since the decrease in the luminescence intensity is relatively small. Thus, all the homogeneous assays involving either Er(III), Ho(III) or Tm(III) nanosized UCPs were performed after functionalization by silylation procedures to obtain the donors.

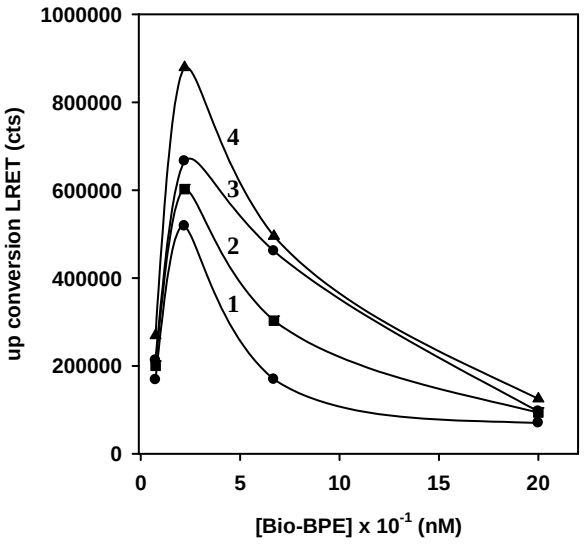

Figure 5. Homogeneous acceptor titration curves obtained after different silylation procedures. Volumes of Triton X-100 used were: (1) 1.3 mL, (2) 2,7 mL, (3) 5,3 mL and (4) adding Triton 2.7 mL of Triton X-100 at the end. LRET signals were calculated as indicated in Figure 3.

BPE and RPE are very fluorescent proteins commercially available, but they are relatively expensive. Thus, the feasibility of other alternative fluorophores, with suitable wavelengths to produce LRET was checked. Figure 6 shows the titration curves obtained for SA-Er(III)-doped (6.A) and SA-Ho(III)-doped (6.B) UCP donors with bio-BPE and bio-AF546 as acceptors. The LRET intensity was much lower for bio-AF546 and the increase of SA-Ho(III)-doped UCP concentration did not improve the LRET signal unlike it happened for the pairs with SA-Er(III)-doped UCPs and bio-BPE as donor and acceptor, respectively. The same behaviour was observed for SA-Tm(III) donors, in which the acceptors used were bio-RPE, bio-AF488 and bio-ATTO 495 (Fig. 6.C). All of them provided LRET signal, but the highest intensity was obtained using bio-RPE, so this pair was chosen to develop further homogeneous affinity assays for biotin with Tm(III)-doped UCPs as donors.

3.3 Determination of biotin using homogeneous LRET assays

Several donor-acceptor pairs were used to perform homogeneous LRET assays for biotin. Figure 7 shows the curves for biotin obtained for the donor-acceptor pairs studied. These pairs were chosen amongst those which provided better LRET intensities with minimal acceptor concentrations.

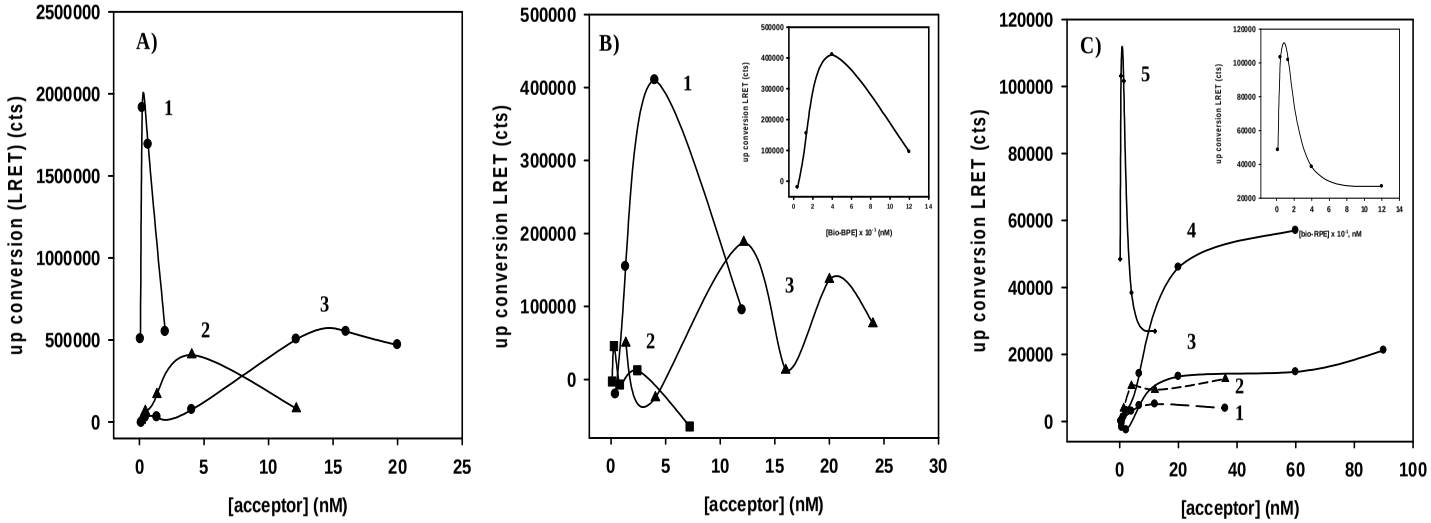

Figure 6. Homogeneous titration curves obtained for different donor-acceptor pairs. In 6.A) [Er(III)-doped UCP = 0.015 mg/mL and acceptors were: (1) bio-BPE; (2) AF680 and (3) AF546. In 6.B) [Ho(III)-doped UCP] were (1) 0.030 mg/mL with bio-BPE as acceptor, (2) 0.015 mg/mL with bio-AF546 as acceptor and in (3) 0.030 mg/mL with AF546 as acceptor. In (C) [Tm(III)-doped UCP] was used as donor and the conditions were (1) [donor] = 0.0075 mg/mL and bio-AF488 as acceptor, in (2) [donor] = 0.0075 mg/mL and bio-ATTO 495 as acceptor, in (3) [donor] = 0.045 mg/mL and bio-AF488 as acceptor, in (4) [donor] = 0.045 mg/mL and bio-ATTO495 as acceptor, in (5) [donor] = 0.015 mg/mL and bio-RPE as acceptor. LRET signals were calculated as indicated in Figure 3.

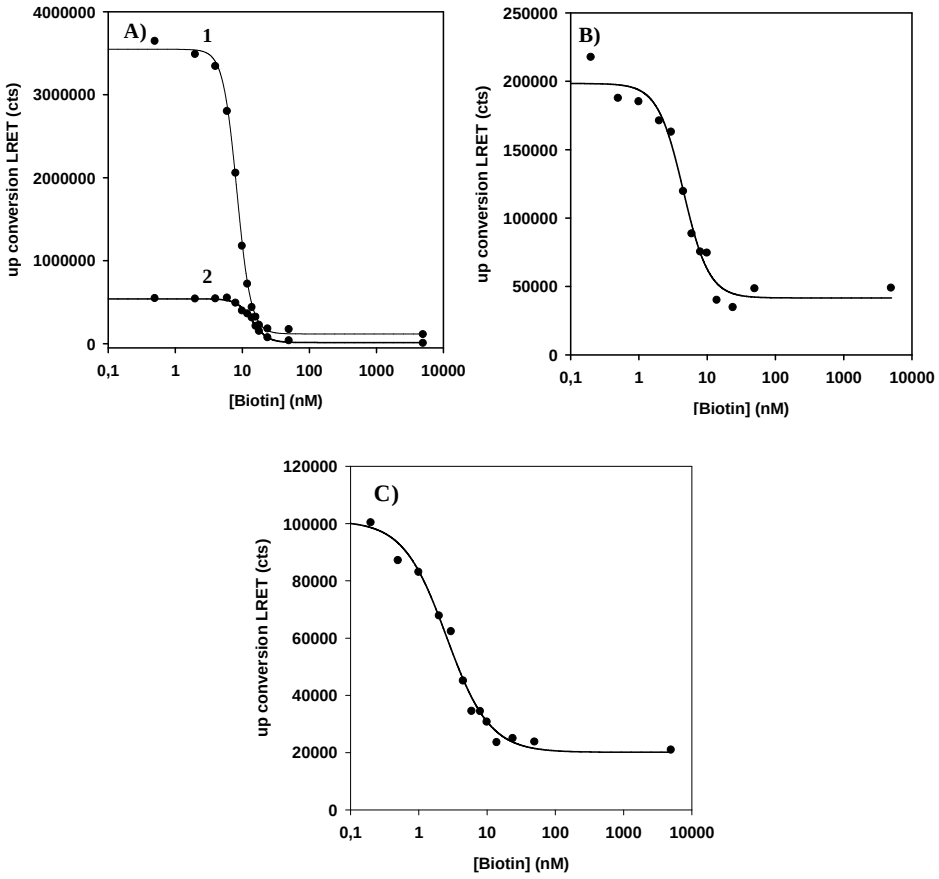

Figure 7. Homogeneous LRET affinity assays for D-biotin with donor-acceptor pairs giving the best results. In A) with Er(III)-doped UCP (0.015 mg/mL) and (1) 0.4 nM BPE and (2) 4 nM AF680. In (B) Ho(III)-doped UCP (0.030 mg/mL) and 0.2 nM BPE. In (C) Tm(III)-doped UCP (0.030 mg/mL) and 1.33 nM RPE. LRET signals were calculated as indicated in Figure 3.

As it can be also seen from the Figure, the highest luminescence intensities were obtained for Er(III)-doped UCPs with BPE and AF680 nm. However, the Table 1 shows the different assays performed according to

the results obtained for homogeneous acceptor assays and the IC50 obtained for biotin.

Table 1. IC50 values for biotin assays using different donor-acceptor pairs

	IC50 for biotin (nM)			
Acceptor / Donor	Bio-BPE (0.2 nM)	Bio-BPE (0.4 nM)	Bio-RPE (1.33 nM)	Bio-AF680 (4 nM)
Er(III)-doped UCP (0.015 mg/mL)	---	8.57*	---	14.37
Ho(III)-doped UCP, 0.015 mg/mL)	5.7	---	---	---
Ho(III)-doped UCP, 0.015 mg/mL)	---	7.20	---	---
Tm(III)-doped UCP (0.030 mg/mL)	---	---	3.35	---

*The concentration of bio-BPE was 0.3 nM

These IC50 values were calculated after adjusting the normalized intensities of the calibration curves for biotin to 4-parameter logistic curves, which regression coefficients (r) were higher than 0.99 in all instances. The lowest IC50 was obtained for the pair SA-Tm(III)-UCP with bio-RPE in spite of its low LRET intensity. The highest IC50 was obtained for the SA-Er(III)-doped UCP functionalized with silica and bio-AF680, which was about 14.4 nM. The values obtained are comparable, and in some instances better than those obtained by some previously reported methods [11,12]

using Er(III)-doped UCPs coated with Additol as donors and bio-BPE as acceptor.

4. Conclusions

A systematic study on the suitability of different UCP donor-acceptor pairs has been performed using biotin as model analyte. The use of Er(III)-doped UCPs has resulted in higher LRET intensities, the maximum of which have been obtained using bio-BPE as acceptor. Although BPE and RPE have shown to provide the best LRET intensities, the use of other fluorophores, such as AF680 allows determinations of biotin with IC50 values in the nM range.

The results obtained show the potential feasibility of multiplexed assays using different LRET donor-acceptor pairs.

References

(1) Gnach A., Bednarkiewicz A. Lanthanide-doped up-coverting nanoparticles: merits and challenges. *Nano Today* **(2012) *7*,** 532 – 536.

(2) Wang F., Banerjee D., Liu Y., Chen X., Liu X. *Analyst* **(2010)** *135*, 1839 – 1854.

(3) Misiak M., Prorok K., Cichy B., Berdnarkiewicz, Strek W. Thulium cocentration quenching in the up-converting a-Tm^{3+}/Yb^{3+} $NaYF_4$ colloidal nanocrystals. *Opt. Mat*. **(2013)** *35*, 1124 – 1128.

(4) Jiang T., Song W., Liu S. Qin W., Synthesis and upconversion luminescene properties study of $NaYbF_4$:Tm^{3+} crystals with different dopant concentration. *J. Fluorine Chem*. **(2012)** *140*, 70 -75.

(5) Prorok K., Gnach A., Beednarkiewicz A., Strek W. Energy up-conversion in Tb^{3+}/Yb^{3+} co-doped colloidal a-$NaYF_4$ nanocrystals. *J. Luminesc*. **(2013)** *140*, 103 – 109.

(6) Koepke C., Piatkowski D., Wisniewski K., Naftaly M. On competition between two types of anti-Stokes emission in the Ho^{3+} and Nd^{3+} ions in glasses. *J. Non-Cryst. Solids* **(2010)** *356*, 435 – 440.

(7) Wnuk A., Kaczkan M., Frukacz Z., Pracka I., Chadeyron G., Joubert M.F., Malinowski M. Infra-red to visible up-conversion in holmium-doped materials. *J. Alloys Compounds* **(2002)** *341*, 353 – 357.

(8) Ukonaho T., Rantanen T., Jämsen L. Kuningas K., Päkkilä, T. Lövgren, T. Soukka. Comparison of infrared-excited up-converting phosphors and europium nanoparticles in a two-site immunoassay. *Anal. Chim. Acta* **(2007)** *596*, 106 – 115.

(9) Kuningas K., Rantanen T., Lövgren T., Soukka T. Enhanced photoluminescence of up-converting phosphors in a solid phase bioaffinity assay. *Anal. Chim. Acta* **(2005)** *543*, 130 – 136.

(10) Kuningas K., Rantanen T., Karhunen U., Lövgren T., Soukka T. Simultaneous use of time-resolved fluorescence and anti-Stokes Photoluminescence in a Bioaffinity Assay. *Anal. Chem*. **(2005)** *77*, 2826 – 2834.

(11) Kuningas K., Rantanen T., Ukonaho T., Lövgren T., Soukka T. Homogeneous assay technology based on upconverting phosphors. *Anal. Chem*. **(2005)** *77*, 7348 – 7355.

(12) Kuningas K., Ukonaho T.,Pakkilä H., Rantanen T., Rosenberg J. Lövgren T., Soukka T. Upconversion fluorescence resonance energy

transfer in a homogeneous immunoassay for estradiol. *Anal. Chem*. **(2006**) *78*, 4690 – 4696.

(13) Rantanen T., Päkkilä H., Jämsen L., Kuningas K., Ukonaho t., Lövgren T., Soukka T. Tandem dye acceptor used to enhance upconversion fluorescence resonance energy transfer in homogeneous assays. *Anal. Chem*. **(2007)** *29,* 6312 – 6318.

(14) Rantanen T., Jarvenpää M.L., Vuojola J., Kuningas K., Soukka T. Fluorescence quenching-based enzyme activity assay using photon up-conversion. *Angew. Chem. Int. Ed*. **(2008)** *47*, 3811 – 3813.

(15) Kong Y.L., Wang Z.L., Lin C.K., Quan Z.W., Li Y.Y., Li C.X. Biofunctionalization of CeF3:Tb^{3+} nanoparticles. *Nanotechnology* **(2007)** *18,* 075601.

(16) Hyppänen I., Hölsä J., Kankare M., Lastusaart M., Pihlgren L., Soukka T., Terrae Rarae. Preparation and up-conversion luminescence properties of NaYF4:Yb3+,Er3+ nanomaterials. *Terra Rarae* **(2009)** *16,* 1 – 6.

(17) Godoy-Navajas J., Aguilar-Caballos M.P., Gómez-Hens J. Synthesis and characterization of oxazine-doped silica nanoparticles for their potential use as stable fluorescent reagents. *J. Fluoresc.* **(2010**) *20,* 171 – 180.

CAPÍTULO 5

CHAPTER 5

Discusión de resultados

Discussion of the results

Introducción

En este capítulo se discuten las características de los métodos desarrollados en esta Memoria, realizando un estudio comparativo de sus ventajas y limitaciones frente a métodos previamente descritos en la bibliografía. También se discute la utilidad de las metodologías propuestas mediante su aplicación al análisis de alimentos.

El capítulo se ha dividido en tres apartados: 1) Nanopartículas de sílice en análisis de alimentos, 2) Nuevas estrategias para la determinación de antioxidantes en alimentos y 3) Nuevas investigaciones en el uso de "upconverting phosphors" en sistemas de transferencia de energía de resonancia luminiscente.

1. Nanopartículas de sílice en análisis de alimentos.

Como ya se ha indicado, el uso de nanomateriales está teniendo un importante auge en distintas áreas de la Química Analítica [1 – 5]. Dentro de la gran diversidad de nanomateriales existentes en la actualidad, la utilización de nanopartículas de sílice (SiO_2NPs) se ha extendido rápidamente a lo largo de la última década gracias a sus excelentes propiedades que las hacen viables para su uso como marcadores en el campo del bioanálisis. En el siguiente apartado se discutirán los resultados obtenidos con estas NPs en tres de los artículos incluidos en esta Memoria.

- Síntesis y caracterización de nanopartículas dopadas con fluoróforos de larga longitud de onda

El uso de SiO_2NPs para formar marcadores tiene interés en los métodos con detección óptica debido principalmente a la transparencia de la sílice a la radiación visible, además de otra serie de ventajas descritas en la Introducción de esta Memoria.

En los dos métodos generales para la síntesis de SiO_2NPs, el método Stöber y el de formación de microemulsión de micelas inversas, se utilizan precursores de sílice tales como el tetrametoxisilano (TMOS) y el tetraetoxisilano (TEOS), los cuales, tras reacciones de hidrólisis y condensación dan lugar a NPs esféricas dispersas [6]. La elección de uno u otro método va a depender de las propiedades físicas y químicas de las especies que se pretenden encapsular en estas NPs [2, 4].

En la Memoria presentada se describe el procedimiento para sintetizar SiO_2NPs con emisión a larga longitud de onda, basado en la formación de una microemulsión de micelas inversas, dopando las NPs con dos fluoróforos de larga longitud de onda (LWFs): violeta de cresilo y azul nilo. Para ello se han optimizado todas las variables implicadas en el proceso de síntesis y se han comparado sus características (tamaño de NP, cantidad de nanomaterial, intensidad de fluorescencia, etc) con las que presentan las obtenidas mediante el método Stöber.

La formación de la microemulsión utilizada para la síntesis de las NPs dopadas con los fluoróforos anteriormente indicados implica el uso de un tensoactivo, una disolución acuosa y un disolvente orgánico, mientras que para la formación de la base estructural de las NPs es necesario un precursor de sílice. Dependiendo de las cantidades relativas de estos

componentes se puede obtener una microemulsión de agua-en-aceite (rica en disolvente orgánico) o bien una microemulsión de aceite-en-agua (rica en agua). De acuerdo a lo descrito en la bibliografía, se ensayó el uso de ciclohexano, 1-hexanol y Tritón X-100 para formar la microemulsión, y mientras que el precursor de sílice seleccionado fue el TEOS [2, 4, 6, 8 – 10]. Sin embargo, las condiciones experimentales anteriormente descritas no fueron satisfactorias para la síntesis de NPs dopadas con azul nilo o violeta de cresilo. Los estudios realizados sobre la posible composición de la microemulsión pusieron de manifiesto que las NPs sintentizadas en ausencia de ciclohexano presentaban similares características a las obtenidas en presencia de este disolvente, en lo referente a número de NPs y tamaño, pero la intensidad de fluorescencia obtenida fue ligeramente mayor. Como puede observarse en las imágenes presentadas en la Figura 1, obtenidas mediante microscopía electrónica de transmisión (TEM), la cantidad y tamaño de las NPs en ausencia de ciclohexano (Figura 1a) fue comparable con las NPs obtenidas utilizando 7,5 mL de ciclohexano (Figura 1c). Sin embargo, el uso de volúmenes intermedios de ciclohexano (Figura 1b) proporciona NPs de mayor tamaño y una elevada distribución de tamaños. Según estos resultados, se prescindió del ciclohexano en el proceso de síntesis de las NPs dopadas con azul nilo y violeta de cresilo, utilizándose agua, Tritón X-100 y 1-hexanol para la formación de la microemulsión.

Tras estudiar la influencia de la cantidad de Tritón X-100, se observó que el número de NPs dopadas con azul nilo aumentaba con la cantidad de tensoactivo utilizada, mientras que el tamaño de las NPs

decrecía. Los mejores resultados fueron obtenidos utilizando 510-520 mg de Tritón X-100 (Figura 1f), ya que menores cantidades de este tensoactivo proporcionaron NPs de tamaño superior a los 200 nm de diámetro (Figuras 1d y 1e). En cambio, cuando la cantidad de Tritón X-100 era próxima a 1,0 g se obtenían NPs muy pequeñas y parcialmente agregadas.

También se estudió la posibilidad de encapsular el fluoróforo en las SiO_2NPs mediante el proceso de formación de microemulsión de micelas inversas con una ligera modificación adicional. Esta modificación consiste en un paso previo de reacción, donde el fluoróforo reacciona con un precursor de sílice, 3-aminopropiltrietoxisilano (APS), para que, una vez unido covalentemente a este precursor, ambos se incluyan en el proceso de polimerización de las NPs. El objetivo de este procedimiento fue evitar posibles pérdidas de fluoróforo a través de la matriz de la sílice, reduciendo también el número de lavados necesarios para eliminar el exceso de fluoróforo, etapa previa a la utilización de las NPs. No obstante, como puede observarse en la Figura 1g, la cantidad de NPs resultante fue considerablemente menor a la obtenida sin la formación del precursor APS-azul nilo, además de presentar una elevada distribución de tamaños. Por lo tanto, se descartó la posibilidad de utilizar este tipo de NPs para la obtención de marcadores utilizables en posteriores ensayos, puesto que no mejoraban las características de las NPs frente a las obtenidas sin incluir esta modificación. Este comportamiento se puede atribuir a la estabilización de los fluoróforos, cargados positivamente, con los grupos silanoles, cargados negativamente, característicos de la matriz de sílice.

Además, se requiere una etapa adicional en el proceso de síntesis, con un mayor consumo de reactivos y tiempo.

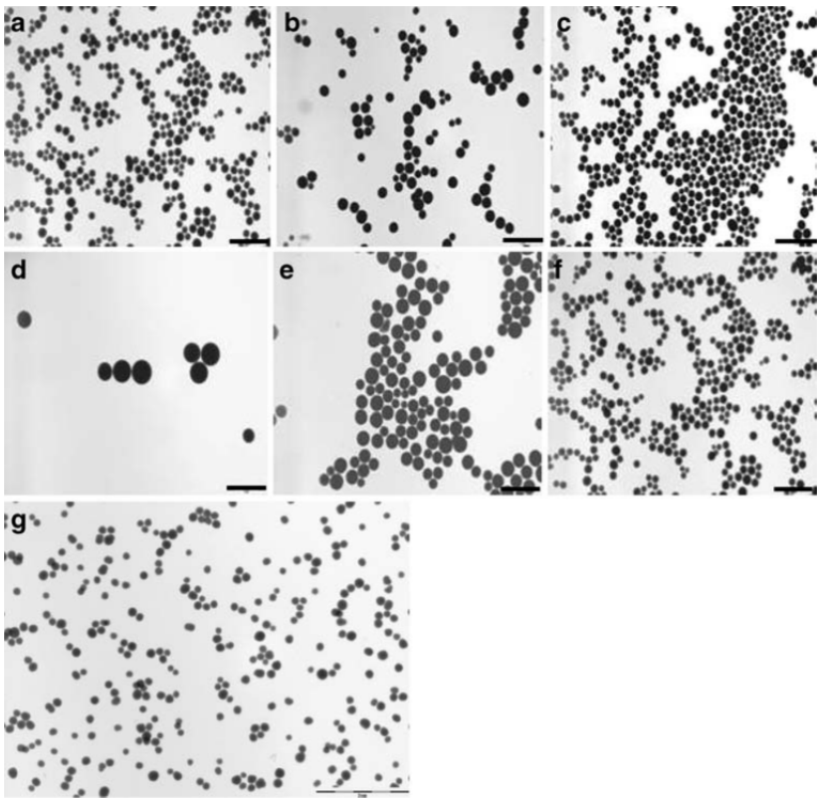

Figura 1. Imágenes obtenidas mediante microscopía electrónica de transmisión (TEM) de NPs dopadas con azul nilo utilizando diferentes volúmenes de ciclohexano (**a, b** y **c**), diferentes concentraciones de Tritón X-100 (**d, e** y **f)** y NPs dopadas con (3-aminopropiltrietoxisilano) APS-Azul Nilo (**g**). Condiciones experimentales: 100 μL (0,44 mmol) TEOS, 0,2 mL de $1x10^{-3}$ (0,2 μmol) azul nilo, 3 mL (0,024 mol) hexanol, 70 μL (0,9 mmol) NH_4OH. En (Figuras 1a - c): 510 – 520 mg (0,79 – 0,82 mmol) Tritón X-100. En Figura 1a 11,3 mL (0,63 mol) agua, 0 mL ciclohexano, en Figura 1b, 7,5 mL (0,42 mol) agua, 3,75 mL (0,034 mol) ciclohexano, en Figura 1c, 3,8 mL (0,21 mol) agua, 7,5 mL (0,068 mol) ciclohexano. En Figura 1d – f, 11,3 mL (0,63 mol) de agua, en Figura 1d, 0 mg, en Figura 1e, 310,9 mg (0,48 mmol), en figura 1f, 510,9 (0,79 mmol) de Tritón X-100. Barra de escala: 1 μm. En figura 1g, condiciones experimentales: 510 – 520 mg (0,79 – 0,81 mmol) de Tritón X-100, 10,3 mL (0,57 mol) de agua, 100 μL (0,44 mmol) TEOS, 1,2mL precursor de reacción, 3 mL (0,024 mol) hexanol, 70 μL (0,9 mmol) de NH_4OH. Barra de escala: 2 μm.

También se estudiaron las proporciones óptimas entre diferentes reactivos, observándose que la relación Tritón X-100/hexanol es una variable crítica en el proceso de síntesis. Como puede observarse en la Figura 2, una cantidad de 170 mg de Tritón X-100 por mL de hexanol proporciona NPs con una intensidad de fluorescencia máxima.

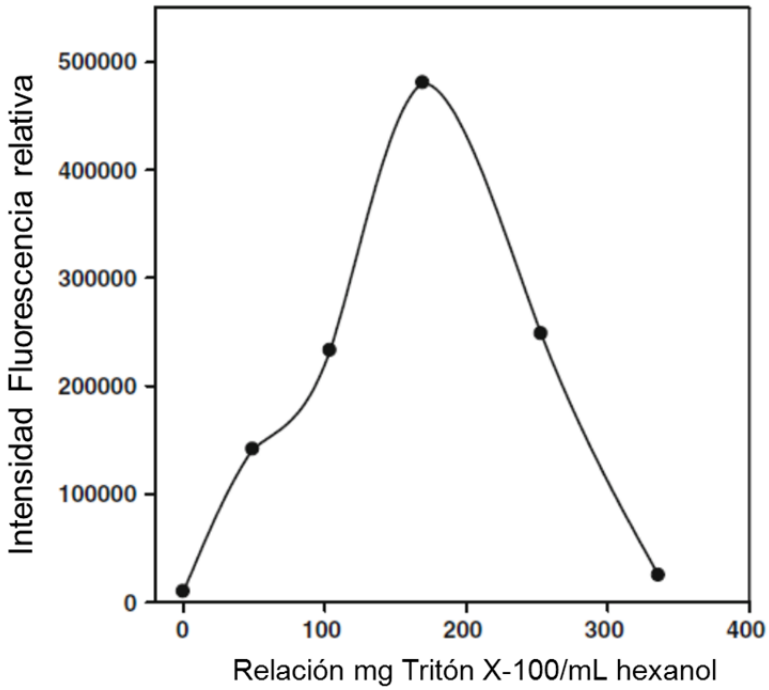

Figura 2. Influencia de la relación Tritón X-100/hexanol en la intensidad de fluorescencia de las NPs-azul nilo. Condiciones experimentales: 11,3 mL (0,63 mol) de agua, 100 μL (0,44 mmol) TEOS, 0,2 mL de $1x10^{-3}$ M (0,2 μmol) azul nilo, 3 mL (0,024 mol) hexanol, 70 μL (0,9 mmol) NH_4OH.

La cantidad de azul nilo utilizada en el proceso de síntesis es otra variable crítica. Como puede observarse en la Figura 3, la intensidad de fluorescencia máxima se obtuvo con 1,8 μmol de azul nilo. La disminución

de esta intensidad de fluorescencia con cantidades de fluoróforo mayores, puede atribuirse a la formación de agregados moleculares de azul nilo, cuya fluorescencia es menor que la del monómero [7].

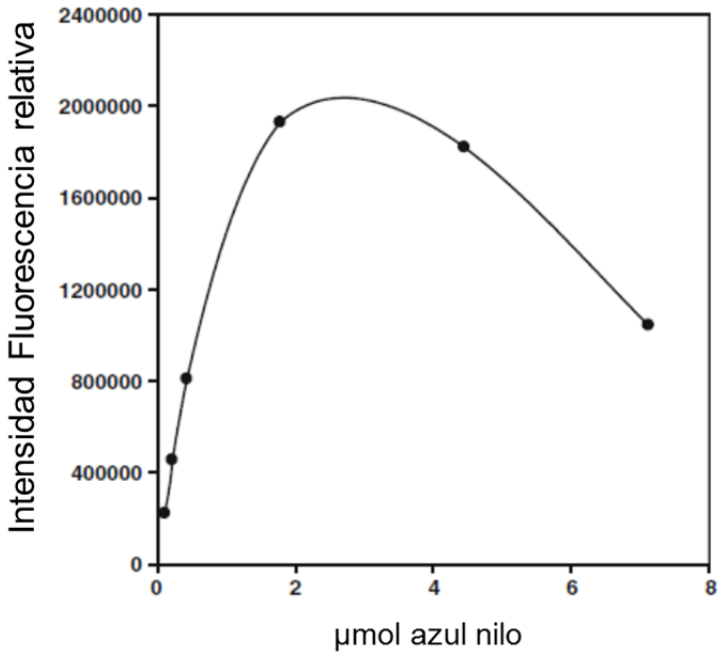

Figura 3. Influencia de la cantidad de azul nilo adicionada en la intensidad de fluorescencia de las NPs dopadas con este fluoróforo. Condiciones experimentales: 510-520 mg (0,79 – 0,81 mmol) de Tritón X-100, 11,3 mL (0,63 mol) de agua, 100 µL (0,44 mmol) TEOS, 3 mL (0,024 mol) hexanol y 70 µL (0,9 mmol) NH_4OH.

Tras estudiar la influencia de todas las variables involucradas en el proceso de síntesis mediante el método de microemulsión de micelas inversas, las NPs obtenidas fueron comparadas con las sintetizadas mediante el método Stöber. En la Tabla 1 se recogen diferentes características de las NPs dopadas con violeta de cresilo obtenidas por

ambos métodos. Con el fin de comparar las características luminiscentes de ambos tipos de NPs se prepararon suspensiones de igual concentración, observándose que el diámetro medio de las NPs obtenidas por el método de microemulsión es ligeramente mayor que el de las obtenidas por el segundo método, aunque las diferencias no son excesivamente elevadas. En cambio, sí existen diferencias destacables en los valores de intensidades de fluorescencia. Este estudio se realizó preparando suspensiones en medio acuoso de las NPs obtenidas mediante ambos métodos, encontrando que las NPs del método optimizado presentaban una intensidad de fluorescencia 12 veces mayor que las obtenidas en el método Stöber, lo que puede atribuirse a la menor degradación del violeta de cresilo en el medio alcalino utilizado durante el proceso de síntesis, gracias a la protección que le proporciona el medio micelar.

Tabla 1. Comparación de las propiedades de las NPs dopadas con violeta de cresilo.

	Método de microemulsión de micelas inversas	**Stöber method**
Concentración, mg/mL	0.1	0.1
Cantidad de partículas, mg	0.02	0.02
Diámetro, nm	178	133
Número de Partículas	2.94×10^{9}	7.06×10^{9}
Intensidad[a]	125563	10138
Relación Intensidad/Nº partículas	4.27×10^{-5}	1.44×10^{-6}
Intensidad específica	1.45×10^{7}	1.17×10^{6}

[a] Las medidas fueron realizadas utilizando microplacas (200 μL) y filtros de excitación y emisión de 531/25 y 620/8 nm (longitud de onda nominal/paso de banda), respectivamente.

La comparación de los espectros de emisión de las NPs dopadas con cada uno de los fluoróforos con los obtenidos para los mismos fluoróforos en disolución y para las NPs sin dopante, mostró que la sílice por sí sola no presenta emisión fluorescente a las longitudes de onda típicas de los fluoróforos y que el máximo de emisión de las NPs dopadas con estas oxacinas sufre un ligero desplazamiento hipsocrómico de unos 9 nm frente a los fluoróforos en disolución. Para llevar a cabo los estudios de foto-descomposición, se irradiaron los fluoróforos en disolución y las NPs dopadas durante una hora a las longitudes de onda de máxima excitación y emisión. La intensidad de fluorescencia disminuyó un 75 % para el violeta de cresilo y un 62 % para el azul nilo, ambos en disolución, mientras que la fluorescencia de las NPs prácticamente no se alteró. El mismo estudio se realizó con las SiO_2NPs preparadas en presencia de la mezcla azul nilo y APS, obteniendo una disminución de fluorescencia de aproximadamente el 10%. La estabilidad del fluoróforo encapsulado en las NPs también se estudió a lo largo del tiempo, comprobándose que la señal fluorescente permanecía constante durante al menos un mes.

En resumen, se puede afirmar que el método modificado de microemulsión de micelas para la síntesis de NPs dopadas con dos LWFs (azul nilo y violeta de cresilo) proporciona unas NPs de similares características (tamaño, cantidad de material, diámetro medio) que las obtenidas mediante el método Stöber, considerado como método de referencia. Sin embargo, la intensidad de fluorescencia de las NPs sintetizadas en el primer caso es mucho mayor que la obtenida por el

método Stöber, atribuibles a la estabilidad y protección que les confiere a los LWFs la microemulsión donde tiene lugar la polimerización de la sílice.

- Utilización de nanopartículas de sílice en inmunoensayo heterogéneo para la determinación de macromoléculas y moléculas pequeñas

La determinación de biomoléculas constituye un campo de aplicación de la Química Analítica de gran interés. Se han desarrollado numerosos métodos cromatográficos y electroforéticos para la determinación de macromoléculas y moléculas pequeñas [11 – 15]. Normalmente, este tipo de técnicas requiere que el analito presente una propiedad medible como, por ejemplo, absorbancia o fluorescencia. En caso contrario, es imprescindible el uso de una etapa de derivatización que complica y aumenta la duración del análisis [16, 17]. Se han desarrollado diferentes métodos cromatográficos acoplados a espectrometría de masas para la determinación de biomoléculas, los cuales requieren instrumentación sofisticada y costosa [18 – 20]. Además, en algunos casos, es necesario incluir etapas previas para la eliminación de la matriz de la muestra, que alargan el proceso y aumentan la manipulación por parte del analista. Los métodos de "screening" desempeñan dos funciones muy importantes en el análisis de biomoléculas: por un lado, el número de muestras susceptibles de ser sometidas a métodos confirmatorios es menor y, por otro lado, se reduce el coste del análisis. Los inmunoensayos, extensamente utilizados en análisis cuantitativo y semicuantitativo, presentan una serie de ventajas para su uso como métodos de "screening" en la determinación de sustancias antigénicas, ya sean moléculas pequeñas

(haptenos) o macromoléculas. Se han descritos varios inmunoensayos heterogéneos que utilizan marcadores enzimáticos (ELISA) comerciales y no comerciales [21 – 25]. Un porcentaje destacable de estos métodos hace uso de medidas fotométricas, obteniéndose límites de detección próximos a ng/mL, mientras que para obtener menores límites de detección es necesario el uso de sistemas de detección quimioluminiscente [26] o bien, el uso de quelatos de europio (III) para formar el marcador [27, 28].

La utilización de NPs inorgánicas funcionalizadas para obtener marcadores en inmunoensayo es un campo relativamente nuevo y de gran proyección gracias a las versátiles propiedades físicas y químicas que presentan estos materiales, mejorando frecuentemente las características de los ensayos [29 – 31]. Entre las NPs inorgánicas, las SiO_2NPs dopadas son una opción muy útil debido a las propiedades anteriormente indicadas. Además, presentan la capacidad de encapsular una gran variedad de compuestos, que quedan protegidos frente a los agentes ambientales, gran área superficial y fácil funcionalización de su superficie. Estas propiedades han dado lugar a numerosos inmunoensayos para la determinación de macromoléculas y haptenos [32, 33]. Por ejemplo, se ha desarrollado un método para la determinación de *E. Coli* utilizando NPs dopadas con el complejo rutenio (II) tris(bipiridina) ($Ru(bpy)_3^{2+}$) inmovilizando el anticuerpo en la superficie de la NP, lo que ha permitido llegar a determinar una sola bacteria sin requerir la amplificación de la señal [34]. De manera similar, se ha determinado albúmina de suero bovino (BSA) mediante un ensayo de afinidad biotina-estreptavidina utilizando NPs dopadas con rodamina 6G para formar el marcador [35], así como la

determinación de α-fetoproteina (AFP) y antígeno de superficie de la hepatitis B (HBsAg) utilizando SiO_2NPs dopadas con fluoresceína [36, 37]. Estas SiO_2NPs también pueden encapsular otras especies como quelatos de terbio y europio, que han sido utilizados como marcadores para la determinación de HBsAg, antígeno carcinoembriónico (CEA) y antígeno prostático específico (PSA) [38 – 40]. De los ejemplos citados, se deduce que las SiO_2NPs dopadas han sido principalmente utilizadas en análisis clínico, pero su uso para desarrollar inmunoensayos aplicables al análisis de alimentos está claramente justificado.

En los inmunoensayos presentados en esta Memoria se utilizan SiO_2NPs dopadas con azul nilo para obtener el marcador, aplicándolas a la determinación de proteínas de soja (macromoléculas) y del antibiótico de uso veterinario monensín, cuya presencia en los alimentos de origen animal está regulada a nivel europeo. Los resultados obtenidos han demostrado que el uso de estas NPs proporciona algunas ventajas respecto a otros tipos de inmunoensayos, como son límites de detección más bajos y, en el caso del enzimoinmunoensayo, un menor número de etapas ya que no es necesaria la adición de un sustrato para medir la actividad de la enzima.

La incorporación de azul nilo a las SiO_2NPs ha tenido como objetivo el uso de medidas de fluorescencia a larga longitud de onda, las cuales proporcionan una selectividad espectral adecuada al eliminar las señales de fondo producidas por la matriz de la muestra. Como se ha indicado anteriormente, el uso de SiO_2NPs podría estar limitado por la posible pérdida de fluoróforo a través de la matriz de sílice. No obstante,

como ya se ha comentado, las SiO_2NPs dopadas con azul nilo muestran una excelente estabilidad debida a las interacciones electrostáticas del fluoróforo cargado positivamente con los grupos silanoles de la sílice.

A continuación se discuten los resultados obtenidos en los inmunoensayos desarrollados en esta Memoria.

- Determinación de proteínas de soja en alimentos mediante inmunoensayo heterogéneo.

En los últimos años, el consumo de alimentos enriquecidos con proteínas de soja se ha incrementado sustancialmente debido a los aspectos beneficiosos para la salud que se han descrito para estas proteínas, tales como un descenso del colesterol en sangre, prevención de enfermedades como el cáncer, la diabetes o la obesidad, así como protección frente a enfermedades que dañan el intestino o el riñón. Sin embargo, también se ha descrito que el consumo de estas proteínas puede originar reacciones alérgicas.

En esta Memoria se describe el desarrollo de un inmunoensayo heterogéneo competitivo para la determinación de proteínas de soja en muestras de alimentos utilizando SiO_2NPs dopadas con azul nilo para formar el marcador, estudiándose dos modalidades de inmunoensayo, con captura de analito y con captura de anticuerpo, como se esquematiza en las Figuras 4 y 5. Las NPs fueron unidas a proteínas de soja y a anticuerpos anti-proteína de soja para estudiar su viabilidad como trazadores en los dos formatos de inmunoensayo. El primero de ellos (Figura 4), con captura de analito, implica la inmovilización de anticuerpos anti-IgG de conejo en

la superficie de los pocillos seguida de la inmovilización de los anticuerpos anti-proteína de soja y el posterior uso de las NPs unidas a la proteína de soja como marcador. Se utilizaron anticuerpos anti-IgG debido al menor coste que suponen frente al uso de anticuerpos anti-proteína de soja, para recubrir la totalidad de los pocillos. El uso de dichos anticuerpos sobre los que se unen los anticuerpos frente al analito disminuye la concentración necesaria de estos últimos y, por lo tanto, el coste total del inmunoensayo. La superficie de los pocillos que forman la microplaca fue tratada con albúmina de suero bovino (BSA) a diferentes concentraciones para evitar uniones no específicas entre el marcador y los anticuerpos anti-IgG inmovilizados previamente. No obstante, los ensayos realizados demostraron que el procedimiento no fue suficientemente adecuado ya que, pese a dicho recubrimiento con BSA, aún se producían dichas uniones no específicas.

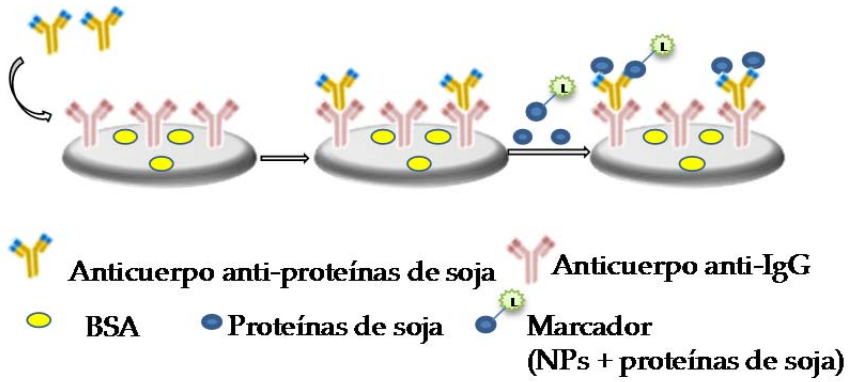

Figura 4: Inmunoensayo heterogéneo competitivo con captura de analito utilizando como marcador SiO_2NPs dopadas con azul nilo unidas a proteína de soja.

Para solucionar este problema, se optó por hacer uso del formato de inmunoensayo con captura de anticuerpo (Figura 5). Para ello, las proteínas de soja se inmovilizaron sobre la superficie de la microplaca, adicionando posteriormente BSA para evitar posibles uniones no específicas con el marcador, formado por anticuerpos anti-proteínas de soja marcados con las NPs. A continuación, tras adicionar la muestra y el marcador a los pocillos, se produjo el inmunoensayo basado en la competencia entre la proteína de soja presente en la muestra y la inmovilizada en la placa por enlazarse al marcador. Después de incubar, se elimina la mezcla de reacción, se lavan los pocillos para eliminar las especies no unidas a la superficie y se llevan a cabo las medidas de fluorescencia en la superficie de los pocillos.

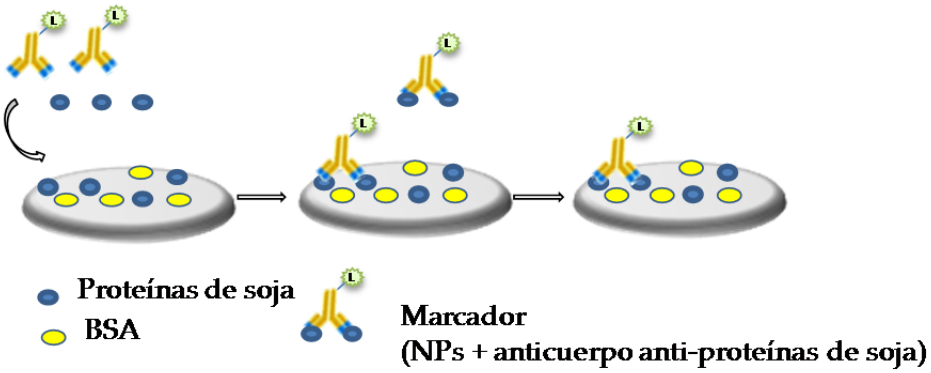

Figura 5: Inmunoensayo heterogéneo competitivo con captura de anticuerpo utilizando como marcador SiO_2NPs dopadas con azul nilo unidas a anticuerpos anti-proteínas de soja.

Las medidas se realizaron a λ_{ex} 620 y λ_{em} 680 nm, obteniéndose un intervalo lineal de 0,1 – 10 mg/L y un límite de detección de 0,05 mg/L, el

cual es 10 veces menor que el obtenido con el kit comercial ELISA [41]. Además, a diferencia del método ELISA, en este caso no es necesaria la adición de sustrato enzimático, reduciéndose así el número de etapas del ensayo y la duración del análisis.

La precisión, expresada como desviación estándar relativa, ensayada a dos concentraciones diferentes, 0,5 y 5 mg/L, fue de 9,6 % y 6,1% respectivamente. La selectividad del método depende principalmente de la selectividad de los anticuerpos anti-proteína de soja. De acuerdo con las especificaciones indicadas por el proveedor de estos anticuerpos, estos presentan cierta reactividad cruzada con extractos de harina de arroz y ovoalbúmina tras su tratamiento con urea caliente. En cambio, no interaccionan con extractos de carne, maíz o caseínas, así como arroz o patata. Además, en un estudio previo en el que se utiliza el mismo anticuerpo anti-proteína de soja, se describe que las concentraciones de BSA, ϒ-globulinas, mioglobina y hemoglobina toleradas son 80 veces mayores que la concentración de analito [42].

El método fue aplicado al análisis de muestras de leche, yogur y zumo de frutas que contenían soja. Estas muestras también fueron analizadas con un kit comercial ELISA [41] y, en ambos casos, las muestras fueron sometidas a un tratamiento de desnaturalización-renaturalización de acuerdo con las recomendaciones procedentes del distribuidor de los anticuerpos anti-proteína de soja. Los resultados obtenidos se muestran en la Tabla 2, los cuales fueron sometidos al test de la *t* por parejas con un nivel de confianza del 95 %, sin encontrarse diferencias estadísticamente significativas entre el método propuesto y el kit comercial.

Tabla 2. Determinación de proteínas de soja en muestras de alimentos

Muestra	Método Propuesto[a,b]	Kit comercial ELISA[a,b]
Leche de soja	74 ± 6	84 ± 3
Zumo de fruta y soja	8,4 ± 0,7	10,5 ± 0,3
Yogur de soja	64 ± 4	60 ± 3

[a] Media ± DE (n = 3)
[b] Unidades: leche de soja en g/L; zumo de frutas y soja y yogur de soja en g/Kg

Para llevar a cabo el estudio de recuperaciones, se añadieron tres cantidades diferentes de proteínas de soja a las muestras, obteniéndose unos valores de recuperación entre 81,5 % y 111,0 %, como se muestra en la Tabla 3, lo que pone de manifiesto la utilidad del método para realizar estos análisis.

Tabla 3. Recuperaciones de proteínas de soja de muestras de alimentos

Muestra	Añadido[a, b]	Encontrado[a, b]	Recuperación (%)
Leche de soja	24	27 ± 2	111,0
	72	69 ± 4	95,7
	123	110 ± 10	89,4
Zumo de frutas y soja	2,7	2,2 ± 0,2	81,5
	8,1	7,7 ± 0,6	95,1
	13,5	12 ± 1	88,9
Yogur de soja	23	21 ± 2	91,3
	65	61 ± 4	93,2
	113	95 ± 7	84,1

[a] Media ± DE (n=3)
[b] Unidades: leche de soja en g/L; zumo de frutas y soja y yogur de soja en g/Kg

- Determinación de monensín en muestras de leche mediante inmunoensayo heterogéneo.

El monensín es un antibiótico de uso veterinario con actividad antibacteriana y coccidiostática, usado tradicionalmente para prevenir la coccidiosis en pollos [43]. Este antibiótico es utilizado también como promotor del crecimiento, ya que previene enfermedades que retrasan el crecimiento de los pollos como diarreas hemorrágicas y pérdidas de peso asociadas. Aunque el uso de promotores del crecimiento comenzó a prohibirse a partir de 2006, algunos de estos aún pueden ser administrados bajo regulación de la Unión Europea [44]. Además, el tratamiento con monensín ha sido ampliado por la Unión Europea a terneros, estableciéndose límites máximos de residuo para este antibiótico.

La preocupación por la seguridad alimentaria ha llevado a buscar y desarrollar nuevos métodos analíticos de "screening" y confirmatorios para detectar la presencia de residuos de antibióticos en alimentos, los cuales, al llegar al consumidor, pueden dar lugar a un incremento de la resistencia bacteriana a antibióticos.

En esta Memoria se ha presentado un método que constituye el primer inmunoensayo para la determinación de monensín utilizando SiO_2NPs dopadas con azul nilo para formar el marcador. Se ha demostrado su utilidad para mejorar las características analíticas, tales como el límite de detección, respecto a los inmunoensayos descritos anteriormente para la determinación de este fármaco utilizando marcadores enzimáticos [22, 45 – 48].

Como se ha indicado anteriormente, el uso de SiO_2NPs dopadas con azul nilo puede mejorar los límites de detección gracias a la selectividad espectral que presentan los LWFs ya que se minimiza la señal de fondo procedente de la matriz de la muestra. Además, la excelente estabilidad del fluoróforo encapsulado en las NPs frente a agentes ambientales y a la radiación excitante, evitando su fotodescomposición, así como la estabilidad temporal de estas NPs dopadas, justifican la utilización de este nanomaterial para formar marcadores y aplicarlos en inmunoensayos. Otra ventaja del método propuesto es el uso de microplacas con pocillos de 100 μL, a diferencia de las microplacas tradicionales con pocillos de 300 μL. De esta manera, se reducen los volúmenes de reactivos utilizados durante el desarrollo del método, disminuyéndose así el coste total del inmunoensayo y los volúmenes de residuos generados. Se utilizan este tipo de placas ya que las medidas se realizan en superficie sólida y el fondo de estos pocillos está a una mayor altura que en las placas tradicionales, de forma que la distancia entre la superficie sólida y el detector disminuye, minimizando pérdidas de señal luminiscente y mejorando la sensibilidad.

Al igual que en el apartado anterior, se estudiaron dos posibles formatos competitivos para este inmunoensayo heterogéneo, con captura de anticuerpo y con captura de analito. El primero de ellos se basó en la inmovilización en la microplaca de un conjugado BSA-monensín y un marcador formado por NPs sobre las que se inmovilizó el anticuerpo anti-monensín. En cambio, el segundo formato necesitó un marcador formado por NPs-monensín, sintetizado via carbodiimida usando EDAC

(clorhidrato de N-(3-dimetilaminopropil)-N´-etilcarbodiimida), la inmovilización del anticuerpo anti-IgG de oveja sobre los pocillos y la posterior unión del anticuerpo anti-monensín sobre esta superficie sólida. En ambos ensayos se obtuvo una diferencia apreciable entre los valores de intensidad de fluorescencia obtenidos en ausencia y en presencia (0,2 μg/L) de monensín. Sin embargo, esta diferencia de señal fue tres veces mayor utilizando el formato de captura de anticuerpo, por lo que se seleccionó este formato para la determinación de monensín en muestras de leche.

El método desarrollado presenta un intervalo lineal dinámico de 0,05 – 5 μg/L y unos límites de detección y cuantificación de 0,015 y 0,05 μg/L, respectivamente, que corresponden a 0,12 y 0,40 μg/Kg en muestras de leche. Este último valor es 5 veces menor que el límite máximo de residuo (MRL) establecido por la Comisión de Regulación de la Unión Europea en la normativa 37/2010/EC en muestras de leche. Además, el límite de detección es cuatro veces menor que el descrito en el kit ELISA con detección quimioluminiscente [32]. La precisión, expresada como desviación estándar relativa, fue ensayada a dos concentraciones de monensín, 0,2 y 1 μg/L, obteniéndose unos porcentajes de 5,8 % y 4,0 %, respectivamente.

El método se aplicó al análisis de muestras de leche entera, semi-desnatada y desnatada, realizando un tratamiento previo sencillo basado en una etapa de desproteinización y la posterior evaporación del disolvente. Para validar el método se llevó a cabo un estudio de recuperaciones (Tabla 4), obteniendo valores entre 83,3 % y 107,5 %, lo que demuestra su utilidad para el análisis de estas muestras.

Tabla 4. Recuperaciones obtenidas para monensín añadido a muestras de leche

Muestra	**Monensín**		
	Añadido[a, b] (μg/Kg)	Encontrado[a, b] (μg/Kg)	Recuperación (%)
Leche desnatada	1,5	1,6 ± 0,1	106,7
	2	1,96 ± 0,09	98,0
	4	4,1 ± 0,2	102,5
Leche semi-desnatada	1,5	1,5 ± 0,1	100,0
	2	2,0 ± 0,1	100,0
	4	3,4 ± 0,3	85,0
Leche entera	1,5	1,25 ± 0,07	83,3
	2	1,7 ± 0,1	85,0
	4	4,3 ± 0,3	107,5

[a] Media ± DE (n=3)

En resumen, los estudios realizados utilizando SiO_2NPs dopadas con un LWF para obtener los correspondientes marcadores, ponen de manifiesto su aplicabilidad para la determinación de macromoléculas (proteínas) y moléculas pequeñas (antibióticos) en análisis de alimentos. Se consiguen menores límites de detección que en ELISA y se evita la etapa final para la medida de la actividad de la enzima. Asimismo, los métodos propuestos han contribuido a expandir el uso de la nanotecnología en esta área analítica.

2. Nuevas estrategias para la determinación de antioxidantes en alimentos

Los procesos de oxidación que se producen en el organismo implican la formación de radicales libres responsables del desarrollo de algunas enfermedades, tales como enfermedades cardiovasculares, Alzheimer y cáncer. Este fenómeno redox es producido por especies reactivas de oxígeno (ROS), capaces de dañar las membranas celulares, aunque este efecto puede ser reducido por la ingesta de compuestos antioxidantes. La capacidad antioxidante de algunos alimentos viene dada principalmente por la presencia de polifenoles, como los flavonoides, y de las vitaminas C y E, entre otros [49].

En esta Memoria se ha desarrollado un método para la determinación de la capacidad antioxidante de algunos alimentos, en el que se demuestra la utilidad de medidas de fluorescencia a larga longitud de onda, y otro método para la determinación de polifenoles en el que se propone el uso de nanomateriales como activadores de la enzima laccasa. A continuación, se discuten las características de estos métodos y su aplicabilidad.

- Determinación fluorimétrica a larga longitud de onda de la capacidad antioxidante de alimentos utilizando azul nilo como reactivo

Desde el punto de vista analítico, existen dos tipos de métodos para la determinación de la capacidad antioxidante de los alimentos. El primer grupo implica reacciones de transferencia de electrones, las cuales pueden

seguirse mediante algún cambio de color o de fluorescencia detectable en el medio de reacción. El segundo grupo se basa en reacciones de transferencia de protones, en las que el antioxidante y un sustrato compiten por los radicales libres generados. El método ORAC (capacidad de absorción de radicales de oxígeno), perteneciente a este segundo grupo, utiliza un generador de radicales libres que ataca directamente a un cromóforo o a un fluoróforo, experimentando éstos una disminución de su absorbancia o de su fluorescencia, respectivamente. Para este ensayo se han utilizado cromóforos, tales como el rojo de pirogalol [50], y en mucha mayor extensión diferentes tipos de fluoróforos tales como la β-ficoeritrina y la fluoresceína [51 – 57]. A pesar de la buena sensibilidad que ofrecen estos compuestos, el desplazamiento Stokes que muestran es bastante estrecho (alrededor de 27 nm), lo cual favorece los fenómenos de dispersión de la radiación. Además, el coste de la β-ficoeritrina es relativamente elevado y suele sufrir fenómenos de fotodescomposición, mientras que la emisión de la fluoresceína normalmente solapa con las señales de fondo procedentes de la matriz de la muestra. El uso de LWFs puede evitar estos inconvenientes, aunque su potencial en ensayos de actividad antioxidante no ha sido investigado hasta ahora.

En esta Memoria se describe un método analítico para la determinación de la capacidad antioxidante de algunos alimentos mediante el ensayo ORAC utilizando azul nilo como reactivo fluorescente, diclorhidrato de 2,2'-azobis(2-amidinopropano) (AAPH) como generador de radicales libres, y ácido 6-hidroxi-2,5,7,8-tetrametilcroman-2-carboxílico (Trolox) como analito de referencia. Las medidas de fluorescencia se

llevaron a cabo en modo cinético registrando su variación con el tiempo y utilizando como parámetro analítico el área neta bajo la curva normalizada, $AUC_{neta} = (AUC_{muestra} - AUC_{blanco})/AUC_{blanco}$), obtenida para diferentes concentraciones de analito.

Como se ha comentado anteriormente, los fluoróforos tradicionalmente utilizados para este tipo de ensayos han sido la β-ficoeritrina y la fluoresceína, los cuales ven inhibida su pérdida de fluorescencia en este tipo de ensayos en presencia de compuestos antioxidantes, pero su utilización presenta las limitaciones ya indicadas. Con objeto de evitar estas limitaciones, se estudió la posibilidad de usar otros tipos de fluoróforos que emitan a larga longitud de onda, como son las oxacinas y las tiacinas, siendo el azul nilo, azure A y azure B los fluoróforos seleccionados. Para llevar a cabo este estudio, se registraron las curvas cinéticas para los tres fluoróforos en presencia y ausencia de Trolox. Como puede observarse en la Figura 6, en los tres casos existen diferencias entre la curva del blanco y la del estándar, aunque se obtuvo una mayor diferencia con el fluoróforo azul nilo. La influencia del pH fue estudiada en el intervalo de 4 – 11, utilizando las disoluciones reguladoras acetato, fosfato, borato y carbonato, a una concentración de 0,075 M, para mantener constante el valor de pH deseado.

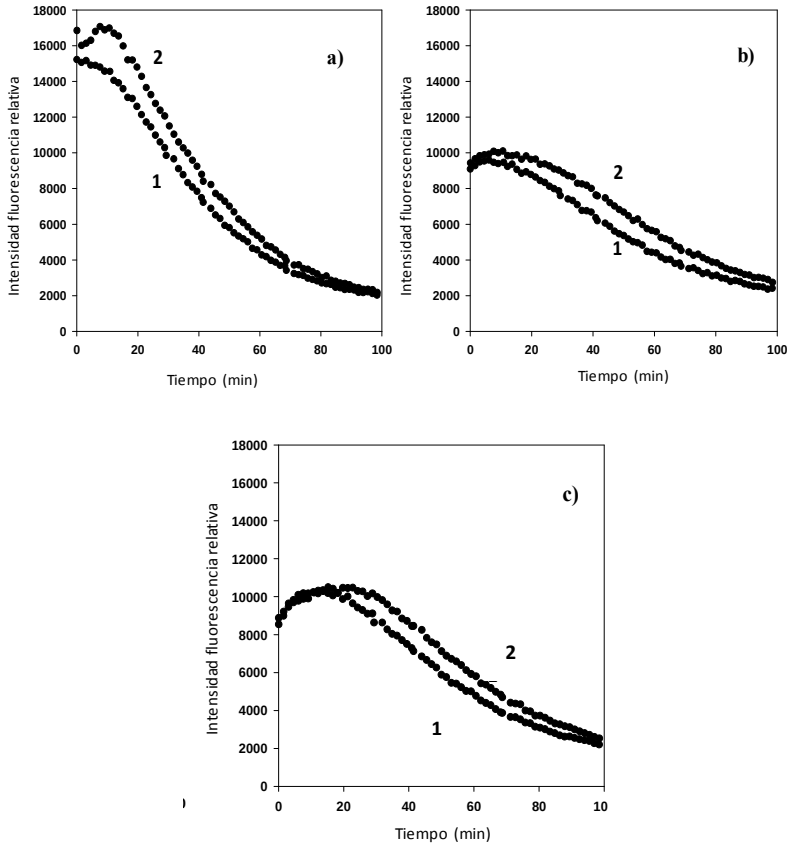

Figura 6: Curvas obtenidas para el ensayo ORAC con los fluoróforos (a) azul nilo, (b) azure A, y (c) azure B: (1) blanco y (2) en presencia de Trolox (2 μM).

Como puede observarse en la Figura 7, el área bajo la curva normalizada no es apreciable para valores inferiores a 5,8 y superiores a 8, obteniéndose los mejores resultados en el intervalo de 6 a 7. El comportamiento del sistema a valores de pH bajos puede deberse al pK_a del Trolox (3,89), cuya solubilidad disminuye al aproximarse a este valor.

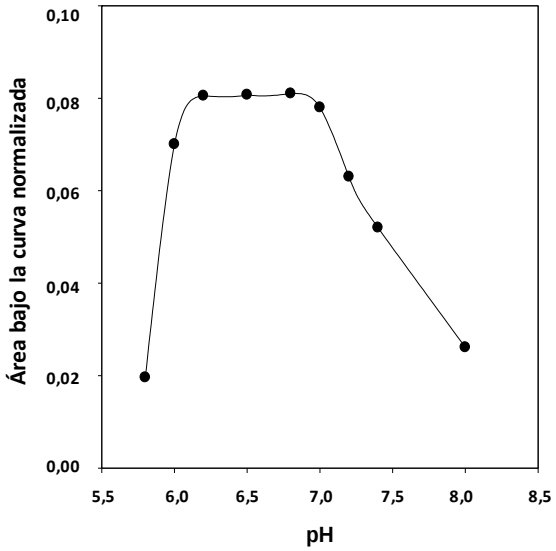

Figura 7. Influencia del pH en el método ORAC-azul nilo. Condiciones experimentales: [azul nilo] = 120 nM; [tampón] = 0,075 M; [AAPH] = 0,024 M, [Trolox] = 2 μM y temperatura = 27 ºC.

La influencia de la concentración del fluoróforo se estudió en el intervalo de 60 a 370 nM (Figura 8), encontrándose que el sistema era prácticamente independiente de esta variable en el intervalo de 80 a 130 nM, por lo que se eligió una concentración óptima de fluoróforo de 89 nM. Cabe indicar que se estudió la posibilidad de utilizar SiO_2NPs dopadas con azul nilo como alternativa al uso del fluoróforo en disolución, pero los resultados no fueron satisfactorios, como era previsible, debido a la protección que ejercen las NPs sobre la fluorescencia del azul nilo encapsulado. Se evaluó la concentración de AAPH, en un intervalo de 6 a 24 mM, encontrándose que las diferencias del área bajo la curva entre el

blanco y en presencia de una concentración determinada de Trolox disminuyen al aumentar la concentración de AAPH. Sin embargo, las curvas obtenidas a bajas concentraciones de AAPH mostraron escasa reproducibilidad, por lo que se optó por seleccionar una concentración de AAPH de 12 mM como óptima.

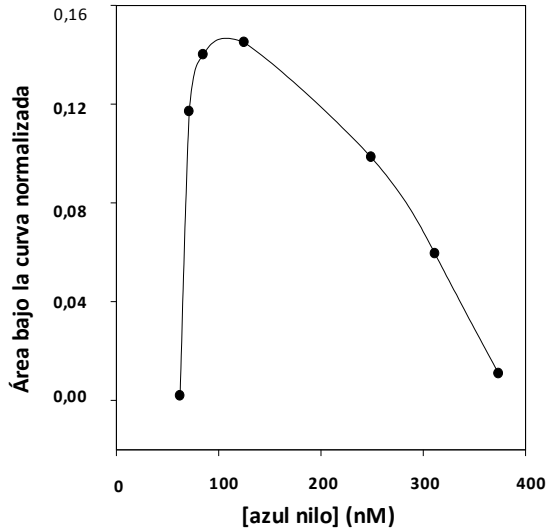

Figura 8. Influencia de la concentración de azul nilo sobre el método ORAC-azul nilo. Condiciones experimentales: [AAPH] = 0,012 M; [Trolox] = 2 μM; pH = 6,9; [fosfato] = 0,085 M; y temperatura = 37 ^{o}C.

El intervalo lineal dinámico obtenido fue de 0,8 – 8 μM de Trolox y el límite de detección fue de 0,45 μM, el cual es menor o similar a los obtenidos en otros métodos ORAC donde se utiliza la fluoresceína como fluoróforo. La precisión del método se ensayó a dos concentraciones

diferentes de Trolox, 1 y 5 μM, obteniéndose una desviación estándar relativa de 5,6 % y 2,9 %, respectivamente.

El método propuesto se aplicó al análisis de muestras de diferentes tipos de vinos y zumos de frutas, comparando los resultados con los obtenidos en el método ORAC convencional utilizado como método de referencia. El tratamiento de las muestras fue igual para ambos métodos, siendo sólo necesario ajustar el pH hasta la neutralidad y diluir las muestras hasta adecuar la concentración de antioxidante al intervalo lineal dinámico de la curva de calibrado.

En la Tabla 5 se muestran los resultados obtenidos con ambos métodos. El ensayo estadístico de la *t* por parejas demostró que no existían diferencias significativas entre ellos, lo cual confirma la utilidad del método propuesto en esta Memoria.

Tabla 5. Capacidad antioxidante de muestras de alimentos analizadas por los métodos ORAC-azul nilo y ORAC-fluoresceína

Muestra	**ORAC-azul nilo[a,b]**	**ORAC-fluoresceína[a,b]**
Vino blanco (Manzanilla)	1,50 ± 0,09	1,3 ± 0,2
Vino semi-seco	7,7 ± 0,9	4,4 ± 0,4
Vino tinto	15,3 ± 0,4	10,4 ± 0,9
Zumo de melocotón	2,222 ± 0,001	1,93 ± 0,09
Zumo de piña	2,7 ± 0,3	2,399 ± 0,006
Zumo de manzana	2,7 ± 0,3	3,5 ± 0,4

[a]Media ± DE (n=3)
[b]Expresada como mili-equivalentes de Trolox en la muestra

Se llevó a cabo un estudio de recuperaciones para validar el método mediante la adición de tres concentraciones diferentes de Trolox a cada una de las muestras analizadas y sometiéndolas al mismo tratamiento mencionado anteriormente. En la Tabla 6 se muestran los resultados obtenidos en el estudio de recuperación, oscilando estos resultados entre 72,7 % y 113,6 %, con unos valores medios de 92,0 % y 92,9% para muestras de vinos y de zumos, respectivamente. Esta validación interna confirma la utilidad del método desarrollado para el análisis de muestras reales.

Tabla 6. Valores de recuperación obtenidos para las diferentes muestras analizadas

	Estudio de recuperaciones		
Muestra	**Añadido[a]**	**Encontrado[a,b]**	**Recuperación (%)**
Vino blanco	2,2	2,0 ± 0,2	92,0
	8,9	6,7 ± 0,9	75,2
	11,1	9,2 ± 0,8	82,9
Vino semi-seco	4,4	3,6 ± 0,2	81,8
	8,8	8,1 ± 0,3	92,1
	13,2	12,9 ± 0,6	97,0
Vino tinto	17,8	18 ± 2	101,1
	35,6	38 ± 4	106,7
	44,4	44 ± 4	99,1
Zumo de melocotón	2,2	2,1 ± 0,1	95,5
	4,4	3,5 ± 0,4	79,5
	5,5	4,3 ± 0,2	78,2
Zumo de piña	2,2	2,5 ± 0,2	113,6
	4,4	4,5 ± 0,3	102,3
	5,5	5,8 ± 0,4	105,5
Zumo de manzana	4,4	3,2 ± 0,2	72,7
	8,8	7,9 ± 0,5	89,6
	11,1	11 ± 1	99,1

[a]Unidades en mili-equivalentes de Trolox en la muestra
[b]Media ± DE (n=3)

Los resultados obtenidos muestran la utilidad de la fluorescencia a larga longitud de onda para la determinación de la capacidad antioxidante de alimentos utilizando el fluoróforo azul nilo. El uso de este reactivo en lugar de otros fluoróforos previamente utilizados con este propósito, como son la fluoresceína y la β-ficoeritrina, supone una alternativa para reducir posibles señales de fondo procedentes de la matriz de la muestra, las cuales pueden aparecer al excitar a longitudes de onda más cortas. Además, el relativamente ancho desplazamiento Stokes que presenta el azul nilo minimiza los efectos de dispersión de la radiación, muy comunes al usar fluoróforos con desplazamientos Stokes relativamente estrechos. Por último, la pérdida de fluorescencia debida a la fotodescomposición del azul nilo es menor que en el caso de la β-ficoeritrina, siendo también su coste inferior.

- Determinación automática de polifenoles en vinos utilizando laccasa y nanopartículas de óxido de terbio

Los polifenoles constituyen un importante grupo de compuestos antioxidantes naturales presentes en alimentos que, tras numerosos estudios clínicos, han mostrado su eficacia para la prevención de algunas enfermedades crónicas. Como se ha descrito en el apartado anterior, se ha desarrollado una gran diversidad de métodos analíticos cromatográficos [58, 59] y electroforéticos [60, 61] para la determinación de estos antioxidantes naturales. Sin embargo, debido al elevado número de compuestos fenólicos que pueden encontrarse en muestras alimenticias, es frecuente el uso de métodos analíticos que determinan el contenido

fenólico total así como la capacidad antioxidante total. Estos parámetros han sido ampliamente determinados mediante métodos fotométricos o fluorimétricos haciendo uso de generadores de radicales libres o bien reacciones enzimáticas, que compiten con los antioxidantes con el fin de inhibir la pérdida de fluorescencia o absorbancia que tendría lugar en ausencia de los mismos [56, 62 – 67].

La laccasa es una enzima feniloxidasa que ha sido utilizada para la determinación del contenido fenólico total y la capacidad antioxidante, utilizando diferentes condiciones experimentales. Como ya se ha comentado anteriormente en esta Memoria, esta enzima cataliza la oxidación de compuestos fenólicos a quinonas o radicales mediante reducción del oxígeno disuelto en el medio, lo cual ha sido utilizado para el desarrollo de sensores amperómetricos [68 – 70] así como métodos con detección fotométrica [71 – 73] y fluorimétrica [74].

En esta Memoria se muestra la utilidad analítica del uso combinado de nanopartículas de óxido de terbio (Tb_4O_7NPs), laccasa, y el fluoróforo 8-hidroxipireno-1,3,6-trisulfonato trisódico (HPTS) para la determinación de polifenoles en muestras de vino. Al igual que en el método expuesto en el apartado anterior, las medidas de fluorescencia se llevaron a cabo en modo cinético registrando su variación con el tiempo y utilizando como parámetro analítico el área bajo las curvas obtenidas a diferentes concentraciones de ácido gálico, utilizado como estándar de calibración.

En primer lugar, se investigó el comportamiento de diversos fluoróforos como posibles sustratos de la laccasa. Con tal fin se ensayó la capacidad de Styryl 7, 2-Di-1-ASP, azure B, azul de toluidina, azul nilo, fluoresceína y HPTS para competir con los compuestos fenólicos por los

sitios activos de la enzima. Aunque el verde de indocianina ha sido descrito anteriormente como sustrato para la laccasa [74], no pudo ensayarse debido a que el lector de placas utilizado no tiene capacidad para medir la fluorescencia a la larga longitud de onda que presenta este compuesto. El estudio realizado demostró que sólo el fluoróforo HPTS experimentaba una disminución relativamente rápida y notable de su fluorescencia en presencia de la laccasa.

Como puede observarse en la Figura 9, el fluoróforo HPTS tiene un grupo fenólico en su estructura, lo cual puede explicar este comportamiento, dando lugar a su oxidación enzimática por el oxígeno disuelto.

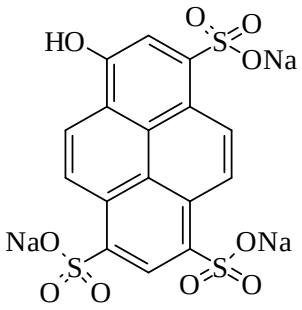

Figura 9. Estructura del fluoróforo 8-hidroxipireno-1,3,6-trisulfonato trisódico (HPTS).

Con objeto de mejorar las características del sistema, se estudió el posible efecto activador de diferentes tipos de NPs en la reacción catalizada por la laccasa. Para este estudio se utilizaron NPs de diamante, Eu_2O_3, Tb_4O_7, Ag y magnéticas recubiertas de oro, en el intervalo de concentraciones 0,1 – 2 mg/mL, encontrándose que sólo las Tb_4O_7NPs proporcionaban un aumento notable de la velocidad de reacción del sistema. Como puede observarse en la Figura 10, las áreas bajo la curva en presencia y en ausencia de ácido gálico fueron menores al utilizar estas

NPs, lo cual proporciona un aumento en la velocidad de muestreo. Además, se estudió la influencia de estas NPs sobre la intensidad de fluorescencia del fluoróforo en ausencia de laccasa, permaneciendo dicha fluorescencia constante con el tiempo. En cambio, las NPs de diamante y las magnéticas recubiertas de oro dieron lugar a una pérdida de fluorescencia del fluoróforo en ausencia de laccasa, las AgNPs inhibían el efecto catalítico de la laccasa y las Eu_2O_3NPs no alteraban las características del sistema.

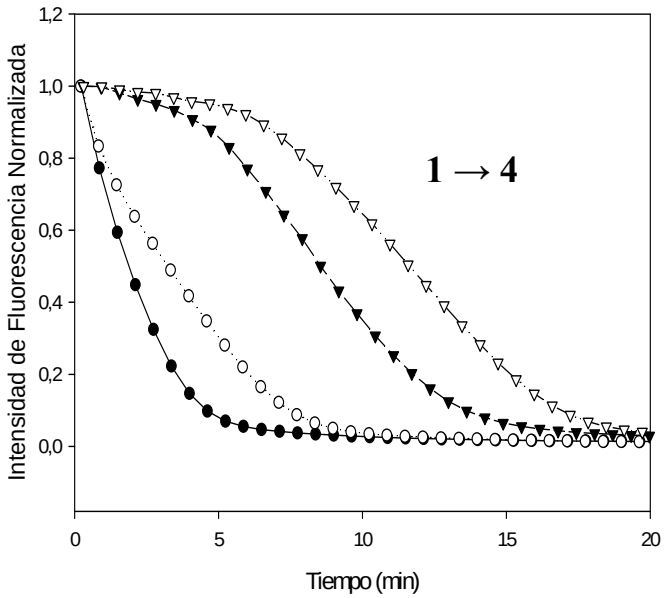

Figura 10. Curvas cinéticas obtenidas para el sistema HPTS-laccasa en ausencia (curvas 1 y 2) y en presencia (curvas 3 y 4) de 2 μM de ácido gálico, y en presencia (curvas 1 y 3) y en ausencia (curvas 2 y 4) de 1 mg/mL de Tb_4O_7NPs. [HPTS] = 10 μM, [laccasa] = 1 U/mL, pH = 7,0, [fosfato] = 0,4 M, temperatura = 37 ^{0}C.

También se estudió la posibilidad de utilizar iones Tb(III) en lugar de las Tb_4O_7NPs para aumentar la velocidad de reacción del sistema. Con

este fin se utilizaron concentraciones equivalentes de Tb(III) a las utilizadas en forma de NPs, obteniéndose áreas bajo la curva netas menores, lo cual ratifica la utilidad de estas Tb_4O_7NPs como activadoras en el sistema enzimático.

Las variables implicadas en el sistema fueron optimizadas mediante el método univariante utilizando el área bajo la curva neta (AUC) como parámetro analítico. Sin embargo, fue necesario alcanzar una solución de compromiso entre este parámetro y el tiempo necesario para llevar a cabo la medida, con el fin de obtener una sensibilidad y una duración del ensayo adecuadas.

La influencia del pH en el sistema se estudió entre 4,0 – 9,0 utilizando diferentes disoluciones reguladoras, obteniéndose que la intensidad de fluorescencia prácticamente desaparecía a valores de pH ácidos, mientras que dicha señal era muy elevada a pH 8,0 – 9,0, pero la laccasa no presentaba actividad sobre el fluoróforo a estos valores de pH. Sin embargo, a valores próximos a la neutralidad, 7,0 – 7,5, la intensidad de fluorescencia del HPTS era bastante elevada y se inhibía en presencia de la enzima. Por lo tanto, el valor de pH seleccionado para desarrollar el método fue 7,0, utilizando una disolución de fosfato, de concentración 0,4 M, para ajustar el pH. El estudio de la influencia de la concentración de HPTS en el sistema demostró que ésta era independiente de esta variable en el intervalo de concentraciones 8 - 12 μM, seleccionándose el valor intermedio, 10 μM, como concentración óptima.

La actividad de la laccasa y la concentración de Tb_4O_7 NPs son dos variables críticas que afectan notablemente al valor neto de AUC y a la velocidad de reacción. Ambas variables fueron estudiadas en los intervalos

de 0,5 – 2 U/mL y 0,2 – 2 mg/mL para la actividad de la laccasa y la concentración de NPs, respectivamente. Para valores elevados de ambas variables, el aumento de la velocidad de reacción era muy considerable, proporcionando AUC netas muy pequeñas, lo cual iba en detrimento de la sensibilidad del método. En cambio, para valores muy bajos de estas variables, estas áreas netas, y por ende, la sensibilidad del método, aumentaban considerablemente, pero la duración del ensayo era excesivamente larga. Por lo tanto, los valores seleccionados como óptimos, con el fin de obtener valores adecuados de sensibilidad con tiempos de ensayo relativamente cortos, fueron 1 U/mL de laccasa y 1 mg/mL de NPs.

Como se ha descrito anteriormente, el parámetro analítico utilizado en este método fue el AUC, obtenida a partir de las curvas cinéticas normalizadas para diferentes concentraciones de ácido gálico. La Figura 11 muestra las curvas registradas a λ_{ex} 450 nm y λ_{em} 535 nm, bajo las condiciones experimentales óptimas.

El intervalo lineal dinámico de la curva de calibrado fue 0,5 – 12 μM de ácido gálico, obteniéndose un límite de detección de 0,14 μM, el cual es unas tres veces menor que el obtenido (0,4 μM) en ausencia de Tb_4O_7NPs. Esta diferencia demuestra el efecto positivo de las Tb_4O_7NPs, no sólo en la velocidad de reacción, sino también en el límite de detección. El límite de detección obtenido en presencia de Tb_4O_7NPs es menor que los límites de detección descritos utilizando biosensores amperométricos, los cuales oscilaban entre 0,19 y 50 μM [69, 70]. Aunque se ha obtenido un límite de detección de 0,04 μM para ácido gálico utilizando verde de indocianina [74], dicho método implica el análisis secuencial de cada muestra, lo que conlleva una velocidad de muestreo mucho menor. La

precisión del método, expresada como desviación estándar relativa, fue ensayada para dos concentraciones diferentes de ácido gálico, 0,7 y 5 μM, obteniéndose valores de 6,3 y 2,5 %, respectivamente.

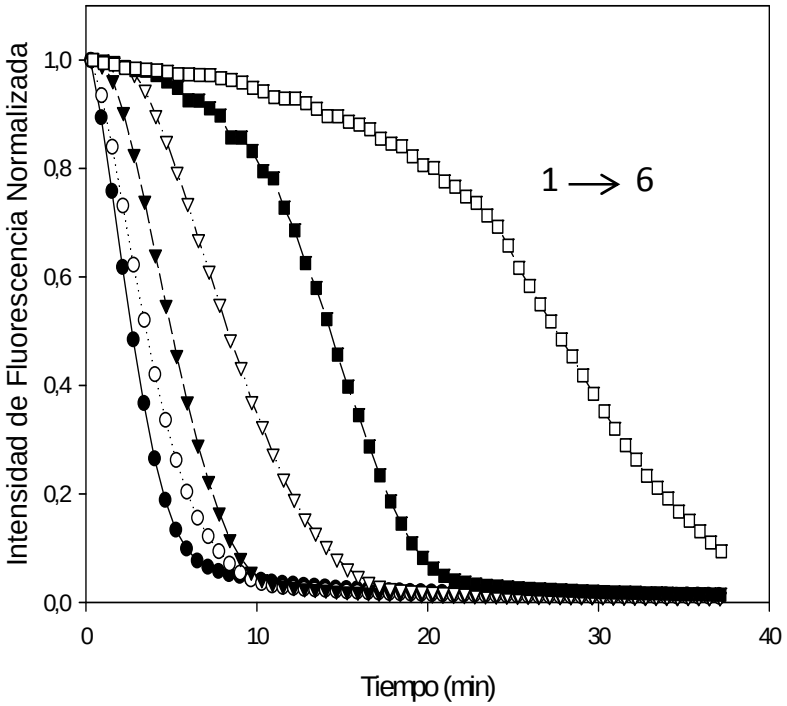

Figura 11. Curvas cinéticas obtenidas con diferentes concentraciones de ácido gálico: (1) 0 μM, (2) 0,5 μM, (3) 1 μM (4) 2 μM (5) 5 μM y (6) 10 μM. Condiciones experimentales: [HPTS] = 10 μM, [laccasa] = 1 U/mL, [NPs] = 1 mg/mL, pH = 7,0, [fosfato] = 0,4 M, temperatura = 37 ^{o}C.

Para aplicar el método al análisis de muestras reales, previamente se realizó un estudio de selectividad, comprobando la influencia de otras sustancias reductoras no fenólicas que pueden estar presentes en las

muestras de vinos utilizadas para demostrar la aplicabilidad del método. La Tabla 7 recoge los resultados obtenidos para varios posibles interferentes. El principal interferente fue el ácido ascórbico cuya concentración tolerada fue igual a la concentración molar del analito. Sin embargo, hay que tener en cuenta que la concentración máxima de ácido ascórbico que puede hallarse como aditivo en vinos es de 0,85 mM [75], menor que la concentración de polifenoles que normalmente existe en vino. La concentración de sulfito tolerada es 20 veces mayor que la concentración de analito y, aunque los sulfitos pueden ser eliminados de la muestra mediante un tratamiento previo [70], no es necesaria dicha etapa ya que la presencia de sulfitos está regulada en función del contenido total de sustancias reductoras [76].

Tabla 7. Influencia de algunos agentes reductores en el método propuesto para la determinación de antioxidantes fenólicos a una concentración de ácido gálico de 2 μM

Compuestos	**Relación maxima tolerada interferente/analito***
Ácido málico	100
Ácido cítrico	100
Sacarosa	100
Glucosa	25
Sulfito sódico	20
Ácido ascórbico	1

*La concentración máxima ensayada fue 100 veces mayor que la del analito

El método propuesto fue aplicado al análisis de muestras de vino tinto, blanco y dulce, las cuales solo requirieron como tratamiento previo la dilución adecuada para que la concentración de polifenoles presente al ser

analizadas estuviera dentro del intervalo lineal dinámico del método, utilizando ácido gálico como estándar y la AUC neta como parámetro analítico. La Tabla 8 muestra el contenido en polifenoles de las muestras analizadas mediante el método propuesto y el método de Folin-Ciocalteu, el cual suele ser considerado como método de referencia.

Tabla 8. Concentración de antioxidante (expresado como equivalente milimolar de ácido gálico)

Muestra	**Método propuesto[a,b]**	**Método Folin-Ciocalteu[a,b]**
Vino tinto (Rioja)	7,0 ± 0,4	11,5 ± 0,1
Vino tinto (Cuenca)	9,5 ± 0,5	14,04 ± 0,18
Vino blanco (Rueda)	1,00 ± 0,06	1,92 ± 0,04
Vino blanco (Valdepeñas)	1,00 ± 0,03	2,028 ± 0,005
Vino dulce (Montilla)	1,27 ± 0,09	3,64 ± 0,05

[a]Media ± DE (n = 3)
[b]Unidades: equivalente mM de ácido gálico

Como puede observarse en la Tabla 8, los valores obtenidos mediante el método de Folin-Ciocalteu son mayores que los obtenidos por el método de la laccasa, lo que se atribuye a la capacidad de este método para reaccionar con sustancias reductoras no fenólicas. Los valores obtenidos por el nuevo método son similares a los descritos haciendo uso de otros métodos para el análisis de este tipo de muestras [68, 69].

Se llevó a cabo un estudio de recuperaciones para validar el método mediante la adición de tres concentraciones diferentes de ácido gálico a cada una de las muestras analizadas y sometiéndolas al método

determinativo propuesto. Como puede observarse en la Tabla 9, los porcentajes de recuperación obtenidos oscilaron entre 81,0 % y 108,3 %, con unos valores medios de 90,9 %, 92,4 % y 99,5 % para las muestras de vino tinto, blanco y dulce, respectivamente.

Tabla 9. Valores de recuperación para las muestras de vino analizadas.

Muestra	Añadido[a]	Encontrado[a,b]	Recuperación (%)
Vino tinto (La Rioja)	4	4,3 ± 0,5	108,3
	12	10,0 ± 0,5	84,1
	20	16 ± 1	81,0
Vino tinto (Cuenca)	4	3,2 ± 0,2	80,0
	12	11,7 ± 0,3	97,4
	20	18,9 ± 0,8	94,5
Vino blanco (Rueda)	0,25	0,24 ± 0,03	97,2
	0,75	0,77 ± 0,04	102,8
	1,25	1,08 ± 0,03	86,7
Vino blanco (Valdepeñas)	0,25	0,23 ± 0,03	92,0
	0,75	0,70 ± 0,04	92,2
	1,25	1,0 ± 0,1	83,3
Vino dulce (Córdoba)	1	1,01 ±0,09	101,5
	3	3,0 ± 0,3	102,0
	5	4,7 ± 0,3	95,0

[a]Media ± DE (n = 3)
[b]Unidades: equivalentes mM de ácido gálico

Los resultados obtenidos demuestran la utilidad del uso combinado de la enzima laccasa, Tb_4O_7NPs y el fluoróforo HPTS para la determinación de polifenoles en muestras de vino. La presencia de laccasa

y NPs permite aumentar la velocidad de muestreo del método y mejorar los valores de sensibilidad, siendo estos superiores a los obtenidos en la mayoría de los métodos descritos anteriormente [68, 69]. Como aspecto más novedoso de la investigación realizada, cabe destacar que se describe por primera vez el efecto activador de las Tb_4O_7NPs en un sistema enzimático. Además, el uso del lector automático de microplacas, permite el procesamiento simultáneo de las muestras consiguiendo una velocidad de muestreo de 35 muestras a la hora, analizando cada muestra por triplicado.

3. Nuevas investigaciones en el uso de "upconverting phosphors" en sistemas de transferencia de energía resonante luminiscente

Este estudio se ha realizado durante la estancia de tres meses en el Departamento de Biotecnología de la Universidad de Turku (Finlandia). Debido a la corta duración de dicha estancia, la investigación se centró en la evaluación sistemática de diferentes dadores y aceptores para el diseño de un sistema de transferencia de energía resonante luminiscente (LRET) haciendo uso del fenómeno anti-Stokes en ensayos de afinidad biotina-estreptavidina. Este estudio tuvo como objetivo la selección del sistema más adecuado para su posterior aplicación analítica.

Como se ha descrito en la Introducción de esta Memoria, los "upconverting phosphors" (UCPs) son un tipo de NPs inorgánicas que pueden ser dopadas con iones lantánidos para llevar a cabo el fenómeno de emisión de fluorescencia anti-Stokes. En esta investigación se presenta el estudio sistemático de diferentes UCPs dopados con Er(III), Ho(III) y

Tm(III), utilizados como dadores, y varios fluoróforos, utilizados como aceptores, para el desarrollo de nuevas metodologías basadas en el fenómeno LRET. Para que se produzca este fenómeno son imprescindibles dos condiciones: 1) el espectro de excitación del aceptor tiene que solapar con el espectro de emisión del dador, y 2) la distancia entre dador y aceptor tiene que cumplir la ecuación de Förster.

Entre la gran variedad de fluoróforos existentes, las ficobiliproteínas, tales como la β-ficoeritrina (BPE) y la R-ficoeritrina (RPE), han sido utilizadas anteriormente como aceptores en diferentes ensayos LRET [77 – 79]. Su uso se debe principalmente a su elevada emisión de fluorescencia, aunque tienen el inconveniente de un coste relativamente elevado. Por este motivo se ha estudiado la posibilidad de utilizar otros tipos de fluoróforos de menor coste para el desarrollo de ensayos de afinidad LRET, como los Alexa Fluor o los ATTO. Para llevar a cabo este estudio sistemático entre dadores y aceptores, los UCPs fueron marcados con estreptavidina (SA) mientras que los fluoróforos fueron marcados con biotina (Bio).

En la Figura 12 se muestran los espectros de emisión de los dadores y los espectros de excitación de los aceptores. Las Figuras 12.A-12.C corresponden a la combinación del UCP dopado con Er(III) con la proteína fluorescente BPE y los fluoróforos Alexa Fluor 546 (AF546) y 680 (AF680), observándose un buen solapamiento entre los espectros de emisión y excitación de dador y aceptor, respectivamente.

Similares espectros fueron obtenidos al utilizar los UCPs dopados con Ho(III) (Figura 12.D-12.E) ensayados con BPE y AF546. Al igual que ocurre al usar el Er(III), el ancho espectro de excitación de la BPE permite excitarla eficientemente mientras que al usarse AF546, esta transferencia de energía presenta un menor rendimiento.

Los UCPs dopados con Tm(III) se combinaron con RPE, Alexa Fluor 488 (AF488) y el fluoróforo ATTO495 (Figura 12.F-12.H). En este caso, el dador presenta un máximo de emisión a una longitud de onda menor que el Er(III) y el Ho(III), con un buen solapamiento teórico con el fluoróforo AF488, aunque, como podrá observarse posteriormente, no siempre un adecuado solapamiento teórico da lugar en la práctica a una transferencia de energía eficaz.

Como ya se indicó en la Introducción de esta Memoria, la ausencia de grupos funcionales en este tipo de nanomateriales inorgánicos hace imprescindible llevar a cabo previamente su recubrimiento y funcionalización para, posteriormente, unirlos a biomoléculas. Después de este proceso, los diferentes dadores y aceptores fueron marcados con SA y Bio, respectivamente, para llevar a cabo la optimización de las concentraciones de cada uno de ellos y, finalmente, obtener las curvas de calibrado para la Bio, utilizada como analito modelo, en las mejores condiciones. Para evitar el elevado coste de las ficobiliproteínas BPE y RPE, se estudió la alternativa de utilizar otros fluoróforos para diseñar el sistema LRET, comparando los resultados con los obtenidos usando estas proteínas.

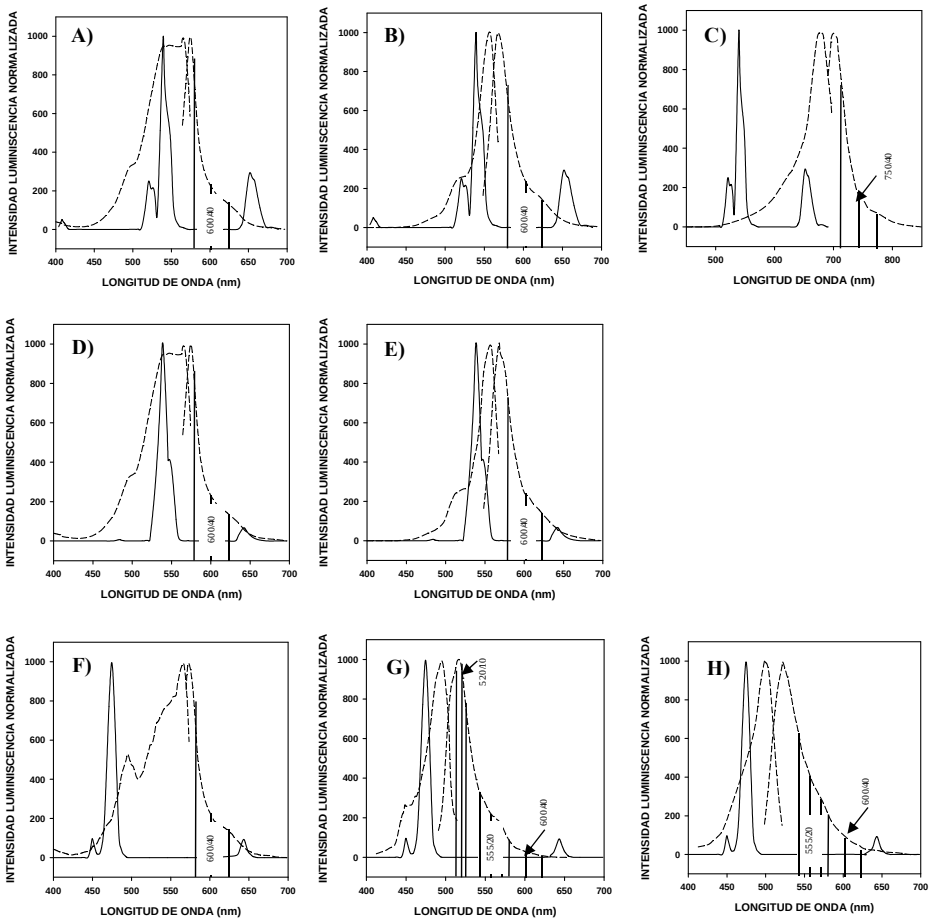

Figure 12: Espectros de emisión de los UCPs y aceptores utilizados en este estudio. En 12.A-12.C, espectro de emisión de UCP dopado con Er (III) junto con BPE (12.A), AF546 (12.B) y AF680 (12.C). En 12.D y 12.E, el UCP utilizado es el dopado con Ho (III) junto con BPE (12.D) y AF546 (12.E). En 12.F-12.H, los UCPs dopados con Tm (III) son combinados con RPE (12.F), AF488 (12.G) y ATTO495 (12.H).

En la Figura 13, se muestran las curvas de calibración obtenidas para biotina con UCPs como dadores dopados con Er(III)-SA (13.A y 13.B),

Ho(III)-SA (13.C) y Tm(III)-SA (13.D), combinados con diferentes fluoróforos. En todos los casos se obtuvo emisión luminiscente, pero los mejores resultados se lograron con las combinaciones Er(III)-BPE, Er(III)-AF680, Ho(III)-BPE y Tm(III)-RPE, las cuales se utilizaron para obtener dichas calibraciones.

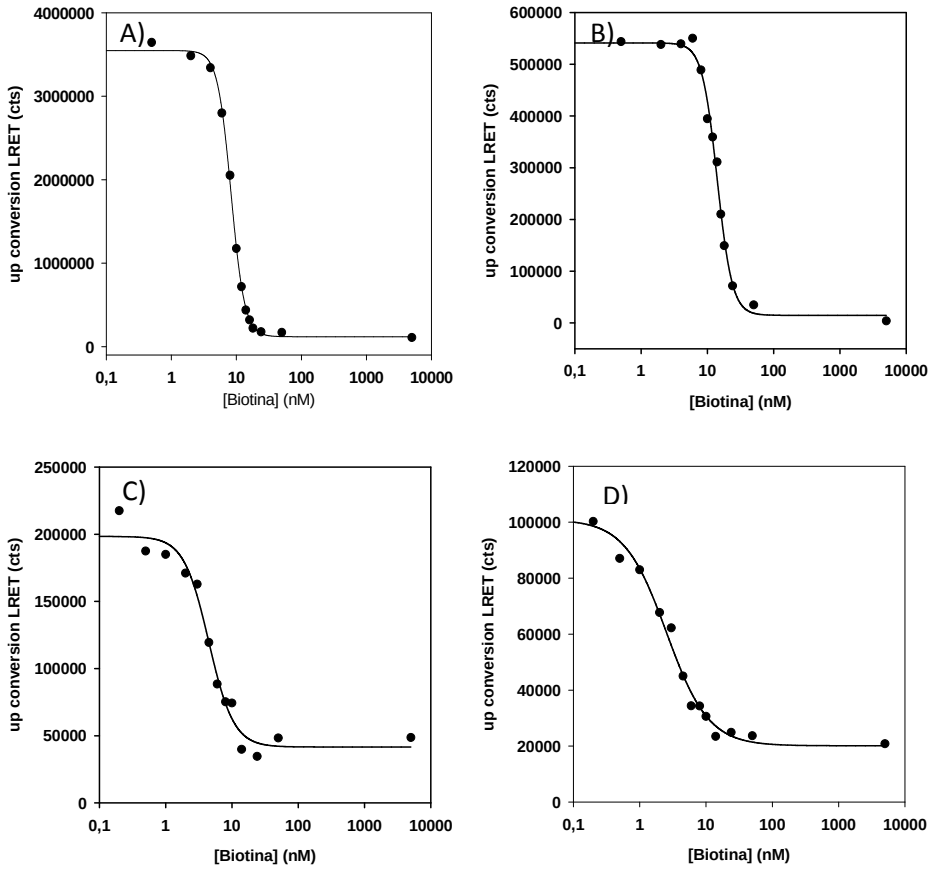

Figura 13. Ensayos homogéneos LRET de afinidad para biotina con los pares dador-aceptor que proporcionan los mejores resultados. A) UCP-Er (III) (0,015 mg/mL) y 0,4 nM BPE. B) UCP-Er (III) (0,015 mg/mL) y 4 nM AF680. C) UCP-Ho (III) (0,030 mg/mL) y 0,2 nM BPE. D) UCP-Tm (III) (0,030 mg/mL) y 1,33 nM RPE. Las intensidades de luminiscencia fueron calculadas restando la señal de fondo (exceso de biotina) a la señal máxima (ausencia de biotina), cts: cuentas.

Como se observa en la Figura 13, la mayor intensidad de fluorescencia fue obtenida con el UCPs-Er(III) junto con BPE y AF680. Sin embargo, como puede apreciarse en la Tabla 10, donde se resumen los diferentes ensayos llevados a cabo para la valoración homogénea de biotina así como los valores de IC50 obtenidos, los menores valores de este parámetro correspondieron al par UCP-Tm(III)-SA y RPE, pese a registrarse la intensidad de luminiscencia más baja. El mayor valor de IC50 fue obtenido para UCP-Er(III)-SA y Bio-AF680, el cual fue próximo a 14,4 nM. Los valores obtenidos son similares y, en algunos casos, mejoran los descritos previamente en los métodos propuestos utilizando UCPs-Er(III) recubierto de aditol como dador y BPE como aceptor [77, 78]

Tabla 10. Valores de IC50 para los ensayos de biotina utilizando diferentes pares dador-aceptor.

	IC50 para biotina (nM)			
Aceptor / **Dador**	**Bio-BPE (0,2 nM)**	**Bio-BPE (0,4 nM)**	**Bio-RPE (1,33 nM)**	**Bio-AF680 (4 nM)**
UCP dopado con Er(III) (0,015 mg/mL)	---	8,57*	---	14,37
UCP dopado con Ho(III) (0,015 mg/mL)	5,7	---	---	---
UCP dopado con Ho(III) (0,015 mg/mL)	---	7,20	---	---
UCP dopado con Tm(III) (0,030 mg/mL)	---	---	3,35	---

*La concentración de Bio-BPE fue de 0,3 nM

En resumen, del estudio sistemático realizado para evaluar la posible utilidad de diferentes UCPs como dadores de energía y diferentes fluoróforos como aceptores de energía en sistemas LRET, cabe destacar lo siguiente: 1) El dador UCP-Er(III) proporciona los mejores resultados al utilizar Bio-BPE como aceptor; 2) La utilización del fluoróforo AF680 como aceptor alternativo a las ficobiliproteínas permite también obtener una elevada señal fluorescente, aunque el valor de IC50 alcanzado para biotina es mayor que los obtenidos en presencia de las ficobiliproteínas. No obstante, la utilización de dicho fluoróforo también permite la determinación de biotina a nivel nanomolar, evitando el mayor coste que supone el uso de las ficobiliproteínas.

Como resumen de las investigaciones descritas en esta Memoria, se presentan en el siguiente esquema las principales ventajas y limitaciones de las metodologías analíticas desarrolladas en esta Memoria:

Ventajas	**Limitaciones**
SiO_2NPs dopadas con LWFs	
• Síntesis reproducibles mediante el método de formación de microemulsiones de micelas inversas • Aumento de estabilidad frente a fluoróforos en disolución • Diversas opciones de funcionalización disponibles por la variedad de reactivos organosilano	• No existen NPs comercialmente disponibles • Las condiciones de síntesis dependen de las características físico-químicas del fluoróforo

• Los inmunoensayos heterogéneos propuestos mejoran los ELISAs ya que: – Se obtienen menores límites de detección. – Se requieren menos etapas, se simplifican los ensayos. – Se mejora la selectividad espectral	
Ensayos para determinación de sustancias antioxidantes	
• **Ensayo ORAC a larga longitud de onda** – Disminución de los fenómenos de dispersión de la radiación – Mejora selectividad espectral • **Determinación de polifenoles mediante laccasa y Tb_4O_7NPs** – Límites de detección menores que los obtenidos mediante biosensores – El uso de Tb_4O_7 NPs permite: o Reducir la cantidad de enzima requerida o Acortar los tiempos de ensayo – Tb_4O_7NPs disponibles comercialmente	• Carencia de métodos normalizados • La enzima no se puede reutilizar
Estudio sistemático de UCPs en fenómenos LRET	
• La luminiscencia anti-Stokes utiliza excitación en el IR que minimiza la interferencia de la matriz de la muestra • Es posible utilizar diferentes pares dador-aceptor para su uso en ensayos multiplex • Se ha demostrado la utilidad de fluoróforos alternativos a las ficobiliproteínas para ser utilizados como aceptores	• No se pueden utilizar (espectro) fluorímetros convencionales

Referencias

(1) A. Gómez-Hens, J.M. Fernández-Romero, M. P. Aguilar-Caballos. Nanostructures as analytical tools in bioassays. *Trends Anal. Chem.* **(2008)** *27*, 394 – 406.

(2) J. Yan, M. C. Estévez, J. E. Smith, K. Wang, X. Ho, L. Wang, W. Tan. Dye-doped nanoparticles for bioanalysis. *Nanotoday* **(2007)** *2*, 44 – 50.

(3) M. Seydack. Nanoparticles labels in immunosensing using optical detection methods. *Biosens. Bioelectron.* **(2005)** *20*, 2454 – 2469.

(4) N. C. Tansil, Z. Gao. Nanoparticles in biomolecular detection. *Nanotoday* **(2006)** *1*, 28 – 37.

(5) G. Liu, Y. Lin. Nanomaterial labels in electrochemical immunosensors and immunoassays. *Talanta* **(2007)** *74*, 308 – 317.

(6) F. J. Arriagada, K. Osseo-Asare. Synthesis of nanosize silica in a noionic water-in-oil microemulsion: effects on the water/surfactant molar ratio and ammonia concentration. *J. Colloid Interf. Sci.* **(1999)** *211*, 210 – 220.

(7) G. Yao, L. Wang, G. Wu, J. Smith, J. Xu, W. Zhao, E. Lee, W. tan. FlotDots: luminescent nanoparticles. *Anal. Bioanal. Chem.* **(2006)** *385*, 518 – 524.

(8) X. He, J. Chen, K. Wang, D. Qin, W. Tan. Preparation of luminescent Cy5 doped core-shell SFNPs and its application as a near-infrared fluorescent marker. *Talanta* **(2007)** *72*, 1519 – 1526.

(9) X-L. Chen, J-L. Zou, T-T. Zhao, Z-B. Li. Preparation and fluoroimmunoassay application of new red-region fluorescent silica nanoparticles. *J. Fluoresc.* **(2007)** *17*, 235 – 241.

(10) W. Yang, C-G. Zhang, H-Y. Qu, H-H. Yang, J-G. Xu. Novel fluorescent silica nanoparticle probe for ultrasensitive immunoassays. *Anal. Chim. Acta* **(2004)** 503, 163 – 169.

(11) Z. Zhang, F. Zhang, Y. Liu. Recent advances in enhancing the sensitivity and resolution of capillary electrophoresis. *J. Chromatogr. Sci.* **(2013)** *51*, 666 – 683.

(12) G. A. Saleh, H. F. Askal, I. H. Refaat, F. A. M. Abdel-Aal. Review on recent separation methods for determination of some fluoroquinolones. *J. Liq. Chromatogr.* **(2013)** *36*, 1401 – 1420.

(13) M. Szultka, B. Buszewki, K. Papaj, W. Szeja, A. Rusin. Determination of flavonoids and their metabolites by chromatographic techniques. *Trends Anal. Chem.* **(2013)** *47*, 47 – 67.

(14) B. Tang, K. H. Row. Development of gas chromatography analysis of fatty acids in marine organisms. *J. Chromatogr. Sci.* **(2013)** *51*, 599 – 607.

(15) I. G. Zenkevich, Y. S. Drugov. Gas chromatographic methods for the determination of trace organic pollutans in environmental samples. *J. Anal. Chem.* **(2013)** *68*, 845 – 861.

(16) C. T. Elliot, D. G. Kennedy, W. J. McCaughey. Methods for the detection of polyether ionophore residues in poultry. *Analyst* **(1998)** *123*, 45R – 56R.

(17) M. Sokolic, M. Pokorny. Comparative determination of salinomycin by high-performance liquid chromatography,

microbiological and colorimetric methods in testing production processes and animal feed preparations. *J. Pharmaceut. Biomed.* **(1991)** *9*, 1047 – 1053.

(18) S. Magiera. Fast, simultaneous quantification of three novel cardiac drugs in human urine by MEPS-UHPLC-MS/MS for therapeutic drug monitoring. *J. Chromatogr. B* **(2013)** *938*, 86 – 95.

(19) R. Ciayadi, G. F. Kelso, M. K. Potdar, S. J. Harris, K. L. Walton, C. A. Harrison, M. T. W. Hearn. Identification of protein binding partners of ALK-5 Kinase inhibitors. *Bioorgan. Med. Chem.* **(2013)** *21*, 6496 – 6500.

(20) G. Pierri, D. Kotoni, P. Simone, C. Villani, G. Pepe, P. Campiglia, P. Dugo, F. Gasparrini. Analysis of bovine milk caseins on organic monolithic columns:An integrated capillary liquid chromatography-high resolution mass spectrometry approach for the study of time-dependent casein degradation. *J. Chromatogr. A* **(2013)** *1313*, 259 – 269.

(21) T. F. McGrath, C. T. Elliot, T. L. Fodey. Biosensors for the analysis of microbiological and chemical contaminants in foods. *Anal. Bioanal. Chem.* **(2012)** *403*, 75 – 92.

(22) X. Pei, B. Zhang, J. Tang, B. Liu, W. Lai, D. Tang. Sandwich-type immunosensors and immunoassays exploiting nanostructure labels: A review. *Anal. Chim. Acta* **(2013)** *758*, 1 – 18.

(23) S. Girotti, S. Ghini, E. Maiolini, L. Bolelli, E. N. Feri. Trace analysis of pollutants by use of honeybees, immunoassays, and chemiluminescence detection. *Anal. Bioanal. Chem.* **(2013)** *405*, 555 – 571.

(24) L. Anfossi, C. Baggiani, C. Giavannoli, G. D´Arco, G. Giraudi. Lateral-flow immunoassays for mycotoxins and phycotoxins: A review. *Anal. Bioanal. Chem.* **(2013)** *405*, 467 – 480.

(25) D. L. Brandon, M. Friedman. Immunoassays of Soy Proteins. *J. Agr. Food Chem.* **(2002)** *50*, 6635 – 6642.

(26) M. A. J. Godfrey, M. F. Luckey, P. Kwasowski. IAC/cELISA detection of monensin elimination from chicken tissues, following oral therapeutic dosing. *Food Add. Contam.* **(1997)** *14*, 281 – 286.

(27) S. R. H. Crooks, T. L. Fodey, G. R. Gilmore, C. T. Elliot. Rapid screening for monensin residues in poultry plasma by a dry reagent dissociation enhanced lanthanide fluoroimmunoassay. *Analyst* **(1998)** *123*, 2493 – 2496.

(28) V. Hagren, P. Peippo, M. Tuomola, T. Lövgren. Rapid time-resolved fluoroimmunoassay for the screening of monensin residues in eggs. *Anal. Chim. Acta* **(2006)** *557*, 164 – 168.

(29) C. Cháfer-Pericás, A. Maquieira, R. Puchades. Functionalized inorganic nanoparticles used as labels in solid-phase immunoassays. *Trends Anal. Chem.* **(2012)** *31*, 144 – 156.

(30) A. Gómez-Hens, J. M. Fernández-Romero, M. P. Aguilar-Caballos. Nanostructures as analytical tolos in bioassays. *Trends Anal. Chem.* **(2008)** *27*, 394 – 406.

(31) D. Knopp, D. Tang, R. Niessner. Review: Bioanalytical applications of biomolecule-functionalized nanometer-sized doped silica nanoparticles. *Anal. Chim. Acta* **(2009)** *647*, 14 – 30.

(32) M. A. J. Godfrey, M. F. Luckey, P. Kwasowski. IAC/cELISA detection of monensin elimination from chicken tissues, following oral therapeutic dosing. *Food Addit. Contam.* **(1997)** *14*, 281 – 286..

(33) M. Hazansadeh, N. Shadjou, E. Omidina, M. Eskandani, M. de la Guardia. Mesoporous silica materials for use in electrochemical immunosensing. *TrAC – Trends Anal. Chem.* **(2013)** *45*, 93 – 106.

(34) X. Zhao, L. R. Hilliard, S. J. Mechery, Y. Wang, R. P. Bagwe, S. Jin, W. Tan. A rapid bioassay for single bacterial cell quantitation using bioconjugated nanoparticles. *P. Ntl. Aca. Sci. USA* **(2004)** *101*, 15027 – 15032.

(35) R. Tapec, X. J. Zhao, W. Tan. Development of organic dye-doped silica nanoparticles for bioanalysis and biosensors. *J. Nanosci. Nanotech.* **(2002)** *2*, 405 – 409.

(36) H-H. Yang, H-Y. Qu, P. Lin, S-H. Li, M-T. Ding, J-G. Xu. Nanometer fluorescent hybrid silica particle as ultrasensitive and photostable biological labels. *Analyst* **(2003)** *128*, 462 – 466.

(37) W. Yang, C. G. Zhang, H. Y. Qu, H. H. Yang, J. G. Xu. Novel fluorescent silica nanoparticles probe for ultrasensitive immunoassays. *Anal. Chim. Acta* **(2004)** *503*, 163 – 169.

(38) M. Tan, G. Wang, X. Hai, Z. Ye, J. Yuan. Development of functionalized fluorescent europium nanoparticles for biolabelling and time-resolved fluorometric applications. *J. Mater. Chem.* **(2004)** *14*, 2896 – 2901.

(39) Z. Ye, M. Tan, G. Wang, J. Yuan. Novel fluorescent europium chelate-doped silica nanoparticles: preparation, characterization

and time-resolved fluorometric application. *J. Mater. Chem.* **(2004)** *14*, 851 – 856.

(40) Z. Ye, M. Tan, G. Wang, J. Yuan. Preparation, Characterization, and time-resolved fluorometric application of ailica-coated terbium (III) fluorescent nanoparticles. *Anal. Chem.* **(2004)** *76*, 513 – 518.

(41) L. L´Hocine, J. I. Boye, C. Munyana. Detection and quantification of soy allergens in food: study of two commercial enzyme-linked immunosorbent assays. *J. Food Sci.* **(2007)** *72*, C145 - C153.

(42) M. L. Sánchez-Martínez, M. P. Aguilar-Caballos, A. Gómez-Hens. Homogeneous immunoassay for soy protein determination in food samples using gold nanoparticles as labels and light scattering detection. *Anal. Chim. Acta* **(2009)** *636*, 58 – 62.

(43) Opinion of the scientific panel on contaminants in the food chain. *EFSA Journal* **(2008)** *592*, 1 – 40.

(44) Regulation (EC) No 1831/2003 of the European Parliament and of the Council of 22 Septembre 2003 on additives for use in animal nutrition. *Official Journal of European Union* **(2003)** *L268*, 29 – 43.

(45) H. Watanabe, A. Satake, M. Matsumoto, Y. Kido, A. Tsuji, K. Ito, M. Maeda. Monoclonal-based enzyme-linked immunosorbent assay and immunochromatographic rapid assay for monensin. *Analyst* **(1998)** *123*, 2573 – 2578.

(46) Monensin ELISA kit (Cat # KA1422 V.01), http://www.abnova.com/.

(47) Monensin ELISA. Enzyme-linked immunosorbent assay for the determination of monensin in feed and contaminated samples. http://abraxiskits.com/.

(48) S. R. H. Crooks, I. M. Traynor, C. T. Elliott, W. J. McCaughey. Detection of monensin residues in poultry liver using an enzyme immunoassay. *Analyst* **(1997)** *122*, 161 – 163.

(49) M. Ciz, H. Cizova, P. Deneb, M. Kratchanova, A. Slavov, A. Lojek. Different methods for control and comparison of the antioxidant properties of vegetables. *Food Control* **(2010)** *21*, 518 – 523.

(50) E. Atala, L. Vásquez, H. Speisky, E. Lissi, C. López-Alarcón. Ascorbic acid contribution to ORAC values in berry extracts: An evaluation by the ORAC-pyrogallol red methodology. *Food Chem.* **(2009)** *113*, 331 – 335.

(51) M. D. Rivero-Pérez, M. L. González-Sanjosé, M. Ortega-Herás, P. Muñiz. Antioxidant potential of single-variety red wines aged in the barrel and in the bottle. *Food Chem.* **(2008)** *111*, 957 – 964.

(52) E. Sofic, Z. Rimpapa, Z. Kundurovic, A. Sapcanin, I. Tahirovic, A. Rustembegovic, G. Cao. Antioxidant capacity of the neurohormone melatonin. *J. Neural Transm.* **(2005)** *112*, 349 – 358.

(53) G. Cao, H. M. Alessie, R. G. Cutler. Oxygen-radical absorbance capacity assay for antioxidants. *Free Radical Bio. Med.* **(1993)** *14*, 303 – 311.

(54) W. Mullen, S. C. Marks, A. Crozier. Evaluation of phenolic compounds in commercial fruit juices and fruit drinks. *J. Agr. Food Chem.* **(2007)** *55*, 3148 – 3157.

(55) J. Tabart, C. Kevers, J. Pincemail, J. O. Defraigne, J. Dommes. Comparative antioxidant capacities of phenolic compounds measured by various tests. *Food Chem.* **(2009)** *113*, 1226 – 1233,

(56) L. Müller, S. Groyke, A. M. Popken, V. Böhm. Antioxidant capacity and related parameters of different fruit formulations. *Food Sci. Technol.* **(2010)** *43*, 992 – 999.

(57) N. Nenadis, O. Lazaridou, M. Z. Tsimidou. Use of reference compounds in antioxidant activity assessment. *J. Agr. Food Chem.* **(2007)** *55*, 5452 – 5460.

(58) B. Lorrain, I. Ky, L. Pechamat, P. L. Teissedre, Evolution of analysis of polyphenols from grapes, wines, and extracts. *Molecules* **(2013)** *18*, 1076 - 1100.

(59) M. Medić-Ŝarić, V. Rastija, M. Bojić. Recent advances in the application of high performance liquid chromatography in the analysis of polyphenols in wine and propolis. *J. AOAC Int*. **(2011)** *94*, 32 - 42.

(60) H. Franquet-Griell, A. Checa, O. Núñez, J. Saurina, S. Hernández-Cassou, L. Puignou. Determination of polyphenols in Spanish wines by capillary zone electrophoresis. Application to wine characterization by using chemometrics. *J. Agr. Food. Chem*. **(2012)** *60*, 8340 - 8349.

(61) A. Sánchez-Arribas, M. Martínez-Fernández, M. Chicharro. The role of electroanalytical techniques in analysis of polyphenols in wine. *Trends Anal. Chem*. **(2012)** *34*, 78 - 96.

(62) L. M. Magalhães, M. A. Segundo, S. Reis, J. L. C. Lima, A. O. S. S. Rangel. Automatic method for the determination of Folin-Ciocalteu reducing capacity in food products. *J. Agr. Food Chem*. **(2006)** *54*, 5241 - 5246.

(63) J. C. Sánchez-Rangel, J. Benavides, J. B. Heredia, L. Cisneros-Zevallos, D. A. Jacobo-Velázquez. The Folin-Ciocalteu assay revisited: improvement of its specificity for total phenolic content determination. *Anal. Methods* **(2013)** *5*, 5990 - 5999.

(64) J. Sochor, M. Ryvolova, O. Krystofova, P. Salas, J. Hubalek, V. Adam, L. Trnkova, L. Havel, M. Beklova, J. Zehnalek, I. Provaznik, R. Kizek. Fully automated spectrometric protocols for determination of antioxidant activity: advantages and disadvantages. *Molecules* **(2010)** *15*, 8618 - 8640.

(65) A. L. Dawidowicz, D. Wianowska, M. Olszowy. On practical problems in estimation of antioxidant activity of compounds by DPPH method (Problems in estimation of antioxidant activity). *Food Chem*. **(2012)** *131*, 1037-1043.

(66) E. Nkhili, P. Brat. Reexamination of the ORAC assay: effect of metal ions. *Anal. Bioanal. Chem*. **(2011)** *400*, 1451 - 1458.

(67) J. Godoy-Navajas, M. P. Aguilar-Caballos, A. Gómez-Hens. Long-wavelength fluorimetric determination of food antioxidant capacity using nile blue as reagent. *J. Agr. Food Chem*. **(2011)** *59*, 2235-2240.

(68) M. Gamella, S. Campuzano, A. J. Reviejo, J. M. Pingarrón. Electrochemical estimation of the polyphenol index in wines using a laccase biosensor. *J. Agric. Food Chem.* **(2006)** *54*, 7960 - 7967.

(69) M. Di Fusco, C. Tortolini, D. Deriu, F. Mazzei. Laccase-based biosensor for the determination of polyphenol index in wine. *Talanta* **(2010)** *81*, 235 - 240.

(70) M.R. Montereali, L. Della Seta, W. Vastarella, R. Pilloton. A disposable laccase-tyrosinase based biosensor for amperometric

detection of phenolic compounds in must and wine. *J. Mol. Catal. B-Enzym*. **(2010)** *64*, 189 - 194.

(71) J. Kulys, I. Bratkovskaja. Antioxidants determination with laccase. Talanta **(2007)** *72*, 526 – 531.

(72) E. Nugroho Prasetyo, T. Kudanga, W. Steiner, M. Murkovic, G. S. Nyanhongo, G. M. Guebitz. Laccase-generated tetramethoxy azobismethylene quinone (TMAMQ) as a tool for antioxidant activity measurement, *Food Chem*. **(2010)** *118*, 437 - 444.

(73) E. Nugroho Prasetyo, T. Kudanga, W. Steiner, M. Murkovic, G. S. Nyanhongo, G. M. Guebitz. Antioxidant activity assay based on laccase-generated radicals. *Anal. Bioanal. Chem*. **(2009)** *393*, 679 - 687.

(74) A. Andreu-Navarro, J. M. Fernández-Romero, A. Gómez-Hens. Determination of polyphenolic content in beverages using laccase, gold nanoparticles and long wavelength fluorimetry. *Anal. Chim. Acta* **(2012)** *713*, 1-6.

(75) J. Robinson (Ed.) "Oxford companion to wine" 3rd edition. (2006) 35 – 36.

(76) Maximum acceptable limits of various substances contained in wine. *Compendium of International Methods of Analysis*, OIV, OIV-MA-C1-01:R2011.

(77) K. Kuningas, T. Rantanen, T. Ukonaho, T. Lövgren, T. Soukka. Homogeneous assay technology based on upconverting phosphors. *Anal. Chem.* **(2005)** *77*, 7348 – 7355

(78) K. Kuningas, T. Ukonaho, H. Pakkilä, T. Rantanen, J. Rosenberg, T. Lövgren, T. Soukka. Upconversion fluorescence resonance energy

transfer in a homogeneous immunoassay for estradiol. *Anal. Chem.* **(2006)** *78*, 4690 – 4696.

(79) T. Rantanen, H. Päkkilä, L. Jämsen, K. Kuningas, T. Ukonaho, T. Lövgren, T. Soukka. Tandem dye acceptor used to enhance upconversion fluorescence resonance energy transfer in homogeneous assays. *Anal. Chem.* **(2007)** *79*, 6312 – 6318.

Introduction

The features of the methods developed in this Dissertation are discussed in this chapter. A comparative study of their advantages and disadvantages to the methods previously described on the literature is carried out. Also, the usefulness of the proposed methodologies by their application to food analysis is discussed.

This chapter is structured in three sections: 1) Silica nanoparticles in food analysis, 2) New strategies for the determination of antioxidants in foods and 3) New investigations in the use of upconverting phosphors in luminescence resonance energy transfer systems.

1. Silica nanoparticles in food analysis.

As it has been previously described, the use of nanomaterials is having a huge growth in different areas of Analytical Chemistry [1 – 5]. Among the wide range of nanomaterials currently available, the use of silica nanoparticles (SiO_2NPs) has rapidly grown in the last decade due to their excellent properties, which are especially appropriate for their use as labels in bioanalysis. The results achieved with these NPs in the three articles included in this Dissertation will be discussed in the next section.

- Synthesis and characterization of long-wavelength fluorophore-doped silica nanoparticles

The use of SiO_2NPs as alternative labels in methods with optical detection is very interesting due to transparency of silica to visible light, as

well as other advantages already described in the Introduction of this Dissertation.

Two general routes for the synthesis of silica NPs, namely Stöber method and reverse-micelle microemulsion method, involve the use of different silica precursors, such as tetramethoxysilane (TMOS) and tetraethoxysilane (TEOS). These precursors undergo hydrolysis and polycondensation reactions, giving rise to the formation of monodisperse spherical SiO_2NPs [6]. The choice of the most appropriate synthesis procedure will depend on the physical and chemical properties of the species to be encapsulated [2, 4].

The synthesis of fluorescent SiO_2NPs doped with two long-wavelength fluorophores (LWFs), cresyl violet and nile blue, is described in this Dissertation using the reverse-micelle microemulsion method. All the variables involved in this synthesis procedure have been optimized for this purpose and their features have been compared (NP size, nanomaterial amount, fluorescence intensity, etc) with those of the NPs obtained by the Stöber method.

The formation of the microemulsions involves the use of a surfactant, an aqueous solution, an organic solvent, and a silica precursor, which is added to perform the SiO_2NP synthesis. Depending on the relative amounts of the components, water-in-oil microemulsions (rich in organic solvent) or oil-in-water microemulsions (rich in water) can be formed. Cyclohexane, 1-hexanol, Triton X-100 and water were chosen to form the microemulsion, according to the procedures previously reported,

and TEOS was selected as the silica precursor [2, 4, 6, 8 – 10]. However, the use of the experimental conditions previously described did not give rise to satisfactory results for the synthesis of the cresyl violet and nile blue-doped silica NPs. Several assays were carried out to optimize the microemulsion composition. This study showed that the NPs synthesized in the absence of cyclohexane had similar features (number and size) as those obtained using cyclohexane, but their fluorescence intensity was slightly higher. Figure 1 shows transmission electronic microscopy (TEM) images of the NPs obtained in the presence of different volumes of ciclohexane. As can be seen, the amount and sizes of the NPs synthesized in the absence of cyclohexane (Figure 1a) were comparable to those achieved using 7.5 mL of cyclohexane (Figure 1c). However, the use of intermediate volumes of cyclohexane (Figure 1b) provided larger NPs with wider size distributions. According to these results, the use of cyclohexane was precluded and only water, Triton X-100 and 1-hexanol were selected as the components of the microemulsion.

The study of the influence of Triton X-100 amount showed that the number of nile blue-doped NPs increases and their size decreases as Triton X-100 amount increases. The best results were obtained using 510 – 520 mg of Triton X-100 (Figure 1f) because lower amounts gave NPs of sizes higher than 200 nm (Figure 1d and 1e). Very small and partially aggregated NPs were obtained when the Triton X-100 amount was close to 1.0 g.

The feasibility of a slight modification of the reverse-micelle microemulsion procedure for fluorophore-doped SiO_2NPs by introducing the use of silica precursors was also studied. This modification includes a

previous reaction step in which the covalent linking between the primary amino groups of the fluorophore and 3-aminopropyl triethoxysilane (APS) was assayed in order to prevent the dye leakage from the silica matrix.

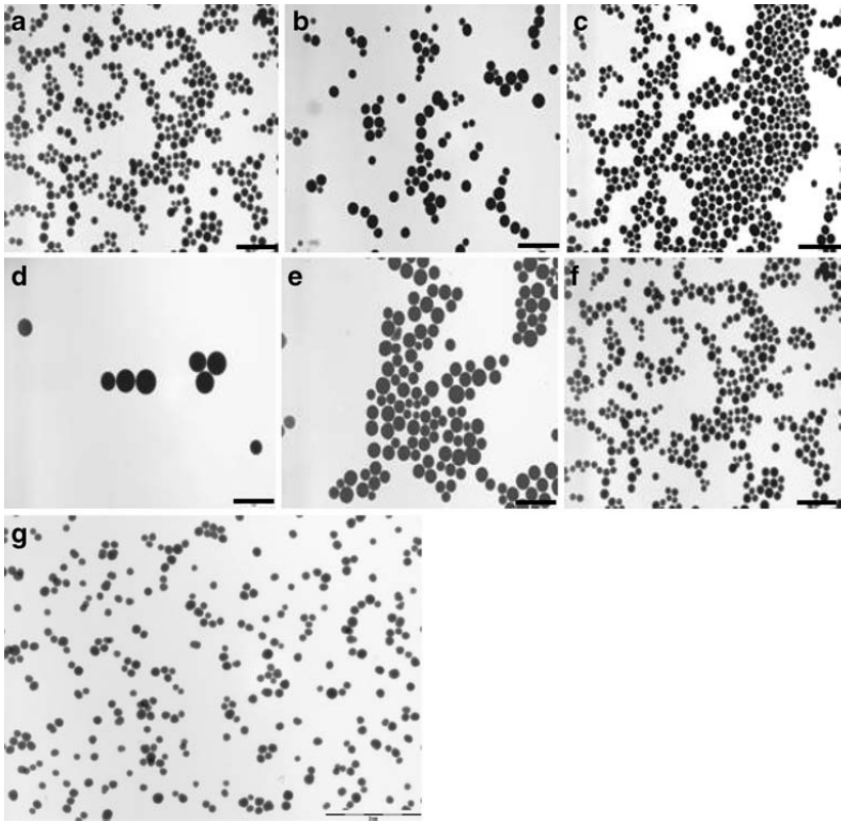

Figure 1. TEM images of nile blue-doped NPs synthesized using different cyclohexane volumes (**a, b** and **c**), different Triton X-100 concentrations (**d, e, f**) and those for nile-blue-APS doped silica NPs (**g**). Experimental conditions: 100 μL (0.11 mmol) TEOS, 0.2 mL of 1 x 10^{-3} M (0.2 μmol) nile blue, 3 mL (0.024 mol) hexanol, 70 μL (0.9 mmol) NH_4OH. In (Figure 1a-c): 510 – 520 mg (0.79 – 0.82 mmol) Triton X-100. In Figure 1a 11.3 mL (0.63 mol) water, 0 mL cyclohexane, in Figure 1b, 7.5 mL (0.42 mol) water, 3.75 mL (0.034 mol) cyclohexane, in Figure 1c 3.8 mL (0.21 mol) water, 7.5 mL (0.068 mol) cyclohexane. In Figure 1d – f 11.3 mL (0.63 mol) of water, in Figure 1d 0 mg, in Figure 1e 310.9 mg (0.48 mmol), in Figure 1f 510.9 (0.79 mmol) of Triton X-100. Scale bar: 1 μm. In Figure 1g experimental conditions: 510 – 520 mg (0.79 – 0.81 mmol) of Triton X-100, 10.3 mL (0.57mol) of water, 100 μL (0.44 mmol) TEOS, 1.2 mL precursor reaction mixture, 3 mL (0.024 mol) hexanol, 70 μL (0.9 mmol) of NH_4OH. Scale bar: 2 μm.

Nevertheless, as can be seen in Figure 1g, the NPs amount collected was substantially lower than that obtained in the absence of APS. Also, these NPs showed a wide size distribution. Thus, the use of these NPs as potential labels for further assays was discarded as they do not improve the features of the NPs obtained without this modification. Also, this synthesis procedure requires an additional step and an increased reagent and time consumption.

It was checked that the Triton X-100/hexanol ratio is a critical variable, as Figure 2 shows. As it can be seen, a ratio of 170 mg Triton X-100/mL hexanol provided the maximum fluorescence intensity of the synthesized material.

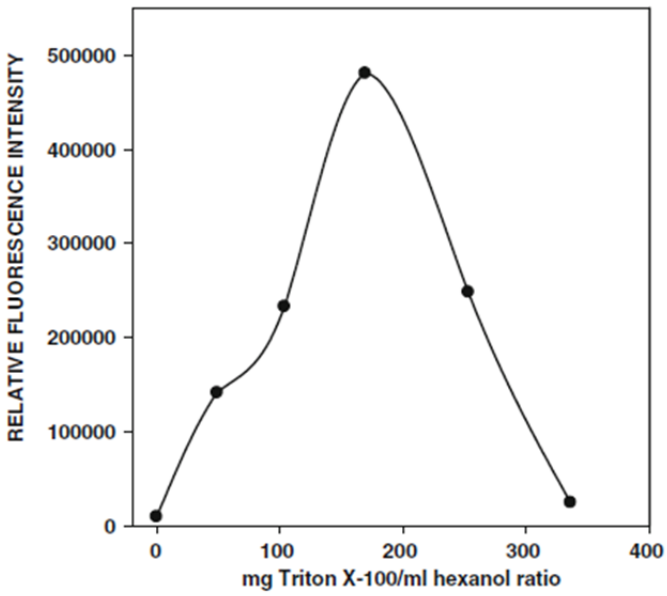

Figure 2. Influence of Triton X-100/hexanol ratio on the fluorescence intensity of nile blue-doped NPs. Experimental conditions: 11.3 mL (0.63 mol) of water, 100 μL (0.44 mmol) TEOS, 0.2 mL of 1 x 10^{-3} M (0.2 μmol) nile blue, 3 mL (0.024 mol) hexanol, 70 μL (0.9 mmol) NH_4OH.

The amount of fluorophore used is another critical variable. The influence of this variable on the fluorescence intensity is shown in the Figure 3, in which can be seen that the maximum value was obtained using 1.8 μmol of nile blue. The decrease in the fluorescence intensity at higher values is ascribed to the formation of fluorophore aggregates, which are less fluorescent than the monomers [7].

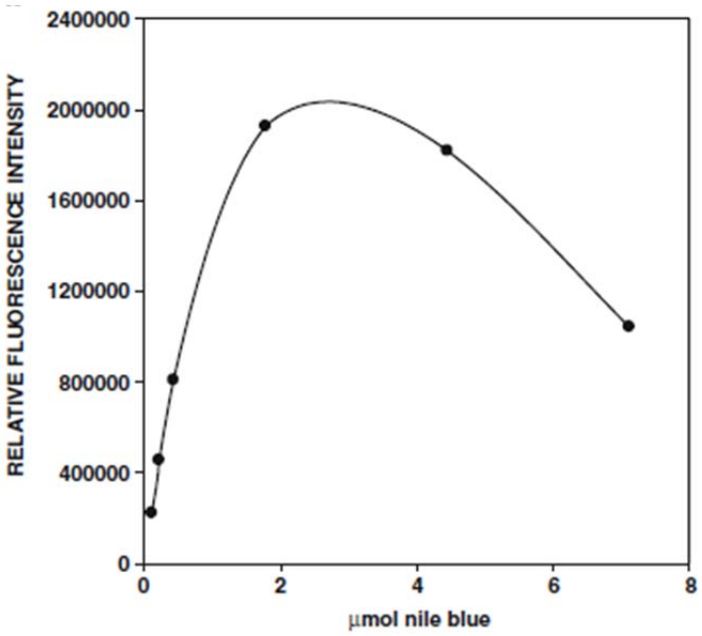

Figure 3. Influence of the amount of nile blue added on the fluorescence intensity of fluorophore-doped NPs. Experimental conditions: 510 – 520 mg (0.79 – 0.81 mmol) Triton X-100, 11.3 mL (0.63 mol) water, 100 μL (0.44 mmol) TEOS, 3 mL (0.024 mol) 1-hexanol and 70 μL (0.9 mmol) NH_4OH.

After studying of all the variables involved in the synthesis process, the NPs obtained by means of the reverse-micelle microemulsion method were compared to the NPs synthetized by the Stöber method. Table 1 shows the comparison of the cresyl violet-doped silica NPs obtained by both methods, using the same NP concentration. It was found that the average diameter of the NPs obtained by the microemulsion method was slightly greater, whereas the number of NPs is higher using the Stöber method, although the differences were not very significant in any instance. However, the fluorescence intensity and the specific intensity of the NPs obtained by the modified microemulsion method were about 12 times higher than the corresponding values obtained for the NPs synthesized by the Stöber procedure. These results can be ascribed to the fact that cresyl violet is less degraded under the alkaline conditions of the synthesis procedure owing to the protective effect of the micelles.

Table 1. Comparison of the properties of cresyl violet-doped NPs obtained by the proposed reverse-micelle microemulsion and Stöber methods.

	Reverse micelle microemulsion method	**Stöber method**
Concentration, mg/mL	0.1	0.1
Particle amount, mg	0.02	0.02
Diameter, nm	178	133
Particle number	2.94×10^{9}	7.06×10^{9}
Intensity[a]	125563	10138
Intensity/particle ratio	4.27×10^{-5}	1.44×10^{-6}
Specific intensity	1.45×10^{7}	1.17×10^{6}

[a]Measurements performed in microplates (200 μl) using excitation and emission filters of 620/8 and 680/10 nm, respectively

The spectral features of the synthesized NPs were compared to those shown by the dyes in solution and by bare SiO_2NPs. The emission maxima of the oxazine-doped SiO_2NPs showed a hypsochromic shift of about 9 nm, when compared to the emission maxima of the fluorophores in solution, whereas the bare SiO_2NPs did not show any fluorescent signal.

The synthesized NPs in aqueous solution were irradiated at their corresponding maximum excitation wavelength for one hour to investigate their potential photobleaching and the results were compared to those obtained for the dyes in solution. The fluorescence intensity of cresyl violet and nile blue in solution showed a fluorescence decrease of about 72 % and 65 %, respectively, but the fluorescence intensity of both cresyl violet and nile blue-doped NPs remained almost constant. The same study was carried out for the SiO_2NPs prepared by using the nile blue-APS mixture, obtaining a decrease of about a 10 % of the initial fluorescence intensity. Also, the stability of the fluorescent SiO_2NPs was checked over time and it was found that the luminescence intensity was constant for at least one month.

In summary, it can be confirmed that the modified reverse-micelle microemulsion method to synthesize two types of LWFs-doped silica NPs, using nile blue and cresyl violet, provides NPs with similar characteristics (size, amount and average diameter) as those obtained by means of the Stöber method, which is considered as a reference method. However, the fluorescence intensity of the NPs synthetized by the first method is higher than that of NPs obtained by the Stöber method. This behavior can be

ascribed to the stability and protection that the microemulsion used to perform the synthesis confers to the LWFs.

- Utilization of silica nanoparticles in heterogeneous immunoassay for the determination of macromolecules and small molecules

The determination of biomolecules is an application field of great interest in Analytical Chemistry. A high number of chromatographic and electrophoretic methods have been developed for the determination of macromolecules and small molecules [11 – 15]. Usually, these techniques require that the analyte shows a measurable property, such as absorbance or fluorescence. Otherwise, the use of a derivatization step is required, which lengthens and complicates the analysis [16, 17]. Although chromatographic methods with mass spectrometry detection are available, they require sophisticated and expensive instrumentation [18 – 20]. Also, these methods usually involve time-consuming sample treatment steps to remove the sample matrix. The use of screening methods plays two essential roles: in one hand, the number of samples subjected to confirmatory analysis is lower and, on the other, the cost of the analysis is reduced. Immunoassays, which can be used for quantitative or semi-quantitative purposes, have shown their usefulness as screening methods for the determination of antigenic substances, either small molecules (haptens) or macromolecules. Numerous commercial and non-commercial enzyme-linked immunosorbent assays (ELISAs) have been described for this purpose [21 – 25]. A high percentage of these methods involve the use of photometric measurements, reaching detection limits close to ng/mL,

but lower values can be obtained using chemiluminescence detection [26] or time-resolved luminescence detection with europium(III) chelates as labels [27, 28].

The use of functionalized inorganic NPs as labels in immunoassays is a relatively new trend justified by their versatile physicochemical properties, which allow the improvement of these assays features [29 – 31]. Among these NPs, doped SiO_2NPs are a useful option owing to their above mentioned characteristics. These SiO_2NPs can encapsulate a wide variety of compounds, which are protected from environmental factors. Also, they show large surface area and easy surface functionalization. These properties have given rise to a great variety of immunoassays devoted to the determination of macromolecules and haptens [32, 33]. For example, a method for the determination of *E. Coli* using tris(bipyridine)ruthenium (II)-doped NPs has been developed by immobilizing the antibody on the NP surface, which has allowed the determination of only one bacteria without using of an enhancement signal procedure [34]. Similarly, bovine serum albumin (BSA) has been determined by a streptavidin-biotin affinity assay using rhodamine 6G-doped SiO_2NPs as labels [35]. Also, the determination of α-fetoprotein (AFP) and hepatitis B surface antigen (HBsAg) have been reported by using fluorescein-doped SiO_2NPs [36, 37]. These SiO_2NPs can also encapsulate other species such as terbium and europium chelates, which have been used as labels to determine HBsAg, carcinoembrionic antigen (CEA) and prostate-specific antigen (PSA) [38 – 40]. From these examples it can be inferred that doped SiO_2NPs have been

mainly used in clinical analysis, which clearly justifies the investigations performed to develop immunoassays for food analysis.

The immunoassays described in this Dissertation have used nile blue-doped SiO_2NPs as labels for the determination of soy proteins (macromolecules) and the veterinary antibiotic monensin, which presence in food is regulated by the European Union. The results obtained have demonstrated that the use of these NPs provides some advantages over other immunoassays, such as lower detection limits and, in the case of ELISAs, fewer steps because the use of a substrate to measure the enzymatic activity is not required.

Nile blue-doped SiO_2NPs were chosen to use long-wavelength fluorescence measurements, which provide a suitable spectral selectivity, avoiding the background signal from the sample matrix. As mentioned above, a potential limitation of doped SiO_2NPs is the potential leakage of the fluorophore from the silica matrix. However, nile blue-doped SiO_2NPs show an excellent stability due to the electrostatic interactions between the positively charged fluorophore and the negatively charged silanol groups.

The results obtained in the immunoassays developed in this Dissertation are discussed below.

- Determination of soy proteins by heterogeneous immunoassay

In recent years, the global consumption of soy foodstuffs has increased because of their reported beneficial effect on nutrition and health, such as decrease of plasma cholesterol, prevention of cancer,

diabetes and obesity, and protection against bowel and kidney diseases. However, it has also been described that soy proteins can produce allergic responses in some people.

A competitive heterogeneous immunoassay for the determination of soy proteins in food samples, using nile blue-doped SiO_2NPs as labels, has been developed in this Dissertation. For this purpose, two different formats either involving analyte capture or antibody capture were assayed, respectively (Figures 4 and 5). These NPs were coupled to either soy proteins or to anti-soy protein antibodies to study the potential use of the corresponding tracers for the development of the two immunoassay formats. The analyte capture format (Figure 4) involves the immobilization of anti-soy protein onto the wells, after the previous immobilization of anti-rabbit IgG antibodies, and the use of the tracer composed of soy protein linked to nile blue-doped SiO_2NPs. The use of anti-rabbit IgG antibodies to immobilize the anti-soy protein antibodies reduces the consumption of these antibodies and, therefore, the total cost of the immunoassay. However, although the well surface was coated with BSA at different concentrations, non-specific interactions of the tracer with the anti-rabbit IgG antibodies were still observed, so that this approach was unsuitable.

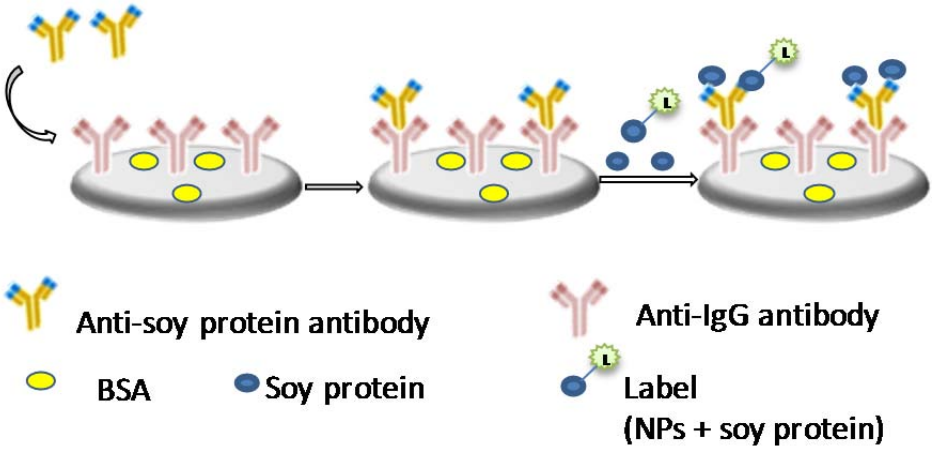

Figure 4. Competitive heterogeneous immunoassay with antigen capture using nile blue-doped SiO_2NPs as label linked to soy protein.

The antibody capture format was assayed to overcome this problem (Figure 5). Thus, soy proteins were immobilized first onto the wells, and the remaining sites of the well were blocked with BSA. Then, a preincubated mixture of soy protein standard or sample together with a conjugate anti-soy protein-nile blue-doped silica NPs (tracer) was added, competing both immobilized and in solution soy proteins for the active sites of the conjugate. After incubation and washing steps, the fluorescence from the bound tracer fraction was measured onto the well surface.

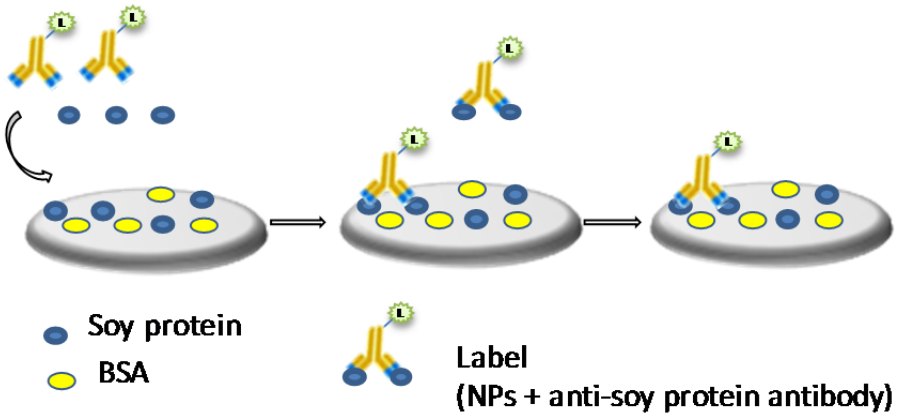

Figure 5. Competitive heterogeneous immunoassay with antibody capture using nile blue-doped SiO_2NPs as label linked to anti-soy protein antibodies.

Fluorescence intensity measurements were performed at the maximum excitation and emission wavelengths of the tracer, λ_{ex} 620 and λ_{em} 680 nm, respectively. The method presented a dynamic range of 0.1 – 10 mg/L and the detection limit was 0.05 mg/L, which is about ten times lower than that provided by the ELISA kit used as reference method [41]. Also, as the addition of an enzymatic substrate is not required, the assay steps and the analysis time are reduced. The precision, expressed as the percentage of relative standard deviation and assayed at two different soy protein concentrations, 0.5 and 5 mg/L, gave values of 9.6 % and 6.1 %, respectively.

The selectivity of the method mainly depends on anti-soy protein antibodies selectivity. According to the antibody specification sheet, these antibodies present some cross-reactivity towards hot urea extracts of wheat and ovalbumin, but no cross-reactivity is observed in extracts form meat,

corn or casein, and rice or potato flour. Additionally, in a previous work that involved the use of the same anti-soy protein antibodies, it was found that bovine serum albumin, ϒ-globulins, myoglobin and hemoglobin were tolerated in excess higher than 80-fold the analyte concentration [42].

The method was applied to the analysis of milk, yoghourt and fruit juice samples containing soy proteins. These samples were also analyzed using a commercial ELISA kit [41]. Samples were subjected to a denaturation-renaturation treatment according to the procedure indicated by the anti-soy protein antibody manufacturer. Table 2 shows the soy protein content found by the reported immunoassay and by the ELISA method, which were compared by a paired *t*-test carried out at a 95 % significance level, finding that there were not statistically significant differences among them.

Table 2. Determination of soy protein content in food samples

Sample	Reported method[a, b]	Commercial ELISA[a, b]
Soy milk	74 ± 6	84 ± 3
Fruit and soy juice	8.4 ± 0.7	10.5 ± 0.3
Soy yoghourt	64 ± 4	60 ± 3

[a] Mean ± SD (n = 3)
[b] Units: fruit and soy juice, soy yoghourt, g/Kg; soy milk, g/L

A recovery study was also carried out to validate the method (Table 3). It was performed by adding three different amounts of soy protein to each sample and subtracting the results obtained from similarly treated non-spiked samples. The values obtained ranged from 81.5 % and 111.0 %.

Table 3. Recovery of soy protein added to food samples

Sample	Added[a, b]	Found[a, b]	Recovery (%)
Soy milk	24	27 ± 2	111.0
	72	69 ± 4	95.7
	123	110 ± 10	89.4
Fruit and soy juice	2.7	2.2 ± 0.2	81.5
	8.1	7.7 ± 0.6	95.1
	13.5	12 ± 1	88.9
Soy yoghourt	23	21 ± 2	91.3
	65	61 ± 4	93.2
	113	95 ± 7	84.1

[a] Mean ± SD (n = 3)

[b] Units: fruit and soy juice, soy yoghourt, g/kg; soy milk, g/L

- Determination of monensin by heterogeneous immunoassay in milk samples

Monensin is a veterinary drug that exhibits both antibacterial and anticoccidial activities and has been traditionally used to prevent coccidiosis in poultry [43]. This antibiotic has been considered as a growth-promoter, since this disease prevents the growth of poultry owing to the bloody diarrhea and weight loses associated. Although the use of many

veterinary antibiotics as growth promoters has been banned since 2006, they can be still administered to some species according to the European Union regulation [44]. Also, the treatment with monensin has been extended to calves for the European Union with maximum residue limits.

The concern on food safety has led to the search for reliable analytical methods to screen and confirm the presence of antibiotic residues in foodstuffs, which contribute to increase bacterial resistance to antibiotics.

The first immunoassay for monensin determination using nile blue-doped SiO_2NPs as labels has been presented in this Dissertation. The usefulness of this approach to improve the analytical features, such as the detection limit, of the immunoassays previously described using enzymatic labels for the determination of this drug is shown [22, 45 – 48].

As it has been previously indicated, the use of nile blue-doped SiO_2NPs as labels provides the spectral selectivity required to avoid interferences from the sample matrix. In addition, the encapsulated fluorophore inside the NPs shows an excellent stability to the action of environmental agents and the incident light, avoiding photobleaching phenomena. These features justify the use of these NPs as labels in immunoassays. Another advantage of the new method is the use of 96-well microplates with 100-μL wells, which reduces the sample and tracer volumes required in comparison to the conventional 300-μL wells, which contributes to minimize the costs associated with the immunoassay and the amount of waste generated. This plate type facilitates the use of front-

surface measurements as the distance between the well bottom and the detector is shorter than that for conventional plates, which minimizes fluorescence signal losses and improves the sensitivity.

As in the previous section, two heterogeneous immunoassays, involving antibody or antigen capture format, were assayed to choose the best option for monensin determination using nile blue-doped SiO_2NPs as labels. The first format was based on the immobilization of a BSA-monensin conjugate and the use of an anti-monensin antibody-NP tracer. The second assay needed a monensin-NP tracer, synthesized via a carbodiimide reaction using EDAC (N-(3-methylaminopropyl)-N′-ethylcarbodiimide hydrochloride), and the immobilization of anti-monensin antibodies by coating the wells with anti-sheep IgG. A significant difference between the fluorescence intensity values obtained in the absence and in the presence (0.2 μg/L) of monensin was reached in both assays, but this difference was about 3-fold higher for the antibody-capture format. Thus, this format was chosen to develop the new immunoassay for monensin determination.

The method presents a dynamic range of 0.05 – 5 μg/L and the detection and quantification limits are 0.015 and 0.05 μg/L, respectively, which would correspond to 0.12 and 0.40 μg/Kg in the milk samples. The latter value is about 5 times lower than the maximum residue limit (MRL) set by the 37/2010/EC Commission Regulation for monensin in milk samples. Also, the detection limit is four times lower than that reported using ELISA with chemiluminescence detection [32]. The precision, expressed as the percentage of relative standard deviation and assayed at

two different monensin concentrations, 0.2 and 1 μg/L, gave values of 5.8 and 4.0 %, respectively.

The method was applied to the analysis of skimmed, semi-skimmed and whole milk samples. The sample treatment was quite simple as it only required the deproteinization of samples and a further solvent evaporation step. A recovery study was also carried out to validate the method (Table 4), obtaining values in the range of 83.3 – 107.5 %.

Table 4. Recoveries obtained for monensin added to milk samples

Sample	**Monensín**		
	Added[a, b] (μg/Kg)	Found[a, b] (μg/Kg)	Recovery (%)
Skimmed milk	1.5	1.6 ± 0.1	106.7
	2	1.96 ± 0.09	98.0
	4	4.1 ± 0.2	102.5
Semi-skimmed milk	1.5	1.5 ± 0.1	100.0
	2	2.0 ± 0.1	100.0
	4	3.4 ± 0.3	85.0
Whole milk	1.5	1.25 ± 0.07	83.3
	2	1.7 ± 0.1	85.0
	4	4.3 ± 0.3	107.5

[a] Mean ± SD (n = 3)

In summary, the results obtained show the usefulness of LWF-doped SiO_2NPs as labels to determine macromolecules (proteins) and small molecules (antibiotics) in food analysis. This approach provides lower detection limits than ELISA and avoids the last step for the enzyme activity measurement. Likewise, the proposed methods have contributed to expand the use of nanotechnology in this analytical area.

2. New strategies for the determination of antioxidants in foods

Oxidation processes involving free radicals contribute to the development of many illnesses, such as cardiovascular disease, Alzheimer´s disorder and cancer. This redox phenomenon is produced by reactive oxygen species (ROS), which damage cell membranes, but this effect can be minimized by the intake of antioxidant compounds. The antioxidant capacity of foods is mainly ascribed to polyphenols, such as flavonoids, and vitamins C and E, among others [49].

A method for the determination of the antioxidant capacity of some food samples has been described in this Dissertation, which shows the usefulness of long-wavelength measurements. Another method for the determination of polyphenols using nanomaterials as laccase enzyme activators is also included. The features of both methods and their applicability are discussed below.

- Long-wavelength fluorimetric determination of food antioxidant capacity using nile blue as reagent

From an analytical point of view, there are two types of methods for assessing food antioxidant capacity. The first group involves a single electron-transfer reaction, which can be followed by a change in the solution color or fluorescence. The second group is based on the use of a hydrogen atom transfer reaction, where the antioxidant and a substrate compete for the free radicals generated. The oxygen radical absorbance capacity (ORAC) assay, which belongs to the second group, involves the use of a free radical generator that directly attacks either a chromophore or

a fluorophore, leading to the decrease of their absorbance or fluorescence, respectively. The chromophore pyrogallol red [50] and the fluorophores β-phycoerythrin and fluorescein [51 – 57], have been used to develop this assay. Despite the high sensitivity that the above-mentioned fluorophores offer, these compounds feature a relatively short Stokes shift (about 27 nm), which favors scattering phenomena. Also, β-phycoerythrin is relatively expensive and suffers from photobleaching, while fluorescein emission is usually overlapped by the static background signals from the sample matrix. The use of long-wavelength fluorophores can avoid these problems, but their potential application to the determination of the antioxidant capacity has not been studied up to now.

An analytical method has been described in this Dissertation for food antioxidant capacity determination by the ORAC assay using nile blue as fluorescent probe, 2,2′-azo-bis-(2-methylpropionamidine) dihydrochloride (AAPH), as free radical generator, and 6-hydroxi-2,5,7,8-tetramethylcroman-2carboxylic acid (Trolox) as model analyte have been used for this purpose. Fluorescent measurements were carried out in the kinetic mode by monitoring the change of fluorescence over time and using the normalized net area under the curve, $AUC_{net} = (AUC_{sample} - AUC_{blanck})/AUC_{blanck}$), obtained for different analyte concentrations, as the analytical parameter.

As it has been already mentioned, the traditional fluorophores used for these assays have been β-phycoerythrin and fluorescein, which show a delay in their fluorescence quenching in the presence of antioxidant compounds, but their use has the limitations above indicated. The potential

use of long wavelength fluorescent dyes as alternative reagents to avoid these limitations was assessed. Several oxazine and thiazine dyes, namely, nile blue, azure A, and azure B, were assayed for this purpose. Figure 6 shows the curves obtained for each fluorophore, in the presence and absence of Trolox. As can be seen, the three fluorophores gave rise to significant AUC_{net} values, but the best results were obtained with nile blue.

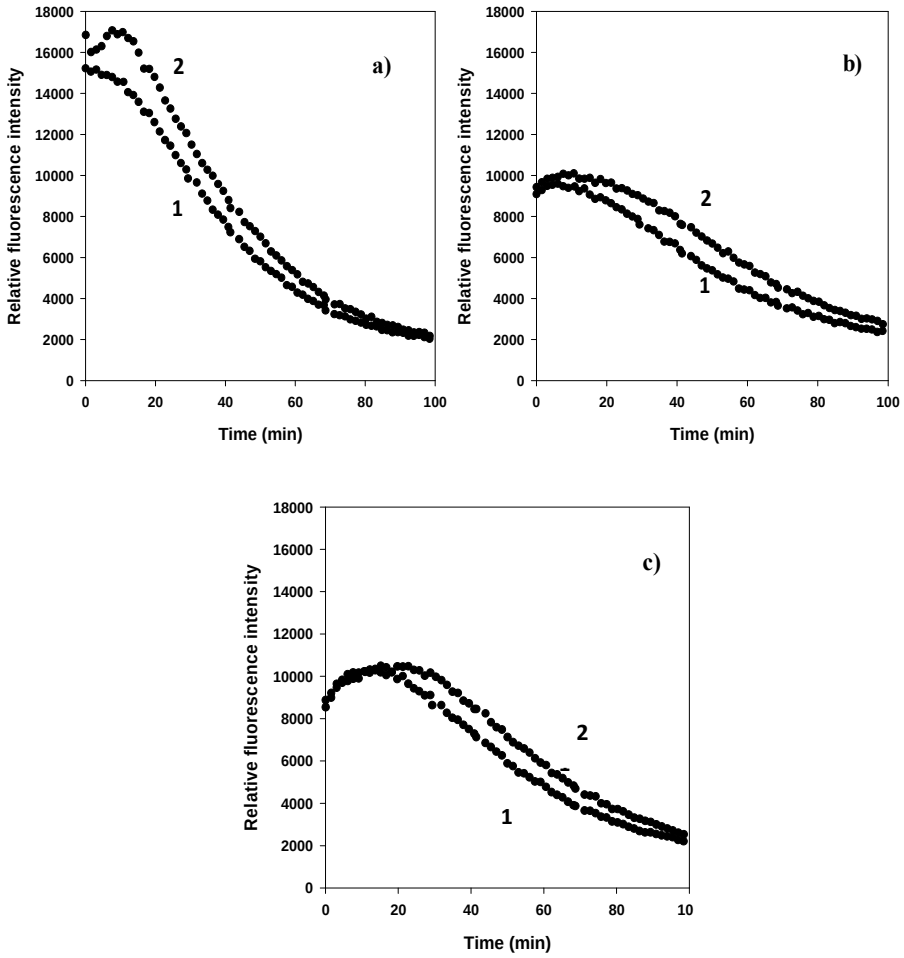

Figure 6: Curves obtained for the ORAC assay using (a) nile blue, (b) azure A, and (c) azure B fluorophores: (1) blank and (2) 2 μM Trolox.

The influence of the pH was investigated in the range of 4 - 11, using 0.075 M acetate, phosphate, borate, and carbonate buffer solutions to keep the pH constant in the buffering region of each solution. As Figure 7 shows, the net AUC values were very low at pH below 5.8 and above 8, obtaining the best results in the pH range of 6.0 – 7.0. The behavior of the system at low pH values could be ascribed to the fact that the pK_a of Trolox is about 3.89, showing a low solubility at this pH.

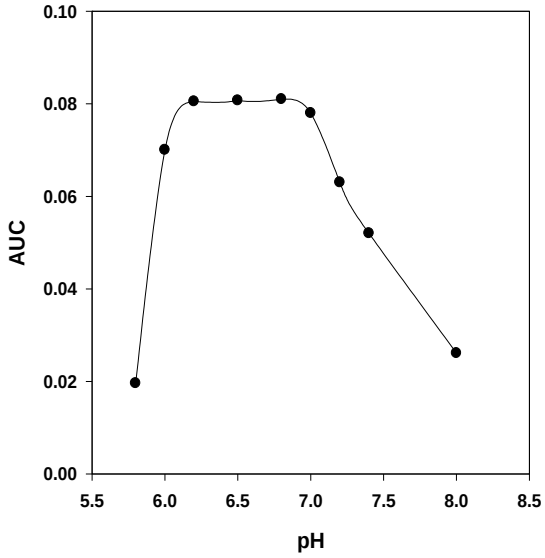

Figure 7: Influence of pH on the ORAC-nile blue method. Experimental conditions: [nile blue] = 120 nM; [buffer] = 0.075 M; [AAPH] = 0.024 M; [Trolox] = 2 μM; temperature = 37 °C.

The influence of the fluorophore concentration was studied in the range of 60 – 370 nM (Figure 8), obtaining that the system was practically independent of this variable in the range of 80 – 130 nM, choosing 89 nM

nile blue concentration for the development of the method. It is worth indicating that the potential use of nile blue doped SiO_2NPs as an alternative to the fluorophore in solution was studied but, as it was foreseen, unsatisfactory results were obtained, owing to the protection provided by the NPs on the fluorescence of the encapsulated dye. The effect of the AAPH concentration on the system was evaluated in the range of 6 to 24 mM, finding that the AUC values of both analyte and blank solutions decrease when the AAPH concentration increases. However, the curves obtained at low AAPH concentrations were less defined and showed a low reproducibility. Thus, a 12 mM AAPH concentration was chosen.

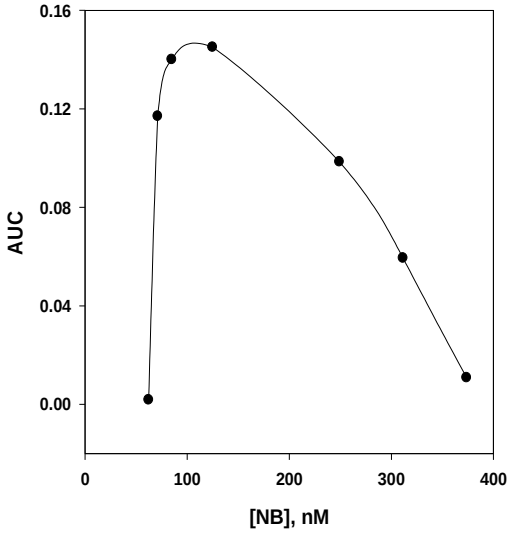

Figure 8: Influence of nile blue concentration on the ORAC-nile blue method. Experimental conditions: [AAPH] = 0.012M; [Trolox] = 2 μM; pH = 6.9; [phosphate] = 0.085 M; temperature = 37 °C.

The dynamic range of the calibration graph was 0.8 – 8 μM Trolox and the detection limit was 0.45 μM, which is lower or similar to those obtained in other ORAC methods involving fluorescein. The precision of the method was assessed at two different Trolox concentrations, 1 and 5 μM, obtaining relative standard deviations of 5.6 and 2.9 %, respectively.

The new method was applied to the analysis of wines and commercial fruit juices and the results were compared to those obtained with the traditional ORAC method. The treatment of the samples was the same for both methods, which just required to adjust the pH until neutral values and the further sample dilution to match the dynamic ranges of the corresponding calibration curves. Table 5 lists the content found in the samples using both methods. The paired *t* test was applied to the results at the 95 % significance level, and it was found that there were not significant differences in the results provided by both methods, which confirms the practical usefulness of the new method described in this Dissertation.

Table 5. Antioxidant capacity of food samples analyzed by ORAC-nile blue and ORAC-fluorescein methods

Sample	ORAC-nile blue[a,b]	ORAC-fluorescein[a,b]
White wine (Manzanilla)	1.50 ± 0.09	1.03 ± 0.2
Semi-dry wine	7.7 ± 0.9	4.4 ± 0.4
Red wine	15.3 ± 0.4	10.4 ± 0.9
Peach juice	2.222 ± 0.001	1.93 ± 0.09
Pineapple juice	2.7 ± 0.3	2.399 ± 0.006
Apple juice	2.7 ± 0.3	3.5 ± 0.4

[a] Mean ± standard deviation (SD) (n=3)
[b] Expressed as millimolar Trolox equivalents of sample

A recovery study was also carried out to validate the method. It was performed by adding three different amounts of Trolox to each sample and subtracting the results obtained from similarly treated unspiked samples. Table 6 shows the recovery percentages, which ranged from 72.7 % to 113.6 %. The mean recovery values obtained were 92.0 and 92.9 % for wine and juice samples, respectively. This internal validation also confirms the usefulness of the developed method for the analysis of real samples.

Tabla 6. Recovery values obtained for the different samples analyzed

	Recovery study		
Sample	Added[a]	Found[a,b]	Recovery (%)
White wine	2.2	2.0 ± 0.2	92.0
	8.9	6.7 ± 0.9	75.2
	11.1	9.2 ± 0.8	82.9
Semi-dry wine	4.4	3.6 ± 0.2	81.8
	8.8	8.1 ± 0.3	92.1
	13.2	12.9 ± 0.6	97.0
Red wine	17.8	18 ± 2	101.1
	35.6	38 ± 4	106.7
	44.4	44 ± 4	99.1
Peach juice	2.2	2.1 ± 0.1	95.5
	4.4	3.5 ± 0.4	79.5
	5.5	4.3 ± 0.2	78.2
Pineapple juice	2.2	2.5 ± 0.2	113.6
	4.4	4.5 ± 0.3	102.3
	5.5	5.8 ± 0.4	105.5
Apple juice	4.4	3.2 ± 0.2	72.7
	8.8	7.9 ± 0.5	89.6
	11.1	11 ± 1	99.1

[a] Units in millimolar Trolox equivalents of sample

[b] Mean ± SD (n=3)

The results obtained show the feasibility of long wavelength fluorimetry for the determination of the antioxidant capacity in food using the fluorophore nile blue. The use of this reagent instead of other fluorophores previously reported for this purpose, such as fluorescein or β-phycoerythrin, is a useful alternative to avoid potential background signals from the sample matrix, which can appear at lower wavelengths. Also, the relatively wide Stokes shift of nile blue reduces the scattering signals. Finally, the probability of photobleaching for nile blue is lower than that for β-phycoerythrin, as well as its cost.

- Automatic determination of polyphenols in wine using laccase and terbium oxide nanoparticles

Polyphenols are an important group of natural antioxidant compounds present in the human diet that, after numerous clinical studies, have shown their usefulness in the prevention of various chronic diseases. As it has been above mentioned, numerous chromatographic [58, 59] and electrophoretic [60, 61] methods have been developed for the determination of these natural antioxidants. However, the high variety of phenolic compounds that can be found in food samples justifies the use of analytical methods to determine total phenolic content and total antioxidant capacity. Both parameters have been widely determined by using photometric or fluorimetric methods involving free radical generators or enzymatic reactions, which compete with the antioxidant in order to inhibit the fluorescence or absorbance decrease observed in absence of these antioxidants [56, 62 – 67].

Laccase is a phenoloxidase enzyme that has been described for the determination of both phenolic content and antioxidant activity, using different experimental conditions. As it has been already mentioned, this enzyme catalyzes the oxidation of phenolic compounds to quinones or radicals by reducing the dissolved oxygen to water, which has been used to develop amperometric sensors [68 – 70] as well as photometric [71 – 73] and fluorimetric [74] methods.

The usefulness of terbium oxide nanoparticles (Tb_4O_7NPs), laccase and the fluorophore 8-hydroxypyrene-1,3,6-trisulfonic acid trisodium salt (HPTS) for the determination of polyphenols in wine samples is described in this Dissertation. As for the method reported in the previous section, fluorescence measurements were carried out in the kinetic mode, by measuring the change of fluorescence over time and using as analytical parameter the net AUC values obtained for different concentrations of gallic acid, which was used as the calibration standard.

Firstly, several potential fluorescent laccase substrates (Styryl 7, 2-Di-1-ASP, azure B chloride, toluidine blue O, nile blue chloride, sodium fluorescein and HPTS) were assayed to study their capability to compete with phenolic antioxidants for the active sites of the enzyme. Although indocyanine green has been described as a laccase substrate [74], it was not assayed because its long excitation and emission wavelengths were not adequate for the microplate reader used in this study. The results obtained from the study of the behavior of the different fluorophores assayed proved that only HPTS showed a relatively fast and remarkable decrease in its fluorescence intensity in the presence of laccase.

As can be seen in Figure 9, the fluorophore HPTS has a phenolic group in its structure, which can explain this behavior, giving rise to its enzymatic oxidation by the dissolved oxygen.

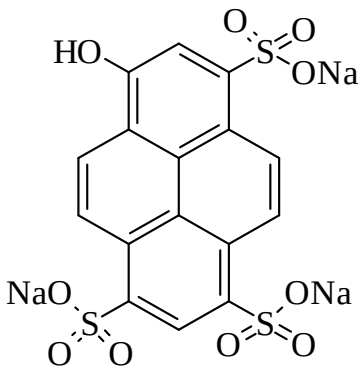

Figure 9. Structure of the fluorophore 8-hydroxypyrene-1,3,6-trisulfonate trisodium (HPTS)

Another investigation carried out to improve the features of the system was the study of the potential activator effect of different NPs on the catalytic behavior of laccase. Several NPs, such as diamond, Eu_2O_3, Tb_4O_7, Ag and magnetic-gold NPs were assayed in the concentration range of 0.1 – 2 mg/mL, finding that only Tb_4O_7NPs notably increased the reaction rate of the system. As can be seen in Figure 10, both blank and analyte AUC decreased, which allows an increase in the sample throughput. Also, the effect of Tb_4O_7NPs on the system was checked in the absence of laccase, finding that the NPs did not modify the fluorescence of HPTS. However, diamond and magnetic-gold NPs caused the fluorescence quenching of HPTS, AgNPs inhibited the catalytic effect of laccase, while

no change in the kinetic behavior of the system was found in the presence of Eu_2O_3NPs.

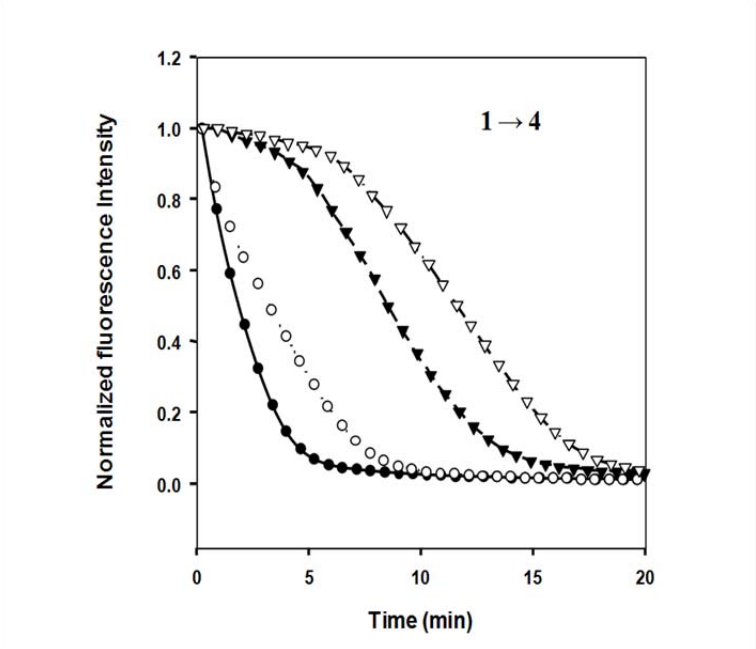

Figure 10. Kinetic curves obtained for the HPTS-laccase system in the absence (curves 1 and 2) and in the presence (curves 3 and 4) of 2 μM gallic acid, and in the presence (curves 1 and 3) and in the absence (curves 2 and 4) of 1mg/mL Tb_4O_7 NPs. [HPTS] = 10 μM, [laccase] = 1 U/mL, pH = 7.0, [phosphate] = 0.4 M, temperature = 37 °C.

The potential use of terbium(III) ions in solution, instead of Tb_4O_7NPs, was also studied using a concentration equivalent to that of the NPs, but lower net AUC values were obtained. These results show the usefulness of these NPs as activators of the enzymatic system.

The variables affecting the system were optimized by the univariate method using the net AUC as the analytical parameter. However, it was

necessary to find a compromised solution between this parameter and the time required for each measurement, in order to obtain an adequate sensitivity but avoiding the excessive duration of the assay.

The influence of the pH on the system was studied in the range of 4.0 – 9.0 using different buffer solutions. The fluorescence of HPTS was very low at acid pH values and very high in the range of 8.0 - 9.0, but laccase did not show any enzymatic activity at the higher pH values. However, the HPTS fluorescence intensity was high enough at pH 7.0 – 7.5 and decreased in the presence of laccase. Thus, a pH of 7.0 was selected for the method development, using a 0.4 M phosphate buffer solution to adjust this pH value. The study of the influence of the HPTS concentration demonstrated that the system was independent of this variable in the range of 8 – 12 μM, and the intermediate value (10 μM) was chosen as the optimum concentration.

The laccase activity and the Tb_4O_7NPs concentration are two critical variables that have a remarkable effect on both the net AUC and the reaction rate. Both variables were studied in the ranges of 0.5 – 2 U/mL and 0.2 – 2 mg/mL for laccase activity and Tb_4O_7NPs concentration, respectively. High values of both variables gave rise to very high reaction rates and low net AUC values, which negatively affected the method sensitivity. On the contrary, very low values of these variables caused a notable increase of the net AUC and, therefore, the improvement of the method sensitivity, but the duration of the assay was excessively long. Thus, the values selected to obtain appropriate net AUC and duration of the process were 1 U/mL laccase activity and 1 mg/mL NPs concentration.

As it has been above mentioned, the analytical parameter used in this method was the net AUC, obtained from the normalized kinetic curves for different gallic acid concentrations. Figure 11 show the kinetic curves obtained to λ_{ex} 450 nm y λ_{em} 535 nm under the optimum experimental conditions.

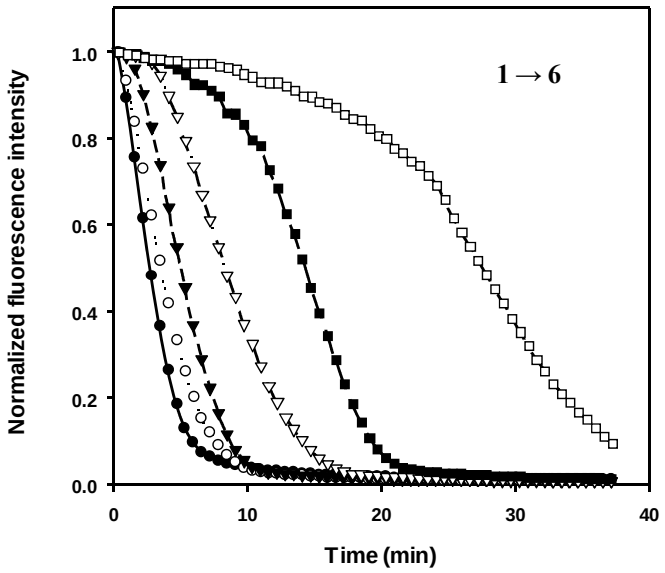

Figure 11. Kinetic curves obtained for different gallic acid concentrations: (1) (1) 0 μM, (2) 0.5 μM, (3) 1 μM (4) 2 μM (5) 5 μM y (6) 10 μM. Experimental conditions: [HPTS] = 10 μM, [laccasa] = 1 U/mL, [NPs] = 1 mg/mL, pH = 7.0, [phosphate] = 0.4 M, temperature = 37 ^{o}C.

The dynamic range of the calibration graph was 0.5 – 12 μM gallic acid and the detection limit was 0.14 μM, which is about three times lower than that obtained in the absence of Tb_4O_7 NPs (0.4 μM). This difference shows the positive effect of the NPs on the method, improving both the reaction rate and the detection limit. The detection limit reached in the presence of the NPs is lower than those described for gallic acid using

some amperometric biosensors, which were ranged between 0.19 and 50 μM [69, 70]. Although a detection limit for gallic acid of 0.04 μM has been obtained using indocyanine green [74], this method involves the sequential analysis of each sample, obtaining lower sample throughput. The precision of the method, expressed as the percentage of relative standard deviation, was assessed at 0.7 and 5 μM gallic acid concentrations, providing values of 6.3 and 2.5 %, respectively.

The selectivity of the method was checked by assaying some non-phenolic reducing substances, which could be present in the wine samples used to demonstrate the applicability of the method. Table 7 shows the results obtained after assaying different potential interfering compounds. The most serious interference was caused by ascorbic acid, which was tolerated at the same molar concentration than that of the analyte. However, this interference would be negligible because the maximum limit allowed for ascorbic acid when used as an additive in wine is 0.85 mM [75], which is lower than the usual content of polyphenols in wines. Sulfites were tolerated in a concentration 20-fold that of the analyte. Although this interference could be removed using a pre-treatment step [70], it was not necessary as the presence of sulfites is controlled according to their total content in reducing substances [76].

Table 7. Influence of some reducing agents on the proposed determination of phenolic antioxidants at 2 μM gallic acid

Compound	Maximum tolerated interferent/analyte ratio*
Malic acid	100
Citric acid	100
Sucrose	100
Glucose	25
Sodium sulfite	20
Ascorbic acid	1

*Maximum ratio assayed was 100

The method was applied to the analysis of red, white and sweet wines. The sample treatment only required the dilution of the sample to match the dynamic range of the calibration curve, using gallic acid standards and the net AUC as analytical parameter. Table 8 shows the content of polyphenols found in these samples analyzed by the new method and by the Folin-Ciocalteu method, which is usually considered as a reference method.

Table 8. Antioxidant concentration (expressed as millimolar equivalents of gallic acid) for each sample

Sample	Proposed method	Folin-Ciocalteu method[a,b]
Red wine (Rioja)	7.0 ± 0.4	11.5 ± 0.1
Red wine (Cuenca)	9.5 ± 0.5	14.04 ± 0.18
White wine (Rueda)	1.00 ± 0.06	1.92 ± 0.04
White wine (Valdepeñas)	1.00 ± 0.03	2.028 ± 0.005
Sweet wine (Montilla)	1.27 ± 0.09	3.64 ± 0.05

[a]Mean ± SD (n=3)
[b]Units: mM gallic acid equivalents of sample

As it can be seen from the Table 8, the values provided by the Folin-Ciocalteu method were higher in all instances than those provided by the laccase method, which is ascribed to the capability of the later to also detect non-phenolic substances. The values obtained by the new method are similar to those obtained using other methods for the analysis of this type of samples [68, 69].

A recovery study was performed by adding three different amounts of gallic acid to each sample and subtracting the results obtained from similarly treated unspiked samples. As it can be seen in the Table 9, the recovery percentages obtained ranged from 81.0 to 108.3 % and the mean recoveries for red, white and sweet wines were 90.9, 92.4 and 99.5 %, respectively.

Table 4. Recovery study for the wine samples analyzed

Sample	Added[a]	Found[a,b]	Recovery (%)
Red wine (La Rioja)	4	4.3 ± 0.5	108.3
	12	10.0 ± 0.5	84.1
	20	16 ± 1	81.0
Red wine (Cuenca)	4	3.2 ± 0.2	80.0
	12	11.7 ± 0.3	97.4
	20	18.9 ± 0.8	94.5
White wine (Rueda)	0.25	0.24 ± 0.03	97.2
	0.75	0.77 ± 0.04	102.8
	1.25	1.08 ± 0.03	86.7
White wine (Valdepeñas)	0.25	0.23 ± 0.03	92.0
	0.75	0.70 ± 0.04	92.2
	1.25	1.0 ± 0.1	83.3
Sweet wine (Montilla)	1	1.01 ±0.09	101.5
	3	3.0 ± 0.3	102.0
	5	4.7 ± 0.3	95.0

[b]Mean ± SD (n=3)

[a]Units: mM gallic acid equivalents of sample

The results obtained evidence the usefulness of the combined use of laccase, Tb_4O_7NPs and the fluorophore HPTS for the determination of polyphenols in wine samples. It is noteworthy to mention that the activator effect of Tb_4O_7NPs on an enzymatic system is described for the first time. The use of laccase and NPs increases the sample throughput of the method and improves the sensibility, being these values better than those obtained for other methods previously described [68, 69]. Also, the use of an automatic microplate reader enables the simultaneous processing of the samples, reaching an overall sample throughput of about 35 samples h^{-1}, when analyzed in triplicate.

3. New investigations in the use of upconverting phosphors in luminescence resonance energy transfer

This study was developed during the three-month stay at the Department of Biotechnology of the University of Turku (Finland). Due to the short duration of this period, the research was focused to the systematic evaluation of several donors and acceptors to design a luminescence resonance energy transfer system (LRET) using the anti-Stokes phenomenon in biotin-streptavidin affinity assays. This study aimed the selection of the most appropriate system for its subsequent analytical application.

As it has been described in the Introduction of this dissertation, upconverting phosphors (UCPs) are composed of inorganic host lattices usually doped with lanthanide ions to achieve the phenomenon of anti-Stokes fluorescence emission. The research presented here reports a

systematic study of the behavior of different UCPs doped with Er(III), Ho(III) and Tm(III), used as donors, and several fluorophores, used as acceptors, to develop new methodologies based in the LRET phenomenon. Two main requirements have to be fulfilled for this process to happen: 1) The excitation spectrum of the acceptor should overlap with the donor emission spectrum; 2) The distance between donor and acceptor should follow the Förster equation.

Among the wide variety of existing fluorophores, phycobiliproteins, such as β-phycoerythrin (BPE) and R-phycoerythrin (RPE) have been previously used as acceptors in different LRET assays [77 – 79]. Their use is mainly due to their excellent fluorescence emission, although their price is relatively high. For this reason, the possibility to use less costly fluorophores, such as Alexa Fluor or ATTO, to develop LRET affinity assays has been studied. These fluorophores could also be used to develop multiplexed assays, since they feature different excitation and emission wavelengths. To perform this systematic study between donors and acceptors, streptavidin (SA) was used to coat UCP donors, whereas biotin (Bio) was coupled to fluorescent acceptors.

Figure 12 shows the excitation and emission spectra of the different donor-acceptor pairs used in this study. Figures 12.A-12.C show the combination between the UCP doped with Er(III) and the fluorescent protein BPE and Alexa Fluor 546 (AF546) and 680 (AF680) fluorophores. As it can be seen, there is an excellent overlap between the emission and excitation spectra of donors and acceptors, respectively..

Similar spectra were obtained when the UCPs doped with Ho(III) (Figure 12.D-12.E) were assayed with BPE and AF546. In a similar way to the Er(III)-doped UCP behavior, the wide excitation spectrum of BPE allows its efficient excitation while the energy transfer using AF546 shows a lower yield.

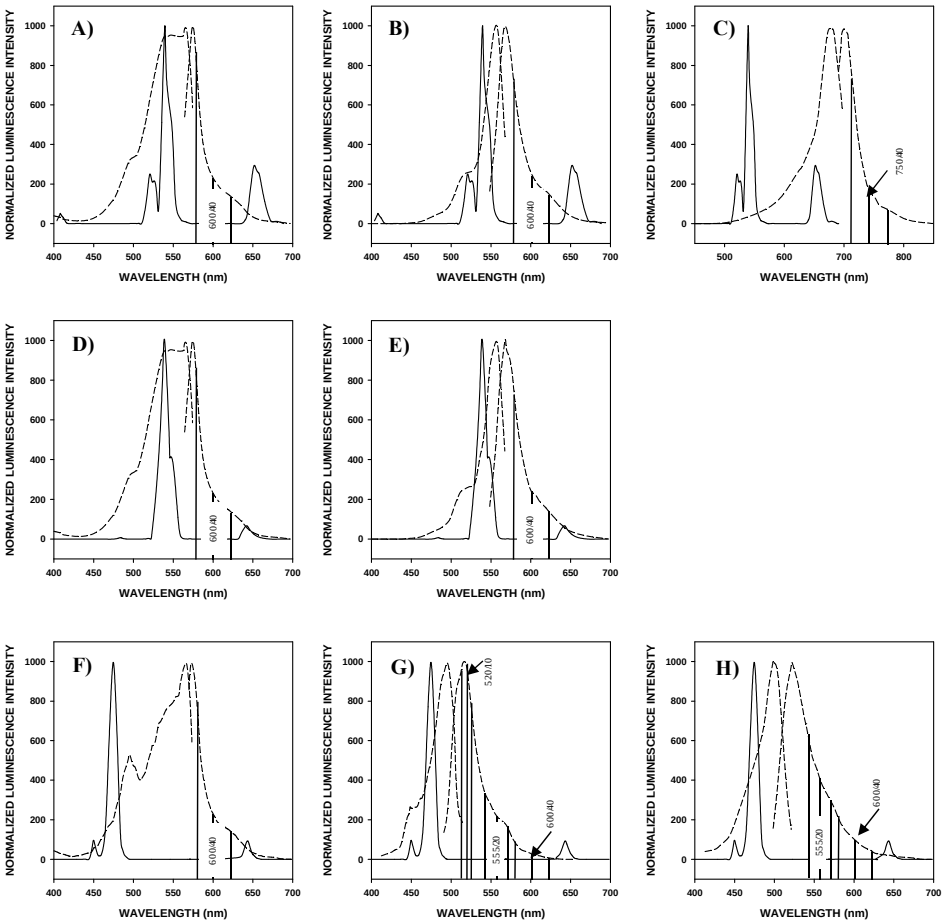

Figure 12. Emission spectra from UCPs and acceptors used in this study. In 12.A-12.C, Er(III)-doped UCP emission spectra together with BPE (12.A), AF546 (12.B) and AF680 (12.C). In 12.D and 12.E, Ho(III)-doped UCPs with BPE (12.D) and AF546 (12.E). In 12.F-12.H, Tm(III)-doped UCPs with RPE (12.F), AF488 (12.G) and ATTO495 (12.H).

The Tm(III)-doped UCPs were combined with RPE, Alexa Fluor 488 (AF488) and ATTO495 fluorophores (Figure 12.F-12.H). In this case, the donor has a lower emission wavelength than Er(III) and Ho(III), with a good theoretical overlap with the AF488 fluorophore, although, as it will be discussed below, an appropriate theoretical overlap does not always provide a suitable energy transfer process.

As has been described in the Introduction of this Dissertation, the absence of functional groups in this type of inorganic nanomaterials makes it essential to perform a coating and functionalization process, before they can be linked to biomolecules. After this step, the different donors and acceptors were labeled with SA and Bio, respectively, to carry out the optimization of their concentrations and, finally, to obtain the calibration curves under the best conditions for biotin, which was used as model analyte.

The possibility of designing LRET systems using alternative fluorophores to the phycobiliproteins BPE and RPE, in order to avoid their relatively high cost, was studied. Figure 13 shows the titration curves obtained with Er(III)-SA (13.A), Ho(III)-SA (13.B) and Tm(III)-SA-doped UCPs as donors, combined with different fluorophores. Luminescence emission was obtained in all instances, but the best results were achieved with the Er(III)-BPE, Er(III)-AF680, Ho(III)-BPE and Tm(III)-RPE pairs, which were used to obtain the titration curves for biotin. As it can be seen from Figure 13, the highest luminescence intensities were obtained for Er(III)-doped UCPs with BPE and AF680.

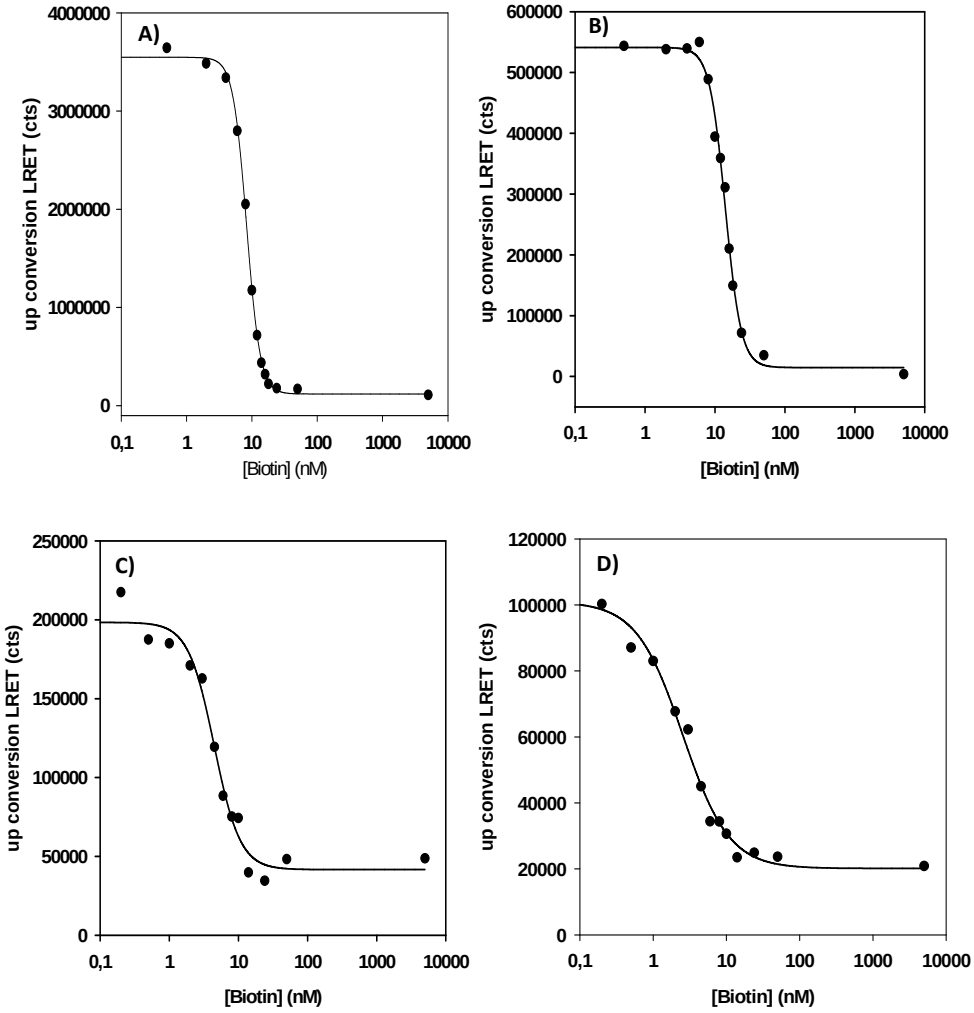

Figure 13. Homogeneous LRET affinity assays for biotin with donor-acceptor pairs giving the best results. In A) with Er(III)-doped UCP (0.015 mg/mL) and (1) 0.4 nM BPE and (2) 4 nM AF680. In (B) Ho(III)-doped UCP (0.030 mg/mL) and 0.4 nM BPE. In (C) Tm(III)-doped UCP (0.030 mg/mL) and 1.33 nM RPE. LRET signals were calculated by subtracting the background signal of the assay (excess of biotin) from the maximum signal (absence of biotin), cts: counts.

However, according to the results shown in Table 10, which summarizes the different assays carried out and the IC50 values obtained for biotin, the lowest value for this parameter was achieved with the pair SA-Tm(III)-UCP with RPE, in spite of its low LRET intensity. The highest IC50 was obtained for the SA-Er(III)-doped UCP with AF680, which was about 14.4 nM. The values obtained are comparable and, in some instances, better than those obtained by other previously reported methods [77, 78] using Er(III)-doped UCPs as donors and BPE as acceptor.

Table 10. IC50 values for biotin assays using different donor-acceptor pairs

	IC50 for biotin (nM)			
Acceptor / Donor	**Bio-BPE (0.2 nM)**	**Bio-BPE (0.4 nM)**	**Bio-RPE (1.33 nM)**	**Bio-AF680 (4 nM)**
Er(III)-doped UCP (0.015 mg/mL)	---	8.57*	---	14.37
Ho(III)-doped UCP, 0.015 mg/mL)	5.7	---	---	---
Ho(III)-doped UCP, 0.015 mg/mL)	---	7.20	---	---
Tm(III)-doped UCP (0.030 mg/mL)	---	---	3.35	---

*The concentration of Bio-BPE was 0.3 nM

In summary, it is possible to draw several conclusions after the systematic study carried out to evaluate the potential usefulness of several

UCPs as donors and several fluorophores as acceptors in LRET systems: 1) The donor UCP-Er(III) provides the best results when it is used together with Bio-BPE as acceptor; 2) The use of the fluorophore AF680 as alternative acceptor to phycobiliproteins provides a high fluorescent signal, although the IC50 value reached for biotin is higher than that obtained in presence of the phycobiliproteins. Nevertheless, the use of this fluorophore also allows the determination of biotin at nanomolar concentration level, avoiding the relatively high cost of these phycobiliproteins.

As a final summary of this chapter, the main advantages and limitations of the new analytical methodologies developed in this Dissertation are included in the following table:

Advantages	**Limitations**
LWF-doped SiO_2NPs	
• Synthesis procedures using reverse-micelle microemulsion method are reproducible • Increased stability compared to the fluorophores in solution • Many functionalization procedures are feasible owing to the great variety of organosilane reagents • Improvement of spectral selectivity • The heterogeneous immunoassays improve some features of ELISAs methods used for this purpose since: – Lower detection limits are obtained – Lesser steps are required, so they are simpler to perform.	• These NPs are not commercially available • A previous study of the synthesis conditions needs to be done according to physical chemical properties of the LWF

New methods for antioxidant determination	
• **Long-wavelength ORAC assay** – Decrease of light scattering phenomena – Improvement of spectral selectivity • **Determination of polyphenols using laccase and Tb_4O_7NPs** – Lower detection limits than those provided by biosensors – The use of Tb_4O_7 NPs also allows: o A decrease of the amount of enzyme required o Shorter assay times – Tb_4O_7NPs are commercially available	• Lack of standardised methods • The enzyme cannot be re-used
Systematic study of UCPs in LRET phenomena	
• Interference of sample matrices is decreased owing to excitation in the IR region of spectrum • It is posible to obtain LRET from different donor-acceptor pairs, so the feasibility of multiplexed systems can expand the application field of this technique • Fluorophores other than phycobiliproteins can be used to develop LRET assays, which can decrease the costs of these assays	• Conventional spectro-fluormeters can not be used

References

(1) A. Gómez-Hens, J.M. Fernández-Romero, M. P. Aguilar-Caballos. Nanostructures as analytical tools in bioassays. *Trends Anal. Chem.* **(2008)** *27*, 394 – 406.

(2) J. Yan, M. C. Estévez, J. E. Smith, K. Wang, X. Ho, L. Wang, W. Tan. Dye-doped nanoparticles for bioanalysis. *Nanotoday* **(2007)** *2*, 44 – 50.

(3) M. Seydack. Nanoparticles labels in immunosensing using optical detection methods. *Biosens. Bioelectron.* **(2005)** *20*, 2454 – 2469.

(4) N. C. Tansil, Z. Gao. Nanoparticles in biomolecular detection. *Nanotoday* **(2006)** *1*, 28 – 37.

(5) G. Liu, Y. Lin. Nanomaterial labels in electrochemical immunosensors and immunoassays. *Talanta* **(2007)** *74*, 308 – 317.

(6) F. J. Arriagada, K. Osseo-Asare. Synthesis of nanosize silica in a noionic water-in-oil microemulsion: effects on the water/surfactant molar ratio and ammonia concentration. *J. Colloid Interf. Sci.* **(1999)** *211*, 210 – 220.

(7) G. Yao, L. Wang, G. Wu, J. Smith, J. Xu, W. Zhao, E. Lee, W. tan. FlotDots: luminescent nanoparticles. *Anal. Bioanal. Chem.* **(2006)** *385*, 518 – 524.

(8) X. He, J. Chen, K. Wang, D. Qin, W. Tan. Preparation of luminescent Cy5 doped core-shell SFNPs and its application as a near-infrared fluorescent marker. *Talanta* **(2007)** *72*, 1519 – 1526.

(9) X-L. Chen, J-L. Zou, T-T. Zhao, Z-B. Li. Preparation and fluoroimmunoassay application of new red-region fluorescent silica nanoparticles. *J. Fluoresc.* **(2007)** *17*, 235 – 241.

(10) W. Yang, C-G. Zhang, H-Y. Qu, H-H. Yang, J-G. Xu. Novel fluorescent silica nanoparticle probe for ultrasensitive immunoassays. *Anal. Chim. Acta* **(2004)** 503, 163 – 169.

(11) Z. Zhang, F. Zhang, Y. Liu. Recent advances in enhancing the sensitivity and resolution of capillary electrophoresis. *J. Chromatogr. Sci.* **(2013)** *51*, 666 – 683.

(12) G. A. Saleh, H. F. Askal, I. H. Refaat, F. A. M. Abdel-Aal. Review on recent separation methods for determination of some fluoroquinolones. *J. Liq. Chromatogr.* **(2013)** *36*, 1401 – 1420.

(13) M. Szultka, B. Buszewki, K. Papaj, W. Szeja, A. Rusin. Determination of flavonoids and their metabolites by chromatographic techniques. *Trends Anal. Chem.* **(2013)** *47*, 47 – 67.

(14) B. Tang, K. H. Row. Development of gas chromatography analysis of fatty acids in marine organisms. *J. Chromatogr. Sci.* **(2013)** *51*, 599 – 607.

(15) I. G. Zenkevich, Y. S. Drugov. Gas chromatographic methods for the determination of trace organic pollutans in environmental samples. *J. Anal. Chem.* **(2013)** *68*, 845 – 861.

(16) C. T. Elliot, D. G. Kennedy, W. J. McCaughey. Methods for the detection of polyether ionophore residues in poultry. *Analyst* **(1998)** *123*, 45R – 56R.

(17) M. Sokolic, M. Pokorny. Comparative determination of salinomycin by high-performance liquid chromatography,

microbiological and colorimetric methods in testing production processes and animal feed preparations. *J. Pharmaceut. Biomed.* **(1991)** *9*, 1047 – 1053.

(18) S. Magiera. Fast, simultaneous quantification of three novel cardiac drugs in human urine by MEPS-UHPLC-MS/MS for therapeutic drug monitoring. *J. Chromatogr. B* **(2013)** *938*, 86 – 95.

(19) R. Ciayadi, G. F. Kelso, M. K. Potdar, S. J. Harris, K. L. Walton, C. A. Harrison, M. T. W. Hearn. Identification of protein binding partners of ALK-5 Kinase inhibitors. *Bioorgan. Med. Chem.* **(2013)** *21*, 6496 – 6500.

(20) G. Pierri, D. Kotoni, P. Simone, C. Villani, G. Pepe, P. Campiglia, P. Dugo, F. Gasparrini. Analysis of bovine milk caseins on organic monolithic columns:An integrated capillary liquid chromatography-high resolution mass spectrometry approach for the study of time-dependent casein degradation. *J. Chromatogr. A* **(2013)** *1313*, 259 – 269.

(21) T. F. McGrath, C. T. Elliot, T. L. Fodey. Biosensors for the analysis of microbiological and chemical contaminants in foods. *Anal. Bioanal. Chem.* **(2012)** *403*, 75 – 92.

(22) X. Pei, B. Zhang, J. Tang, B. Liu, W. Lai, D. Tang. Sandwich-type immunosensors and immunoassays exploiting nanostructure labels: A review. *Anal. Chim. Acta* **(2013)** *758*, 1 – 18.

(23) S. Girotti, S. Ghini, E. Maiolini, L. Bolelli, E. N. Feri. Trace analysis of pollutants by use of honeybees, immunoassays, and chemiluminescence detection. *Anal. Bioanal. Chem.* **(2013)** *405*, 555 – 571.

(24) L. Anfossi, C. Baggiani, C. Giavannoli, G. D´Arco, G. Giraudi. Lateral-flow immunoassays for mycotoxins and phycotoxins: A review. *Anal. Bioanal. Chem.* **(2013)** *405*, 467 – 480.

(25) D. L. Brandon, M. Friedman. Immunoassays of Soy Proteins. *J. Agr. Food Chem.* **(2002)** *50*, 6635 – 6642.

(26) M. A. J. Godfrey, M. F. Luckey, P. Kwasowski. IAC/cELISA detection of monensin elimination from chicken tissues, following oral therapeutic dosing. *Food Add. Contam.* **(1997)** *14*, 281 – 286.

(27) S. R. H. Crooks, T. L. Fodey, G. R. Gilmore, C. T. Elliot. Rapid screening for monensin residues in poultry plasma by a dry reagent dissociation enhanced lanthanide fluoroimmunoassay. *Analyst* **(1998)** *123*, 2493 – 2496.

(28) V. Hagren, P. Peippo, M. Tuomola, T. Lövgren. Rapid time-resolved fluoroimmunoassay for the screening of monensin residues in eggs. *Anal. Chim. Acta* **(2006)** *557*, 164 – 168.

(29) C. Cháfer-Pericás, A. Maquieira, R. Puchades. Functionalized inorganic nanoparticles used as labels in solid-phase immunoassays. *Trends Anal. Chem.* **(2012)** *31*, 144 – 156.

(30) A. Gómez-Hens, J. M. Fernández-Romero, M. P. Aguilar-Caballos. Nanostructures as analytical tolos in bioassays. *Trends Anal. Chem.* **(2008)** *27*, 394 – 406.

(31) D. Knopp, D. Tang, R. Niessner. Review: Bioanalytical applications of biomolecule-functionalized nanometer-sized doped silica nanoparticles. *Anal. Chim. Acta* **(2009)** *647*, 14 – 30.

(32) M. A. J. Godfrey, M. F. Luckey, P. Kwasowski. IAC/cELISA detection of monensin elimination from chicken tissues, following oral therapeutic dosing. *Food Addit. Contam.* **(1997)** *14*, 281 – 286..

(33) M. Hazansadeh, N. Shadjou, E. Omidina, M. Eskandani, M. de la Guardia. Mesoporous silica materials for use in electrochemical immunosensing. *TrAC – Trends Anal. Chem.* **(2013)** *45*, 93 – 106.

(34) X. Zhao, L. R. Hilliard, S. J. Mechery, Y. Wang, R. P. Bagwe, S. Jin, W. Tan. A rapid bioassay for single bacterial cell quantitation using bioconjugated nanoparticles. *P. Ntl. Aca. Sci. USA* **(2004)** *101*, 15027 – 15032.

(35) R. Tapec, X. J. Zhao, W. Tan. Development of organic dye-doped silica nanoparticles for bioanalysis and biosensors. *J. Nanosci. Nanotech.* **(2002)** *2*, 405 – 409.

(36) H-H. Yang, H-Y. Qu, P. Lin, S-H. Li, M-T. Ding, J-G. Xu. Nanometer fluorescent hybrid silica particle as ultrasensitive and photostable biological labels. *Analyst* **(2003)** *128*, 462 – 466.

(37) W. Yang, C. G. Zhang, H. Y. Qu, H. H. Yang, J. G. Xu. Novel fluorescent silica nanoparticles probe for ultrasensitive immunoassays. *Anal. Chim. Acta* **(2004)** *503*, 163 – 169.

(38) M. Tan, G. Wang, X. Hai, Z. Ye, J. Yuan. Development of functionalized fluorescent europium nanoparticles for biolabelling and time-resolved fluorometric applications. *J. Mater. Chem.* **(2004)** *14*, 2896 – 2901.

(39) Z. Ye, M. Tan, G. Wang, J. Yuan. Novel fluorescent europium chelate-doped silica nanoparticles: preparation, characterization

and time-resolved fluorometric application. *J. Mater. Chem.* **(2004)** *14*, 851 – 856.

(40) Z. Ye, M. Tan, G. Wang, J. Yuan. Preparation, Characterization, and time-resolved fluorometric application of silica-coated terbium (III) fluorescent nanoparticles. *Anal. Chem.* **(2004)** *76*, 513 – 518.

(41) L. L´Hocine, J. I. Boye, C. Munyana. Detection and quantification of soy allergens in food: study of two commercial enzyme-linked immunosorbent assays. *J. Food Sci.* **(2007)** *72*, C145 - C153.

(42) M. L. Sánchez-Martínez, M. P. Aguilar-Caballos, A. Gómez-Hens. Homogeneous immunoassay for soy protein determination in food samples using gold nanoparticles as labels and light scattering detection. *Anal. Chim. Acta* **(2009)** *636*, 58 – 62.

(43) Opinion of the scientific panel on contaminants in the food chain. *EFSA Journal* **(2008)** *592*, 1 – 40.

(44) Regulation (EC) No 1831/2003 of the European Parliament and of the Council of 22 Septembre 2003 on additives for use in animal nutrition. *Official Journal of European Union* **(2003)** *L268*, 29 – 43.

(45) H. Watanabe, A. Satake, M. Matsumoto, Y. Kido, A. Tsuji, K. Ito, M. Maeda. Monoclonal-based enzyme-linked immunosorbent assay and immunochromatographic rapid assay for monensin. *Analyst* **(1998)** *123*, 2573 – 2578.

(46) Monensin ELISA kit (Cat # KA1422 V.01), http://www.abnova.com/.

(47) Monensin ELISA. Enzyme-linked immunosorbent assay for the determination of monensin in feed and contaminated samples. http://abraxiskits.com/.

(48) S. R. H. Crooks, I. M. Traynor, C. T. Elliott, W. J. McCaughey. Detection of monensin residues in poultry liver using an enzyme immunoassay. *Analyst* **(1997)** *122*, 161 – 163.

(49) M. Ciz, H. Cizova, P. Deneb, M. Kratchanova, A. Slavov, A. Lojek. Different methods for control and comparison of the antioxidant properties of vegetables. *Food Control* **(2010)** *21*, 518 – 523.

(50) E. Atala, L. Vásquez, H. Speisky, E. Lissi, C. López-Alarcón. Ascorbic acid contribution to ORAC values in berry extracts: An evaluation by the ORAC-pyrogallol red methodology. *Food Chem.* **(2009)** *113*, 331 – 335.

(51) M. D. Rivero-Pérez, M. L. González-Sanjosé, M. Ortega-Herás, P. Muñiz. Antioxidant potential of single-variety red wines aged in the barrel and in the bottle. *Food Chem.* **(2008)** *111*, 957 – 964.

(52) E. Sofic, Z. Rimpapa, Z. Kundurovic, A. Sapcanin, I. Tahirovic, A. Rustembegovic, G. Cao. Antioxidant capacity of the neurohormone melatonin. *J. Neural Transm.* **(2005)** *112*, 349 – 358.

(53) G. Cao, H. M. Alessie, R. G. Cutler. Oxygen-radical absorbance capacity assay for antioxidants. *Free Radical Bio. Med.* **(1993)** *14*, 303 – 311.

(54) W. Mullen, S. C. Marks, A. Crozier. Evaluation of phenolic compounds in commercial fruit juices and fruit drinks. *J. Agr. Food Chem.* **(2007)** *55*, 3148 – 3157.

(55) J. Tabart, C. Kevers, J. Pincemail, J. O. Defraigne, J. Dommes. Comparative antioxidant capacities of phenolic compounds measured by various tests. *Food Chem.* **(2009)** *113*, 1226 – 1233,

(56) L. Müller, S. Groyke, A. M. Popken, V. Böhm. Antioxidant capacity and related parameters of different fruit formulations. *Food Sci. Technol.* **(2010)** *43*, 992 – 999.

(57) N. Nenadis, O. Lazaridou, M. Z. Tsimidou. Use of reference compounds in antioxidant activity assessment. *J. Agr. Food Chem.* **(2007)** *55*, 5452 – 5460.

(58) B. Lorrain, I. Ky, L. Pechamat, P. L. Teissedre, Evolution of analysis of polyphenols from grapes, wines, and extracts. *Molecules* **(2013)** *18*, 1076 - 1100.

(59) M. Medić-Ŝarić, V. Rastija, M. Bojić. Recent advances in the application of high performance liquid chromatography in the analysis of polyphenols in wine and propolis. *J. AOAC Int*. **(2011)** *94*, 32 - 42.

(60) H. Franquet-Griell, A. Checa, O. Núñez, J. Saurina, S. Hernández-Cassou, L. Puignou. Determination of polyphenols in Spanish wines by capillary zone electrophoresis. Application to wine characterization by using chemometrics. *J. Agr. Food. Chem*. **(2012)** *60*, 8340 - 8349.

(61) A. Sánchez-Arribas, M. Martínez-Fernández, M. Chicharro. The role of electroanalytical techniques in analysis of polyphenols in wine. *Trends Anal. Chem*. **(2012)** *34*, 78 - 96.

(62) L. M. Magalhães, M. A. Segundo, S. Reis, J. L. C. Lima, A. O. S. S. Rangel. Automatic method for the determination of Folin-Ciocalteu reducing capacity in food products. *J. Agr. Food Chem*. **(2006)** *54*, 5241 - 5246.

(63) J. C. Sánchez-Rangel, J. Benavides, J. B. Heredia, L. Cisneros-Zevallos, D. A. Jacobo-Velázquez. The Folin-Ciocalteu assay revisited: improvement of its specificity for total phenolic content determination. *Anal. Methods* **(2013)** *5*, 5990 - 5999.

(64) J. Sochor, M. Ryvolova, O. Krystofova, P. Salas, J. Hubalek, V. Adam, L. Trnkova, L. Havel, M. Beklova, J. Zehnalek, I. Provaznik, R. Kizek. Fully automated spectrometric protocols for determination of antioxidant activity: advantages and disadvantages. *Molecules* **(2010)** *15*, 8618 - 8640.

(65) A. L. Dawidowicz, D. Wianowska, M. Olszowy. On practical problems in estimation of antioxidant activity of compounds by DPPH method (Problems in estimation of antioxidant activity). *Food Chem*. **(2012)** *131*, 1037-1043.

(66) E. Nkhili, P. Brat. Reexamination of the ORAC assay: effect of metal ions. *Anal. Bioanal. Chem*. **(2011)** *400*, 1451 - 1458.

(67) J. Godoy-Navajas, M. P. Aguilar-Caballos, A. Gómez-Hens. Long-wavelength fluorimetric determination of food antioxidant capacity using nile blue as reagent. *J. Agr. Food Chem*. **(2011)** *59*, 2235-2240.

(68) M. Gamella, S. Campuzano, A. J. Reviejo, J. M. Pingarrón. Electrochemical estimation of the polyphenol index in wines using a laccase biosensor. *J. Agric. Food Chem.* **(2006)** *54*, 7960 - 7967.

(69) M. Di Fusco, C. Tortolini, D. Deriu, F. Mazzei. Laccase-based biosensor for the determination of polyphenol index in wine. *Talanta* **(2010)** *81*, 235 - 240.

(70) M.R. Montereali, L. Della Seta, W. Vastarella, R. Pilloton. A disposable laccase-tyrosinase based biosensor for amperometric

detection of phenolic compounds in must and wine. *J. Mol. Catal. B-Enzym*. **(2010)** *64*, 189 - 194.

(71) J. Kulys, I. Bratkovskaja. Antioxidants determination with laccase. Talanta **(2007)** *72*, 526 – 531.

(72) E. Nugroho Prasetyo, T. Kudanga, W. Steiner, M. Murkovic, G. S. Nyanhongo, G. M. Guebitz. Laccase-generated tetramethoxy azobismethylene quinone (TMAMQ) as a tool for antioxidant activity measurement, *Food Chem*. **(2010)** *118*, 437 - 444.

(73) E. Nugroho Prasetyo, T. Kudanga, W. Steiner, M. Murkovic, G. S. Nyanhongo, G. M. Guebitz. Antioxidant activity assay based on laccase-generated radicals. *Anal. Bioanal. Chem*. **(2009)** *393*, 679 - 687.

(74) A. Andreu-Navarro, J. M. Fernández-Romero, A. Gómez-Hens. Determination of polyphenolic content in beverages using laccase, gold nanoparticles and long wavelength fluorimetry. *Anal. Chim. Acta* **(2012)** *713*, 1-6.

(75) J. Robinson (Ed.) "Oxford companion to wine" 3rd edition. (2006) 35 – 36.

(76) Maximum acceptable limits of various substances contained in wine. *Compendium of International Methods of Analysis*, OIV, OIV-MA-C1-01:R2011.

(77) K. Kuningas, T. Rantanen, T. Ukonaho, T. Lövgren, T. Soukka. Homogeneous assay technology based on upconverting phosphors. *Anal. Chem.* **(2005)** *77*, 7348 – 7355

(78) K. Kuningas, T. Ukonaho, H. Pakkilä, T. Rantanen, J. Rosenberg, T. Lövgren, T. Soukka. Upconversion fluorescence resonance energy

transfer in a homogeneous immunoassay for estradiol. *Anal. Chem.* **(2006)** *78*, 4690 – 4696.

(79) T. Rantanen, H. Päkkilä, L. Jämsen, K. Kuningas, T. Ukonaho, T. Lövgren, T. Soukka. Tandem dye acceptor used to enhance upconversion fluorescence resonance energy transfer in homogeneous assays. *Anal. Chem.* **(2007)** *79*, 6312 – 6318.

CONCLUSIONES

CONCLUSIONS

Las investigaciones presentadas en esta Memoria han contribuido a expandir la aplicabilidad de la Nanotecnología al análisis de alimentos mediante el desarrollo de diversos métodos que presentan niveles adecuados de sensibilidad y selectividad. El uso de microplacas ha permitido la automatización de estos métodos con un bajo consumo de muestras y reactivos y una elevada velocidad de muestreo. A partir del trabajo realizado se extraen las siguientes conclusiones:

- Se han sintetizado nanopartículas de sílice dopadas con los fluoróforos de larga longitud de onda violeta de cresilo y azul nilo. La utilización de estos nanomateriales con fines analíticos permite mejorar simultáneamente la selectividad espectral, evitando la señal de fondo de la matriz de la muestra, y la sensibilidad, consecuencia de su elevada relación superficie/volumen. Los principales resultados obtenidos con estas nanopartículas se resumen a continuación:
    - La síntesis mediante el método de formación de microemulsiones en micelas inversas proporciona nanopartículas con un mayor porcentaje de fluoróforo encapsulado que con el método Stöber, que en general ha sido el más utilizado.
    - Los nuevos nanomateriales desarrollados presentan mayor estabilidad fotoluminiscente que los fluoróforos orgánicos en disolución.
    - La interacción entre las cargas positivas de estos fluoróforos y las cargas negativas de la matriz de sílice favorece la

estabilización de los fluoróforos encapsulados, no siendo necesario su enlace covalente a dicha matriz de sílice.

- La versatilidad y aplicabilidad analítica de las nanopartículas de sílice dopadas con azul nilo se ha puesto de manifiesto mediante su uso para formar marcadores en fluorinmunoensayo heterogéneo. Se ha demostrado su utilidad para la determinación de macromoléculas como las proteínas de soja y moléculas pequeñas como el antibiótico de uso veterinario monensín.
- Los dos métodos de inmunoensayo desarrollados constituyen una alternativa útil frente a los métodos ELISA normalmente usados para la determinación de estas especies, ya que alcanzan menores límites de detección y evitan la etapa adicional para la medida de la actividad enzimática.
- La elevada sensibilidad obtenida con estos marcadores permite realizar medidas de fluorescencia en superficie sólida utilizando pocillos de menor volumen que los convencionales, lo que disminuye el consumo de reactivos y el coste de los ensayos.

- Se ha desarrollado un nuevo método ORAC para la determinación de la capacidad antioxidante en zumos y vinos con el uso del fluoróforo de larga longitud de onda azul nilo como reactivo, mejorando la selectividad espectral de las determinaciones convencionales basadas en el uso de fluoresceína o de β-ficoeritrina.

- Se ha propuesto un nuevo método enzimático con detección fluorimétrica para la determinación de polifenoles en vinos basado en el uso del fluoróforo 8-hidroxipireno 3-sulfonato sódico como nuevo sustrato de la laccasa y de nanopartículas de óxido de terbio como activadores de esta enzima. Se ha demostrado que el límite de detección del método en presencia de estas nanopartículas es tres veces inferior al obtenido en su ausencia.

- Se ha ampliado el campo de aplicación de los procesos basados en transferencia de energía de resonancia luminiscente (LRET) utilizando nanocristales de iones lantánidos que presentan luminiscencia anti-Stokes, denominados "upconverting phosphors", como dadores de energía, y fluoróforos orgánicos que emiten en el visible, como aceptores. Las conclusiones más destacables de este estudio son las siguientes:
    - Se han obtenido señales LRET adecuadas utilizando nanocristales dopados con Er(III), Ho(III) y Tm(III), con diámetros medios entre 10 y 20 nm, como dadores y, β-ficoeritrina, R-ficoeritrina y Alexa Fluor 680 como aceptores.
    - Mediante ensayos de afinidad homogéneos, utilizando el sistema biotina-estreptavidina, se ha obtenido la mayor luminiscencia con el par formado por nanocristales dopados con Er(III) y β-ficoeritrina. No obstante, se ha demostrado que los pares formados por nanocristales dopados con Ho(III) y Tm(III) como dadores y β-ficoeritrina

y R-ficoeritrina como aceptores también originan señales luminiscentes adecuadas, permitiendo en todos los casos la determinación de biotina a nivel nM.

- Se ha demostrado la utilidad analítica de la mayoría de los métodos desarrollados mediante su aplicación al análisis de diversos alimentos, tales como vinos, zumos y leche. Las propiedades analíticas que presentan estos métodos han permitido que las determinaciones realizadas no requieran tratamientos de muestra complejos, siendo sólo necesaria la dilución de las muestras de vinos y zumos y la desproteinización de las muestras de leche.

The investigations included in this Dissertation have contributed to expand the application of Nanotechnology to food analysis by the development of several methods that present adequate levels of sensitivity and selectivity. The use of the microplate format has allowed the automation of these methods, also featuring low sample and reagent consumption and a relatively high sample throughput. Bearing in mind the results obtained, the following conclusions can be drawn:

- Silica nanoparticles doped with the long-wavelength fluorophores cresyl violet and nile blue have been synthesized. The use of these nanomaterials for analytical purposes allows the simultaneous improvement of the spectral selectivity, by avoiding the background signal of simple matrix, and the sensitivity, this later as a consequence of their high surface/volume ratio. The main results obtained with these nanoparticles can be summarized as follows:
    - The reverse-micelle microemulsion synthesis procedure provides nanoparticles with a higher percentage of encapsulated fluorophore than the Stöber method, which has been generally used.
    - The newly developed nanomaterials feature better photoluminescent stability than the organic fluorophores in solution.
    - The interaction between the positive charges of these fluorophores and the negative charges of silica matrix favours the stabilization of the encapsulated fluorophores, which avoids their covalent linking to the silica matrix.

- The versatility and analytical usefulness of nile blue-doped silica nanoparticles has been shown by their application to the synthesis of tracers to be used in heterogeneous fluoroimmunoassays. Their analytical potential has been demonstrated by developing methods for the determination of macromolecules, such as soy proteins, and for small molecules (haptens), namely the veterinary antibiotic monensin.
- The two immunoassay methods developed can be regarded as useful alternatives to the ELISA methods commonly used for the determination of these species, since lower detection limits are achieved and the addition of a substrate to measure the enzymatic activity of the tracer is avoided.
- The high sensitivity obtained with these tracers allows the performance of front-surface fluorescence measurements using wells with a lower volume than the conventional ones, which lowers reagent consumption and decreases the cost of assays.

- A new ORAC method to determine the antioxidant capacity in juice and wine samples has been developed by using the long-wavelength fluorophore nile blue as reagent. This approach has improved the spectral selectivity of the conventional determinations based on the use of fluorescein or β-phycoerythrin.

- A new enzymatic method for polyphenol determination in wines with fluorometric detection has been developed using the fluorophore 8-hydroxypyrene 3-sulfonate trisodium and terbium oxide nanoparticles as new laccase substrate and activator, respectively. This study has shown that the detection limit obtained using nanoparticles is about three times lower than that obtained in their absence.

- The application field of luminescence resonance energy transfer (LRET) processes has been expanded using nanocrystals of lanthanide ions capable of providing anti-Stokes luminescence, so called "upconverting phosphors". These nanocrystals have been used as energy donors and organic fluorophores emitting in the visible region as energy acceptors. The main conclusions of this study are:
    - Suitable LRET signals have been obtained using nanocrystals doped with Er(III), Ho(III) y Tm(III), which feature mean diameters between 10 and 20 nm, as donors, and β-phycoerythrin, R-phycoerythrin and Alexa Fluor 680 as acceptors.
    - The performance of homogeneous affinity assays for the biotin-streptavidin system has shown that the highest luminescence is obtained with the pair integrated by Er(III)-doped nanocrystals and β-phycoerythrin. Nevertheless, it has been shown that the pairs integrated by Ho(III) and Tm(III) doped nanocrystals as donors and β-phycoerythrin and R-phycoerythrin as acceptors also provide adequate

luminescent signals, allowing the biotin determination at nM level in all instances.

- The analytical usefulness of most developed methods has been demonstrated by their application to the analysis of several foods, such as wine, juice and milk. The analytical features of these methods have allowed the use of very simple sample treatments, such as the dilution of wine and juice samples or the protein removal from milk samples.

ANEXO

ANNEX

Producción Científica

Scientific Production

ARTÍCULOS CIENTÍFICOS

Tipo de publicación	Artículos científico
Autores	Juan Godoy-Navajas, María Paz Aguilar-Caballos, Agustina Gómez Hens
Título	**Synthesis and caracterization of oxazine-doped silica nanoparticles for their potential use as stable fluorescent reagents**
Revista	Journal of Fluorescence Volumen 20 (2010), Páginas 171 - 180
ISSN	1053-0509 (Print) 1573-4994 (Online)
Índice de impacto	1.966 (31ª posición en la sección de Química Analítica del *Journal of Citation Report* de 2010)

Tipo de publicación	Artículos científico
Autores	Juan Godoy-Navajas, María Paz Aguilar-Caballos, Agustina Gómez Hens
Título	**Long-wavelength fluorimetric determination of food antioxidant capacity using nile blue as reagent**
Revista	Journal of Agricultural and Food Chemistry Volumen 59 (2011), Páginas 2235 – 2240
ISSN	0021-8561 (Print) 1520-5118 (Online)
Índice de impacto	2.816 (12ª posición en la sección de Química Aplicada del *Journal of Citation Report* de 2011)

Tipo de publicación	Artículos científico
Autores	Juan Godoy-Navajas, María Paz Aguilar-Caballos, Agustina Gómez Hens
Título	**Heterogeneous immunoassay for soy protein determination using nile blue-doped silica nanoparticles as labels and front-surface long-wavelength fluorimetry**
Revista	Analytica Chimica Acta Volumen 701 (2011), Páginas 194 – 199
ISSN	0003-2670
Índice de impacto	4.555 (5ª posición en la sección de Química Analítica del *Journal of Citation Report* de 2011)

Tipo de publicación	Artículos científico
Autores	Juan Godoy-Navajas, María Paz Aguilar-Caballos, Agustina Gómez Hens
Título	**Determination of monensin in milk samples by front-surface long-wavelength fluoroimmunoassay using nile blue-doped silica nanoparticles as labels**
Revista	Talanta Volumen 94 (2012), Páginas 195 - 200
ISSN	0039-9140
Índice de impacto	3.498 (12ª posición en la sección de Química Analítica del *Journal of Citation Report* de 2012)

Tipo de publicación	Artículos científico
Autores	Juan Godoy-Navajas, María Paz Aguilar-Caballos, Agustina Gómez Hens
Título	**Automatic determination of polyphenols in wines using laccase and terbium oxide nanoparticles**
Revista	Enviado a Food Chemistry
ISSN	0308-8146

Tipo de publicación	Artículos científico
Autores	Juan Godoy-Navajas, Terhi Riuttamäki, Tero Soukka
Título	**Evaluation of different donor-acceptor pairs for the development of homogeneous bioaffinity assays using up-conversion luminescence resonance energy transfer**
Revista	En redacción

CONTRIBUCIONES A CONGRESOS

Autores	Juan Godoy-Navajas, María Paz Aguilar-Caballos, Agustina Gómez-Hens
Título	**Synthesis of nile blue- and cresyl violet-doped silica nanoparticles for their potential use as labels**
Tipo de participación	Comunicación oral
Congreso	XIII International Symposium of Luminiscence Spectrometry
Lugar y fecha de celebración	Bologna (Italy), del 7 al 11 de Septiembre de 2008

Autores	Juan Godoy-Navajas, María Paz Aguilar-Caballos, Agustina Gómez-Hens
Título	**Development and assessment of new luminescent silica nanoparticles as labels in long-wavelength fluoroimmunoassays**
Tipo de participación	Póster
Congreso	12ª Jornadas de Análisis Instrumental
Lugar y fecha de celebración	Barcelona (España), del 21 al 23 de Octubre de 2008

Autores	Juan Godoy-Navajas, María Paz Aguilar-Caballos, Agustina Gómez-Hens
Título	**Long wavelength dye-doped silica nanoparticles as potential labels**
Tipo de participación	Póster
Congreso	I Encuentro sobre Nanociencia y Nanotecnología de investigadores y tecnólogos de la Universidad de Córdoba (I Nano-UCO)
Lugar y fecha de celebración	Córdoba (España), 12 de Diciembre de 2008

Autores	Juan Godoy-Navajas
Título	**Investigación del potencial analítico de nuevos nanomateriales luminiscentes a larga longitud de onda**
Tipo de participación	Póster
Congreso	VII Jornadas Doctorales Andaluzas
Lugar y fecha de celebración	Carmona (Sevilla, España), del 28 de Junio al 3 de Julio (2009)

Autores	Juan Godoy-Navajas
Título	**Nuevas metodologías en análisis de alimentos y ambiental con el uso de nanopartículas**
Tipo de participación	Comunicación Oral
Congreso	I Congreso Científico de Investigadores en Formación
Lugar y fecha de celebración	Córdoba (España), 15 y 16 de Octubre de 2009

Autores	Juan Godoy-Navajas, María Paz Aguilar-Caballos, Agustina Gómez-Hens
Título	**Long-wavelength homogeneous fluoroimmunoassay for the veterinary antibiotic monensin using doped silica nanoparticles**
Tipo de participación	Póster
Congreso	II Encuentro sobre Nanociencia y Nanotecnología de Investigadores y Tecnólogos de la Unversidad de Córdoba (II Nano-UCO)
Lugar y fecha de celebración	Córdoba (España), 15 de Enero de 2010

Autores	Juan Godoy-Navajas, María Paz Aguilar-Caballos, Agustina Gómez-Hens
Título	**Determinación de proteínas de soja mediante fluoroinmunoensayo a larga longitude de onda utilizando nanopartículas de sílice dopadas con azul nilo como marcador**
Tipo de participación	Comunicación Oral
Congreso	XII Reunión del grupo regional andaluz de la Sociedad Española de Química Analítica
Lugar y fecha de celebración	Córdoba (España), 10 y 11 de Junio de 2010

Autores	Juan Godoy-Navajas, María Paz Aguilar-Caballos, Agustina Gómez-Hens
Título	**Determinación fluorimétrica a larga longitud de onda de la actividad antioxidante de muestras de alimentos con azul nilo como reactivo**
Tipo de participación	Póster
Congreso	XII Reunión del grupo regional andaluz de la Sociedad Española de Química Analítica
Lugar y fecha de celebración	Córdoba (España), 10 y 11 de Junio de 2010

Autores	T. Riuttamäki (née Rantanen), J. Godoy-Navajas, E. Harju, J. Hölsa, T. Soukka
Título	**Resonance energy transfer from upconverting phosphors doped with different lanthanide ions**
Tipo de participación	Póster
Congreso	International Conference on Luminiscence of Lanthanides (ICLL)
Lugar y fecha de celebración	Odessa (Ukraine), del 5 al 9 de Septiembre de 2010

Autores	Juan Godoy-Navajas, María Paz Aguilar-Caballos, Agustina Gómez-Hens
Título	**Use of nile blue-doped silica nanoparticles as labels in heterogeneous immunoassay for antibiotic determination**
Tipo de participación	Póster
Congreso	III Encuentro sobre Nanociencia y Nanotecnología de Investigadores Andaluces (III Nano-UCO)
Lugar y fecha de celebración	Córdoba (España), 10 y 11 de febrero de 2011

Autores	Juan Godoy-Navajas, María Paz Aguilar-Caballos, Agustina Gómez-Hens
Título	**Front-surface long-wavelength fluorescence immunoassay for monensin determination**
Tipo de participación	Póster
Congreso	12th International Conference on Methods and Applications of Fluorescence
Lugar y fecha de celebración	Strasbourg (France), del 11 al 14 de Septiembre de 2011

Autores	Juan Godoy-Navajas
Título	**Nuevas metodologías analíticas en análisis de alimentos y ambiental con el uso de nanopartículas**
Tipo de participación	Comunicación Oral
Congreso	I Congreso Científico de Investigadores en Formación en Agroalimentación de la eidA3 y II Congreso Científico de Investigadores en Formación de la Universidad de Córdoba
Lugar y fecha de celebración	Córdoba (España), 8 y 9 de mayo de 2012

Autores	Juan Godoy-Navajas, María Paz Aguilar-Caballos, Agustina Gómez-Hens
Título	**Utilidad Analítica del uso combinado de nanopartículas de Tb_4O_7 para la determinación de antioxidantes en alimentos**
Tipo de participación	Póster
Congreso	IV Encuentro sobre Nanociencia y Nanotecnología de Investigadores y Tecnólogos Andaluces (IV Nano-UCO)
Lugar y fecha de celebración	Córdoba (España), 7 y 8 de febrero de 2013

Autores	Juan Godoy-Navajas, María Paz Aguilar-Caballos, Agustina Gómez-Hens
Título	**Analytical usefulness of the combined use of Tb_4O_7 nanoparticles and laccase enzyme for the determination of antioxidants in food samples**
Tipo de participación	Póster
Congreso	Trends in Nanotechnology
Lugar y fecha de celebración	Sevilla (España), del 9 al 13 de septiembre de 2013

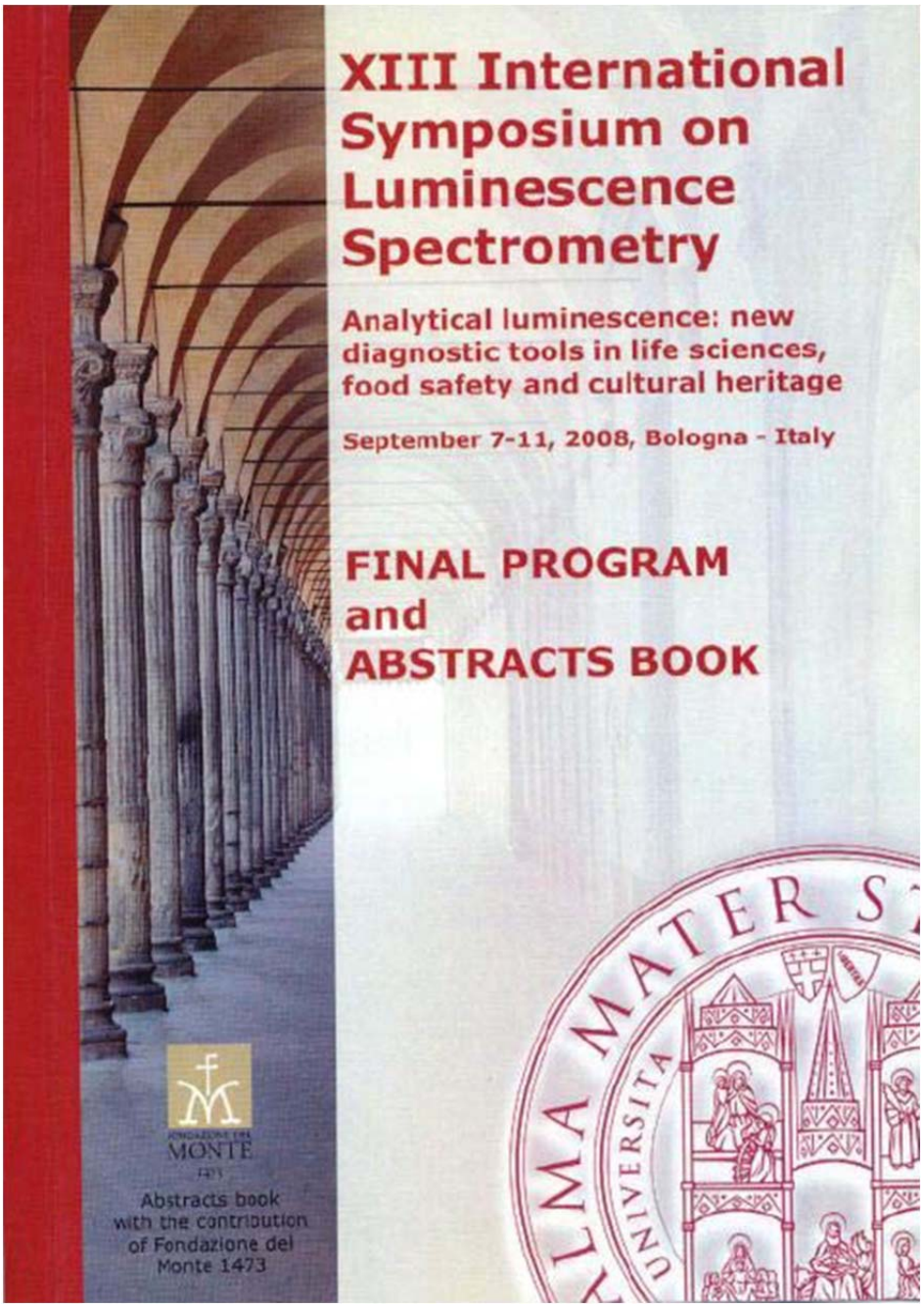
XIII International Symposium on Luminescence Spectrometry
Analytical luminescence: new diagnostic tools in life sciences, food safety and cultural heritage
September 7-11, 2008, Bologna - Italy
FINAL PROGRAM and ABSTRACTS BOOK
MONTE
Abstracts book with the contribution of Fondazione del Monte 1473
ALMA MATER
UNIVERSITA

XIII International Symposium on Luminescence Spectrometry **OC28**

SYNTHESIS OF NILE BLUE- AND CRESYL VIOLET-DOPED SILICA NANOPARTICLES FOR THEIR POTENTIAL USE AS LABELS

J. Godoy-Navajas, M.P. Aguilar-Caballos, A. Gómez-Hens
Dept. of Analytical Chemistry, University of Córdoba, Córdoba, Spain. Email: qa1agcam@uco.es

The aim of the work presented here has been the synthesis of dye-doped silica nanoparticles for their further use as labels in fluoroimmunoassay at long wavelength. For this purpose, two different oxazine dyes, cresyl violet and nile blue, have been used. These nanoparticles have been synthesized by a modification of the conventional sol-gel method based on the formation of water-in-oil microemulsions. A systematic study of the variables involved in the process, such as the dye chosen, the type and concentration of precursor, surfactant, cosurfactant as well as their molar ratio, time and temperature of formation, among others, has been performed. The formation of nanoparticles is followed by Transmission Electron Microscopy (TEM) and fluorescence measurements using a microplate reader. The size of nanoparticles obtained, which ranges between 10 and 400 nm, depends on the experimental conditions assayed. Also, the modification of the surface of these nanoparticles using 3-aminopropyltriethoxysilane is being investigated to obtain suitable tracers for the development of fluoroimmunoassay methods.
The picture included below is a TEM image of the nanoparticles obtained using hexanol, tetraethoxysilane, Triton X-100, ammonium hydroxide and cresyl violet. The diameter of these particles ranges from 85 to 130 nm.

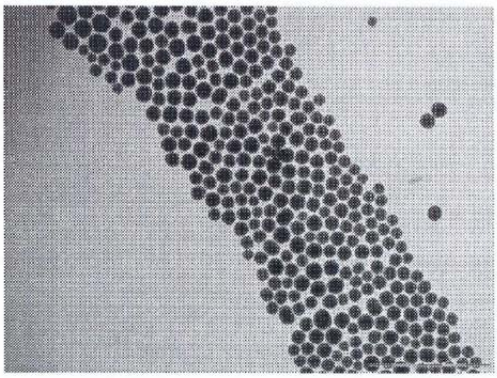

12as JORNADAS DE ANÁLISIS INSTRUMENTAL

LIBRO DE RESÚMENES

Barcelona
21-23 de Octubre de 2008

PO-NANO-3

DEVELOPMENT AND ASSESSMENT OF NEW LUMINESCENT SILICA NANOPARTICLES AS LABELS IN LONG-WAVELENGTH FLUORO IMMUNOASSAYS

J. Godoy-Navajas, M.P. Aguilar-Caballos, A. Gómez-Hens

Department of Analytical Chemistry. University of Córdoba. Campus of Rabanales. Marie-Curie Annex building. 14071-Córdoba. Phone: +34-957218645. Fax: +34-957218644. e-mail: godoynavajas@hotmail.com

The use of silica nanoparticles for the development of biosensors and bioassays is desirable because of some of their properties [1]: 1) high emission intensity, as a result of the encapsulation of a high number of dye molecules inside the nanosphere, 2) good photostability due to the protection that the silica shell of the nanoparticle confers to the encapsulated fluorophore, thus minimizing the interaction of the fluorophore with dissolved oxygen, 3) high water solubility, what makes them compatible for their use in bioassays, and 4) efficient conjugation of surface-modified silica nanoparticles after different modification procedures to the species of interest. In addition, long-wavelength organic dyes exhibit some good properties such as lower probability of photobleaching and good spectral selectivity compared to those from conventional fluorophores.

The synthesis of silica nanoparticles doped with two oxazine dyes, nile blue and cresyl violet, has been investigated. A modification of the reverse micelle microemulsion method for the synthesis of nanoparticles has been used. A micellar medium provided by the non-ionic surfactant Triton X-100, in a hexanol:water mixture, is used to provide the organized medium. Tetraethoxysilane has been used as the initiator of the polymerization and condensation reaction after its hydrolysis in basic medium using ammonium hydroxide. Size distribution and fluorescence of the synthesized nanoparticles, which were monitored using Transmision Electron Microscopy (TEM) and a microplate reader, respectively, depend on the molar ratio of the reagents involved in the synthesis. Nanoparticles obtained using the developed synthesis procedure had sizes below 400 nm in most instances and the best luminescent properties were observed for nanoparticles with sizes ranging from 100 to 300 nm. Lower sizes result in a decrease in the fluorescence intensities of these nanomaterials. The repeatability of the synthesis procedure performed in different days gave a relative standard deviation of 10% for the fluorescence intensity values.

The modification of the surface of these nanoparticles has been performed using 3-aminopropyltriethoxysilane for the further covalent attachment of the analytes of interest in order to carry out different fluoroinmunoassays. Preliminary results have showed that there is a decrease in the fluorescence of the synthesized nanoparticles after modification of the surface, which would be ascribed to the increase in the thickness of the outer silica shell of the nanoparticle.

REFERENCES

[1] G. Yao, L. Wang, Y. Wu, J. Smith, J. Xu, E. Lee, W. Tan, Anal. Bioanal. Chem., 385 (2006) 518.

Vicerrectorado de Política Científica

Universidad de Córdoba

NANO UCO

I ENCUENTRO SOBRE NANOCIENCIA Y NANOTECNOLOGÍA DE INVESTIGADORES Y TECNÓLOGOS DE LA UNIVERSIDAD DE CÓRDOBA

Libro de Resúmenes

Córdoba, 12 de diciembre de 2008

P-3

LONG WAVELENGTH DYE-DOPED SILICA NANOPARTICLES AS POTENTIAL LABELS

J. Godoy-Navajas, M.P. Aguilar-Caballos, A. Gómez-Hens
Dept. of Analytical Chemistry, University of Córdoba, Córdoba, Spain. Phone: +34-957218645. Fax: +34-957218644. e-mail: qa1gohea@uco.es

The aim of the work presented here has been the synthesis of dye-doped silica nanoparticles for their further use as labels in fluoroimmunoassay at long wavelength. For this purpose, two different oxazine dyes, cresyl violet and nile blue, have been used. These nanoparticles have been synthesized by a modification of the conventional sol-gel method based on the formation of water-in-oil microemulsions. A systematic study of the variables involved in the process, such as the dye chosen, the type and concentration of precursor, surfactant, cosurfactant as well as their molar ratio, time and temperature of formation, among others, has been performed. The formation of nanoparticles is followed by Transmission Electron Microscopy (TEM) and fluorescence measurements using a microplate reader. The size of nanoparticles obtained, which ranges between 10 and 400 nm, depends on the experimental conditions assayed. Also, the modification of the surface of these nanoparticles using 3-aminopropyltriethoxysilane is being investigated to obtain suitable tracers for the development of fluoroimmunoassay methods.

7as Jornadas Doctorales Andaluzas
Del 28 de junio
al 3 de julio de 2009
Casa Palacio de los Briones
Carmona (Sevilla)
Universidad Pablo de Olavide
www.upo.es/jornadas/doctoralesandaluzas09

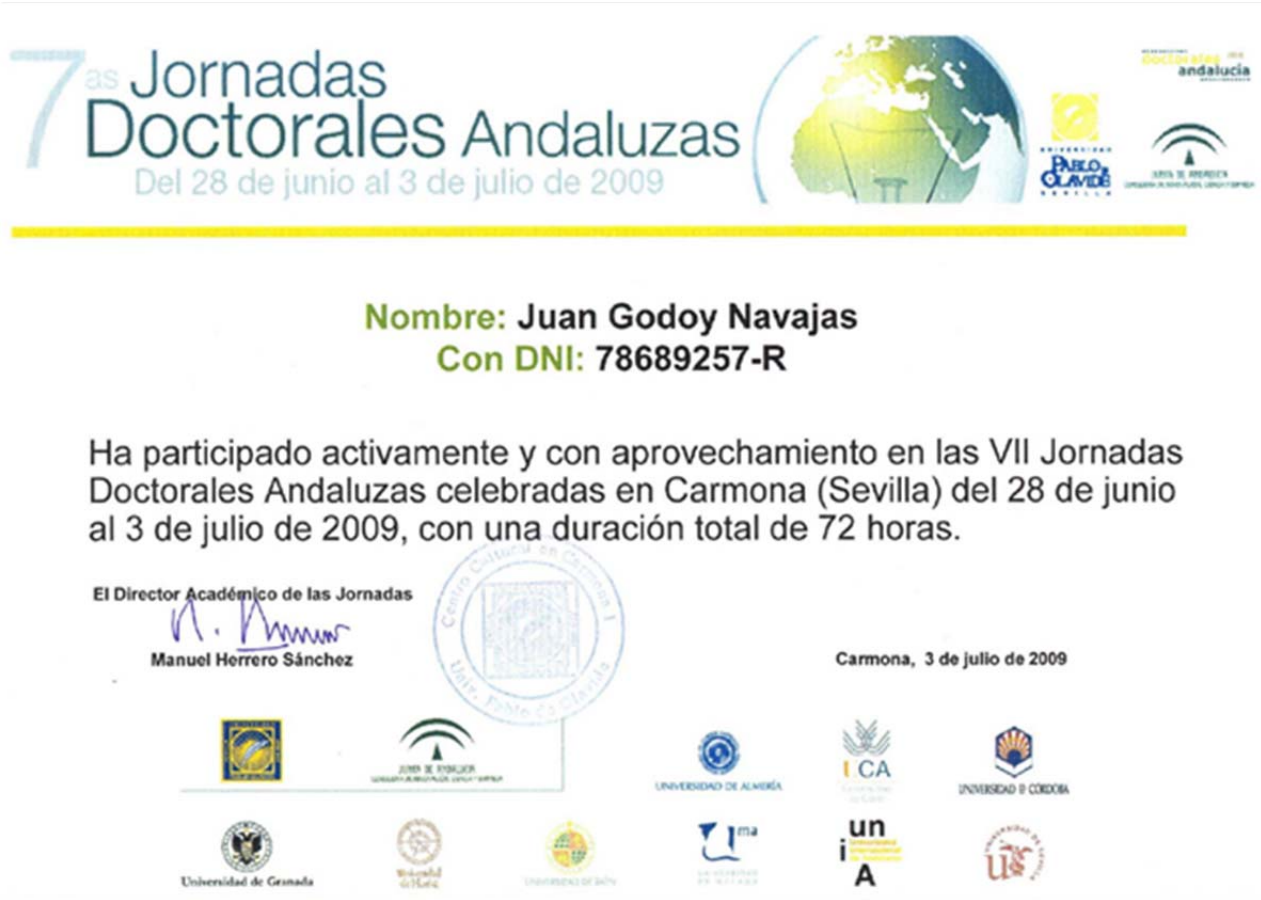

7as Jornadas Doctorales Andaluzas

Del 28 de junio al 3 de julio de 2009

Nombre: Juan Godoy Navajas

Con DNI: 78689257-R

Ha participado activamente y con aprovechamiento en las VII Jornadas Doctorales Andaluzas celebradas en Carmona (Sevilla) del 28 de junio al 3 de julio de 2009, con una duración total de 72 horas.

El Director Académico de las Jornadas

Manuel Herrero Sánchez

Carmona, 3 de julio de 2009


Integrando
Disciplinas

UNIVERSIDAD D CÓRDOBA

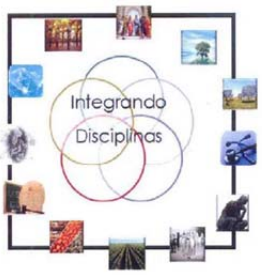

Los Vicerrectores de Estudios de Postgrado y Formación Continua y Política Científica acreditan que D/Dª **JUAN GODOY NAVAJAS** ha presentado la comunicación titulada **NUEVAS METODOLOGÍAS EN ANÁLISIS DE ALIMENTOS Y AMBIENTAL CON EL USO DE NANOPARTÍCULAS**, en el *I Congreso Científico de Investigadores en Formación* celebrado en Córdoba los días 15 y 16 de octubre de 2009.

VICERRECTOR DE ESTUDIOS DE POSTGRADO Y FORMACIÓN CONTINUA

FDO: José Carlos GÓMEZ VILLAMANDOS

VICERRECTOR DE POLÍTICA CIENTÍFICA

FDO: Enrique AGUILAR BENÍTEZ DE LUGO

Universidad de Córdoba

IAQFN
Instituto Andaluz de Química Fina y Nanoquímica

JUNTA DE ANDALUCIA
Consejería de Innovación, Ciencia y Empresa

NANO UCO

II ENCUENTRO SOBRE NANOCIENCIA Y NANOTECNOLOGÍA DE INVESTIGADORES Y TECNÓLOGOS DE LA UNIVERSIDAD DE CÓRDOBA

Córdoba, 14 de enero de 2010

P-26

Long-wavelength homogeneous fluoroimmunoassay for the veterinary antibiotic monensin using nile-blue doped silica nanoparticles

J. Godoy-Navajas, M.P. Aguilar-Caballos, A. Gómez-Hens
Department of Analytical Chemistry
University of Cordoba
Annex to "Marie Curie" Building. Campus of Rabanales.14071-Córdoba
e-mail: qa1gohea@uco.es. Web: http://www.uco.es/FQM-303/

The present method describes for the first time the use of nile blue-doped silica nanoparticles (NPs) as labels to develop a long-wavelength homogeneous fluoroimmunoassay for a hapten, more specifically the veterinary antibiotic monensin. The use of silica NPs as labels has been previously described for the determination of macromolecules [1], but their application to the determination of low molecular weight antigens has been scarce up to date.
Dye-doped silica NPs have several advantages when used as labels compared to organic fluorophores, such as: 1) an enhanced sensitivity since a single NP label contains a high number of fluorophore molecules and 2) the photostability of luminescent organic fluorophores can be improved owing to the protection that the silica matrix confers to the fluorophore molecules. In addition, the use of long-wavelength fluorophores to obtain dye-doped silica NPs provides to these labels with a suitable spectral selectivity since the presence of background signals from the sample matrix can be avoided.

The NPs used in the method reported here have been synthesized according to a reverse-micelle microemulsion sol-gel method previously described [2]. These NPs do not have any moiety suitable for its coupling to biomolecules being necessary the use of a functionalization reaction using 3-aminopropyltriethoxysilane (APS) as reagent for the introduction of amino groups. The use of APS alone gives rise to aggregated NPs but this effect can be overcome using a silane reagent containing phosphonate groups, which reduces the aggregation of NPs. The functionalized NPs are bound to the carboxylic acid group of monensin via a carbodiimide reaction in the presence of N-sulfohydroxysuccinimide and a water soluble carbodiimide reagent. The obtained tracer was purified by washing and centrifuging the NP suspension. The reaction of the synthesized tracer with anti-monensin antibodies originated a fluorescence quenching, which is hindered in the presence of monensin. This can be explained owing to competition phenomena between monensin and the tracer and the fluorescence is recovered when the tracer is free in solution. The method has a dynamic range of 0.1-10 ng mL^{-1}.

REFERENCES

[1] Gómez-Hens, A.; Fernández-Romero, J.M.; Aguilar-Caballos, M.P., Trends Anal. Chem., 2008, 27, 394-406.

[2] Godoy-Navajas, J.; Aguilar-Caballos, M.P.; Gómez-Hens, A.. J. Fluoresc., 2009, DOI 10.1007/s10895-009-0535-2.

REUNIÓN DEL GRUPO REGIONAL ANDALUZ DE LA
SOCIEDAD ESPAÑOLA DE QUÍMICA ANALÍTICA

XII GRASEQA 2010

Córdoba, 10 y 11 de junio

LIBRO DE RESÚMENES

UNIVERSIDAD D CÓRDOBA

GRASEQA 2010

CO-9

Determinación de proteínas de soja mediante fluorinmunoensayo a larga longitud de onda utilizando nanopartículas de sílice dopadas con azul nilo como marcador

J. Godoy-Navajas, M.P. Aguilar-Caballos, A. Gómez-Hens

Departamento de Química Analítica. Universidad de Córdoba
Edificio Anexo al Marie Curie. Campus de Rabanales. 14071-Córdoba. España
Tlfno: +34957218645, fax: +34957218644, correo-e: qa1gohea@uco.es,
Web: http://www.uco.es/investiga/grupos/FQM-303/

Se propone por primera vez un fluorinmunoensayo a larga longitud de onda para la determinación de proteína de soja utilizando como marcador anticuerpos anti-soja unidos a nanopartículas (NPs) de sílice dopadas con azul nilo. Estas NPs se han sintetizado mediante la tecnología sol-gel, usando microemulsiones en micelas inversas[1]. Las NPs obtenidas se han funcionalizado con grupos amino, recubriendo su superficie con 3-aminopropiletoxisilano (APS). La agregación de las NPs se ha evitado utilizando grupos fosfonato. El marcador se ha obtenido mediante la unión de las NPs funcionalizadas con los anticuerpos anti-soja oxidados previamente con peryodato. El formato de inmunoensayo utilizado es heterogéneo competitivo con captura de anticuerpo en microplacas de 96 pocillos de 100 µl de volumen. Las proteínas de soja se incuban en cada micropocillo durante 24 h a 4 °C y, a continuación, se incuba albúmina de suero bovino durante 1 hora para bloquear la superficie y minimizar las interacciones no específicas. En el momento del ensayo, se añaden la proteína de soja (0.2 – 20 mg L^{-1}) y el marcador y se incuban durante 90 minutos, se lavan los pocillos tres veces y se mide la fluorescencia en superficie sólida a λ_{ex} 620 y λ_{em} 680 nm.

La metodología propuesta es más simple que el método ELISA convencional utilizado para la determinación de proteínas de soja en alimentos ya que evita el uso del conjugado enzimático y la adición del sustrato. El método se ha aplicado al análisis de alimentos que contienen proteínas de soja y los resultados obtenidos se han comparado con los obtenidos mediante un kit ELISA comercial, proporcionando ambos resultados muy similares.

[1] Godoy-Navajas, J.; Aguilar-Caballos, M.P.; Gomez-Hens, A. J. *Fluoresc.* **2010,** *20*, 171 – 180.

REUNIÓN DEL GRUPO REGIONAL ANDALUZ DE LA SOCIEDAD ESPAÑOLA DE QUÍMICA ANALÍTICA

XII GRASEQA 2010

Córdoba, 10 y 11 de junio

LIBRO DE RESÚMENES

UNIVERSIDAD D CÓRDOBA

GRASEQA 2010

SC-51

Determinación fluorimétrica a larga longitud de onda de la actividad antioxidante de muestras de alimentos con azul nilo como reactivo

J. Godoy-Navajas, M.P. Aguilar-Caballos, A. Gómez-Hens

Departamento de Química Analítica. Universidad de Córdoba
Edificio Anexo al "Marie Curie". Campus Rabanales
+34-957218644, +34-957218645, correo-e: qa1gohea@uco.es,
web: http://www.uco.es/investiga/grupos/FQM-303/

Se ha desarrollado por primera vez un método para la determinación de la actividad antioxidante basado en el uso de medidas de fluorescencia a larga longitud de onda. El método propuesto es una modificación del método ORAC (Oxigen Radical Antioxidant Capacity) clásico que utiliza los fluoróforos fluoresceína o ficoeritrina y un compuesto generador de radicales, diclorhidrato de 2-metil propionamidina (AAPH). La descomposición de AAPH produce un radical peroxilo que reacciona con el fluoróforo originando la inhibición de su fluorescencia, pero la presencia de especies con actividad antioxidante disminuye la velocidad de esta inhibición. Se propone la utilización del fluoróforo azul nilo como reactivo analítico alternativo a los fluoróforos convencionales, el cual permite obtener medidas de fluorescencia a larga longitud de onda, lo que ofrece las siguientes ventajas: 1) la señal analítica se afecta menos por las señales estáticas procedentes de la matriz de la muestra ya que éstas, normalmente, se originan a longitudes de onda más cortas; 2) la probabilidad de fotodescomposición del fluoróforo es menor, debido a que la excitación se realiza a mayor longitud de onda; 3) El desplazamiento Stokes del azul nilo es mayor que los de los fluoróforos convencionales, lo que minimiza posibles problemas de dispersión de la radiación; y 4), el coste del ensayo es menor que el que implica el uso de ficobiliproteínas.

El sistema se ha estudiado obteniendo las correspondientes curvas cinéticas, mediante el registro de la variación de la fluorescencia (λ_{ex} 620 y λ_{em} 680 nm) con el tiempo, utilizando el formato de microplacas de 96 pocillos, lo que dota al método desarrollado con una frecuencia de muestreo relativamente elevada. El ácido 6-hidroxi-2,5,7,8-tetrametilcroman-2-carboxílico (Trolox) se ha usado como analito modelo y el parámetro analítico utilizado ha sido el área normalizada bajo la curva. El límite de detección del método propuesto es de 0.3 µM, y el intervalo dinámico de la calibración es 0,8 - 8 µM. La precisión del método, estudiada a dos niveles de concentración, 1 y 5 µM, y expresada como desviación estándar relativa, tiene valores comprendidos entre 2,9 y 5,6%. El método se ha aplicado al análisis de muestras de zumos de frutas y vinos, obteniendo resultados similares a los proporcionados utilizando el método ORAC con fluoresceína como reactivo.

ICLL-1

First International Conference on Luminescence of Lanthanides

Program
and
Abstracts Book

5-9 September 2010
Odessa, Ukraine

RESONANCE ENERGY TRANSFER FROM UPCONVERTING PHOSPHORS DOPED WITH DIFFERENT LANTHANIDE IONS

T. Riuttamäki[1], J. Godoy-Navajas[1], E. Harju[2], J. Hölsä[2,3], T. Soukka[1]

[1]*Department of Biotechnology, University of Turku, Tykistökatu 6A, FI-20520 Turku, Finland;*
[2]*Department of Chemistry, University of Turku, FI-20014 Turku, Finland;*
[3]*Turku University Centre for Materials and Surfaces (MatSurf), FI-20014 Turku, Finland*
e-mail: tetrant@utu.fi

Upconverting phosphors (UCPs) are usually inorganic, lanthanide-doped photoluminescent compounds emitting visible light under infrared excitation. The unique upconversion phenomenon offers advantages in bioanalytical diagnostics by enabling the elimination of autofluorescence even without time-resolved fluorometry and allowing more sensitive assays with less complicated instrumentation.

The color of the upconversion photoluminescence depends on the emitting ion, which can be e.g. Er^{3+}, Tm^{3+} or Ho^{3+} (Fig 1a). Diverse UCP materials provide an opportunity to multiplex bioaffinity assays by choosing a distinct measurement wavelength for each analyte. A separation-free competitive model assay for biotin was utilized to demonstrate that UCP materials doped with any of the three above-mentioned lanthanides can be exploited as a donor in upconversion resonance energy transfer (UC-RET) [1]. Hexagonal $NaYF_4$:Yb^{3+}, Er^{3+} is recognized as one of the most efficient upconverting material and it has previously been utilized in UC-RET, but the use of the Tm^{3+} and Ho^{3+} dopants has been marginal or even nonexistent.

B-phycoerythrin acceptor paired with Er^{3+}-doped UCP provided the brightest sensitized acceptor emission, as expected. However, also the Ho^{3+}-doped (B-phycoerythrin acceptor) as well as the Tm^{3+}-doped (R-phycoerythrin acceptor) UCP showed sigmoidal calibration curves easily separated from the background (Fig 1b). By optimizing the synthesis and upconversion efficiency, these UCP materials could be valuable donors in UC-RET applications.

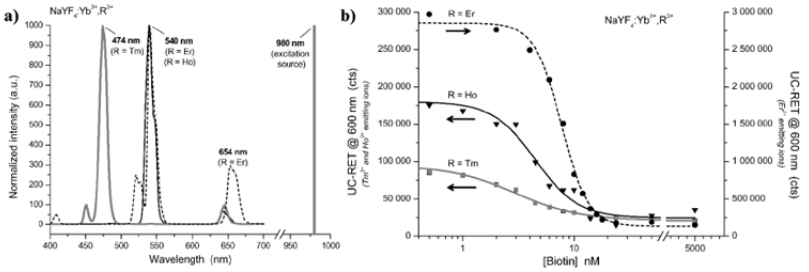

Fig 1. ***(a) The normalized emission spectra of three UCP materials.*** *The host lattice and the absorber ion were common to all UCP materials, but the emitting ion was either Tm^{3+} (gray thick line), Ho^{3+} (black thin line) or Er^{3+} (dashed line).*
(b) Calibration curves for biotin assay. *Tm^{3+}-doped UCP was used as a donor together with R-phycoerythrin acceptor and both Ho^{3+}-doped as well as Er^{3+}-doped UCPs with B-phycoerythrin acceptor. The sensitized emission of all acceptors was measured at 600 nm. The arrows indicate the y-axes related to each curve.*

1. T. Soukka, T. Rantanen, K. Kuningas, *Ann. N.Y. Acad. Sci.* **2008**, *1130*, 188.

NANO UCO

LIBRO DE RESÚMENES

NANOUCO III
Encuentro sobre Nanociencia y Nanotecnología de Investigadores y Tecnólogos Andaluces

Córdoba, 10 y 11 de febrero de 2011

P-9

USE OF NILE BLUE-DOPED SILICA NANOPARTICLES AS LABELS IN HETEROGENEOUS IMMUNOASSAYS FOR ANTIBIOTIC DETERMINATION

J. Godoy-Navajas, M.P. Aguilar-Caballos, A. Gómez-Hens
Department of Analytical Chemistry
University of Córdoba
Campus of Rabanales
Annex to Marie Curie building
14071-Córdoba. Spain
E-mail: qa1gohea@uco.es
Web: http://www.uco.es/FQM-303/

The use of silica nanoparticles (NPs) as labels in immunoassays with optical detection has very interesting features: 1) transparency of silica to visible light, 2) almost negligible photo-bleaching phenomena of encapsulated organic dyes, 3) stability of silica matrix at medium-term, since it is not susceptible to microbiological degradation and, 4) porosity or swelling changes do not happen at moderate pH variations. In addition, the spectral selectivity of conventional fluorophores can be enhanced by using long-wavelength emitting organic compounds, such as cyanines, thiazines and oxazines, since their emission is not overlapped by static background signals from sample matrix, which usually happen at shorter wavelengths. Nile blue-doped silica NPs, synthesized using a simple reverse-micelle method[1], have been assayed for analytical purposes.

The use of these NPs is described for the first time to develop heterogeneous immunoassays for the determination of the veterinary antibiotic monensin. Two different formats, with antigen and antibody capture, have been assayed using black and shallow Proxy-plate 96-well microplates as solid supports. The first assay relies on the immobilization of anti-sheep IgG previously to the incubation of sheep anti-monensin antibodies. Then, a mixture of monensin and tracer (monensin bound to nile blue-doped silica NPs) is added and, after subsequent incubation and washing steps, the fluorescence of the bound tracer fraction is measured onto the dry surface of the well. The second assay format, relies on the competition of the monensin present in the samples with a monensin-BSA conjugate, which has been previously immobilised onto the well surface, for the active sites of anti-monensin antibodies. In both instances, the fluorescence signal obtained can be correlated to the analyte concentration. Preliminary studies have shown that the best results are achieved with the antibody capture heterogeneous immunoassay. The use of NPs as labels allows a decreased number of steps to perform this assay compared to those required for the development of ELISA assays, since the use of enzyme conjugate and substrate solutions is avoided.

[1] Godoy-Navajas, J., Aguilar Caballos, M.P., Gomez-Hens, A. *J. Fluoresc.*, **2010**, 20, 171.

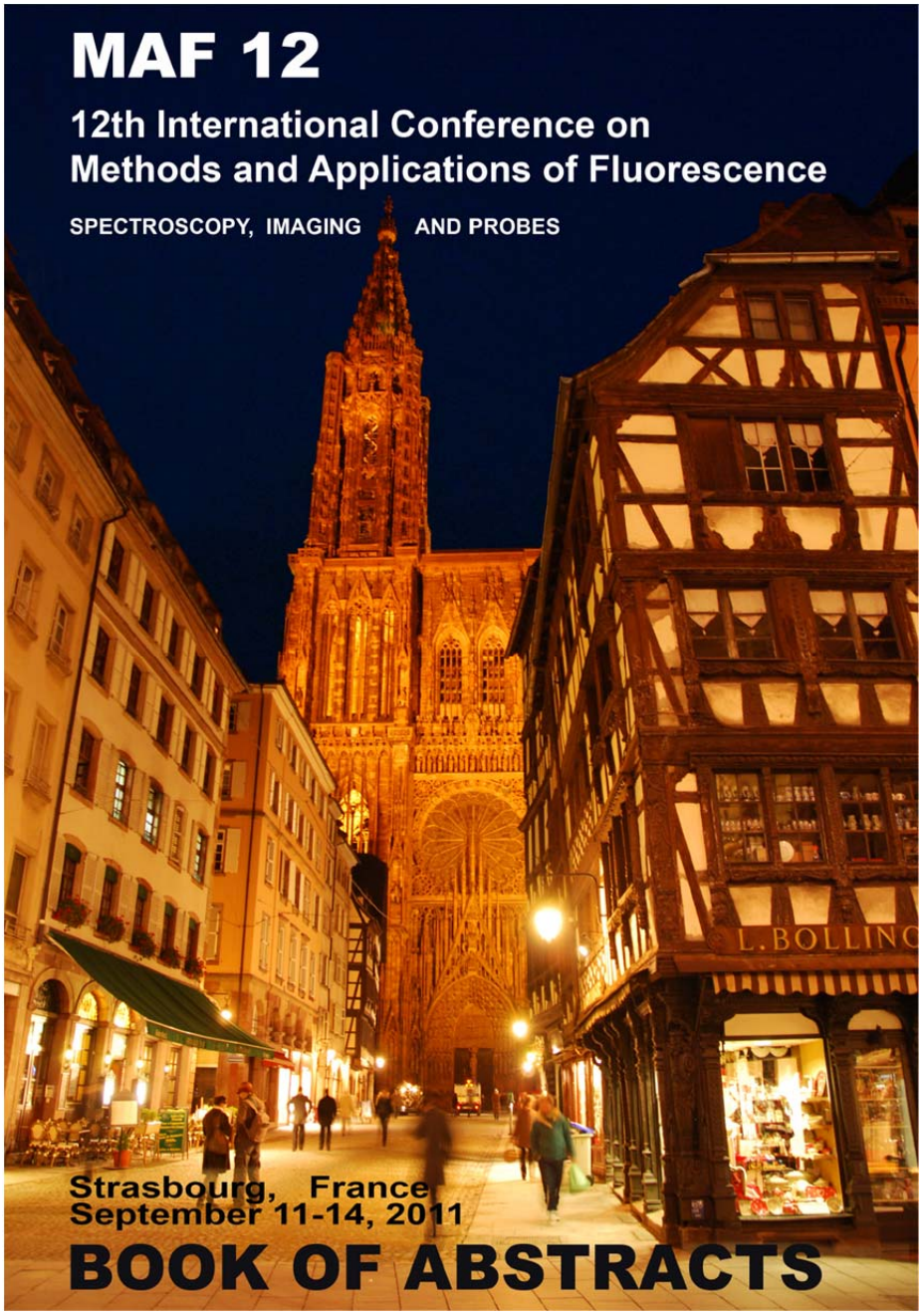
MAF 12
12th International Conference on
Methods and Applications of Fluorescence
SPECTROSCOPY, IMAGING AND PROBES
Strasbourg, France
September 11-14, 2011
BOOK OF ABSTRACTS

Front-surface long-wavelength fluorescence immunoassay for monensin determination

J. Godoy-Navajas[1], M. P. Aguilar-Caballos[1] & A. Gómez-Hens[1*]

[1]*Analytical Chemistry Department, Institute of Fine Chemistry and Nanochemistry (IAQFN). Campus of Rabanales. Marie Curie Building (Annex). University of Cordoba. 14071-Cordoba, Spain*

A long-wavelength heterogeneous fluoroimmunoassay for monensin determination in food samples using nile-blue doped silica nanoparticles (NPs) is described. A luminescent tracer is synthesized by conjugating anti-monensin antibodies to amino-group functionalized nile blue-doped silica NPs, which have been previously synthesized using a reverse-micelle method [1]. Two different formats, with antigen and antibody capture, have been assayed using black and shallow Proxy-plate 96-well microplates as solid supports. The first assay relies on the immobilization of anti-sheep IgG previously to the incubation of sheep anti-monensin antibodies. Then, a mixture of monensin and tracer (monensin bound to nile blue-doped silica NPs) is added and, after subsequent incubation and washing steps, the fluorescence of the bound tracer fraction is measured onto the dry surface of the well. The second assay format relies on the competition of the monensin present in the samples with a monensin-BSA conjugate, which has been previously immobilised onto the well surface, for the active sites of anti-monensin antibodies. In both instances, the fluorescence signal obtained can be correlated to the analyte concentration. The best results have been achieved with the antibody capture heterogeneous immunoassay, which general scheme is depicted in the Figure:

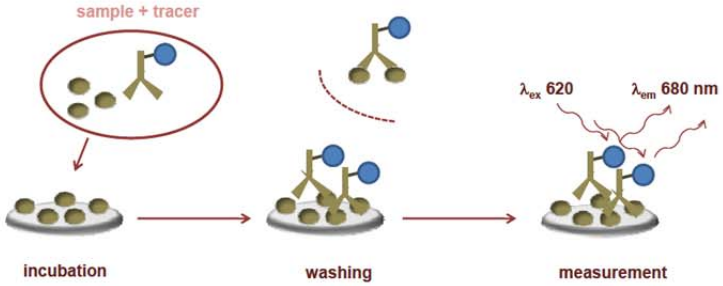

After the optimization of the variables involved, the method features a detection limit of 0.014 ng mL^{-1} and a dynamic range from 0.1 to 5 ng mL^{-1}. The precision of the method, at two different analyte concentrations, 0.2 and 1 ng mL^{-1}, and expressed as relative standard deviation, has given values between 4.0 and 5.9%. The method has been satisfactorily applied to the analysis of food samples, which requires a simple extraction step in order to remove the proteins from samples.

This work has been supported by the Spanish MICINN (Grant No. CTQ2009-08621) and by the Junta of Andalucia (Grant No. P09-FQM4933) and from the FEDER-FSE Program (Grant No. P09-FQM4933). J. Godoy Navajas thanks the Junta of Andalucia (Grant No. P09-FQM4933) for the financial support of his pre-doctoral fellowship.

References: [1] J. Godoy-Navajas et al., J. Fluoresc., **20** (2010) 171.

*Corresponding author: e-mail: qa1gohea@uco.es


ceiA3
campus de excelencia internacional
agroalimentario


eidA3
escuela internacional de doctorado en
agroalimentación

UNIVERSIDAD D CÓRDOBA

El Vicerrector de Estudios de Posgrado y Formación Continua de la Universidad de Córdoba **ACREDITA** que :

JUAN GODOY NAVAJAS

ha presentado la comunicación oral que lleva por título :

" NUEVAS METODOLOGÍAS ANALÍTICAS EN ANÁLISIS DE ALIMENTOS Y AMBIENTAL CON EL USO DE NANOPARTÍCULAS"

en el **I Congreso Científico de Investigadores en Formación en Agroalimentación** de la eidA3 y **II Congreso Científico de Investigadores en Formación de la Universidad de Córdoba** celebrado en Córdoba los días 8 y 9 de Mayo de 2012.

Y para que así conste, se expide y firma este certificado en Córdoba, a 9 de Mayo de 2012

Fdo: JOSE CARLOS GÓMEZ VILLAMANDOS
Vicerrector de Estudios de Posgrado y Formación Continua

ceiA3

eidA3
escuela internacional de doctorado en agroalimentación

Rectorado Universidad de Córdoba – Avnd. Medina Azahara, 5 14002 Córdoba

UNIVERSIDAD D CÓRDOBA

IV Workshop
NANO UCO

LIBRO DE RESÚMENES

NANOUCO IV
Encuentro sobre Nanociencia y Nanotecnología
de Investigadores y Tecnólogos Andaluces

Córdoba, 7 y 8 de Febrero 2013

UNIVERSIDAD D CÓRDOBA

IUIQFN

P47-NA

UTILIDAD ANALÍTICA DEL USO COMBINADO DE NANOPARTÍCULAS DE Tb_4O_7 Y LACCASA PARA LA DETERMINACIÓN DE ANTIOXIDANTES EN ALIMENTOS

Juan Godoy Navajas, María Paz Aguilar Caballos, Agustina Gómez Hens
Departamento de Química Analítica. Instituto de Química Fina y Nanoquímica. Campus de Rabanales. Anexo al Edificio Marie Curie. Universidad de Córdoba. 14071-Córdoba. España.
Teléfono: 34-957218645, Fax. 34-957218644
e-mail: qa1gohea@uco.es, web: http://www.uco.es/investiga/grupos/FQM-303

Se describe por primera vez la utilidad analítica de las nanopartículas de óxido de terbio (Tb_4O_7 NPs) en la determinación de compuestos fenólicos en alimentos. La oxidación enzimática de estos fenoles puede realizarse mediante el uso de laccasa, una enzima fenol oxidasa que se aisla de diversos géneros de plantas, hongos y microorganismos, siendo una de las más utilizadas la obtenida a partir de *Trametes Versicolor*. Esta enzima cataliza la oxidación de compuestos fenólicos a través de la reducción del oxígeno disuelto a agua, la cual puede medirse mediante su acción sobre cromóforos, como el ácido 2,2'-azino-bis(3-etilbenzotiazolín-6-sulfónico (ABTS)[1].

En el presente trabajo, se utiliza el fluoróforo 8-hidroxipireno-3-sulfonato trisódico (HPTS), cuya fluorescencia disminuye en presencia de laccasa, siendo este descenso menor en presencia de compuestos antioxidantes como el ácido gálico, el cual se ha utilizado como analito modelo. El área bajo las curvas cinéticas obtenidas en presencia de este antioxidante es directamente proporcional a su concentración. La presencia de Tb_4O_7 NPs en el medio origina un aumento en la velocidad del sistema que se traduce en tiempos de análisis más cortos, lo que mejora la velocidad de muestreo del método.

El ensayo se ha desarrollado en microplacas de 96 pocillos y se realiza en dos etapas: 1) una etapa de pre-incubación del fluoróforo HPTS y el estándar de ácido gálico o muestra durante 15 min a 37 ºC y 2) adición de una disolución en la que se han mezclado previamente las NPs y la laccasa. Esta mezcla se coloca inmediatamente en el lector de microplacas y se registran las curvas cinéticas del sistema utilizando los filtros con longitudes de onda nominales de excitación y emisión de 450 y 535 nm, respectivamente. El método presenta un límite de detección de 0,14 μM y el intervalo dinámico es 0,5 -12 μM. La precisión, expresada como desviación estándar relativa, se ha ensayado a dos concentraciones diferentes, 0,7 y 5 μM, obteniéndose valores en el intervalo 2,5-6,3%. El método se ha aplicado satisfactoriamente al análisis de muestras de vino y de cerveza, lo que demuestra su utilidad práctica.

Referencias

[1]Branchi, B.; Galli, C., Gentili, P., Org. Biomol. Chem., **2005**, 3, 2604.


TNT 2013
Trends in NanoTechnology
September 09-13, 2013
Seville (Spain)
PHANTOMS foundation
INL
INTERNATIONAL IBERIAN NANOTECHNOLOGY LABORATORY
CiNaM
INDUSTRIALES
ETSII | UPM
TECHNISCHE UNIVERSITÄT DRESDEN
UNIVERSITAS FRIBURGENSIS
ibec Institute for Bioengineering of Catalonia
UAB
Universitat Autònoma de Barcelona
Leti
cea
PURDUE UNIVERSITY
NIMS
Nanomaterials Laboratory
dipc
CAMPUS DE EXCELENCIA INTERNACIONAL
POLITÉCNICA
"Ingeniamos el futuro"
Faculté des Sciences
Aix-Marseille Université
Georgia Tech
UNIVERSITAT DE BARCELONA
Universidad de Oviedo
mana
UAM
UNIVERSIDAD AUTONOMA DE MADRID
CIC nanoGUNE
nanoscience cooperative research center
Abstracts

Analytical usefulness of the combined use of Tb_4O_7 nanoparticles and laccase enzyme for the determination of antioxidants in food samples

Juan Godoy-Navajas, María Paz Aguilar-Caballos, Agustina Gómez-Hens
Analytical Chemistry Department. Institute of Fine Chemistry and Nanochemistry. Campus of Rabanales. Annex to Marie Curie Building. University of Córdoba. 14071-Córdoba. Spain.
Phone number: +34-957218645, Fax: +34-957218644
e-mail: qa1gohea@uco.es, web: http://www.uco.es/investiga/grupos/FQM-303

The analytical usefulness of terbium oxide nanoparticles (Tb_4O_7 NPs) for the determination of phenolic compounds in food samples in combination with the use of laccase enzyme is described for the first time. Laccases are oxidase-phenol enzymes, which are isolated from several types of plants, fungus and microorganisms, the most used variety being T*rametes Versicolor*. Laccase enzyme catalyzes the oxidation of phenolic compounds by reducing the dissolved oxygen present in the medium. This reduction can also be monitored by its action on some chromophores, such as 2,2´-azino-bis-(3-ethylbenzothiazolin-6-sulfonic) acid (ABTS)[1].

The use of the fluorophore 8-hydroxypyrene-3-sulfonate trisodium (HPTS), which fluorescence decreases in presence of laccase, is now reported. The observed decrease is lower in presence of antioxidant compounds, such as gallic acid, which has been used as model analyte. The areas under the kinetic curves obtained in presence of this antioxidant are directly proportional to its concentration. The presence of Tb_4O_7 NPs in the reaction medium gives rise to an increased reaction rate, which provides shorter analysis times, and hence, a better sample throughput.

This novel assay has been developed in a 96-well microplate format and it consists of two steps: 1) Pre-incubation of HPTS together with gallic acid standards or samples for 15 min at 37 °C, and 2) the addition of a pre-mixed solution, which contains a mixture of Tb_4O_7 NPs and laccase. This mixture is placed immediately on the microplate reader and kinetic curves are monitored using filters with nominal excitation and emission wavelengths of 450 and 535 nm, respectively. The method shows a detection limit of 0.14 µM and dynamic range of 0.5 - 12 µM. The precision, expressed as relative standard deviation, has been assayed at two different concentrations, 0.7 and 5 µM, obtaining values between 2.5 and 6.3 %. The method has been applied to the analysis of wine and beer samples, which demonstrates its analytical usefulness.

References

[1]Branchi, B., Galli, C., Gentili, P., Org. Biomol. Chem., **3** (2005) 2604.